

AALTO UNIVERSITY SCHOOL OF SCIENCE AND TECHNOLOGY PO BOX 11000, FI-00076 AALTO http://www.aalto.fi		ABSTRACT OF DOCTORAL DISSERTATION	
Author Ahmed Mohamed Othman Abd El-Maksoud			
Name of the dissertation Enhancing the Performance of Flexible AC Transmission System (FACTS) by Computational Intelligence			
Date of manuscript December 2010		Date of the dissertation	
<input checked="" type="checkbox"/> Monograph		<input type="checkbox"/> Article dissertation (summary + original articles)	
Department Electrical Engineering Department			
Field of research Power Systems			
Opponent(s)			
Supervisor Professor Matti Lehtonen, Aalto University, Finland			
		Professor Mahdi El-Arini, Zagazig University, Egypt	
Abstract <p>FACTS technology concerns the management of active and reactive power in the power networks to improve the performance aiming to reach the best operation criteria. The concept of FACTS technology has the ability to deal with many fields of both system and customer problems, especially related to performance quality issues, since most power quality problems can be attenuated or solved with an adequate control of power flow. In general, the classification of FACTS depends on the technology used in their implementation and the way they are connected to the power system (shunt or series).</p> <p>The subject of the thesis is to study applications of FACTS to control an electric power system. There are some problems like the inability to achieve full utilising of the capacity of the transmission lines, undesirable voltage levels, higher losses, high or low voltages, cascade tripping and outages that must be solved. FACTS devices can be used for adapting the phase angle and the voltage magnitude at certain buses and/or line impedance, which gives the ability to control the power flow in the networks.</p> <p>The main subject of the thesis deals with enhancing the steady-state and dynamics performance of the power grids by Flexible AC Transmission System (FACTS) based on computational intelligence. Control of the electric power system can be achieved by designing the FACTS controller, where the new trends as Artificial Intelligence can be applied to this subject to enhance the characteristics of controller performance. The proposed technique will be applied to solve real problems in a Finnish power grid. The thesis seeks to deal, solve, and enhance performances until the year 2020, where the data used is until the conditions of year 2020.</p> <p>The FACTS device, which will be used in the thesis, is the most promising one, which known as the Unified Power Flow Controller (UPFC). The FACTS control concerns with the active and reactive power levels in the power systems and their performance. So it's better to optimize the type, the location and the size of the power elements to optimize the system performance. The thesis derives the criteria to install the UPFC in an optimal location with optimal parameters and then designs an AI based damping controller for enhancing power system dynamic performance.</p>			
Keywords Unified Power Flow controller (UPFC), Genetic Algorithm (GA), Optimal location, Optimal settings			
ISBN (printed)		ISSN (printed)	
ISBN (pdf)		ISSN (pdf)	
ISBN (others)		Number of pages xii + 172 p.	
Publisher Aalto University School of Science and Technology, Transmission and Power Systems Engineering			
Print distribution Transmission and Power Systems Engineering			
<input checked="" type="checkbox"/> The dissertation can be read at http://lib.tkk.fi/Diss/			

Acknowledgment

First of all I would like to acknowledge my great debt in this work to my Merciful GOD who supported me with patience and strength to complete this thesis.

Cordial thanks and deep gratitude are offered to Prof. Dr. Matti Lehtonen, Electrical Engineering Department, Electrical Power Systems Lab, Aalto University, Finland and to Prof. Mahdi El-Arini, Electrical Power and Machines Department, Faculty of Engineering, Zagazig University, Egypt for valuable guidance and supervision.

The support provided by the Egyptian Educational Missions and Aalto University is thankfully acknowledged.

Special thanks are also offered to staff members and instructors of the Electrical Engineering Department in Aalto University School of Science and Technology, and in Zagazig University, for great help, guidance and for exerted efforts to overcome the difficulties that arose during the work. In addition, special thanks for William Martin, from Aalto University for reviewing and double-checking of the language issues of the thesis.

In fact, I would like to dedicate this thesis to all of our professors and ask GOD to help me to express clearly the aim of this thesis.

At the last, but not least, my deepest thanks also go to my family: my mother, my father, my brother, my sister, my father-in-law and my wife brother and sisters. Finally, my (HANA) and beloved wife, for their patience and endless support.

ESPOO, Aalto,

Ahmed Mohamed Othman Abd El-Maksoud.

Abstract

FACTS technology concerns the management of active and reactive power to improve the performance of AC power systems. The concept of FACTS embraces a wide and diverse field of both system and customer problems, especially related to performance quality issues, since most power quality problems can be attenuated or solved with an adequate control of power flow.

In general, FACTS devices are classified depending on the technology used in their implementation and the way they are connected to the power system (shunt or series). The main subject of the thesis is study the FACTS to control an electric power system. Then the new trends as Artificial Intelligence can be applied to this problem. The inability to achieve full capacity of the transmission lines, undesirable voltage levels, higher losses, high or low voltages, cascade tripping and outages are problems, which must be solved. One can readjust the phase angle, the voltage magnitude at certain buses and/or line impedance using FACTS devices. FACTS devices can control the power flow in power networks.

The main subject of the research deals with enhancing the steady state and dynamics performance of the power networks, as applied on large-scale network and a real Finnish Power Grid, by Flexible AC Transmission System (FACTS) based on Artificial Intelligence (AI), studying the power flow control of the electric power system to design the FACTS controller. Then the new trends as Artificial Intelligence can be applied on this subject to enhance the characteristics of controller performance.

This controller will be applied to solve real problems in the power grid generally and the applied to a real Finnish 110 kV power grid in Helsinki, through real data from the Finnish power system. The thesis will deal with the real Finnish network, solve, and enhance performance until year 2020, where the data used is until the conditions of year 2020.

The FACTS device, which will be used in the research, is the most promising one that is Unified Power Flow Controller (UPFC).

The power flow control concerns the power levels in the power systems and their performance. So it's better to optimize the type, the location and the size of the power elements to optimize the system performance.

The thesis contains a literature survey on the power flow control and a literature survey on the modeling and simulation of the problem and the techniques used to solve this problem. The thesis derives the proposed criteria to install the UPFC in an optimal location with optimal parameters and then to design an AI controller based on the ability of FACTS devices damping controllers in enhancing power system dynamics that to fine tune the system dynamics performance based on Artificial Intelligence. The thesis deals with FACTS especially the most recent UPFC devices. Applying the proposed criteria and controller to power systems (Case Studies) where these models are applied to the power system to show the capability of the proposed algorithm and controller on the system performance and the overall cost.

Optimizing the performance of the UPFC device with respect to the required components, quality of performance, location and the application capability will be considered. Genetic algorithm is used to as an optimization tool for the most suitable controllers' parameters to improve system performance over a wide range of operating conditions. Adaptive neuro-fuzzy inference system (ANFIS) is developed where the outputs of each neuro-fuzzy controller are the desired parameters of FACTS devices controllers.

The controller belongs to adaptive control where the (ANFIS) controller, once trained by a set of input-output patterns, can yield proper control action under any operating conditions providing better performance than a fixed parameters controller. Also the thesis shows the advantages of the proposed controller as applied to many power networks especially in a real Finnish power grid and in the first stage it will be compared with the best known and established controllers.

Table of Contents

Acknowledgment	V
Abstract	VII
Table of Contents	IX
List of Abbreviations	XII
Chapter (1) Introduction and Literature Survey	1
1.1 Introduction	2
1.2 FACTS Concept	3
1.3 Literature Survey on FACTS	5
1.4 Contribution of the thesis	12
Chapter (2) FACTS Devices Modeling	13
2.1 Introduction	14
2.2 The Thyristor Controlled Reactor (TCR)	14
2.3 TCR Based FACTS Devices	16
2.3.1 Static Var Compensators (SVCs)	16
2.3.2 Thyristor Controlled Series Capacitor (TCSC)	17
2.3.2.1 Equivalent impedance of the TCSC	18
2.3.2.2 Resonance firing angle	21
2.4 Synchronous Voltage Source (SVS)	22
2.5 SVS Based FACTS Device	24
2.5.1 Static Compensator (STATCOM)	24
2.5.2 Static Series Synchronous Compensator (SSSC)	26
2.5.3 Unified Power Flow Controller (UPFC)	28
Chapter (3) Artificial Intelligence Concept (AI)	31
3.1 Introduction	32
3.2 Nature and Scope of AI Techniques	32
3.2.1 Artificial Neural Networks	33
3.2.2 Fuzzy Logic Algorithm	35
3.2.2.1 Fuzzy Logic Operators	36
3.4.2.2 If-Then Rules and Fuzzy Inference Systems	37
3.2.3 Evolutionary Algorithms	37
3.2.4 Components of GAs	39
3.2.4.1 Initial Population	39
3.2.4.2 Natural Selection	39
3.2.4.3 Mating	40
3.2.4.4 Mutations	40
3.2.4.5 Continuous-Parameter Genetic Algorithm	40
3.3 Hybrid Intelligent Systems	41
3.3.1 Adaptive Neuro-Fuzzy Inference Systems (ANFIS)	42
3.3.2 ANFIS Hybrid Training Rule	43
3.3.2.1 Training of the consequent parameters	43
3.3.2.2 Training for the antecedent parameters	43

Chapter (4) Unified Power Flow Controller Scope	46
4.1 Introduction	47
4.2 Power Flow UPFC Modeling	47
4.3 Effective Initialization of UPFC Controllers	50
4.3.1 Controllers Represented by Shunt Synchronous Voltage Sources	50
4.3.2 Controllers Represented by Series Synchronous Voltage Sources	50
4.4 Dynamic Modeling of UPFC	52
4.5 Control of UPFC	54
4.5.1 Control of the Shunt Converter	54
4.5.2 Control of the Series Converter	55
Chapter (5) Proposed Techniques	57
5.1 Introduction	58
5.2 Proposed Technique for Optimal Location and Settings	58
5.2.1 Problem Formulation	58
5.2.2. GA Fitness Functions	59
5.2.3. UPFC Modeling for Power Flow	62
5.2.4. Problem Constraints	63
5.3 Performance Ranking Index	64
5.4 The Proposed Genetics Algorithm	65
5.5 Scope on the Simulations Files (UPFC files , GA files)	68
5.6 Dynamics Studies of the system (Concept and Building)	70
5.6.1 Data for dynamics studying of UPFC installation in HELEN network	70
5.7 Importance of Dynamics Tuning	72
5.8 Conventional PI Controller	77
5.9 UPFC Dynamic Controller	79
5.10 Why AI?	80
5.10.1 Why GA with ANFIS?	82
5.10.2 Construction of the adaptive intelligent Controller	83
Chapter (6) Case Studies	96
6.1 Introduction	97
6.2 Network Definition	97
6.3 Application Results on IEEE 6-Bus System	102
6.3.1 Normal Operating with Heavy Loading Pattern	103
6.3.2 Contingency Operating with Outage Pattern	107

6.3.3 Genetics Algorithm Versus another advanced optimization tool (PSO)	111
6.4 Application Results on IEEE Large Scale 57-Bus System	118
6.4.1 Normal Operating with Heavy Loading Pattern	118
6.4.2 Contingency Operating with Outage Pattern	119
6.5 Application Results on HELEN OY 110 KV NETWORK	120
6.5.1 Normal Operating with Heavy Loading Pattern until 2020	120
6.5.2 Contingency Operating with Outage Pattern	126
6.6 Cases Study: Optimal Installation for Load Profile Period	131
6.6.1 Normal Configuration with high loading	131
6.6.2 The contingency Study	132
6.7 Case Study: Fixed Location with Optimal Setting	136
6.8 Case Study: Multiple Optimal UPFC Installation	138
6.9 Optimal Power Flow Case	139
6.10 Dynamics of the system (Concept and Building)	140
6.11 Dynamics Data of the System	142
6.11.1 Scope on some dynamics data values of HELEN network	142
6.12 Importance of Dynamics Tuning	143
6.16 Effect of Adjusting PI Controller on Dynamics	145
6.18 Effect of AI controller installation on the system	146
6.19 Comparing Conventional Fixed PI , Adaptive AI Controller	149
Chapter (7) Conclusions	153
References	157
Appendix	164

List of Abbreviations

AVR	Automatic Voltage Regulator
DVR	Dynamic Voltage Restorer
FACTS	Flexible AC Transmission System
GTO	Gate Turn-Off (Thyristor)
HVDC	High Voltage Direct Current
IGBT	Insulated Gate Bipolar Transistor
IGCT	Integrated Gate Commutated Thyristor
LPF	Low Pass Filter
LP	Low Pressure (turbine)
PSS	Power System Stabilizer
PWM	Pulse Width Modulation
PQ	Power Quality
SSR	Subsynchronous Resonance
SSSC	Static Synchronous Series Compensator
STATCOM	Static (Synchronous) Compensator
SVC	Static Var Compensator
TCBR	Thyristor Controlled Braking Resistor
TCR	Thyristor Controlled Reactor
TCSC	Thyristor Controlled Series Capacitor
UPFC	Unified Power Flow Controller
UPQC	Unified Power Quality Conditioner
VSC	Voltage Source Converter
VSI	Voltage Source Inverter
ANN	Artificial Neural Network
FL	Fuzzy Logic
GA	Genetic Algorithm
ANFIS	Artificial Neuro-Fuzzy Interference System
DNS	Demand Not Supplied
ENS	Energy Not Supplied

Chapter 1

Introduction and Literature Survey

Introduction on Power Flow Control

1.1 Introduction

FACTS Technology is defined as the management of active and reactive power to improve the performance of electrical networks. The concept of FACTS technology embraces a wide and variety of tasks related to both networks and consumers problems, especially related to power quality issues, since most of power quality problems can be improved or enhanced with an adequate control of the power flow.

In general, the concept of power flow control is concerned with two jobs: load support and voltage compensation. In load support, the objectives are to increase the value of the system power factor, to balance the active power from the source, to compensate voltage regulation and to decrease harmonic components produced by large and fluctuating nonlinear loads especially in industry applications. Voltage compensation is generally required to decrease voltage fluctuation at the terminals of a transmission line. Reactive power compensation in transmission systems also enhances the stability of the networks by maximizing the active power that can be transferred. It also assists to keep a substantially regulated voltage profile at all sections of power transmission, it improves HVDC (High Voltage Direct Current) response performance, increases transmission efficiency, controls steady-state bus normal voltage and over voltages, and can avoid serious blackouts.

Series and shunt VAR compensators can modify the performance characteristics of electrical networks. Series compensators change the parameters of the transmission grids or distribution levels, where shunt compensators modify the impedance at the connected terminals. In both of them, the reactive power through the system can significantly improve the performance of the power system.

Classically, rotating and fixed or mechanically switched capacitors or inductors have been applied to VAR power compensators. Even in recent decades, static VAR compensators based on thyristor switched capacitors and thyristor controlled reactors to feed or consume the required reactive power have been installed. Also, the use of self-commutated PWM converters with an control action allows the implementation of static compensators for generating or consuming reactive components faster than the fundamental system period. Based on the reliable high-speed power electronics, efficient analytical tools, intelligent control Flexible AC and microcomputer technologies, Flexible AC Transmission Systems, also known as FACTS, have been presented as a new concept for the operation of power transmission systems.

Inside these concepts, static VAR compensation uses fast response times and plays an important role in improving the amount of total power transfer through a transmission line, near its thermal rate, without violation in its stability boundary. These techniques arise through the power of special static VAR compensators to adapt the related parameters that control the performance of transmission systems with the impedance, current, voltage, phase angle and the damping of oscillations [1].

This thesis presents an overview of FACTS technologies, their operation concepts, also compensation procedure and performance are presented and analyzed. In general, FACTS are classified depending on the technology and implementation and the connection method in the power system (shunt or series).

Conventionally steady-state reactive compensators are not powerful in controlling the transmission power when the network is subjected to disturbances. For explanation, a fault into the transmission grid disrupts the equilibrium between the mechanical input power for the generating units and the electrical output power of the generating units that is directed by the faulted area [2].

Even with sufficient transient stability margin, the power system may not become stable if its steady state stability is insufficient; that is, if the power system has negative damping. It has been shown that both the transient and steady state stabilities of the power system can be improved if the reactive compensation of the transmission system is made rapidly variable.

However, the existing traditional transmission facilities were not designed to handle the stressed control requirements of an interconnected power system. The power flow in the individual lines of the transmission grid is determined by their impedance and it often cannot be restricted to the desired power corridors. Consequently, power flow loops develop and certain lines become over-loaded, with the overall effect of deteriorating voltage profiles and decreased system stability. Furthermore, while the power transmission requirements have been rapidly growing, the difficulties and escalating cost of right-of-ways have serious effect on the construction of new lines [3].

The general layout wants a review of the conventional power transmission principle and practice, and the creation of new technologies that give the complete benefits of current power generation and transmission facilities without effecting system availability and security. The Electric Power Research Institute (EPRI) has developed the Flexible AC Transmission Systems (FACTS) in which power flow is effectively controlled by various power electronic devices. The core of FACTS technology contains high power electronics, a variety of thyristor devices, micro-electronics, communications and advanced control actions [4].

By FACTS, operator governs the phase angle, the voltage profile at certain buses and line impedance. Power flow is controlled and it flows by the control actions using FACTS devices, which include

- Static VAR Compensators (SVC)
- Thyristor Controlled Series Capacitors (TCSC)
- Static Compensators (STATCOM)
- Static Series Synchronous Compensators (SSSC)
- Unified Power Flow Controllers (UPFC)

1.2 FACTS Concept

From the general point of view, the FACTS principle is based on the substantial incorporation of power electronic techniques and algorithms into the system, to make it electronically controllable.

Much of the research upon which FACTS rests evolved over a period of many years. Nevertheless, FACTS, an integrated technology, is a novel concept that was brought to fruition during the 1980s at the Electric Power Research Institute (EPRI) for applications of North American army objectives [5]. FACTS can capitalize on the many breakthroughs taking place in the area of high-voltage and high-current power electronics, to increase the control of power flows in networks during both steady-state and transient conditions. The recent reality of making the power network electronically controllable has initiated a change in the way that power plant equipment is designed and built as well as the technology that goes into the planning and operation of transmission and distribution networks. These developments may also affect the way energy transactions are conducted, as high-speed control of the path of the energy flow is now feasible. FACTS own a lot of promising benefits, technical and economical, which received the support of electrical equipment manufacturers, utilities, and research organizations around the world [6]. Several kinds of FACTS controllers have been commissioned in various parts of the world. The most popular are: load tap changers, phase-angle regulators, static VAR compensators, thyristor-controlled series compensators, inter-phase power controllers, static compensators, and unified power flow controllers.

This thesis covers in breadth and depth the modeling and simulation methods required for a thorough study of the steady-state and dynamic operation of electrical power systems with FACTS controllers. The characteristics of a given power system evolve with time, as load grows and generation is added. If the transmission grid capacity is not updated sufficiently the power network becomes vulnerable to steady state and transient stability problems, as stability margins will be narrower [7].

The powerful of the transmission grid to transmit power has constraint by one or more of the following steady-state and dynamic limitations: Angular stability, Voltage stability, Thermal limits, Transient stability, and Dynamic stability.

These limits affect the maximum electrical power to be transmitted without breakdown to transmission lines and electric devices. In principle, limitations on power transfer can be managed by the addition of new transmission and generation facilities. Alternatively, FACTS controllers can enable the same objectives to be met with no major alterations to system layout. FACTS controllers save a lot of benefits such as reduction of operation and transmission investment cost, increased system security and system reliability, maximize power transfer capabilities, and an overall enhancement of the quality of the electric energy delivered to customers [8].

From the operational point of view, FACTS technology is concerned with the ability to control, in an adaptive trend, the directions of the power flows throughout the network, where before the advent of FACTS, high-speed control was very limited. The ability to control the line impedance and the buses voltage magnitudes and phase angles at both the sending and the receiving ends of transmission lines, with almost no delay, has significantly increased the transmission capabilities of the network while considerably enhancing the security of the system. In many practical situations, it is desirable to include

economical and operational considerations into the power flow formulation, so that optimal solutions, within constrained solution spaces, can be obtained.

The main objective of the thesis is concerned with enhancing the steady state and dynamic performance of the Flexible AC Transmission System (FACTS) using Computational Intelligence methods, like Genetic Algorithms (GA), Fuzzy Logic (FL), Neural Networks, (NN), and Adaptive Neuro-Fuzzy Inference System (ANFIS).

1.3 Literature Survey on FACTS

There is a vast amount of work reported in the literature in the area of Reactive Power Control and FACTS devices. The reactive Power control concepts and methods, as well as FACTS devices research at the initial stage, clarified of the principles of FACTS devices functions. Later, modeling, analysis and control were investigated, resulting in the recent application tests.

In [9], there is a presentation of Parallel Optimal Reactive Power Flow Based on Cooperative Co-Evolutionary Differential Evolution and Power System Decomposition. Differential evolution (DE) is an effective evolutionary technique for solving optimal reactive power flow problems, but it needs mainly a large population to prevent convergence in the suitable time. To recover this disadvantage, a new decomposition and coordination technique, which depends on the cooperative co-evolutionary architecture and the voltage-var sensitivity-based power system decomposition method is applied and united with DE. It is achieved with a three-level parallel computing topology on a PC-cluster. Based on the IEEE 118-bus system test case, the power of the applied method has been tested by comparison with the parallel basic DE, that not employing the decomposition and coordination technique. The limitation of that paper that the application of DE to large-scale systems was not investigated and recommended as a future area of research.

In [10], a hybrid genetic algorithm–interior point method for optimal reactive power flow is presented. By combining a genetic algorithm (GA) with a non-linear Interior Point Method (IPM), a new hybrid technique for the Optimal Reactive Power Flow (ORPF) application is presented in that research. The applied technique can be essentially divided into two sections. The first section is to solve the ORPF with the IPM by releasing the discrete variables. The second section is to divide the original ORPF into two sub-problems: continuous optimization and discrete optimization. The optimal solution can be achieved by solving separately the two sub-problems. A dynamic updating strategy is also presented to make the GA and the IPM complement each other and to improve the efficiency of the hybrid proposed method. The GA is applied to solve the discrete optimization with the continuous variables being fixed, whereas the IPM handles the continuous optimization with the discrete variables being constant.

In [11], a new optimal reactive power flow (ORPF) model in rectangular form is proposed. Where the load tap changing (LTC) transformer element is considered as an ideal transformer and the series impedance becomes a dummy point placed between them. The terminal voltages of the ideal transformer winding are then utilized to exchange the turn ratio of the LTC for making the ORPF model quadratic. The Hessian matrices in this model are constants and require being determined only once inside the optimal procedure, which reduces the required time for the calculation. The solution of the ORPF problem by the predictor corrector primal dual interior point method is presented in this research. Two

separate modules for the new and the traditional methods are developed in MATLAB in order to compare the performances. The limitation on this method that it takes in some cases the same identical iteration counts as the conventional method to reach the solution.

In [12], a presentation of a simple, fast, and efficient method for determining the maximum loading point (MLP) and the voltage stability security margin of electric power systems. The presented technique depends on nonlinear programming methods. The MLP is accurately achieved after a few load change steps. The computational process has two types of load changes. Initially, load increases directed to the MLP are used for minimizing an objective function based on sensitivities. In case an overestimated load increase moves the system outside the stable feasible operating region, another very simple optimization-based process lead to minimize the power mismatches that to calculate the load adjustment curtailment to pull the system back onto the feasible area. Simulation results for small test to large realistic systems are shown to validate the proposed method. The limitation is that the simulation results were for small IEEE test systems. A possible shortcoming of the proposed approach would have been the need of setting parameter t . However, all simulations that have been carried out showed that its setting is straightforward, since it lies within a narrow range for all systems.

In [13], the maximum loading margin (MLM) method is presented in determining generation directions to maximize the static voltage stability margin, where the MLM is calculated at different possible generation tends in the generation space. An easy and short formula indicating the link between the generation direction and the LM is applied to get the MLM point. The presented technique is validated in the modified IEEE 14-bus test system and used for the Thailand power system. LMs of the system with the generation directions are compared for different generator combinations using the proposed technique.

In [14], the Tellegen's theorem and adjoint networks are applied to derive a novel, local voltage-stability index. The new technique makes it available to calculate the Thevenin's values in a various method than adaptive curve-fitting techniques, from two consecutive phasor measurements. The new index was verified on various test systems. The results were achieved on a static two-bus test system and on the dynamic Belgian–French 32-bus test system that contains complete dynamic models of all power-system components crucial to the voltage instability analysis. The simulations indicate the advantages of the presented index: it is simple, computationally very fast, and easy to implement in wide-area monitoring and control center or locally in a numerical relay.

In [15], there is a proposal for a new optimal routing algorithm to minimize power loss and at the same time to maximize the voltage stability in radial power systems. The resultant characteristics of this research can be presented as follows.

- An powerful a voltage stability index (VSI) has been applied to evaluate the voltage stability, which is well suited for frequent switching features. As shown in the case studies, the voltage stability of a radial system can be rapidly evaluated by the proposed VSI. Furthermore, information of all buses along the critical transmission path (CTP) and the critical bus can be automatically determined through the BE procedure. Therefore, operators can prepare a preventive action scheme in a sudden contingency or disturbance environment that may cause the voltage collapse in a regional distribution system.

- The technique can act for both dual and single optimization based on the priority of operational conditions, such as in an ill-conditioned distribution system, operators can use

the network configuration based on the VSI only, or dual optimization with both VSI and loss minimization. While in the well conditions system, it may be sufficient only to use the loss minimization objective function. Operators can make lookup tables concern the ill-conditioned system environments, which could supply them with operational data to enhance the voltage stability while servicing the loss minimization target.

- In addition to, the improved branch exchange (IBE) approach is presented to decrease the computational time. The IBE method depends on the loss calculation index. The index can be applied as an efficient judge to evaluate the change of power loss without solving the iterative load flow during the BEs in a loop network. For calculation of the new tie-branch power flow resulting from load transfer during the BEs, the newly derived TBP equation is used with reasonable accuracy.

- The optimal routing algorithm (ORA) also has used the GA as a global search algorithm to look for an initial radial network. As indicated in numerical results, this hybrid method is very powerful in large-scale systems.

In [16], a new criterion of voltage stability margin is proposed. Voltage instability is usually leading to participating in the progress of power system disturbances. While increasing load admittance, bus voltage reduces to such a level that the apparent power (V^2Y) does not rise. As a result, voltage collapses with all consequences resulting from it. One of the most important defenses is the load shedding at the stations, where the stability margin start to be low, and has bad effects on the large-scale power system disturbance. To do that, there is a request to develop automatic devices, which procedure local signals, detect the decreased margin, and initiate the load shedding. One of the operating requirements for theses devices is measuring the voltage level. The disadvantage of such an approach appears due to the relations between the voltage level and the stability limit that is based mainly on the load power factor. To handle this issue, this research proposes a criterion, which has solid dependence on the concept of voltage stability. It determines the derivative of VA power with respect to the admittance (dS/dY). It may be easily accomplished, because both the power and the admittance are measurable, and the variation of load is due to switching on and off the impedances, and/or actions of the transformer on load tap-changing devices. The limitation of this method, however, is that it is not performed in a real power system, Also there is no comparison between this method and others.

In [17], a proposal of a novel method to determine the optimal SVC allocation to enhance the voltage stability of power systems is presented. By concerning the second-order term of the Taylor's series expansion, the nonlinear bus voltage participation factor is calculated in this research. It gets the nonlinear features of power systems into the process. When we make a comparison between those that are available and the traditional linear technique, some advantages are available when the proposed nonlinear method is used.

- 1) By use of the normal forms of the proposed method, more details about the nonlinearity of the power system can be considered. Therefore, it is more accurate to analyze the complex nonlinear characteristics of power systems.

- 2) For the power systems operating under the light loading condition, as the nonlinearity of the system is not very high, the results from both the nonlinear bus voltage PF and the linear bus voltage PF lead to well outputs. When the power networks are working under stressed conditions, the nonlinearity has an essential role in the power system response. In

this condition, the nonlinearity of the system cannot be ignored. The nonlinear bus voltages PF will lead to results that are more accurate related to the steady-state voltage stability index.

In [18], the modeling of FACTS devices for power flow studies and the role of that modeling in the study of FACTS devices for power flow control are discussed. Three essential generic models of FACTS devices are presented and the combination of those devices into load flow analysis, studies relating to wheeling, and interchange power flow control is explained. The determination of the voltage magnitude and phase angle of the FACTS bus is provided by solving two simultaneous nonlinear equations. These equations are solved with a separate Newton-Raphson approach within each iteration of the large load flow analysis. Therefore, another set of mismatch equations must be met for each iteration of the larger study. It is possible that this smaller Newton-Raphson study will not converge, particularly when voltage magnitudes are significantly less than rating. Therefore, the resultant solution may not converge due to divergence of the internal search. The disadvantage of this model is that the firing angle corresponding to such a compensation level should be calculated by reordering to an iterative process, in addition to the load flow solution. Moreover, it is not possible to evaluate within the load flow solution whether or not the solution is occurring near of a resonant point of a TCSC. The only indication would be a divergent iterative process.

In [19], the issue of UPFC modeling within the context of optimal power flow solutions is addressed. The UPFC model has been presented to control active and reactive power flow at the buses of the sending or receiving end. The UPFC model suitable for optimal power flow solutions is presented for the first time in this study.

In [20], the basic features of controllable reactive series elements (CRSE) (i.e. controllable series compensation (CSC) and a static synchronous series compensator (SSSC)) for power system flow control are presented. Mathematical models of CRSE, containing a simple representation of the transmission system, have been developed. According to these concepts, the CRSE effect on a longitudinal transmission system was analyzed. The theory of physics and the basic difference between a CSC and an SSSC in terms of power flow control has been indicated. According to theoretical considerations, from the point of view of power flow control capability, SSSC is found to be superior to CSC, especially at low transmission angles. Therefore, SSSC is more suitable in cases where power flow requires to be controlled in short lines or under light-load conditions. The disadvantage of this paper is that the difference between an SSSC and a CSC has been studied on the basis of a static model.

In [21], a new method to incorporate the power flow control needs of FACTS in studying the optimal active power flow problem is presented. The linearized (DC) network model is used. Three main types of FACTS devices, namely TCSC, TCPS, and the UPFC, are considered. The proposed method decomposes the solution of such modified optimum power flow (OPF) problem into the iteration of two problems. The first problem is a power flow control sub-problem while the second problem is a normal OPF problem. Further research work is needed for other OPF algorithms with an AC network model.

In [22, 23], a new and comprehensive load flow model for the TCSC and the UPFC is presented. For the TCSC, the state variable is the TCSC's firing angle, which is linked with the nodal voltage magnitudes and angles of the grid in a single format for a combined

iterative process through a Newton-Raphson method. Under different operation of the TCSC models, this model develops account of the loop current that exists in the TCSC under both partial and full conduction operating modes. Also, the model provides proper care of the resonant points characterized by the TCSC fundamental frequency impedance. A group of analytical equations has been derived to make good UPFC initial conditions. Suitable guidelines are proposed for an efficient control coordination of two or more UPFCs operating in series or parallel arrangements.

In [24], using the steady state models of FACTS devices, the controllability and control ranges of the power flow on the transmission line occupied by single FACTS device are studied. That paper mainly concerns with the commitment of several FACTS devices. To handle this issue, a new method based on genetic algorithm (GA) has been presented. With this presented technique, we analyze the number of FACTS to maximum range of the power flow control. It is found that the controllability of the power flow is based on the number of FACTS devices in the system and power flow control range with multiple FACTS devices is larger than that with only one such device. Therefore, the commitment of control performances of various devices is a very essential issue for future power system planning and operation.

A linear optimal controller is proposed [25] to enhance the system dynamics and to coordinate three SVCs depending on two control levels, the local control to insure optimum Performance at the local level and the global control to make the coordination by decoupling the state equation for each area. Also a state observer is suggested to obtain the unmeasured states. PSCAD/MTDC is used to simulate the system. The problem of coordination is also handled in [26], a coordinated controller is designed according to the linear quadratic problem; the gain matrix is modified to allow the controller to depend on output feedback. In addition, the system states are reduced since the controller is concerned with the range of frequencies of the inter-area modes.

A methodology to obtain the robust locations and feedback signals of FACTS controllers is proposed in [27]. The criteria proposed insure good performance for the controller not only at the designed operating condition but also at the different operating conditions of the power system. An eigen-free index is introduced to evaluate the performance of the controller.

In [28], it proposed the application of a Takagi-Sugeno (TS) fuzzy controller to provide regulation of the series and shunt voltage source inverters of the UPFC to damp the inter-area and local modes in a multi-machine power system. The UPFC injection model, which consists of two controllable loads, was used and the dynamics of the DC voltage was expressed by a differential equation. The reactive and active power deviations, which were feedback signals to the active and reactive components of the series voltage source respectively, were fuzzified using two fuzzy sets, positive and negative. By applying Zadeh's rules for AND operation and the general defuzzifier, the output of the controller was obtained. In [29], it proposed a conventional lead-lag controller for UPFC to improve the oscillation damping of a single-machine infinite bus system. The generator speed deviation is the controller input signal. Based on the linearized model, the damping function of the UPFC is investigated.

A robust fixed-structured power system damping controllers using genetic algorithm is indicated in [30]. The designed controllers have a classical structure structuring from a

gain, a washout stage and two lead-lag stages. The GA searches for an optimum solution over the controller's parameter space. The approach is applied to design SVC and TCSC damping controllers to improve the damping of the inter-area modes. Local voltage and current measurements are used to synthesis remote feedback signals.

In [31], various control methods for damping undesirable inter-area oscillations by PSSs, SVCs and STATCOMs are discussed. The oscillation problem is studied from Hopf bifurcations perspective. It is observed that the damping introduced by the SVC and STATCOM controllers with only voltage control was lower than that provided by the PSSs and the STATCOM provides better damping than the SVC as this controller is able to transiently exchange active power with the system.

A supplementary damping controller for a UPFC had been proposed in [32]. The gains of the UPFC supplementary damping controller are adjusted in real time, based on online measured real and reactive power flows in transmission lines. To decrease the time required for the online gain adaptation process, an artificial neural network is designed. Power flows over the transmission line are used as inputs to the adaptive controller. The proposed damping compensator has effectively damped the electromechanical mode with an oscillation frequency of around 0.78 Hz.

In [32], it concerns with minimizing the active losses in the power systems using installation of UPFC in the network. The applications of UPFC in that paper are as series element to work as a series compensator and/or to work as a phase shifter; Genetic Algorithm (GA) is used to find the optimal values of the phase angles for the phase shifters and the optimal values of series reactance for the series compensators to achieve the required criteria. The simulations are applied on IEEE 30-bus system.

In [33], it focuses on optimal power flow with presence of UPFC in the system. And then it applies Genetic Algorithm (GA) to find the optimal dispatch of the generation powers of the generating units in the network to achieve the minimum total cost (\$/hr). The model, which is used in modeling, is the injected model of FACTS device. The simulations are applied on IEEE 14-bus system. The results show that FACTS device doesn't lead to a significant reduction in the cost of the generating power. It can be used in controlling and increase the feasibility of the power network.

In [34], a design of fuzzy damping controller of UPFC through genetic algorithm is presented. It applies a fuzzy controller as external controller provides supplementary damping signal to UPFC. The design includes the shape and the number of membership functions for the input and the output variables. The genetic algorithm is used to optimize the scaling factors, which are used in the scaling portion of the fuzzy controller. The simulations are applied on four machines interconnected power system, which used as a test system. A comparison between the fuzzy controller and the conventional controller and also without presence of controller is performed.

In [35], it studies the optimal location of FACTS devices, in general way. It compares between the simulated annealing method, Tabu search method, and genetic algorithm method; to find the optimal location for some FACTS devices like TCSC, TCVR, TCPST, SVS and UPFC. The study is performed on the steady-state models, and the simulations are occurred on IEEE 118-bus system. The problem is that, this paper represents UPFC as two separated devices, without modeling the UPFC itself as stand-alone device. It presents a limitation of the number of FACTS devices. It states that GA is better in the simulations.

In [36], it studies the application of harmony search algorithm and genetic algorithm in optimal installation of FACTS devices related to voltage stability and losses issues. It concerns with determining the optimal location of FACTS devices. The applied devices, which are used in that paper, are TCPAR, UPFC, and SVC. The concerning criteria are the loss and the voltage stability. The used mathematical model of FACTS devices is the power-injected model. The simulations are applied on IEEE 30-bus system.

In [37], it presents a control method on UPFC based on genetic algorithm, but applied on a single-machine infinite-bus system. The aim of UPFC installation on that system is to damp the system oscillations. The UPFC voltage sources are converted into three power injections at the receiving and sending buses. The applied controller is an external genetic algorithm PI controller trying to return the response deviation to zero. The fitness function is termed on the real and imaginary parts of the dominant eigenvalues.

In [38], it proposes a micro genetic algorithm based fuzzy logic controller to coordinate between TCSC and UPFC in the system. The micro genetic controller is designed to operate to reach the optimal criteria as fast as possible without enhancing the performance. The micro genetic algorithm is applied when it available to use small size and value of population not more than 10. These characteristics direct the simulations to be executed on three-machine power system. The genetic algorithm search for the optimal membership functions. In [39], it studies the same application, in addition to use parallel micro genetic algorithms to speed up the initialization process covering the search-space, also it uses neuro-fuzzy technique to escape from dropping in the local minimum.

In [40], it concerns with enhancement of voltage stability and reduction in investment cost by installing multi-type FACTS devices using genetic algorithm. The fitness functions is termed by the FACTS devices cost functions and the system losses. Three different FACTS devices are used: TCSC, SVC, and UPFC. The paper uses the decoupled model for UPFC, which is less complex but it lacks to the modifications in Jacobian matrix. Multi-type FACTS devices can achieve the required criteria but the economic aspects must be considered.

In [41], it studies the congestion management in deregulated power system; and how to utilize the FACTS devices in that application. It uses the static modeling of TCSC and the static modeling of UPFC, specially for UPFC modeling, it uses the injection model of UPFC. The fitness function is termed by the loading of the transmission lines in exponential mathematical formula. According to the proposed fitness function, to reduce more significantly the loading of the lines, we want to install more than FACTS devices, which may give reflection for the cost of the power in the system. The simulations are applied on IEEE 30-bus system.

In [42, 43], they present a method for optimal location of UPFC in power systems to increase the loadability using genetic algorithm. The model for UPFC, which is used in the papers, is the injection model of UPFC. The analysis studies the comparison of installing one, two or three UPFC in the system. The objective function concerns with maximizing the loadability of the transmission lines, and that is the only technical benefit is taken into consideration. The objective function is termed by exponential mathematical formula to describe the required criteria. The process depends on increase the number of UPFC installed in the system. The simulations are occurred on high loading operating conditions for the transmission lines. The simulations are applied on IEEE 14-bus system. Specially

[43], it takes the same area and analysis with some more case studies for increasing the active power and the reactive power. In [44], it concerns with a hybrid genetic algorithm for determining UPFC optimal control setting. The injected-power model is the static modeling of UPFC, which is the used in the simulations. The objective function is related to optimal power flow to minimize the operating cost especially for the power of the generating units. The optimization process searches the control setting of UPFC to minimize the cost of the operation. The results is achieved by first finding the optimal setting of UPFC using genetic algorithm, then simulate the system and UPFC with that setting to get the objective. The simulations are applied on IEEE 14-bus system. Also, in [45], it discusses the same concept for a hybrid genetic algorithm for optimal power flow included FACTS devices. The static models of FACTS devices, which are used, are for TCSC and UPFC. The objective is to minimize the overall cost. The simulations are applied on IEEE 14-bus system with different loading conditions by increasing loading value at certain one bus.

In [46], it proposes ANFIS system to find the optimal setting UPFC during the static operation of the system. The objective is described in the difference of the desired parameter and the actual one. The analysis concerns with the normal increase in the loading conditions. The method is simulated in many small networks configurations. The approach needs a continusly update in the patterns. The UPFC is installed in the system to control the power flow in certain transmission line. In [47], it presents an external ANFIS controller on UPFC to enhance the stability of the system. The objective is mainly described to maximize the energy function of UPFC. The method is applied for a single-machine infinite-machine bus system. The generating units in the simulations are represented in classical model. The energy function is termed by the total reactive power injected into the network by the UPFC, that energy functions is used as the core of the neuro-fuzzy system; and is applied to generate the input/output patterns of the method.

1.4 Contribution of the Thesis

The contributions of the thesis start with formatting, deriving, coding and programming the network equations required to link UPFC steady-state and dynamic models to the power systems. One of the other contributions of the thesis is deriving GA applications on UPFC to achieve real criteria on a real world sub-transmission network.

An enhanced GA technique is proposed by enhancing and updating the working phases of the GA including the objective function formulation and computing the fitness using the diversity in the population and selection probability. The simulations and results show the advantages of using the proposed technique. Integrating the results by linking the case studies of the steady-state and the dynamic analysis is achieved. In the dynamic analysis section, a new idea for integrating the GA with ANFIS to be applied on the control action procedure is presented.

In addition to, packages of Software for genetics algorithm and adaptive neuro-fuzzy system are developed. In other related work, GA only was used to enhance the system dynamic performance considering all working range of power system at a time that gave a difficulty and inability in some cases to reach the solution criteria. In this thesis, for every operating point GA is used to search for controllers' parameters, parameters found at certain operating point are different from those found at others. ANFISs are required in this case to recognize the appropriate parameters for each operating point.

Chapter 2

FACTS Devices Modeling

FACTS Devices Modeling

2.1 Introduction

This chapter presents an overview of the most prominent characteristics of the power electronic equipment currently used in the electricity supply industry for the purpose of voltage regulation, active and reactive power flow control, and power quality enhancement. A study of the models and procedures with which to assess the steady-state operation of electrical power systems at the fundamental frequency is made.

The modeling of FACTS controllers in both the phase domain and the sequence domain is addressed in this chapter. All models are developed from the first principles, with strong reference to the physical structure of the equipment.

The focus is on steady-state operation and a distinction has been made between power electronic devices, which uses conventional power semiconductor equipments (i.e. thyristors) and the new generation of power system controllers, which use complete controllable semiconductor devices such as GTOs thyristors and IGBTs. Also the latter devices work well with fast switching control techniques, such as the sinusoidal PWM control scheme, and, from the power system perspective, operate like voltage sources, having an almost delay-free response. Devices based on thyristors have a slower response, more than one cycle of the fundamental frequency, and use phase control as opposed to PWM control. From the power system point of view, thyristor-based controllers behave like controllable reactances as opposed to voltage sources.

This chapter presents the structure, operation and the steady state characteristics of FACTS devices that depend in its operation on the Thyristor Controlled Reactor (TCR) or the Synchronous Voltage Source (SVS).

2.2 The Thyristor Controlled Reactor (TCR)

The main components of the basic TCR are shown in Figure 2.1. The controllable element is the antiparallel thyristor pair, Th1 and Th2, which conducts on alternate half cycles of the supply frequency. The other key component is the linear (air-core) reactor of inductance L . In a practical valve, many thyristors (typically 10 to 40) are connected in series to meet the required blocking voltage levels [49]. Applying simultaneously a gate pulse to all thyristors of a thyristor valve brings the valve into conduction. The valve will automatically block approximately at the zero crossing of the AC current, in the absence of the firing signal. Thus, the controlling element is the thyristor valve. The TCR current is essentially reactive, lagging the voltage by nearly 90° . The active component of the current is very small and the losses of the device are of the order of 0.5 – 2 % of the reactive power. Therefore, one of the modeling assumptions is that the resistance of the inductor may be neglected [50].

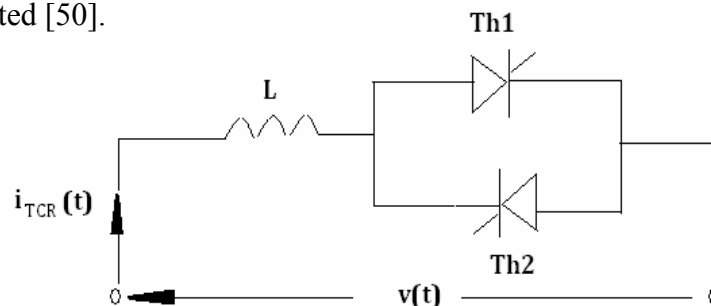


Fig. 2.1, The Thyristor Controlled Reactor

The firing angle α is defined as the angle in electrical degrees between the positive going zero-crossing of the voltage across the inductor and the positive going zero-crossing of the current through it. The thyristors are fired symmetrically; therefore, the maximum possible firing angle is 180° . Complete conduction is achieved with a angle of gate of 90° . Partial conduction is achieved with angles of gates between 90° and 180° with zero current at 180° . Firing angles less than 90° are not allowed, as they generate unsymmetrical currents with a high DC component [51]. The fundamental component of the reactor current is decreased as the firing angle increases. That means an increase in the reactor inductance, reducing both of its reactive power and its current.

In Figure 2.2a, the voltage across the TCR inductor and the current through it are shown at full conduction. The equivalent reactance of the TCR is equal to the inductor reactance. In Figure 2.2b, the current waveform is shown for a firing angle of 100° . Only part of the sinusoidal voltage is applied to the inductor, the current and the voltage are not sinusoidal anymore. The fundamental component of the current is less than that the current at a 90° firing angle, resulting in an equivalent reactance of the TCR higher than the inductor reactance. Figure 2.2c and 2.2d show the TCR current waveform for a firing angle of 130° and 150° . The fundamental component of the current through the inductor is very small, the equivalent reactance of the TCR is very high, and at 180° it becomes practically infinite.

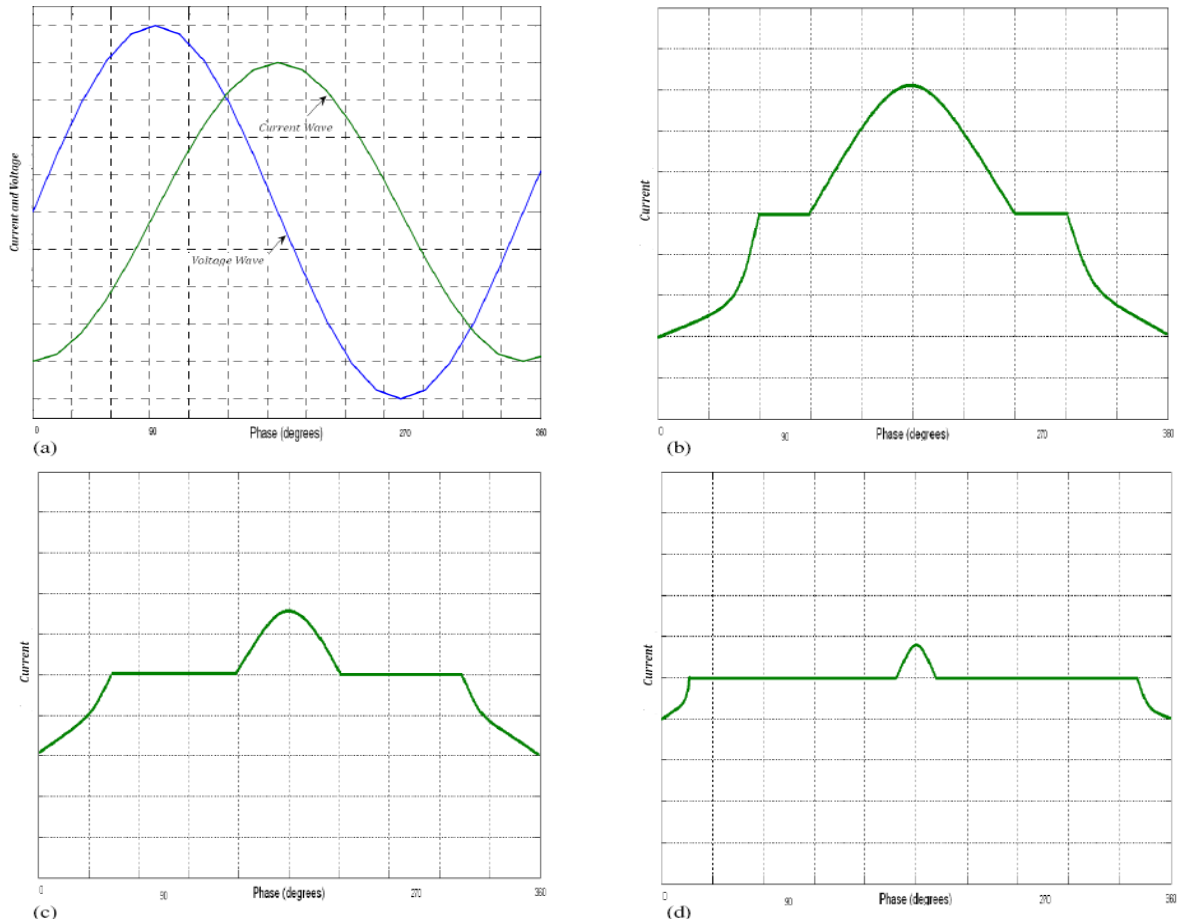


Fig. 2.2, Current waveforms in the basic thyristor-controlled reactor.

Using the Fourier series, the fundamental component of the controllable reactance of the TCR (X_v) is

$$x_v = x_l \frac{\pi}{2(\pi - \alpha) + \sin(2\alpha)}$$

Inside a 3- Φ network, three 1- Φ thyristor controlled reactors are utilized in delta connection. Subjecting to balanced conditions, the odd-order harmonic currents circulate in the delta connected TCRs and do not flow to the power system. For the TCRs arranged in delta, the maximum total harmonic distortion coefficient is less than 10 % [2]. For being used with shunt devices, a step-down transformer is requested in high-voltage applications as the TCR voltages has a constraint for technical and economic reasons to values starting from 50 kV or below.

2.3 TCR Based FACTS Devices

Among the devices that depend on the TCR are Static Var Compensators (SVC) and Thyristor Controlled Series Capacitor (TCSC).

2.3.1 Static Var Compensators (SVCs)

The construction of the SVC consists of a TCR in parallel with a capacitors bank. From a technical perspective, the SVC operates as a shunt-connected variable reactance that can produces or draws reactive power to regulate the voltage level at the location of the connection to the system. It is used efficiently to supply fast reactive power and voltage regulation support. The firing angle control of the thyristor provides the SVC with an instantaneous speed of response [5].

A graphical illustration of the SVC is shown in Figure 2.3, where a three-phase, three winding transformer is utilized to connect the SVC to the system. The transformer has two identical secondary windings: the first is for the delta connection, six-pulse TCR and the second for the star connection, is a three-phase bank of capacitors, with its star point floating. The three transformer windings are also taken to be star-connected, with their star points floating.

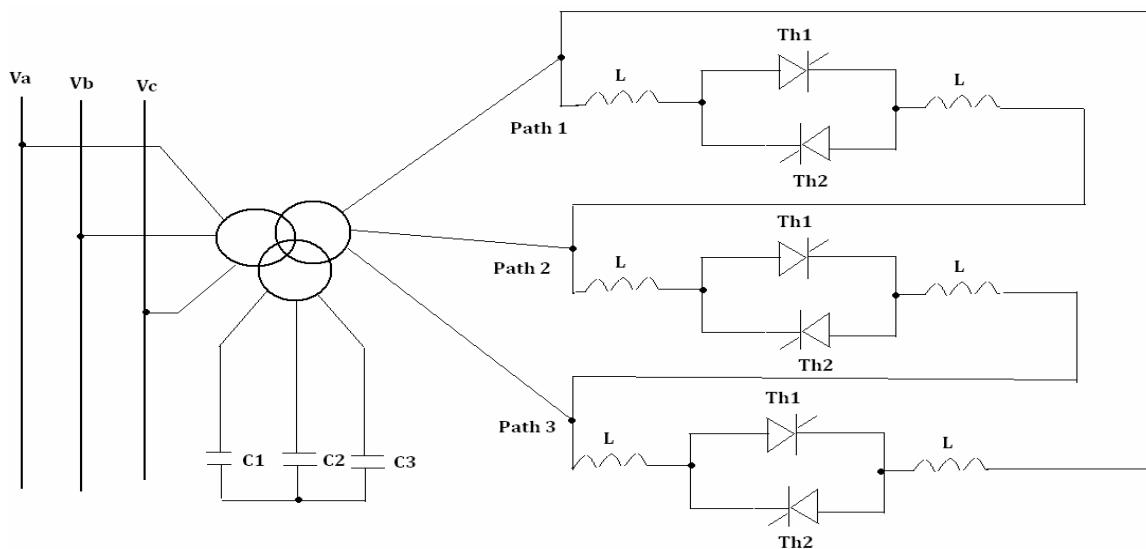


Fig. 2.3, three-phase static VAR compensator (SVC).

The compensator is normally operated to regulate the voltage of the transmission system at a selected terminal. The V-I characteristic of the SVC, shown in Figure 2.4, indicates that regulation with a given slope around the nominal voltage can be achieved in the normal operating range defined by the maximum capacitive and inductive currents of the SVC. While the maximum capacitive current reduces linearly and the produced reactive power in quadrature with the system voltage since the SVC acts as a fixed capacitor when

the maximum capacitive output is achieved. Therefore, the voltage support capability of the conventional thyristor-controlled static Var compensator speedily impairs with reducing system voltage [51].

In addition to voltage support, SVCs are also employed for transient first swing and steady state stability damping improvements. SVC behaves like an ideal mid-point compensator until the maximum capacitive admittance BC_{\max} is reached. From this point on, the power transmission curve becomes identical to that obtained with a fixed, mid-point shunt capacitor whose admittance is BC_{\max} .

The steady state stability enhancement of power oscillation damping can be achieved by changing the output of the SVC between appropriate capacitive and inductive levels to oppose the angular acceleration and deceleration of the units involved. The idea is to increase the transmitted electrical power by increasing the transmission line voltage (via capacitive vars) when the units accelerate and to reduce it by reducing the voltage (via inductive vars) when the units decelerate. The powerful of the SVC in power oscillation damping is a function of the allowed voltage variation.

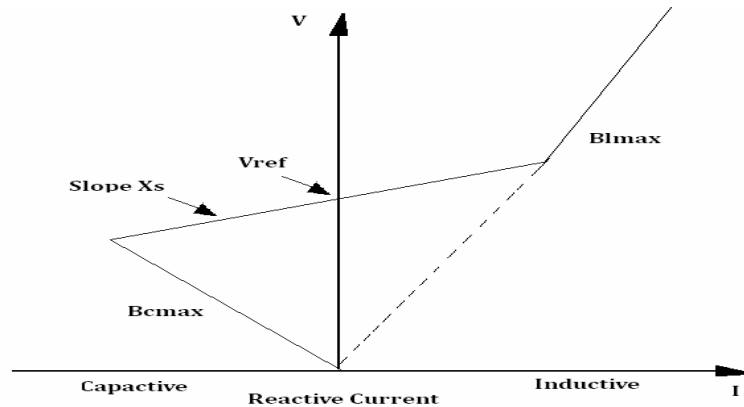


Fig. 2.4, Current V-I characteristics.

2.3.2 Thyristor Controlled Series Capacitor (TCSC)

A basic TCSC module consists of a TCR in parallel with a capacitor. An actual TCSC comprises one or more modules. Figure 2.5 shows the layout of one phase of the TCSC installed in the Slatt substation on USA. The TCSC basically comprises a capacitor bank inserted in series with the transmission line, a parallel metal oxide varistor (MOV) to protect the capacitor against over-voltage and a TCR branch, with a thyristor valve in series with a reactor, in parallel with the capacitor. Mechanically bypass breakers are provided in parallel with the capacitor bank and in parallel with the thyristor valve. During normal operation, the bypass switch is open, the bank disconnect switches (1 and 2) are closed and the circuit breaker is open. When it is required to disconnect the TCSC, the bypass circuit breaker is switched on first, and then the bypass switch is switched on. The damping circuit is used to limit the current when the capacitor is switched on or when the by pass circuit breaker is switched on.

In the fixed-capacitor thyristor-controlled reactor scheme, the degree of series compensation in the capacitive operating region and the admittance of the TCR are kept below that of the parallel connected capacitor is changed with the change in the thyristor conduction angle and also with TCR current. Minimum series compensation is achieved

when the TCR is off. The TCR may be designed to reach the capability to limit the voltage across the capacitor during faults and other system contingencies of similar effect.

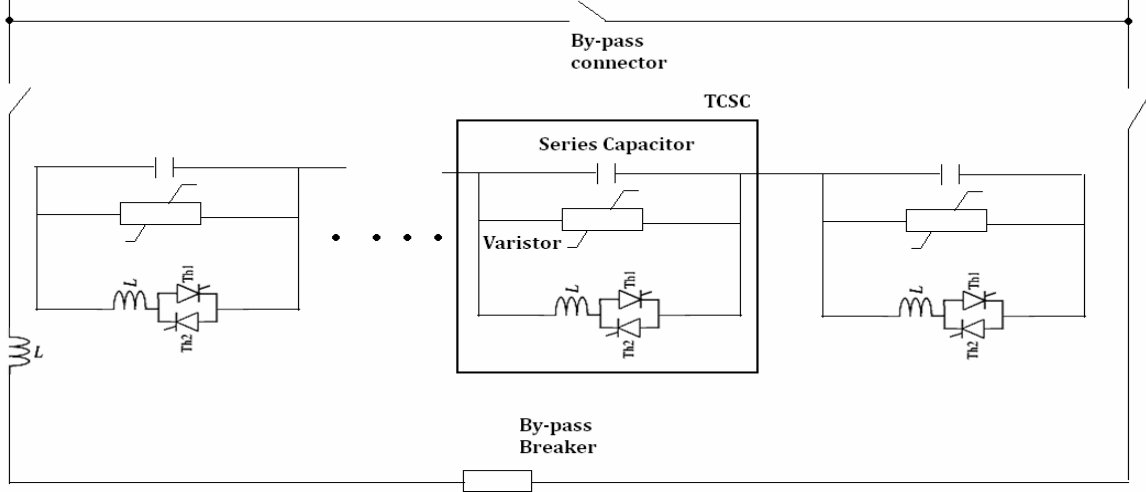


Fig. 2.5, Thyristor controlled series capacitor (TCSC).

The operating range curve of TCSC impedance against the line current is shown in Figure 2.6 [52]. The different operating limits of the TCSC can be explained as follows:

For low line current, the TCSC can provide maximum capacitive and inductive compensation according to the resonant firing angle. In the capacitive region, the minimum firing angle allowed is above the resonant firing angle (limit A). On the other hand, in the inductive region, the maximum firing angle allowed is lower than the resonant firing angle (limit E). In the capacitive region, as the line current increases, the voltage drop across the TCSC increases too. To prevent over-voltage across the TCSC during normal operation, the firing angle increases towards 180 to reduce the equivalent capacitive reactance of the TCSC, hence the voltage drop across it (limit c). In the inductive region, as the magnitude of the line current increases, the harmonic heating limit of the thyristor valves is reached. The firing angle should be reduced to reduce the equivalent inductive reactance of the TCSC so as not to exceed this limit (limit F). Limit G presents the thyristors current limits.

Figure 2.7 shows the block diagram for the TCSC operation under current control mode. The line current is measured and the magnitude of it is compared with the desired value of the line current, the error signal is passed to the TCSC controller to obtain the appropriate firing angle, which can be measured from the zero crossing of the line current. The model for balanced, fundamental frequency operation is shown in Figure 2.8 [53].

2.3.2.1 Equivalent impedance of the TCSC

Previously, attempts have been made to obtain the TCSC equivalent impedance. The overall impedance of the TCSC is given as:

$$X_{TCSC} = \frac{\pi X_C X_L}{X_C [2(\pi - \alpha) + \sin 2\alpha] - \pi X_L} \quad (2.1)$$

The problem of the last equation is that the harmonic analysis has only been conducted for the TCR while the analysis of the capacitor charging has been neglected. The total impedance has been obtained by paralleling the TCR equivalent impedance at the fundamental frequency and the fixed capacitor. This makes (2.1) only valid for the first cycle of the current. The reason is that after the first cycle has elapsed, the capacitor stores

charge, leading to higher steady state voltages compared to cases when the capacitor charging effect is neglected.

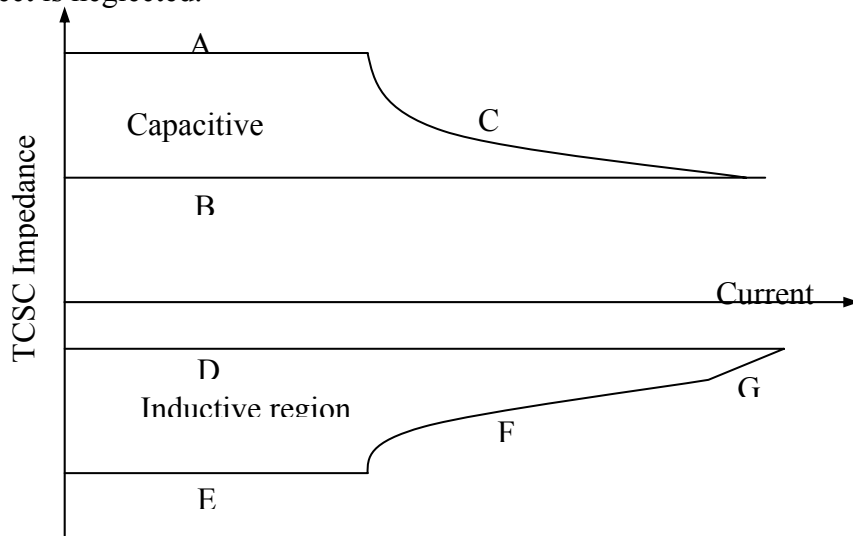


Fig. 2.6, Operating range of TCSC.

- A: Firing angle limit
- B: Thyristor blocked
- C: Maximum voltage limit
- D: Full thyristor conduction
- E: Firing angle limit
- F: Harmonic heating limit
- G: Thyristor current limit

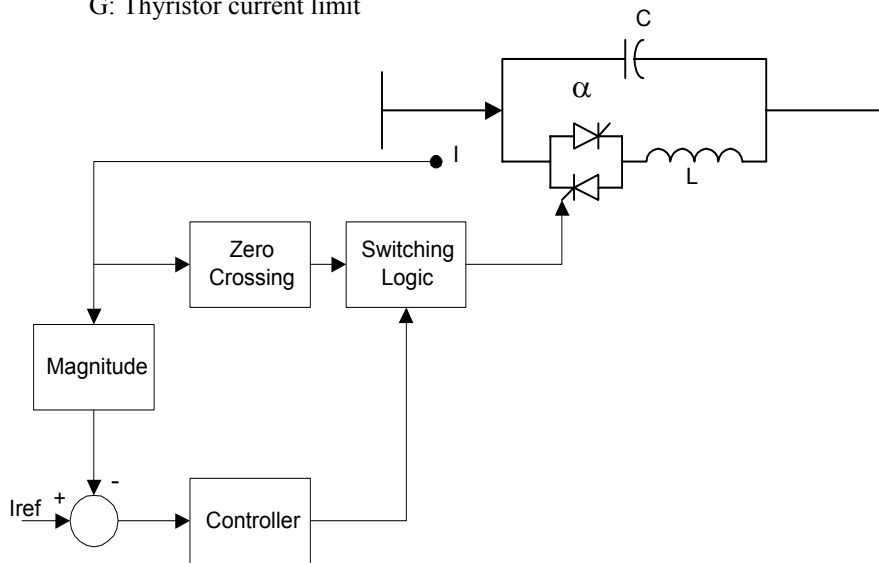


Fig. 2.7, Block diagram of a TCSC operating in current control.

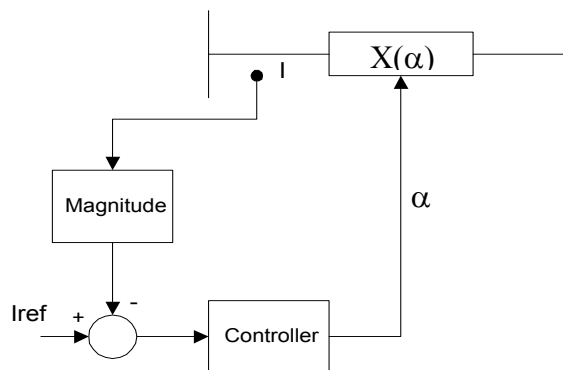


Fig. 2.8, Dynamic model of a TCSC.

The derivation of the TCSC impedance is started by examining the voltages and currents in the TCSC under the full range of operating conditions. The basic equation is:

$$Z_{TCSC(1)} = \frac{V_{TCSC(1)}}{I_{line}} \quad (2.2)$$

$V_{TCSC(1)}$ is the fundamental frequency voltage across the TCSC model, I_{line} is the fundamental frequency line current. The voltage $V_{TCSC(1)}$ is equal to the voltage across the TCSC capacitor and (2.2) can be written as:

$$Z_{TCSC(1)} = \frac{-jX_C I_{cap(1)}}{I_{line}} \quad (2.3)$$

If the external power network is represented by an idealized current source, as seen from the TCSC terminals, this current source is equal to the sum of the currents following through the TCSC capacitor and inductor. The TCSC can then be expressed as:

$$Z_{TCSC(1)} = \frac{-jX_C (I_{line} - I_{TCR(1)})}{I_{line}} \quad (2.4)$$

Substituting the expression for $I_{TCR(1)}$ (The fundamental component of the TCR current) into (2.4) and assuming $I_{line} = I_m \cos \omega t$, leads to the fundamental frequency TCSC equivalent reactance, as a function of the TCSC firing angle α as:

$$X_{TCSC} = -X_C + C_1(2(\pi - \alpha) + \sin(2(\pi - \alpha))) - C_2 \cos^2(\pi - \alpha)(\bar{\omega} \tan(\bar{\omega}(\pi - \alpha)) - \tan(\pi - \alpha)) \quad (2.5)$$

Where

$$\bar{\omega} = \frac{\omega_0}{\omega}, \quad \omega_0^2 = \frac{1}{LC}, \quad C_1 = \frac{X_C + X_{LC}}{\pi}, \quad C_2 = \frac{4X_{LC}^2}{X_L \pi},$$

$$X_{LC} = \frac{X_C X_L}{X_C - X_L}$$

Comparing Equations 2.1 and 2.5, the resonant firing angle in the two equations are not the same. Depending on the ratio between X_C and X_L , there could be more than one resonant angle for the TCSC expressed by Equation 2.5.

Figure 2.9 shows the TCSC equivalent reactances as a function of the firing angle. The TCSC capacitive and inductive reactance values should be chosen carefully in order to ensure that just one resonant point is present in the range of $\Pi/2$ to Π .

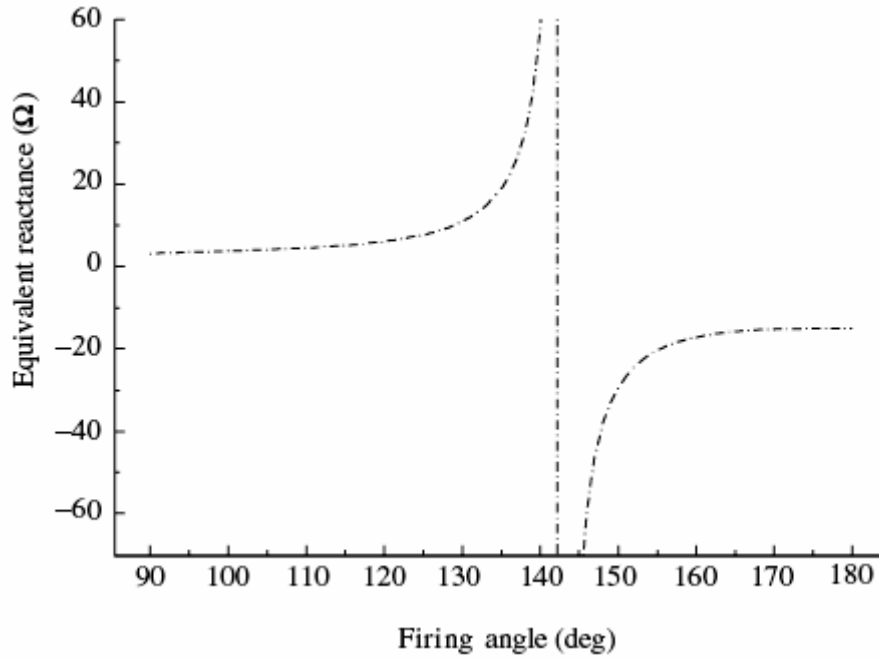


Fig. 2.9, Thyristor-controlled series capacitor (TCSC) fundamental frequency impedance.

2.3.2.2 Resonance firing angle:

Examining (2.5), the firing angle that cause resonance is obtained when

$$\cos(\pi - \alpha_{res}) \cos(\bar{\omega}(\pi - \alpha_{res})) = 0 \quad (2.6)$$

So

$$\alpha_{res} = \pi - \frac{(n+1)\pi}{2} \sqrt{\frac{X_L}{X_C}} \quad \text{where } n = 0, 2, 4, \dots \quad (2.7)$$

Although of the effective enhancement on transmittable power, high levels of series compensation are not typically used. The feasible upper boundary to the limit of series compensation is about 70 % [53], as more steady state compensation may produce uncontrollable variations in the power for low alteration in terminal voltages or angles, and large transient currents and voltages during disturbances at series resonance conditions.

2.4 Synchronous Voltage Source (SVS)

Controllable solid-state synchronous voltage sources are employed for the dynamic compensation and real-time control of the power flow in transmission systems. This method, when compared to conventional compensation approaches employing thyristor-switched capacitors and thyristor-controlled reactors, saves vastly premium performance characteristics and regular applicability for transmission voltage, impedance, and angle control. It also offers the unique potential to direct exchange real power with the AC system, in addition to the independently controllable reactive power compensation, thereby giving a powerful new option for the counteraction of dynamic disturbances.

A functional model of the solid-state synchronous voltage source is shown in Figure 2.10. Reference signals Q_{ref} and P_{ref} define the amplitude and phase angle of the generated output voltage and also the reactive and real power flow between the solid-state voltage source and the network. If the function of dynamic real power exchange is not required ($P_{\text{ref}} = 0$), the SVS becomes a self-sufficient reactive power source, like an ideal synchronous condenser, and the external energy storage device can be disposed of.

Various switching power converters can implement the solid-state synchronous voltage source, although of the switching converter mentioned as the voltage-sourced inverter. This particular DC to AC switching power converter, which is based on gate turn-off (GTO) thyristors [54] in appropriate multi-pulse circuit configurations, is presently applied in the most practical for high power utility applications. The functional and operating characteristics of this type of inverter, which saves the basic functional building block for the comprehensive compensation and power flow control approach, are explained below.

An elementary, six-pulse, voltage-sourced inverter is shown in Figure 2.11. It consists of six self-commutated semiconductor (GTO) switches, each of which is shunted by a reverse-parallel connected diode. It should be noted that in a high power inverter, each solid-state switch consists of a number of series-connected GTO thyristor/diode pairs. With a DC voltage source (which may be a charged capacitor), the inverter can produce a balanced set of three quasi-square voltage wave-forms of a given frequency, as illustrated in Figure 2.12, by connecting the DC source sequentially to the three output terminals via the appropriate inverter switches.

The reactive power exchange between the inverter and the AC system can be controlled by altering the magnitude of the three-phase output voltage generated. That is, if the amplitude of the output voltage is raised over that of the network voltage, then the current flows through the reactance from the inverter to the AC system and the inverter generates reactive (capacitive) power for the AC system. If the amplitude of the output voltage is decreased below that of the AC system, then the reactive current flows from the AC system to the inverter and the inverter absorbs reactive (inductive) power. If the output voltage is equal to the AC system voltage, the reactive power exchange is zero.

Similarly, the real power exchange between the inverter and the AC system can be controlled by phase shifting the inverter output voltage with respect to the AC system voltage. That is, the inverter from its DC energy storage supplies real power to the AC system if the inverter output voltage is made to lead the corresponding AC system voltage. This is because this phase advancement results in a real component of current through the tie reactance that is in phase opposition with the AC system voltage. For the same reason, the inverter absorbs real power from the AC system for DC energy storage, if the inverter

output voltage is made to lag the AC system voltage. The real component of current flowing through the tie reactor is now in-phase with the AC system voltage.

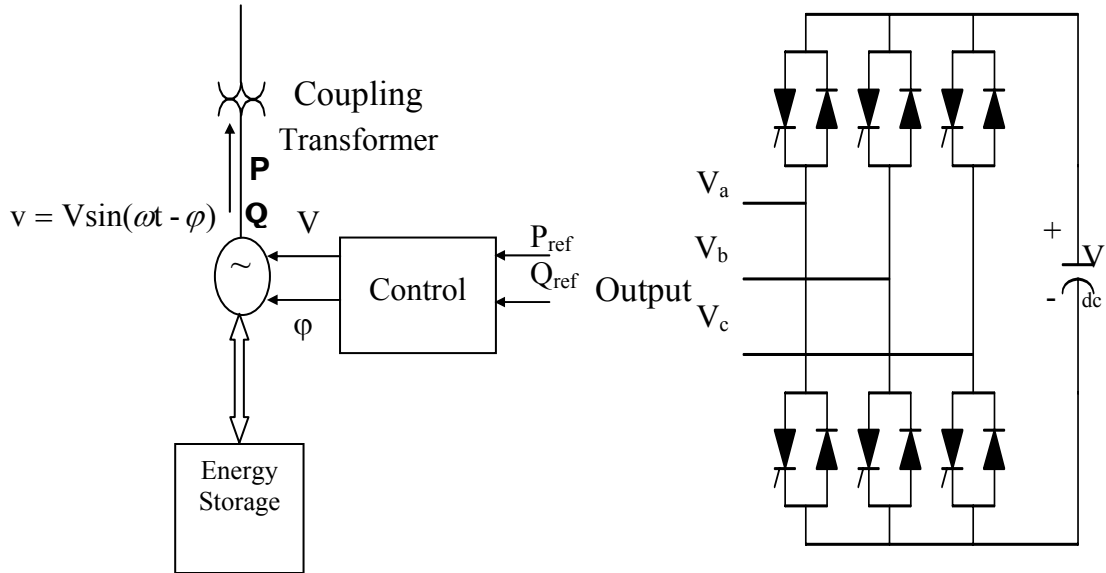


Fig. 2.10, generalized synchronous voltage source.

Fig. 2.11, Basic six-pulse voltage sourced.

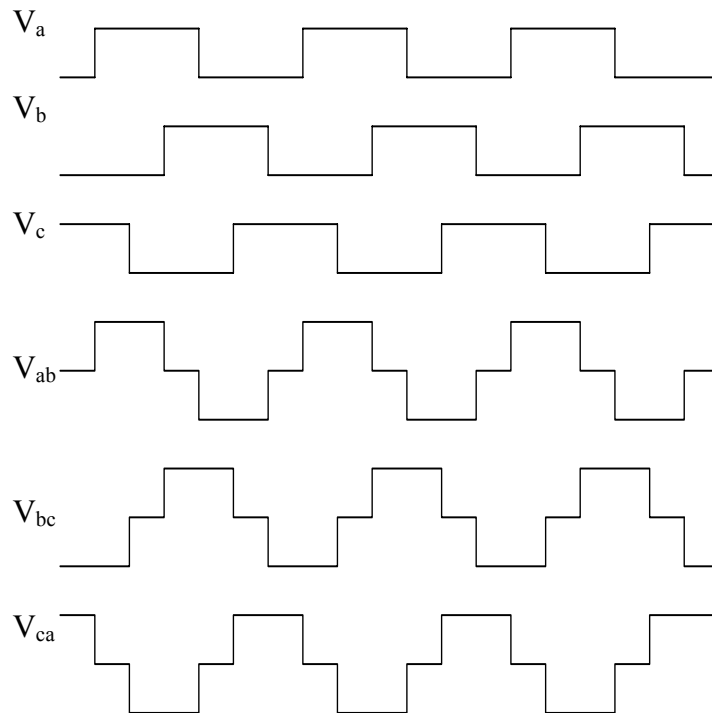


Fig. 2.12, Six pulse inverter output voltage waveforms.

The mechanism by which the inverter internally generates reactive power can be explained simply by considering the relationship between the output and input powers of the inverter. The base of the explanation depends on the physical rule that the process of energy transfer through the inverter, consisting of nothing but arrays of solid-state switches, is absolutely direct. Thus, it is clear that the net instantaneous power at the AC output terminals must always be equal to the net instantaneous power at the DC input terminals when neglecting the losses.

Assume that the inverter is operated to supply only reactive output power. In this case, the active input power provided by the DC source has to be zero. Furthermore, where reactive power, at frequency equals zero, by basics will be zero, the DC source generates no input power and therefore it clearly has no part in the supplying of the reactive output power. In another meaning, the inverter connects internally the three output terminals, like a method that the reactive output currents can flow easily between them. Considering this from the terminals of the network, it could be seen that the inverter produces an exchanged circulating power among the phases [54].

Although reactive power is inherently produced by the action of the solid-state switches, it is still essential to have a relatively small DC capacitor connected across the input terminals of the inverter. The importance for the DC capacitor is primarily requested to satisfy the above-stipulated equality of the instantaneous output and input powers. The output voltage waveform of the inverter is not a perfect sine wave. It is a staircase approximation of a sine wave. However, the multi-pulse inverter absorbs a smooth, almost sinusoidal current from the network through the tie reactance. As a result, the resultant three-phase instantaneous apparent power (VA) at the output terminals of the inverter slightly fluctuates. Thus, for not violating the balance between of the instantaneous output and input powers, the inverter must draw a ripple current from the DC capacitor that keeps a regulated terminal voltage at the input.

The existence of input ripple current components is thus basically due to the ripple components of the output voltage, which depend on the used technique in the output waveform fabrication. In a high power inverter, using a sufficiently high pulse number, the output voltage distortion and, thereby, capacitor ripple current can be mainly decreased to any desired degree. Thus, a perfect inverter would produce sinusoidal output voltage and draw pure DC input current without harmonics. To achieve purely reactive output, the input current of the perfect inverter is zero. In practice, due to system unbalance and other imperfections, as well as to economic considerations, these ideal conditions are not achieved, but approximated satisfactorily by inverters of sufficiently high pulse numbers (24 or higher) .

2.5 SVS Based FACTS Device

Among the SVS based Facts devices are the STATCOM, the SSSC and the UPFC.

2.5.1 Static Compensator (STATCOM)

The STATCOM consists of one VSC and its associated shunt-connected transformer. It is the static form of the rotating synchronous condenser but it supplies or draws reactive power with a fast rate because there is no moving parts inside it. In principle, it performs the same voltage regulation function as the SVC but in a more robust manner because, unlike the SVC, its operation is not impaired by the presence of low voltages. A schematic representation of the STATCOM and its equivalent circuit are shown in Figure 2.13.

If the energy storage is of suitable rating, the SVS can exchange both active and reactive power with the network. The active and reactive power, supplied or drawn by the SVS, can be controlled independently of each other, and any combination of active power, generated or absorbed, with active power, generated or absorbed, is possible. The active power that the SVS exchanges at its network terminals with the grid must, of course, be supplied to, or absorbed from, its DC terminals by the energy storage device. In contrast, the reactive power exchanged is internally generated by the SVS, without the DC energy storage device playing any significant part in it.

The bi-directional real power exchange capability of the SVS, that is, the ability to absorb energy from the AC system and deliver it to the DC energy storage device (large storage capacitor, battery, superconducting magnet) and to reverse this process and deliver power for the AC system from the energy storage device, makes complete, temporary system support possible. Specifically, this capability may be used to improve system efficiency and prevent power outages. In addition, in combination with fast reactive power control, dynamic active power exchange is considered as an extremely powerful method for transient and dynamic stability enhancement.

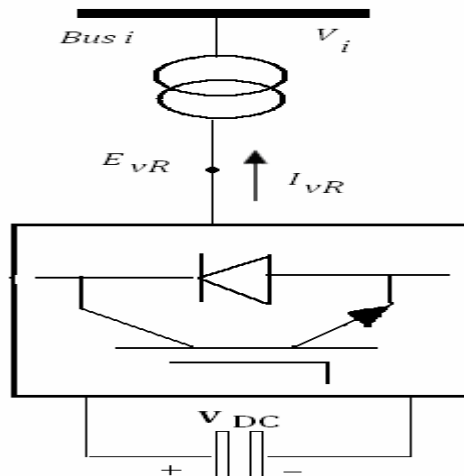


Fig. 2.13 Static compensator (STATCOM) system voltage source converter (VSC) connected to the AC network via a shunt-connected transformer.

If the SVS is used strictly for reactive shunt compensation, like a conventional static Var compensator, then the DC energy storage device can be replaced by a relatively small DC capacitor, as shown in Figure 2.13. In this case, the steady-state power exchange between the SVS and the AC system can only be reactive.

When the SVS is applied for reactive power supplying, the inverter itself can maintain the capacitor charged to the desired voltage level. This is achieved by making lagging in the output voltages of the inverter and the system voltages by a little angle. In this way, the inverter draws a small amount of active power from the grid to replenish its internal losses and keep the capacitor voltage at the required level. The same control procedure can be applied to raise or reduce the capacitor voltage, and thereby the magnitude of the output voltage of the inverter, for the purpose of controlling the reactive power generation or absorption. The DC capacitor also has a function of establishing an energy balance between the input and output during the dynamic changes of the Var output.

The V-I characteristic of the STATCOM is shown in Figure 2.14 [55]. As can be seen, the STATCOM can act as both capacitive and inductive compensators and it is able to control its output current independently over the maximum range of the capacitive or inductive of the network voltage. That is, the STATCOM can produce complete capacitive output current at any grid voltage level. On the other side, the SVC can supply only output current with reducing system voltage as calculated by its maximum equivalent capacitive admittance. The STATCOM is, therefore, superior to the SVC in providing voltage support.

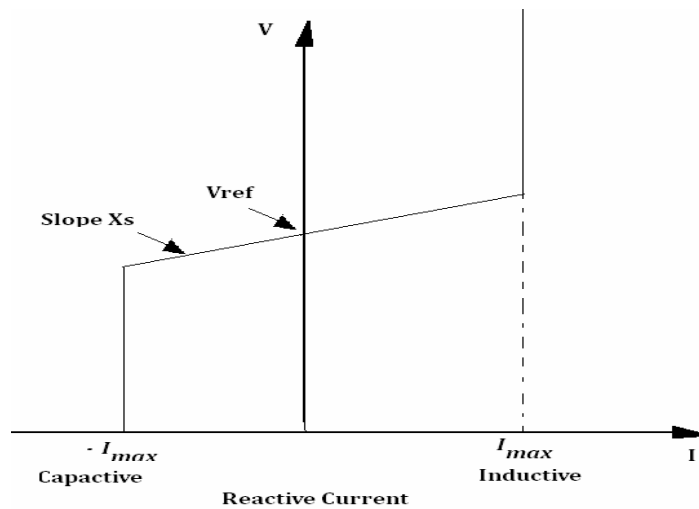


Fig. 2.14 V-I characteristic of STATCOM.

2.5.2 Static Series Synchronous Compensator (SSSC)

The Static Synchronous Series Compensator (SSSC) is a series connected FACTS controller based on VSC and can be viewed as an advanced type of controlled series compensation, just as a STATCOM is an advanced SVC.

A SSSC has several advantages over a TCSC such as (a) elimination of bulky passive components (capacitors and reactors), (b) improved technical characteristics (c) symmetric capability in both inductive and capacitive operating modes (d) the possibility of connecting an energy source on the DC side to exchange real power with the AC network.

A solid-state synchronous voltage source, consisting of a multi-pulse, voltage-sourced inverter and a DC capacitor, is shown in series with the transmission line in Figure 2.15.

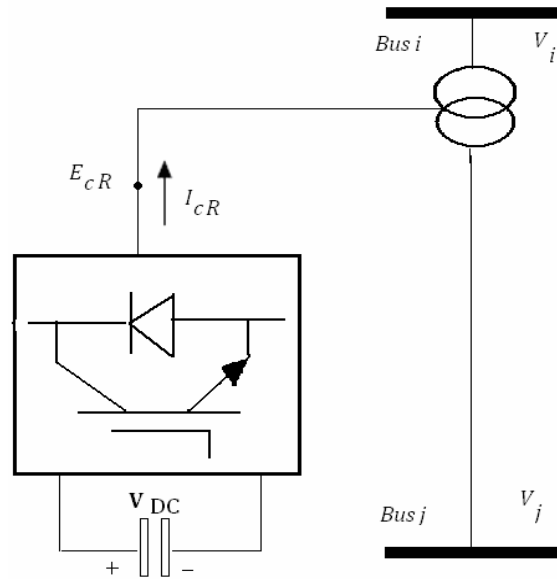


Fig. 2.15, Schematic diagram for the SSSC.

In general, the active and reactive power exchange is controlled by the phase displacement of the injected voltage with respect to the line current. For example, if the injected voltage is in phase with the line current, then only active power is exchanged, and if it is in quadrature with the line current then only reactive power is exchanged

The series-connected synchronous voltage source is an extremely powerful tool for power flow control and, it is able to control both the transmission line impedance and angle. Its capability to exchange active power with the grid makes it very effective in enhancing dynamic stability by means of alternately inserting a virtual positive and negative damping resistor in series with the line in sympathy with the angular acceleration and deceleration of the disturbed generators.

The idea of the solid-state synchronous voltage source for series reactive compensation is based on the rule that the characteristic between the impedance and the frequency of the practically employed series capacitor, which is different than the filter techniques, has no role in achieving the required line compensation. The function of the series capacitor is simply to produce an appropriate voltage at the fundamental AC system frequency in series with the line to partially cancel the voltage drop developed across the inductive line impedance by the fundamental component of the line current. So that the resulting total voltage drop of the compensated line becomes electrically equivalent to that of a shorter line. Therefore, if an AC voltage supply with fundamental frequency, which has a quadrature lagging relationship to the line current and whose magnitude is proportional to the line current is injected in series with the line, a series compensation equivalent to that supplied by a series capacitor at the fundamental frequency is provided.

Mathematically, this voltage source can be defined as follows:

$$V_n = -jkXI$$

where V_n is the injected compensating voltage phasor, I is the line current phasor, X is the series reactive line impedance, and k is the degree of series compensation. For conventional series compensation, k is defined as X_C/X , where X_C is the impedance of the series capacitor.

For regular capacitive compensation, the output voltage must lag the line current by 90 degrees, in order to directly oppose the inductive voltage drop of the line impedance. However, the inverter output voltage can be reversed by a proper control method to direct it to be leading the line current by 90 degrees. At this moment, the injected voltage is in phase with the voltage produced across the inductive line impedance and thus the series compensation has the same effect as if the reactive line impedance was raised. This capability can be invested to increase the effectiveness of power oscillation damping and, with sufficient inverter rating; it can be used for fault current limitation.

Series compensation by a synchronous voltage source that can be limited to the fundamental frequency is worthy to that provided with series capacitive compensation in that it cannot produce undesired electrical resonances with the transmission grid, and for this reason, it cannot cause sub-synchronous resonance. However, by appropriate control it can damp sub-synchronous oscillations, which may happen because of present series capacitive compensations by inserting non-fundamental voltage components with proper magnitudes, phase angles and frequencies, in addition to the fundamental component, in series with the line [55].

Due to the stipulated 90-degree phase relationship between the inverter output voltage and the line current, this, via the series insertion transformer, flows through the inverter as the load current, the inverter in the solid-state voltage source theoretically exchanges only reactive power with the AC system. As explained previously, the inverter can internally generate all the reactive power exchanged and thus can be operated from a relatively small DC storage capacitor charged to an appropriate voltage. In practice, however, the semiconductor switches of the inverter are not loss-less, and therefore the energy stored in the DC capacitor would be used up by the internal losses of the inverter. These losses can be supplied from the AC system itself by making the inverter voltage lag the line current by somewhat less than 90 degrees. The typical deviation from 90 degrees is a fraction of a degree. In this way, the inverter absorbs a small amount of real power from the AC system to replenish its internal losses and keep the DC capacitor voltage at the desired level. This control procedure can also be applied to raise or reduce the DC capacitor voltage by making the inverter voltage lag the line current by an angle smaller or greater than 90 degrees. Thereby, control the magnitude of the AC output voltage of the inverter and the degree of series compensation.

2.5.3 Unified Power Flow Controller (UPFC)

The UPFC may be considered to be constructed of two VSCs sharing a common capacitor on their DC side and a unified control system. A simplified schematic representation of the UPFC is given in Figure 2.16.

The UPFC gives simultaneous control of real and reactive power flow and voltage amplitude at the UPFC terminals. Additionally, the controller may be adjusted to govern one or more of these criteria in any combination or to control none of them. This technique allows not only the combined application of phase angle control with controllable series reactive compensations and voltage regulation, but also the real-time transition from one selected compensation mode into another one to deal with particular system contingencies more effectively. For example, series reactive compensation could be replaced by phase-angle control or vice versa. This may become essentially important when relatively large numbers of FACTS devices will be applied in interconnected power grids, and control

compatibility and coordination may have to be kept in the face of devices failures and system changes. The technique would also give considerable operating flexibility by its inherent adaptability to power system expansions and changes without any hardware alterations.

The implementation problem of the unrestricted series compensation is simply that of supplying or absorbing the real power that it exchanges with the AC system at its AC terminals, to or from the DC input sides of the inverter applied in the solid-state synchronous voltage source. The implementation in the proposed configuration called unified power flow controller (UPFC) [55] employs two voltage-sourced inverters operated from a common DC link capacitor; it is shown schematically in Figure 2.16. This arrangement is actually a practical realization of an AC to DC power converter with independently controllable input and output parameters.

Inverter 2 in the arrangement shown is used to generate voltage $V_B(t) = V_B \sin(\omega t - \delta_B)$ at the fundamental frequency with variable amplitude ($0 \leq V_B \leq V_{Bmax}$) and phase angle ($0 \leq \delta_B \leq 2\pi$), which is added to the AC system terminal voltage by the series connected coupling (or insertion) transformer. With these stipulations, the inverter output voltage injected in series with the line can be used for direct voltage control, series compensation, and phase-shift.

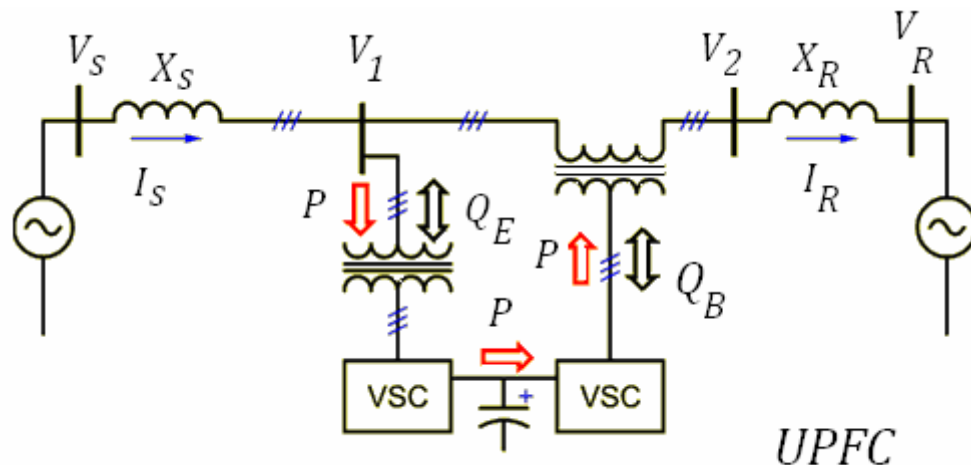


Fig. 2.16, Schematic diagram for the UPFC.

The inverter output voltage inserted in series with the line is considered mainly as an AC voltage source. The current flowing through the injected voltage source is the transmission line current; it depends on the transmitted electric power and the impedance of the transmission line. The product of the maximum injected voltage determines the VA rating of the injected voltage source of Inverter 2 and the maximum line current at which power flow control is still provided.

This total VA consists of two components: the first is the maximum active power, which is calculated by the maximum line current, and the maximum injected voltage component that is in phase with this current. The second is the maximum reactive power, which is calculated by the maximum line current and the maximum injected voltage component that is in quadrature with this current.

As explained before, the voltage-sourced inverter applied in the technique can internally supply or draw, at grid side, the amount of reactive power required by the voltage/impedance/phase-angle control applied, and only the active power amount has to be generated at its DC input terminal.

Inverter 1 (shunt connection with the power network via a coupling transformer) provides primarily the active power required to Inverter 2 at the common DC link terminal from the AC power grid. Since Inverter 1 can also supply or draw reactive power at its AC terminal, independently of the active power it transfers to (or from) the DC terminal, it follows that, with proper controls, it can also fulfill the function of an independent static condenser providing reactive power compensation for the transmission line. Thus executing an indirect voltage regulation at the input terminal of the unified power flow controller is achieved.

It is clear at the outset that Inverter 1 could be cancelled if a proper DC energy storage device was linked to Inverter 2, and the phase-shifting function of the unified power flow controller was applied only to deal with transient disturbances. That is, Inverter 2 would normally provide series reactive compensation and absorb real power at some pre-determined rate to keep the energy storage device charged. During the system disturbances, the UPFC would be controlled to provide phase angle control and/or direct active power to stabilize the network. With this arrangement, the UPFC would become a generalized solid-state series compensator discussed in the previous section.

The inherent control of the solid-state power flow controller is built so as to receive certain reference signals, in an order of designed criteria, for the required reactive shunt compensation, series compensation, transmission angle, and output voltage. These reference signals are used in closed control-loops to force the inverters to produce the AC voltages at the input (shunt-connected) terminals and output (series-connected) terminals of the power flow controller, and thereby establish the transmission parameters desired (Q_{Ref} , V_{Ref} , P_{Ref} , and φ_{Ref} at the output). The control also maintains the necessary DC link voltage and ensures smooth real power transfer between the two inverters.

It is evident that if the unified power flow controller is operated only with the phase angle reference input, it automatically acts as a perfect phase-shifter. It internally supplies the reactive power involved in the phase-shifting process and negotiates the necessary real power from the AC system. Since the active power component is generally smaller than the total VA demand resulting from phase-shifting, the rating of Inverter 1 would be normally less than that of Inverter 2, unless the “surplus” rating of Inverter 1 is, again, intentionally utilized for controllable reactive shunt compensation.

Chapter 3

Artificial Intelligence Scope

Artificial Intelligence Concept (AI)

3.1 Introduction

Soft computing (SC) is a promising new trend to build computationally intelligence systems. It is now recognized that complex real-world problems want intelligent systems that combine knowledge, techniques and methodologies from various sources. These intelligent systems are proposed to possess humanlike expertise within a specific domain, adjust themselves and learn to do better in changing environments, and explain how they make decisions or take actions. It is extremely beneficial to use several cooperatively computing techniques, resulting in the implementation of complementary hybrid intelligent systems.

This chapter introduces the concept of Artificial Intelligence especially the Genetic Algorithm (GA) and Adaptive Neuro-Fuzzy Inference System (ANFIS). Genetic algorithm is applied to the optimization process for optimal locations and optimal setting for FACTS Devices and also ANFIS to be applied in tuning the dynamics response.

3.2 Nature and Scope of AI Techniques

The intelligent Machine concept appeared in 1936, when Alan Turing proposed the concept of a universal mathematics machine, a theoretical base in the mathematical theory of computability. Turing and Emil Post showed that finding the decidability of mathematical propositions is equal to determine an abstract machine contains a package of guidelines could recognize the sort of sequences of a finite number of symbols. That procedure is related to the machine intelligence concept, assessing the arguments against the possibility of creating an intelligent computing machine and determining solutions to those disputations; in 1950, it is suggested the Turing test as an experiential measure of intelligence.

The Turing test judges the performance of a machine against that of a human being. Turing disputes that machines may be considered to be intelligent. In the 1960s, however, computers could not pass the Turing test due to the low processing speed of computers in those days.

The last few years had a novel concept of artificial intelligence (AI) concerning the principles, theoretical issues, and design methodology of algorithms simulated from the natural systems. Artificial neural networks based on neural systems, evolutionary computation based on biological natural selection, simulated annealing based on thermodynamics rules, and swarm intelligence based on the collective behavior of insects or microorganisms, and so on, interacting locally with their environment, has resulted in the emergence of coherent functional global patterns. These techniques have found their way into handling real-world problems in science, economics, technology and also to a great extent in measuring systems.

The new trend is to combine various algorithms to have advantage of integrated features and to produce a hybrid algorithm. Hybrid systems such as neuro-fuzzy systems, evolutionary-fuzzy systems, evolutionary-neural networks, evolutionary-neuro-fuzzy systems, are effectively used for handling real-world problems [56]. In the following sections, the main functional components of computational intelligence are introduced along with their key advantages and application domains.

3.2.1 Artificial Neural Networks

Artificial neural networks (ANN) have been appeared as general mathematical modules simulating biological nervous systems.

In the simple mathematical form of the neuron, the influence of the synapses are included by connection weights that regulate the influence of the corresponding input signals, and the non-linear behavior produced by neurons is presented by an activation function, which is usually the sigmoid, Gaussian-shaped, triangle-metric function, and others.

The neuron output is overall calculated as the weighted sum of the input signals, being processed by the activation function.

The learning ability of an intelligent neuron is done by adapting the weights in accordance to the selected learning method. Most applications of neural networks fall into the following categories:

- **Prediction:** to predict the output variables using input values
- **Classification:** to process the classification stage using input values
- **Data Association:** it is as classification, plus recognizing data that has errors
- **Data conceptualization:** process the inputs to group relationships can be figured out

A typical multilayered neural network and an artificial neuron are illustrated in Figure 3.1. Each neuron is distinguished by an activity level; presenting the polarization status of a neuron; an output value; presenting the firing rate of the neuron; a set of input connections; presenting synapses on the neuron and its dendrite. In addition, bias value; presenting an inherent serene level of the neuron; and finally a set of output connections; presenting a neuron's axonal projections. Each of these aspects of the unit is represented mathematically by real numbers. Thus, each connection has an associated weight (synaptic strength), which determines the effect of the incoming input on the activation level of the unit. The weights may be positive or negative. Referring to Figure 3.1, the signal flow from inputs x_1, \dots, x_n is considered to be unidirectional, indicated by arrows, as is a neuron's output signal flow (O). The neuron output signal O is given by the following relationship:

$$O = f(\text{net}) = f\left(\sum_{j=1}^n w_j x_j\right) \quad (3.1)$$

where w_j is the weight vector and the function $f(\text{net})$ is pointed to an activation transfer function.

The variable net is defined as a scalar product of the weight and input vectors

$$\text{net} = w^T x = w_1 x_1 + \dots + w_n x_n \quad (3.2)$$

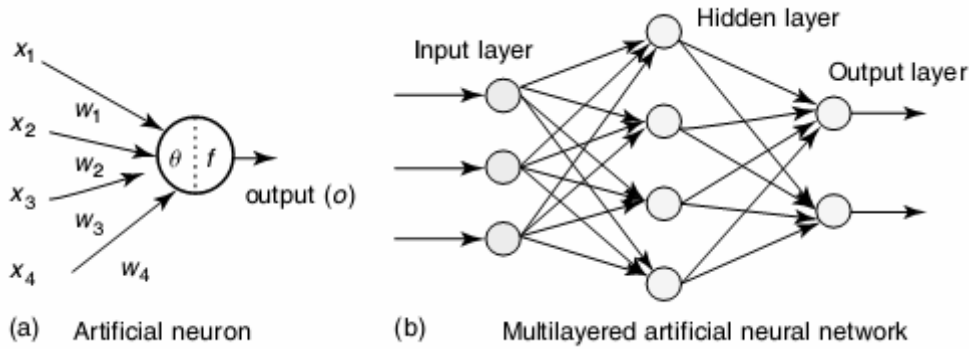


Fig. 3.1 Architecture of an artificial neuron and a multilayered neural network.

where T is the transpose of a matrix and in the simplest case the output value O is computed as

$$O = f(\text{net}) = \begin{cases} 1 & \text{if } w^T x \geq \theta \\ 0 & \text{otherwise} \end{cases} \quad (3.3)$$

where θ is called the threshold level, and this type of node is called a linear threshold unit.

The characteristic of the neural network is mainly a function of the interaction between the different neurons. The basic architecture consists of three types of neuron layers:

1. Input
2. Hidden
3. Output

In feed-forward networks, the signal flow is directed from the input to output layers, by constraint of the feed-forward direction. The data processing can be distribute over the multiple layers, but no feedback connections, that is, connections extending from the outputs of units to inputs of units in the same layer or previous layers.

Recurrent networks have feedback connections. Conflicting with feed-forward networks, the dynamical characteristics of the network are essential. In some cases, the activation values of the units yield to a relaxation process such that the network will extract a stable state in which these activations are constant evermore. In other applications, the changes of the activation values of the output neurons are important, such that the dynamical behavior constitutes the output of the network.

There are many other neural network architectures such as Elman network, adaptive resonance theory maps, competitive networks, and others, depending on the characteristics and field of the application.

A neural network has to be formatted such that the application of a set of inputs develops the required set of outputs. There are many methods to adapt the strengths of the connections. The first technique is to adapt the weights in an explicit way based on a priori knowledge. Another technique is to learn the neural network by feeding it teaching patterns and leaving it to modify its weights according to some learning rule. The learning situations in neural networks may be classified into three distinct sorts of learning:

1. Supervised
2. Unsupervised
3. Reinforcement

In supervised learning, an input vector is represented at the inputs nodes with a set of required performance, one for each node, at the output layer. A forward pass is activated and the errors or discrepancies, between the desired and real response for each node in the output layer, are determined.

These values are then used to calculate weight changes in the network according to the governing learning rule.

The original of supervised learning is due to that the required signals on individual output neurons are available by an external teacher. The famous shapes of this technique are the back propagation training, the delta rule, and perceptron rule. In unsupervised learning or self-organization, an output unit has a training to respond to clusters of pattern within the input. In this paradigm, the system is assumed to detect statistically clear characteristics of the input population. Unlike the supervised learning paradigm, there is no a priori set of categories into which the patterns are to be classified; rather, the system must produce its own organized self-map.

Reinforcement learning depends on learning the actions that should be done and the way to do the actions, by maximizing a well signal. The learner does not define the actions, as in most versions of training, but instead must detect the actions undergoing the most reward by activating them. In the most motivating and challenging situations, actions may affect not only the direct reward but also the next scene and, through that, all subsequent rewards. These two attribute trial and error option and shifted reward, are the most significant characteristics of reinforcement learning [57]-[59].

3.2.2 Fuzzy Logic Algorithm

In 1965, Zadeh presented the theory of fuzzy logic to present obscurity in linguistics and to further implement and express human knowledge and inference ability in a natural way. Fuzzy logic begins with the concept of a fuzzy set. A fuzzy set is a set without a crisp, clearly defined boundary. It can include elements with only a partial degree of membership. A Membership Function (MF) is a plot that maps each point in the input space to a membership value (or degree of membership) between 0 and 1. The input space is sometimes called as the universe of discourse.

Let X be the universe of discourse and x be an inclusive part of X . A classical set A is considered as a group of elements $x \in X$, such that each x can either belong to or not belong to the set A .

By defining a characteristic function (or membership function) on each element x in X , a classical set A can be represented by a set of ordered pairs $(x, 0)$ or $(x, 1)$, where 1 indicates membership and 0, non membership.

The fuzzy set is different from the normal set in expressing the degree to which an element belongs to a set. Hence, the feature function of a fuzzy set is permit to own a value between 0 and 1, referring to the degree of membership of an element in a certain set. If X is a group of elements pointed to generically by x , then a fuzzy set A in X is defined as a set of ordered pairs:

$$A = \{(x, \mu_A(x)) | x \in X\} \quad (3.4)$$

$\mu_A(x)$ is the membership function of the linguistic variable x in A , which directs X to the membership space M , for values between 0, 1. A is crisp and μ_A is identical to the characteristic function of a crisp set.

Triangulated-shape and trapezoidal-shape membership functions are the most simple membership functions based on straight lines. Some of the other shapes are Gaussian, generalized bell, sigmoidal, and polynomial-based curves. Figure 3.2 illustrates the shapes of two commonly used MFs. The most significant issue to know about fuzzy logical reasoning is that it is a superset of standard Boolean logic.

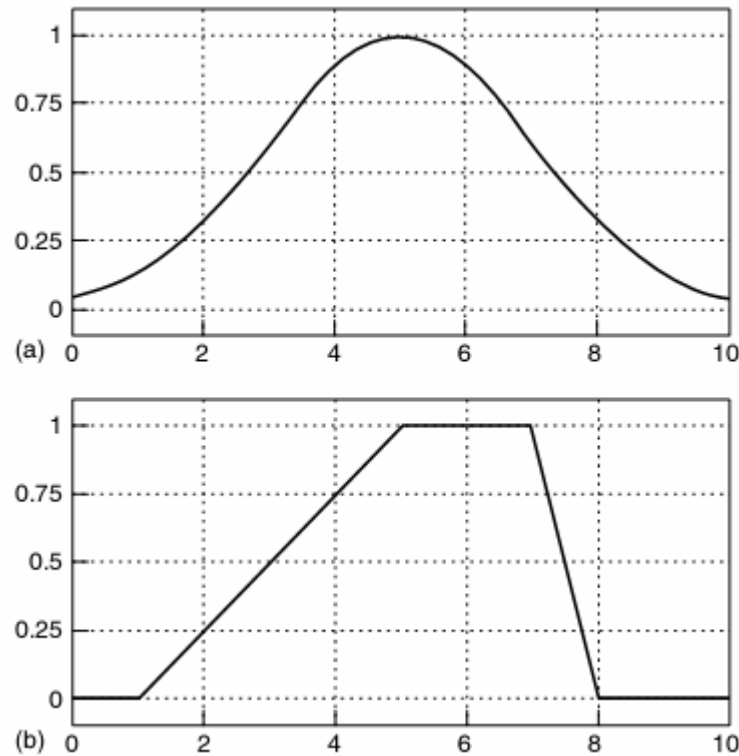


Fig. 3.2. Membership functions; (a) Gaussian and (b) trapezoidal.

3.2.2.1 Fuzzy Logic Operators

There is some coincidence between two-valued and multi-valued logic operations for the AND, OR, and NOT logical operators.

We can explain the statement A AND B , where A and B are between the range (0, 1) by using the operator minimum (A, B). By the way, we can replace the OR operation with the maximum operator, so that A OR B be equal to a maximum (A, B). Finally, the operation NOT A be equal to the operation $1-A$.

There are some terms related to fuzzy logic operators such as fuzzy intersection or conjunction for AND operation, fuzzy union or dis-junction for OR operation, and fuzzy complement for NOT operation. The intersection of two fuzzy sets A and B is generally defined, by a binary mapping T , which aggregates two membership functions as follows:

$$\mu_{A \cap B}(x) = T(\mu_A(x), \mu_B(x)) \quad (3.5)$$

The fuzzy intersection operator is usually pointed to T-norm (Triangular norm) operator. The fuzzy union operator is generally addressed by a binary mapping S .

$$\mu_{A \cup B}(x) = S(\mu_A(x), \mu_B(x)) \quad (3.6)$$

This class of fuzzy union operators is often referred to as T-conorm (S-norm) operators.

3.3.2.2 If-Then Rules and Fuzzy Inference Systems

The fuzzy rule base is featured in the formula of if-then rules in which antecedent and conclusion having linguistic variables. The fuzzy rules format the rule bases for the fuzzy logic system. Fuzzy if-then rules are often applied to achieve the imprecise states of reasoning that have an important part in the human ability to make decisions in an environment of uncertainty and imprecision. A single fuzzy if-then rule assumes the form

If x is A then y is B

where A and B are linguistic values defined by fuzzy sets in the ranges of universes of discourse, X and Y , respectively.

The “if” part of the rule ‘ x is A ’ is called the antecedent or precondition, while the “then” part of the rule ‘ y is B ’ is called the consequent or conclusion. Explaining an if-then rule has estimating the antecedent fuzzification of the input and activating any necessary fuzzy operators and then applying that result to the consequent known as implication. For rules with multiple antecedents, all parts of the antecedent are calculated simultaneously and resolved to a single value using the logical operators. Similarly, all the consequents rules with multiple consequents are affected equally by the result of the antecedent. The consequent specifies a fuzzy set be assigned to the output.

The implication function then adapts that fuzzy set to the degree defined by the antecedent. For multiple rules, the output of each rule is a fuzzy set. The output fuzzy defines for each rule are then aggregated into a single output fuzzy set. Then, the resulting set is defuzzified to a single value.

The defuzzification interface is a map for a space of fuzzy processes known with an output universe of discourse to a space of non-fuzzy processes, due to the output from the inference engine is often a fuzzy set, but in most real problems, crisp numbers are the desired. The most famous defuzzification methods are maximum criterion, center of gravity, and the mean of maximum. The maximum criterion is the simplest one to apply. It develops the state for the possible distribution for achieving a maximum value [65] – [71].

It is basically benefit if the fuzzy rule base is adjustable to a certain application. The fuzzy rule base is often installed manually or by automatic adaptation by some learning techniques using evolutionary algorithms and/or neural network learning techniques.

3.2.3 Evolutionary Algorithms

Evolutionary Algorithm (EA) is an adaptive technique, which may provide solution search and optimization problems, based on the genetic processes of biological natural. Depending on the principles of natural selection and the Charles Darwin rule of ‘survival of the fittest’, and by imitating this procedure, evolutionary algorithms are able to get solutions to real-world problems, provided they have been suitably encoded.

The genetic algorithms (GAs); evolution and evolutionary programming; and learning classifier systems are collections which belong to evolutionary algorithms or evolutionary

computation. They have the similar theoretical concept of emulating the evolution of individual structures by actions of selection, mutation, and reproduction. The processes depend on the realized characteristics of the individual construction as defined by the environment problem.

GA process parameters with finite length, which are programmed using a finite alphabet, not to manipulate the parameters in a direct way. This makes the search to be unrestricted neither by the continuity of the function under investigation nor by the existence of a derivative function.

Figure 3.3 depicts the functional block diagram of a genetic algorithm. It is supposed that an effective solution to a problem may be presented as a set of parameters. These parameters called genes are linked together to construct a string called a chromosome. A gene, also referred to as a feature, character, or detector, refers to a specific attribute that is encoded in the chromosome.

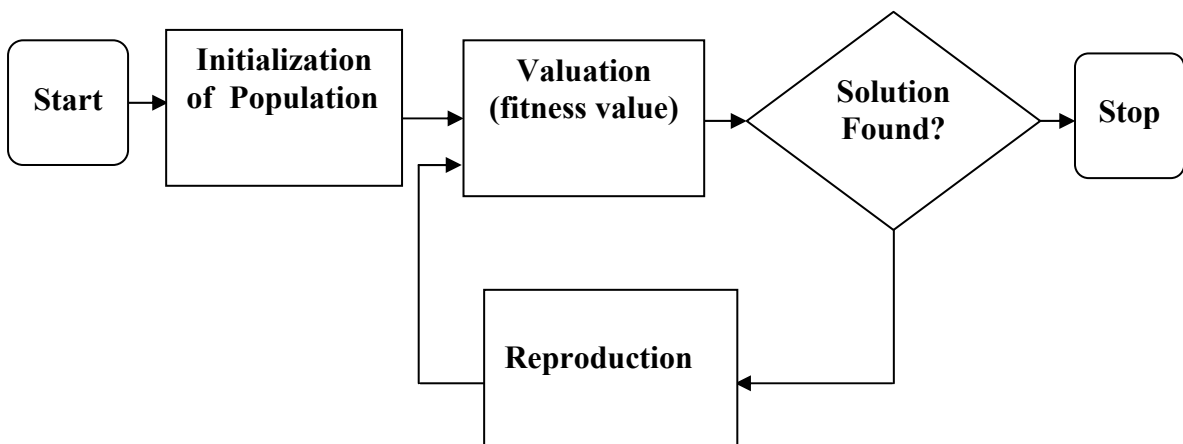


Fig. 3.3. Flowchart of genetic algorithm iteration.

The encoding process presents a solution in a chromosome and, there is no unique method solves all problems. A fitness function must be designed for each problem to be solved. For a certain single chromosome, the fitness function gives a single numerical fitness, which will determine and define the capability of the individual that the chromosome represents in the optimization process.

Reproduction is the second stage of GAs, where two individuals selected from the population are allowed to mate to develop an offspring, which will comprehend the next generation. Having selected the parents, the offsprings are generated, mainly by the procedure of crossover and mutation.

Selection is the survival of the fittest within GAs. It defines the individuals who survive to the next generation. The selection phase consists of three sections.

The first section determines the individual's fitness by the fitness function. A fitness function should be designed for the corresponding application; for a specific chromosome, the fitness function gives a single value, which is proportional to the capability, or utility, of the individual represented by that chromosome. The second stage transfers the fitness function into an expected value, and then is followed by the third and last stage where the expected value is then transferred to a discrete number of offspring.

Examples of the known applied selection techniques are the roulette wheel and stochastic universal sampling. The GA should be properly carried out, ensuring that the population

will involve sequential generations. The fitness of the best and the average individual in each generation rises toward the global optimum [61] – [63].

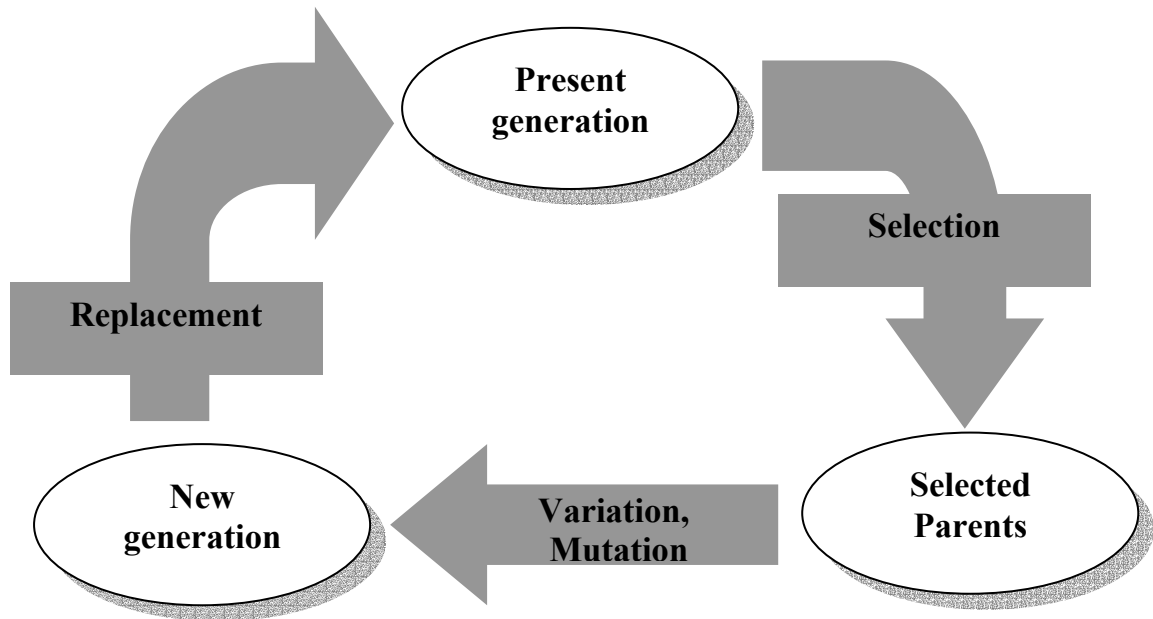


Fig. 3.4 Basic Evolution Cycle.

3.2.4 Components of GA

Major components of GA include initial population, natural selection, mating, and the mutations are explained next.

3.2.4.1 Initial Population

The genetic algorithm starts with a large commune of randomly selected chromosomes known as the initial population. A large initial population provides the genetic algorithm with a good sampling of search space; on the other hand, it increases the time of the search. Usually, not all the initial population chromosomes make the cut for the iterative portion of the genetic algorithm.

3.2.4.2 Natural Selection

A portion of the low fitness chromosomes is discarded through natural selection or survival of the fittest. Only the best members of the population are kept for each iteration of the genetic algorithm. Defining the numbers of the chromosomes to continue is mainly arbitrary. Leaving the survival of some chromosomes to the next generation controls the available genes in the offspring. Keeping too many chromosomes, on the other hand, allows bad performers a chance to contribute their traits to the next generation. 50 % of the population is often kept in the natural selection process.

3.2.4.3 Mating

Mating is the creating of one or more offspring from the parents chosen by natural selection stage. It is the first method a genetic algorithm discovers a fitness surface. The most common form of mating includes two parents that develop two offspring. A crossover point is selected between the first and last bits of the parents' chromosomes. The offspring contains portions of the binary codes of both parents.

3.2.4.4 Mutations

Random mutations change a small percentage of the bits in the last chromosomes. Mutations are the second method a genetic algorithm discovers a fitness surface. It can define attributes not in the master population and saves the genetic algorithm from converging too soon. Raising the number of mutations increases the algorithm freedom to search outside the current region of parameter space. It is also tends to divert the algorithm from converging on a solution. Typically, percentage about 1 % to 5 % of the bits mutate per iteration [76]. After mutations take place, the fitness associated with the offspring, mutated chromosomes are calculated, and the process described is iterated.

3.2.4.5 Continuous-Parameter Genetic Algorithm

When the fitness function parameters are continuous, it is logic to represent them by floating-point numbers. In addition, the binary genetic algorithm has its accuracy conditioned by the binary representation of parameters, using real number represent to the machine precision. This continuous parameter genetic algorithm owns the advantage of requesting less storage than the binary genetic algorithm. The other advantage is in the accurate representation of the continuous parameter, it follows that, representation of the fitness function is also more accurate [72] – [75]. The flow chart in Figure 3.4 provides an overview of a continuous GA.

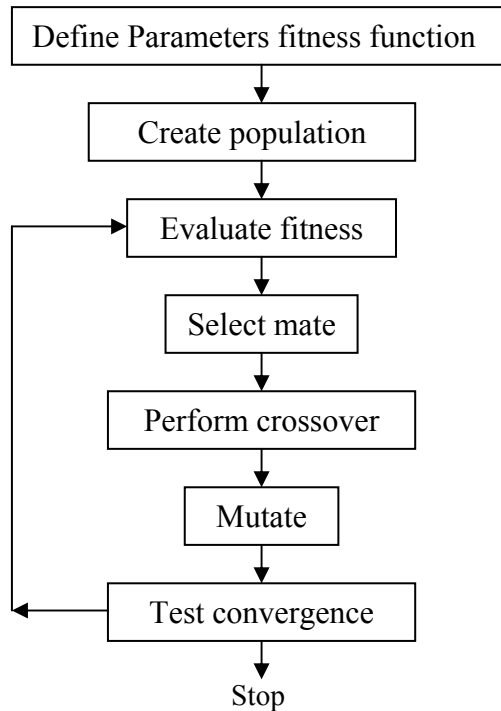


Fig. 3.5 Flow chart of a continuous GA.

The randomly selected initial population is sorted according to the fitness value. Selection is made randomly taking into consideration that the fittest individuals have the highest probability of being selected. If P_1 and P_2 are chosen to perform crossover, the resulting offspring according to the arithmetic crossover are:

$$P'_1 = r.P_1 + (1-r).P_2 \quad (3.7)$$

$$P'_2 = (1-r).P_1 + r.P_2 \quad (3.8)$$

Where r is a random number between 0 and 1.

Mutation introduces a new solution to the population for trial by producing spontaneous random change in various individuals. Non-uniform mutation is defined as follows, if an element P_k of a parent P is selected for mutation, the result would be:

$$P'_k = \begin{cases} P_k + (UB - P_k) f(gen) & \text{if a random digit is 0} \\ P_k - (LB + P_k) f(gen) & \text{if a random digit is 1} \end{cases} \quad (3.9)$$

Where UB and LB are the upper and lower bounds of the individual P_k respectively, gen is the current generation. The function $f(gen)$ should return a value in the range $[0,1]$ such that the probability of $f(gen)$ being close to 0 increases as gen increases. This insures the operator to search the space uniformly initially and very locally at later generations. The following function can be used

$$f(gen) = (r.(1 - \frac{gen}{gen\ max}))^b \quad (3.10)$$

Where r is a random number in the range $[0, 1]$, $genmax$ is the maximum number of generation, and b is called the shape parameter that determines the degree of non-uniformity.

3.3 Hybrid Intelligent Systems

Various adaptive hybrid intelligent systems have been proposed in the last decades, for model expertise, image, and video process techniques, industrial control, mechatronics, robotics, automation applications and others.

Several of these systems combine different knowledge implementation schemes, decision-making modules, and learning strategies to handle a computational application. This integration overcomes the constraints of individual techniques by hybridization various methods.

These concepts direct to the emergence of many various types of intelligent system architectures. Many of the Hybrid Intelligent Systems (HIS) contain three necessary models: artificial neural networks, fuzzy inference systems, and global optimization algorithms as evolutionary algorithms. HIS is developing those appropriate techniques together with the essential advances in other new computing methods.

Experience has indicated that it is decisive for the design of HIS to concern primarily the integration and interaction of different techniques rather than merge different methods to create techniques from scratch. Techniques already well understood should be used to solve specific domain problems within the system. Their drawback must be defined by combining them with complementary methods.

Neural networks have a clear established architecture with learning and generalization power. The generalization capability for new inputs is then based on the internal algebraic structure of the neural network. However, it is very difficult to incorporate human a priori knowledge into a neural network.

In the opposite way, fuzzy inference systems show integral characteristics, allowing a very effective framework for approximate reasoning as it tries to model the human reasoning process at a cognitive scale. Fuzzy systems acquire knowledge from domain experts and this is encoded within the algorithm in terms of the set of if-then rules. Fuzzy systems use this rule-based approach and interpolative reasoning to respond to new inputs. The incorporation and interpretation of knowledge is straightforward, whereas learning and adaptation constitute major problems.

Global optimization is the job of determining the perfectly superior set of parameters to optimize an objective function. Generally, it may be possible to have solutions that are locally optimal but not globally optimal. Evolutionary Computing (EC) is based by simulating evolution on a processing device.

These techniques could be easily applied to optimize neural networks, fuzzy inference systems, and other applications. By the supplementary attributes and strengths of different systems, the trend in the design of hybrid system is to integrate various algorithms into a more efficient integrated system to overcome their individual weaknesses.

3.3.1 Adaptive Neuro-Fuzzy Inference Systems (ANFIS)

Jang and Sun [77] introduced the adaptive Neuro-Fuzzy inference system. This system makes use of a hybrid-learning rule to optimize the fuzzy system parameters of a first order Sugeno system. The Sugeno fuzzy model (also known as TSK fuzzy model) was presented to save a systematic method to produce fuzzy rules of a certain input-output data set. Figure 3.6 shows the architecture of two inputs, two-rule first-order ANFIS Sugeno system, the system has only one output.

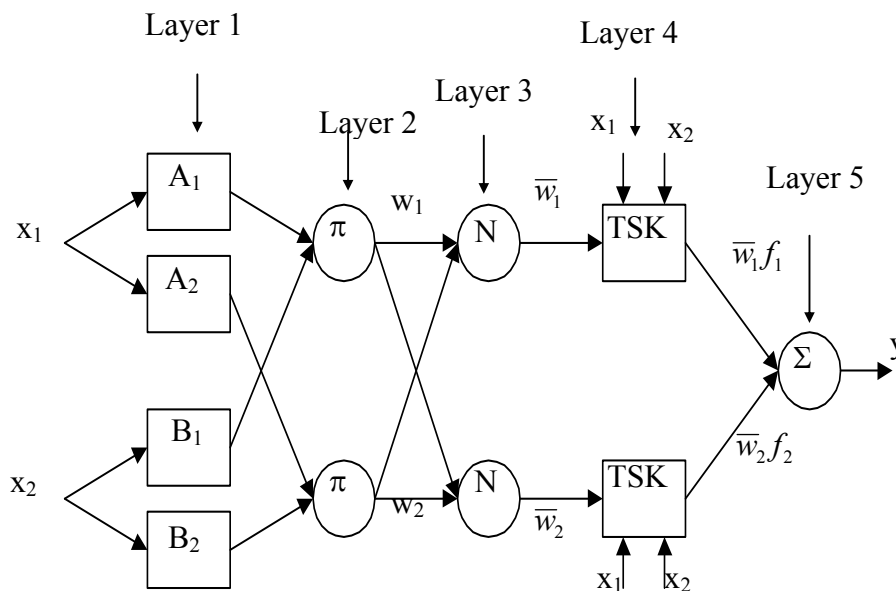


Fig. 3.6, Two input, two-rule first order Sugeno ANFIS system

The first layer of the ANFIS has adaptive nodes with each node has its function

$$O_{1,i} = \mu_A(x_1), \quad \text{for } i = 1,2 \text{ or } O_{1,i} = \mu_{B-2}(x_2), \quad \text{for } i = 3,4 \quad (3.11)$$

Where x_1 and x_2 are the inputs; and A_i and B_i are linguistic labels for the node. And $O_{1,i}$ is the membership grade of a fuzzy set A ($= A_1, A_2, B_1$ or B_2) to define the degree of applying the input to the set A .

The second layer has fixed nodes, where its output is the product of the present signals to act as the firing power of a rule.

$$O_{2,i} = w_i = \mu_A(x_1) \mu_B(x_2), \quad i = 1,2. \quad (3.12)$$

The third layer also has fixed nodes; the i th node computes the ratio of the i th rule's firing strength to the rules' firing strengths sum:

$$O_{3,i} = \bar{w}_i = \frac{w_i}{w_1 + w_2}, \quad i = 1,2. \quad (3.13)$$

The nodes of the forth layers are adaptive nodes, each with a node function

$$O_{4,i} = \bar{w}_i f_i = \bar{w}_i(p_i x_1 + q_i x_2 + r_i) \quad (3.14)$$

Where \bar{w}_i is a normalized firing strength produced by layer 3; $\{p_i, q_i, r_i\}$ is the parameter set of the node, and pointed to consequent parameters.

There is a single node in the fifth layer, which is a fixed node, which calculate the resultant output as the summation of all signals.

$$\text{Overall output} = O_{5,1} = \sum_i \bar{w}_i f_i = \frac{\sum_i w_i f_i}{\sum_i w_i} \quad (3.15)$$

3.3.2 ANFIS Hybrid Training Rule

The ANFIS architecture includes a two training parameter set

1. The antecedent membership function parameters
2. The polynomial parameters $[p, q, r]$

In [77], The ANFIS training systems applies a gradient descent algorithm to optimize the antecedent parameters and a least square algorithm to solve the consequent parameters. Due the researon that it utilizes two different algorithms to minimize the error, the training rule is reffered to as "hybrid". Firstly, The consequent parameters are updated using a least squares algorithm and the antecedent parameters are then updated by backpropagating the errors that still appear.

3.3.2.1 Training of the consequent parameters

Each output of ANFIS can be written as:

$$y_m = \bar{w}_1 f_{1m} + \dots + \bar{w}_n f_{nm} \quad (3.16)$$

Where m is the output number and n the number of the input membership functions. The function f_{nm} in terms of the consequent parameters and two inputs is:

$$f_{nm} = p_{nm}x_1 + q_{nm}x_2 + r_{nm} \quad (3.17)$$

In this case, ANFIS outputs can be rewritten as:

$$y_m = [\bar{w}_1x_1 \quad \bar{w}_1x_2 \quad \bar{w}_1 \quad \cdots \quad \bar{w}_nx_1 \quad \bar{w}_nx_2 \quad \bar{w}_n] \begin{bmatrix} p_{1m} \\ q_{1m} \\ r_{1m} \\ \vdots \\ p_{nm} \\ q_{nm} \\ r_{nm} \end{bmatrix} = XW_m \quad (3.18)$$

If X is not invertable, Pseudo inverse can be used to calculate the vector W_m , i.e.

$$W_m = (X^T X)^{-1} X^T y_m \quad (3.19)$$

3.3.2.2 Training for the antecedent parameters

Each antecedent parameter updating rule can be written as:

$$a(T+1) = a(T) - \frac{\eta_a}{k} \frac{\partial E}{\partial a} \quad (3.20)$$

Where:

a : Parameter to be updated

T : Epoch number

η_a : Learning rate

k : Number of input patterns

E : Sum of square error (SSE)

To calculate the derivatives used to update the antecedent parameters, the chain rule is used which can be written as:

$$\frac{\partial E}{\partial a_{iL}} = \frac{\partial E}{\partial y} \cdot \frac{\partial y}{\partial w_i} \cdot \frac{\partial w_i}{\partial \mu_{iL}} \cdot \frac{\partial \mu_{iL}}{\partial a_{iL}} \quad (3.21)$$

Where i is the number of the membership function of input number L and y is the sum of ANFIS outputs. The partial derivatives are derived below:

$$E = \frac{1}{2}(y - y^t) \quad \text{so} \quad \frac{\partial E}{\partial y} = y - y^t = \text{error} \quad (3.22)$$

Where y^t is the target output.

$$y = \frac{w_1}{\sum_{j=1}^n w_j} (f_{11} + \dots + f_{1m}) + \dots + \frac{w_n}{\sum_{j=1}^n w_j} (f_{n1} + \dots + f_{nm}) \quad (3.23)$$

so

$$\frac{\partial y}{\partial w_i} = \frac{\sum_{j=1}^n w_j - w_i}{\left(\sum_{j=1}^n w_j\right)^2} (f_{i1} + \dots + f_{im}) = \frac{(f_{i1} + \dots + f_{im}) - y_i}{\sum_{j=1}^n w_j} \quad (3.24)$$

$$w_i = \prod_{j=1}^S \mu_{ij} \quad \text{so} \quad \frac{\partial w_i}{\partial \mu_{iL}} = \prod_{\substack{j=1 \\ j \neq L}}^S \mu_{ij} = \frac{w_i}{\mu_{iL}} \quad (3.25)$$

Where S is the number of inputs.

The last term in Equation 3.16, $\frac{\partial \mu_{iL}}{\partial a_{iL}}$, depends on the membership function used. For example if the membership function is trapezoidal as shown in Figure 3.6, the derivatives of the membership function w.r.t. its parameters are:

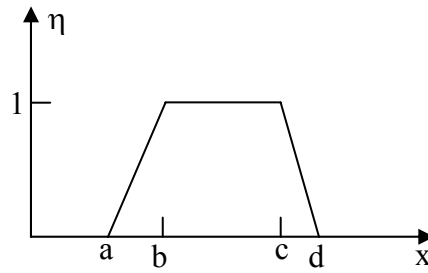


Fig. 3.7, Trapezoidal membership function

If the input pattern x lies between points a and b ,

$$\frac{\partial \eta}{\partial a} = \frac{x-b}{(b-a)^2}, \quad \frac{\partial \eta}{\partial b} = \frac{a-x}{(b-a)^2}, \quad \frac{\partial \eta}{\partial c} = 0 \quad \text{and} \quad \frac{\partial \eta}{\partial d} = 0 \quad (3.26)$$

If the input pattern x lies between points b and c ,

$$\frac{\partial \eta}{\partial a} = 0, \quad \frac{\partial \eta}{\partial b} = 0, \quad \frac{\partial \eta}{\partial c} = 0 \quad \text{and} \quad \frac{\partial \eta}{\partial d} = 0 \quad (3.27)$$

If the input pattern x lies between points c and d ,

$$\frac{\partial \eta}{\partial a} = 0, \quad \frac{\partial \eta}{\partial b} = 0, \quad \frac{\partial \eta}{\partial c} = \frac{d-x}{(d-c)^2} \quad \text{and} \quad \frac{\partial \eta}{\partial d} = \frac{x-c}{(d-c)^2} \quad (3.28)$$

and if point x is outside the range from a to d , the partial derivatives of the membership function w.r.t its parameters are equal to 0.

Chapter 4

UPFC Scope

Unified Power Flow Controller Scope

4.1 Introduction

The Unified Power Flow Controller (UPFC) is the most versatile FACTS controller for the regulation of voltage and power flow in a transmission line.

In this chapter, steady state and dynamic models of the UPFC are investigated. In steady state, the model of the UPFC may consist of two equivalent voltage sources with controlled magnitude and phase angle in series with the transformers' impedance. These sources represent the shunt and the series branches of the UPFC. Incorporation of this model in the load flow of the power system will be discussed and applied.

4.2 Power Flow UPFC Modeling

Power flow UPFC model consists of two voltage source converters (VSC), one shunt connected and the other series connected. The DC capacitors of the two converters are connected in parallel as shown in Figure 4.1. If the switches 1 and 2 are open, the two converters work as STATCOM and SSSC controlling the reactive current and reactive voltage injected in shunt and series respectively in the line. The closing of the switches 1 and 2 enables the two converters to exchange real active power flow between the two converters. The active power can be either absorbed or supplied by the series connected converter [78].

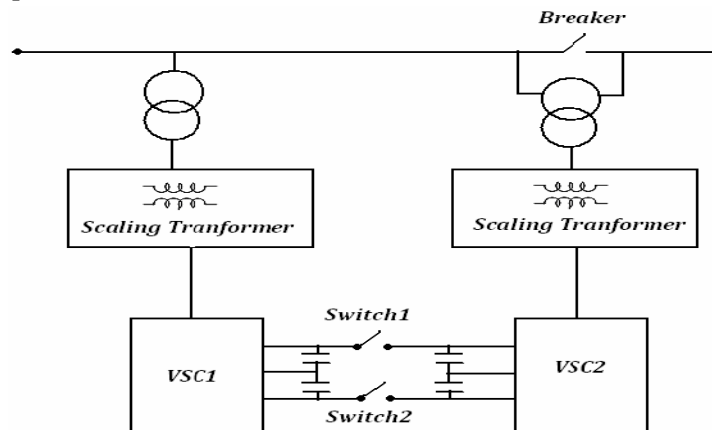


Fig. 4.1 A UPFC schematic.

The general transfer admittance matrix is obtained by applying Kirchhoff current and voltage laws to the electric circuit shown in Figure 4.2

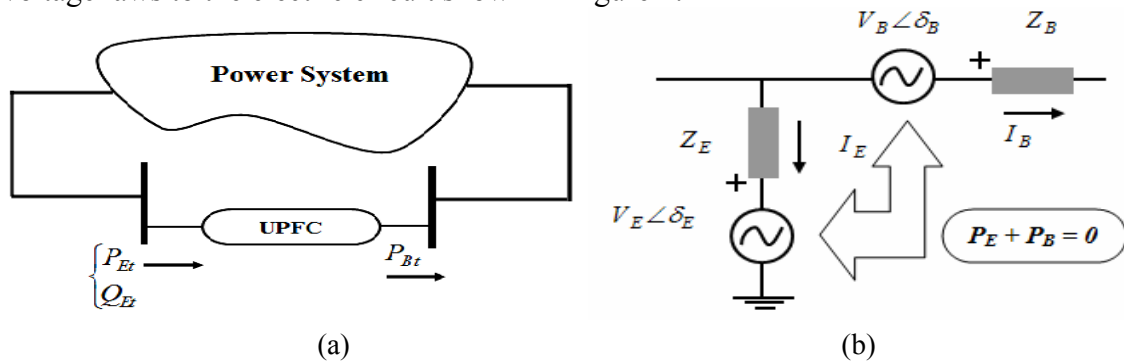


Fig. 4.2 (a) UPFC Power Flow Model (b) UPFC Single Line Diagram.

Considering the sending shunt bus k and the receiving series bus m , and writing the injected currents at m and k buses:

$$\begin{bmatrix} I_k \\ I_m \end{bmatrix} = \begin{bmatrix} y_B + y_E & -y_B & -y_B & -y_E \\ -y_B & y_B & y_B & 0 \end{bmatrix} \begin{bmatrix} V_k \\ V_m \\ V_B \\ V_E \end{bmatrix} \quad (4.1)$$

$$\Delta Y_{bus} = \begin{bmatrix} Y_{kk} & Y_{km} & Y_{kB} & Y_{kE} \\ Y_{mk} & Y_{mm} & Y_{mB} & 0 \end{bmatrix} \quad (4.2)$$

The original Y_{bus} of the system before installing the UPFC is modified to include the UPFC model by adding ΔY_{bus} to it, and in this case the number of columns of the new Y_{bus} will be increased by two corresponding to V_B and V_E [79].

Considering a lossless converter operating, the UPFC will not draw nor supply real power with respect to the network. The real power demanded by the series converter is supplied from the network by the shunt converter via the common DC link voltage. The DC link voltage, V_{dc} , must remain constant so that the stored energy in the capacitor would not be changed. Hence, the active power supplied to the shunt converter, P_E , must satisfy the real power demanded by the series converter, P_B :

$$P_E + P_B = 0.0 \quad (4.3)$$

Where

$$P_B = -\text{real}(V_B^* I_B) = -\text{real}(V_B^* (V_k - V_m - V_B) Y_{mB}) \quad (4.4)$$

$$= V_B^2 G_{mB} - V_B Y_{mB} V_k \cos(\theta_{mB} + \delta_k - \delta_B) + V_B Y_{mB} V_m \cos(\theta_{mB} + \delta_m - \delta_B) \quad (4.5)$$

$$P_E = -\text{real}(V_E^* I_E) = -\text{real}(V_E^* (V_k - V_E) (-Y_{kE}))$$

$$= -V_E^2 G_{kE} + V_E Y_{kE} V_k \cos(\theta_{kE} + \delta_k - \delta_E) \quad (4.6)$$

$$P_B + P_E = V_B^2 G_{mB} - V_E^2 G_{kE} - V_B Y_{mB} V_k \cos(\theta_{mB} + \delta_k - \delta_B) \\ + V_B Y_{mB} V_m \cos(\theta_{mB} + \delta_m - \delta_B) + V_E Y_{kE} V_k \cos(\theta_{kE} + \delta_k - \delta_E)$$

The UPFC linearized power equations are combined with the linearized system equations corresponding to the rest of the network

$$[\Delta f(x)] = [J][\Delta x] \quad (4.7)$$

Where $[\Delta f(x)] = [\Delta P_k \Delta P_m \Delta Q_k \Delta Q_m \Delta P_{mk} \Delta Q_{mk} \Delta(P_B + P_E)]'$, $[\Delta x]$ is the solution and $[J]$ is the Jacobian matrix.

If both nodes k and m are PQ type and the UPFC is controlling active power, flowing from m to k , and reactive power injected at node m , the solution vector and the Jacobian matrix are defined as shown in Equation (4.8). Assuming the power controlled mentioned above and that the UPFC controls voltage magnitude at the AC system shunt converter terminal (node k), the solution vector and the Jacobian matrix are shown in Equation (4.9).

where

$$S_{mk}^* = V_m^* I_{mk}^* = V_m^* (V_m + V_B - V_k) Y_{mB} \quad (4.10)$$

$$P_{mk} = V_m^2 G_{mB} + V_m Y_{mB} V_B \cos(\theta_{mB} + \delta_B - \delta_m) - V_m Y_{mB} V_k \cos(\theta_{mB} + \delta_k - \delta_m) \quad (4.11)$$

$$Q_{mk} = -V_m^2 B_{mB} - V_m Y_{mB} V_B \sin(\theta_{mB} + \delta_B - \delta_m) + V_m Y_{mB} V_k \sin(\theta_{mB} + \delta_k - \delta_m) \quad (4.12)$$

4.3 Effective Initialization of UPFC Controllers

The modeling of UPFC controllers for application in power flow analysis results in highly nonlinear equations, which should be suitably initialized to ensure quadratic convergent solutions when using the Newton–Raphson method. This section concerns such as issue and makes well-grounded recommendations for the use of simple and effective initialization procedures for all FACTS models in power flow and related studies.

4.3.1 Controllers Represented by Shunt Synchronous Voltage Sources

Extensive application of FACTS devices represented by shunt voltage sources shows that elements such as the STATCOM, the shunt source of the UPFC, and the two-shunt sources representing the HVDC-VSC are suitably initialized by choosing 1 p.u. voltage magnitudes and 0 phase angles.

4.3.2 Controllers Represented by Series Synchronous Voltage Sources

Suitable initialization of series voltage sources in load flow analysis is obligatory to guarantee robust solutions. Examples of FACTS devices that use one or more series voltage sources are the static synchronous series compensator (SSSC) and unified power flow controller (UPFC).

Different equations exist for the purpose of initializing the series voltage source, depending on the operating condition exhibited by the controller. For example, for the case when active and reactive powers are specified at bus k , and assuming

$V_k = V_m = 1$ p.u., and $\theta_k = \theta_m = 0$, leads to the following simple expressions:

$$V_B = V_{cR} = X_B (P_{\text{specified}}^2 + Q_{\text{specified}}^2)^{1/2} \quad (4.13)$$

$$\theta_E = \theta_{cR} = \arctan \left(\frac{P_{\text{specified}}}{Q_{\text{specified}}} \right) \quad (4.14)$$

These equations are used to initialize the parameters of series voltage sources within the Newton–Raphson power flow solution.

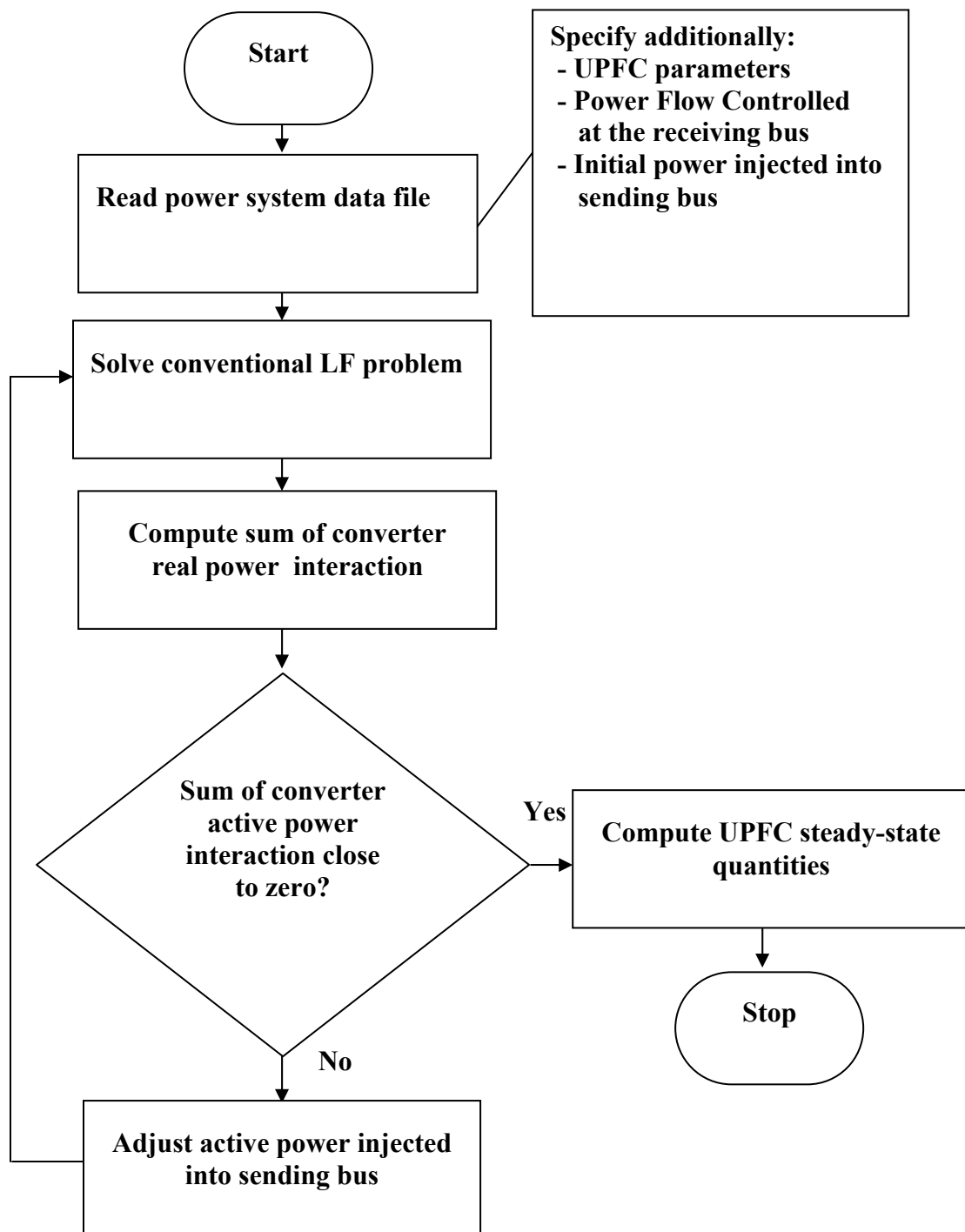


Fig. 4.3, General Load Flow Algorithm with UPFC.

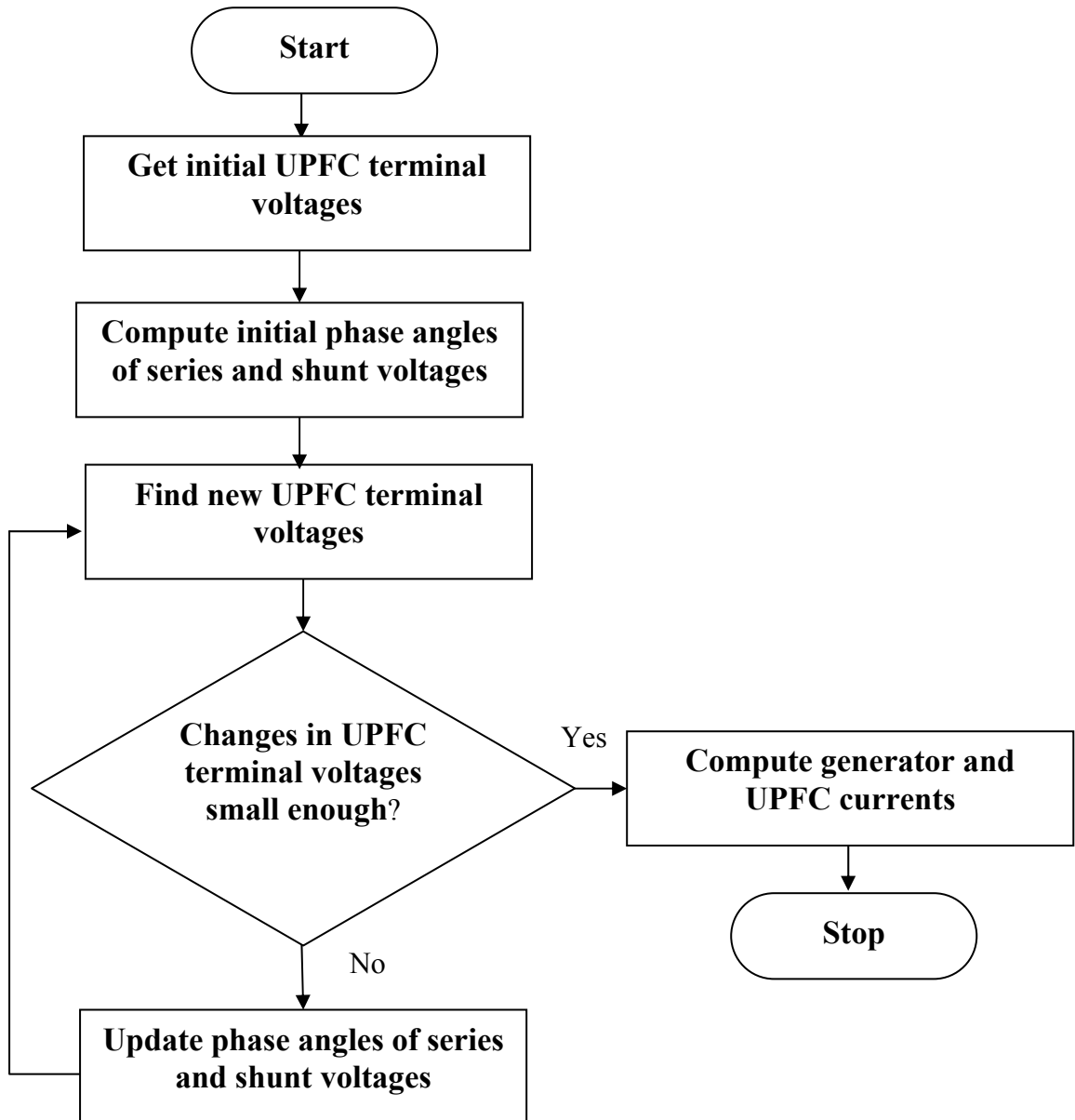


Fig. 4.4, Algorithm for Updating UPFC parameters.

4.4 Dynamic Modeling of UPFC

Figure 4.5 shows the schematic diagram of the UPFC. The two converters in the figure have the same construction except for the variation in their rated values. The magnitude and phase angle of the network output voltages of the two converters can be updated according to the operating requests of the system [80].

Therefore, there are four control inputs : m_E , m_B and δ_E , δ_B , that are the amplitude modulation ratio and phase angle of the control signal of each VSC, as shown in Figure 4.5. In a practical system, the power flow of the transmission line, the voltage of the controlled bus, and the voltage on the DC link capacitor of the device itself can be controlled by regulating these four control variables.

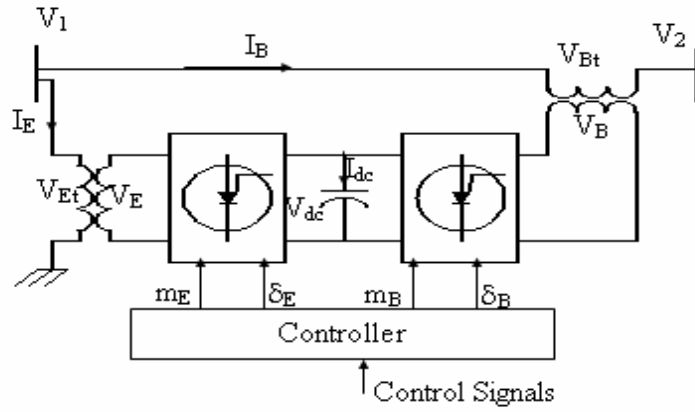


Fig. 4.5, Schematic diagram of the power circuit of a UPFC.

An equivalent UPFC model, which is based on the Pulse Width Modulation (PWM) approach, is shown in Figure 4.6.

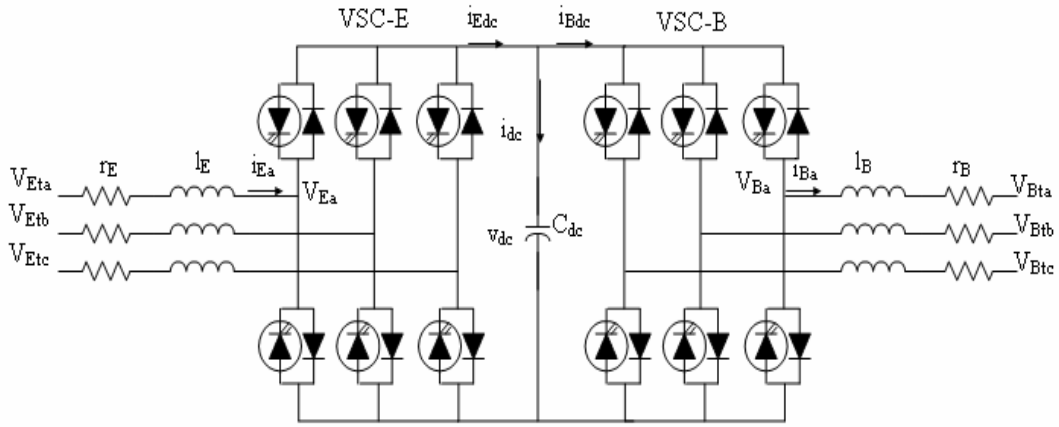


Fig. 4.6, Equivalent UPFC Model.

The three-phase dynamic differential equations of the UPFC are:

$$\begin{bmatrix} \frac{di_{Ea}}{dt} \\ \frac{di_{Eb}}{dt} \\ \frac{di_{Ec}}{dt} \end{bmatrix} = \begin{bmatrix} -\frac{r_E}{l_E} & 0 & 0 \\ 0 & -\frac{r_E}{l_E} & 0 \\ 0 & 0 & -\frac{r_E}{l_E} \end{bmatrix} \begin{bmatrix} i_{Ea} \\ i_{Eb} \\ i_{Ec} \end{bmatrix} + \begin{bmatrix} \frac{1}{l_E} & 0 & 0 \\ 0 & \frac{1}{l_E} & 0 \\ 0 & 0 & \frac{1}{l_E} \end{bmatrix} \begin{bmatrix} v_{Eta} \\ v_{Etb} \\ v_{Etc} \end{bmatrix} - \begin{bmatrix} \frac{1}{l_E} & 0 & 0 \\ 0 & \frac{1}{l_E} & 0 \\ 0 & 0 & \frac{1}{l_E} \end{bmatrix} \begin{bmatrix} v_{Ea} \\ v_{Eb} \\ v_{Ec} \end{bmatrix} \quad (4.15)$$

$$\begin{bmatrix} \frac{di_{Ba}}{dt} \\ \frac{di_{Bb}}{dt} \\ \frac{di_{Bc}}{dt} \end{bmatrix} = \begin{bmatrix} -\frac{r_B}{l_B} & 0 & 0 \\ 0 & -\frac{r_B}{l_B} & 0 \\ 0 & 0 & -\frac{r_B}{l_B} \end{bmatrix} \begin{bmatrix} i_{Ba} \\ i_{Bb} \\ i_{Bc} \end{bmatrix} + \begin{bmatrix} \frac{1}{l_B} & 0 & 0 \\ 0 & \frac{1}{l_B} & 0 \\ 0 & 0 & \frac{1}{l_B} \end{bmatrix} \begin{bmatrix} v_{Bta} \\ v_{Btb} \\ v_{Btc} \end{bmatrix} - \begin{bmatrix} \frac{1}{l_B} & 0 & 0 \\ 0 & \frac{1}{l_B} & 0 \\ 0 & 0 & \frac{1}{l_B} \end{bmatrix} \begin{bmatrix} v_{Ba} \\ v_{Bb} \\ v_{Bc} \end{bmatrix} \quad (4.16)$$

Where V_E , V_B and V_{dc} are given by:

$$\begin{bmatrix} v_{Ea} \\ v_{Eb} \\ v_{Ec} \end{bmatrix} = \frac{\sqrt{2}m_E v_{dc}}{2} \begin{bmatrix} \cos(\omega t + \delta_E) \\ \cos(\omega t + \delta_E - 120^\circ) \\ \cos(\omega t + \delta_E + 120^\circ) \end{bmatrix} \quad (4.17)$$

$$\begin{bmatrix} v_{Ba} \\ v_{Bb} \\ v_{Bc} \end{bmatrix} = \frac{\sqrt{2}m_B v_{dc}}{2} \begin{bmatrix} \cos(\omega t + \delta_B) \\ \cos(\omega t + \delta_B - 120^\circ) \\ \cos(\omega t + \delta_B + 120^\circ) \end{bmatrix} \quad (4.18)$$

V_E and V_B can be written as phasor quantities:

$$V_E = \frac{m_E v_{dc}}{2} \angle \delta_E \quad (4.19)$$

$$V_B = \frac{m_B v_{dc}}{2} \angle \delta_B \quad (4.20)$$

$$\begin{aligned} \frac{dv_{dc}}{dt} = & \frac{m_E}{2C_{dc}} [\cos(\omega t + \delta_E) i_{Ea} + \cos(\omega t + \delta_E - 120^\circ) i_{Eb} + \cos(\omega t + \delta_E + 120^\circ) i_{Ec}] \\ & + \frac{m_B}{2C_{dc}} [\cos(\omega t + \delta_B) i_{Ba} + \cos(\omega t + \delta_B - 120^\circ) i_{Bb} + \cos(\omega t + \delta_B + 120^\circ) i_{Bc}] \end{aligned} \quad (4.21)$$

4.5 Control of UPFC

As the UPFC consists of two converters that are coupled on the DC side, the control of each converter is taken up individually.

4.5.1 Control of the Shunt Converter

The shunt converter absorbs a controlled current from the system. A component of this current is I_p , which is automatically calculated by the requirement to balance the active power supplied to the series converter through the DC link. This power balance is commanded by regulating the DC capacitor voltage by feedback control [81].

Another component of the shunt converter current is the reactive current, I_r that can be controlled with the same method as in a STATCOM.

There are two operating control modes for a STATCOM or the shunt converter. These are,

1. VAR control mode where the reactive current reference is calculated by the inductive or capacitive VAR order. The feedback signals are addressed from current transformers (CT), which positioned at the coupling step-down transformer.

2. Automatic voltage control mode where the reactive current reference is calculated by the output of the feedback voltage controller, which has a droop characteristic as in the case of a SVC or a STATCOM. The voltage feedback signals are available from potential transformers (PT), which measure the voltage V_l at the substation feeding the coupling transformer.

The block diagram of the shunt converter controller is shown in Figure 4.7.

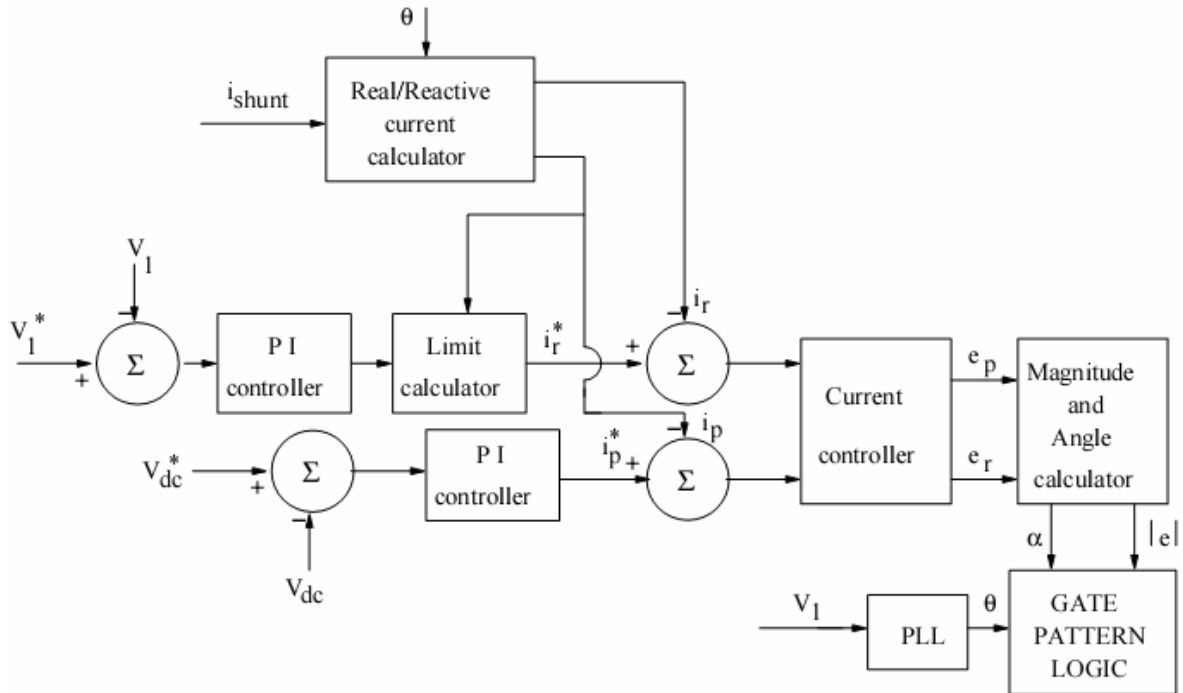


Fig. 4.7, Block diagram of shunt controller.

4.5.2 Control of the Series Converter

The series converter control concerns with injecting a series voltage of the desired magnitude and angle. These are different control modes for the series voltage mentioned next.

1. Direct voltage injection mode where the converter mainly provides a voltage phasor in response to the reference input. A special case happens when the required voltage is a reactive voltage in quadrature with the line current.
2. Phase Angle Shifter Emulation mode where the injected voltage \hat{V}_c is phase shifted with respect to the voltage V_l by an angle determined by the reference input.
3. Line impedance emulation mode where the series injected voltage is controlled in proportion to the line current. The complex impedance, which is calculated by the injected voltage divided by the line current, is determined by the reference inputs. It is necessary to consider in applying this control mode, to prevent instability or resonance. For example, negative values of the resistance can lead to instability. A large value of the capacitive (negative) reactance can make resonance case leading to very high current.

4. Automatic power flow control mode where the reference inputs determine the desired active power (P) and the reactive power (Q) at a given location in the line. Both P and Q can be controlled independently of each other in a feasible area determined by the achieving of different constraints.

In this control mode, the series injected voltage is calculated by a vector control system to guarantee the flow of the required current phasor, which is kept even during system disturbances, unless the system control governs the modulation of the power and reactive power. Although the normal conditions govern the regulation of the complex power flow in the line, the contingency conditions want the controller to enhance the system stability by damping power oscillations.

The feedback signals for the series converter control come from CT and PTs where the line current and the voltages at the two ports of the UPFC are measured. The block diagram of the series converter control is shown in Figure 4.8.

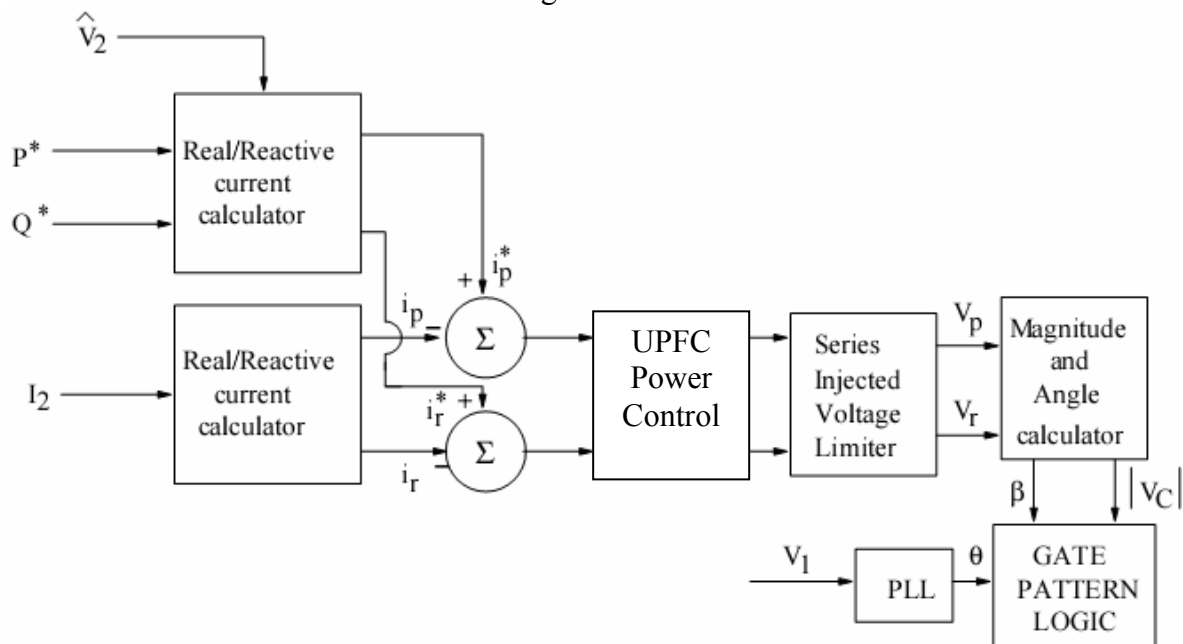


Fig. 4.8, Block diagram of series controller.

Chapter 5

Proposed Techniques

Proposed Techniques

5.1 Introduction

Unified Power Flow Controller (UPFC) was proposed as a family member of Flexible AC Transmission Systems (FACTS). This is a multiple functional FACTS controller with primary duty to control the power flow of the system. The secondary function of the UPFC can be voltage control, transient stability improvement, oscillation damping to enhance the dynamic stability of the system.

The applied proposed technique will be used to solve real problems in the power systems especially in a real Finnish network.

The optimal locations and the optimal settings will be detected using the AI concepts to reach the best performance area during the normal and the contingency operations of the network to solve the reliability issues in the line outage cases to improve the grid performance by finding the optimal locations and the settings for UPFC installation.

The criteria for the optimality will depend on some fitness functions, these fitness functions will involve in the indices terms to include the network buses voltage profile and how to reduce the voltage violations of the network, also the network line loading and how to reduce the lines overloading related to the network lines rate. UPFC has the ability to do both of SVC and SSSC performance simultaneously, and all of these UPFC modes will be applied and investigated.

The effect of UPFC, in enhancing the dynamics performance of the system and in improving the oscillations damping of the system will be discussed. The link between the steady state and the dynamic analysis can be achieved by considering the results from the steady state coupled with the dynamic response analysis. Dynamic controller based modern control theory with damping effect will be designed to insure good damping under various operating conditions and disturbances.

5.2 Proposed Technique for Optimal Location and Optimal Setting

The UPFC installation scenario in the power network will be at the following phases:

- Normal operation (Base load pattern) with normal configuration
- Normal operation with load growth pattern (Load growth coefficients for the year 2020) with normal configuration
- Contingency analysis with elements outage (Base load and load growth)

At each phase, the installation of UPFC will be in the optimal locations and with optimal setting of parameters, which will be achieved according to the following procedure.

5.2.1 Problem Formulation

The normal operation of the power network depends on many factors as the loading conditions, the configuration of the system and the current operating point of the system. All the previous factors affect the stability of the system and the trajectory of the system performance. A contingency can be considered to be the outage of a generator, a transformer or a line. The system may become unstable and enter an insecure state when a contingency event has occurred.

Contingency analysis is one of the most important functions performed in power systems to establish appropriate preventive and/or corrective actions for each contingency. Some indices will be proposed to indicate the overloaded lines and the bus voltage violations, and then ranking of the severest contingencies cases will be performed. For each line outage contingency in the system, we tabulate the all overloaded lines and the buses that have voltage violations, and then the lines are ranked with respect to the severity of the contingency, in another meaning, according to the total resultant number of the thermal and voltage violations limits. Then the most critical contingencies are calculated. After determining the most critical contingencies scenarios, the GA technique is applied to find the optimal location and parameters setting of UPFC. Optimal installation of UPFC with these locations and parameters will prevent or reduce the overloaded lines and the bus voltage violations to the minimum limit under these critical contingencies according to the proposed fitness function.

5.2.2. GA Fitness Functions

The task is concerned with finding the optimal location and the optimal parameter settings of the UPFC in the power network to eliminate or minimize the overloaded lines and the bus voltage violations.

The main general description of the equations is:

$$\text{Min Fitness } F_t(X,U) \quad (5.1)$$

Subject to:

$$G_t(X,U) = 0.0 \quad (5.2)$$

$$H_t(X,U) \leq 0.0 \quad (5.3)$$

Where

$F_t(X,U)$ represents the fitness function to be minimized;

$G_t(X,U)$ represents the vector of the equality constraints corresponding to active and reactive power balance equations;

$H_t(X,U)$ represents the vector of the inequality constraints corresponding to UPFC parameter bounds limits, active and reactive power generation limits, bus voltage limits, and phase angles limits;

X represents the vector of the state of the power system consisting of voltage magnitude and phase angles; and

U represents the vector of control variables to be optimized which the output of the process, the location of UPFC and its parameters setting.

The fitness function will depend on some performance indices, the fitness function and the performance index will be changed according the scope zone of interest as following:

- I) Optimizing with the bus voltage violations (No overloaded lines or out of interest zone):

$$F_t(X,U) = \sum_{i=1}^{nbb: no. of buses} V(BV) \quad (5.4)$$

$$V(BV) = \begin{cases} 0 & ,if \quad 0.95 \leq V_i \leq 1.05 \\ \log \left(\Psi_{V(BV)} * abs \left(\frac{V_{i nominal} - V_i}{V_{i nominal}} \right)^Q \right) & ,otherwise \end{cases} \quad (5.5)$$

Where

$V(BV)$ represents the Bus Voltage Violation function;

V_i represents the voltage magnitude at bus i ;

$V_{i nominal}$ represents the bus i nominal voltage;

$\Psi_{V(BV)}$ represents the weights and is determined in order to have certain index value for various percentage of voltage difference, also used to adjust the slope of the logarithm.

Q represent the integer coefficient is used to penalize more or less voltage variations, it may be varied as 1, 2, 3,

nbb represent the number of the buses in the system.

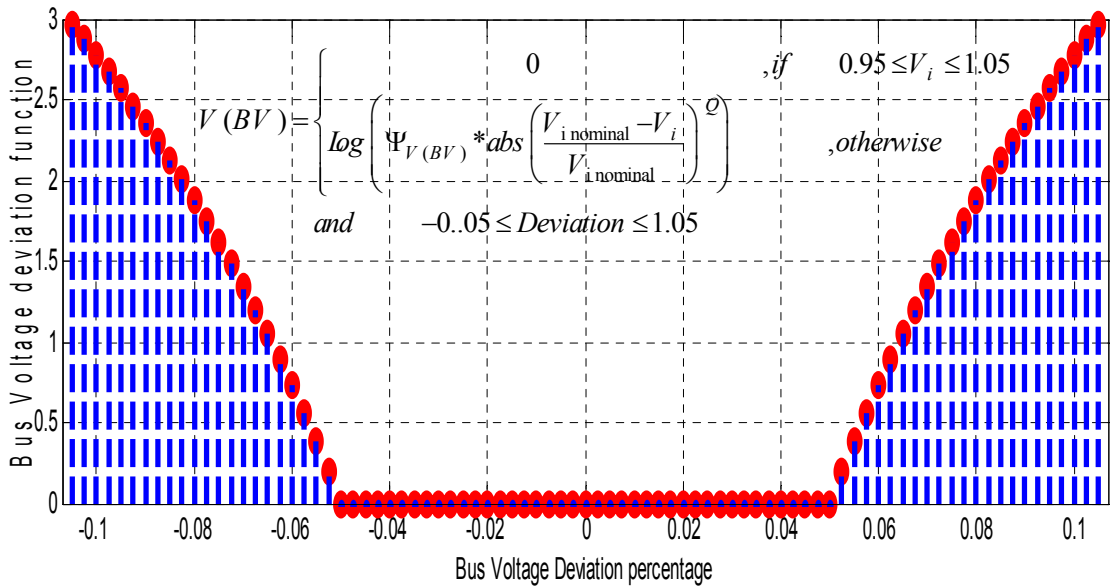


Fig. 5.1 Bus Voltage Violations function.

II) Optimizing with the overloaded lines (No bus voltage violations or out of interest zone):

$$F_t(X,U) = \sum_{i=1}^{ntl: \text{no. of lines}} L(OL) \tag{5.6}$$

$$L(OL) = \begin{cases} 0 & , \text{if } S_{i \text{ operating}} \leq S_{i \text{ max. rate}} \\ \log \left(\Psi_{L(OL)} * \left(\frac{S(MVA)_{i \text{ operating}}}{S(MVA)_{i \text{ max. rate}}} \right)^{2 * R} \right) & , \text{if } S_{i \text{ operating}} > S_{i \text{ max. rate}} \end{cases} \tag{5.7}$$

Where

$L(OL)$ represents the Over Loaded Line function;

S_i represents the current Volt-Ampere power in line i ;

S_i represents the Volt-Ampere power rate of line

$\Psi_{L(OL)}$ represents the weights and is determined in order to have certain index value for various percentage of branch loading, also used to adjust the slope of the logarithm

R represent the coefficient is used to penalize more or less overloads.

ntl represent the number of lines in the system.

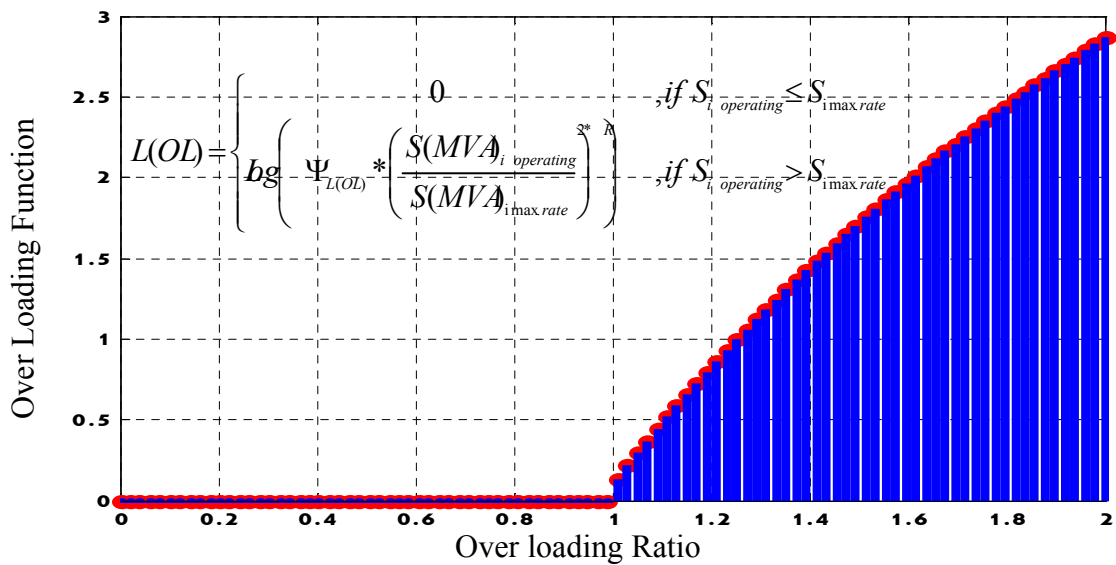


Fig. 5.2 Over Loaded Lines Function.

III) Optimizing with the overloaded lines and the bus voltage violations :

$$F_t(X,U) = \sum_{i=1}^{ntl: no. of lines} L(OL) + \sum_{j=1}^{nbb: no. of buses} V(BV) \quad (5.8)$$

As it is indicated in the Equation (5.4) and (5.5) and related variables

$$L(OL) = \begin{cases} 0 & ,if S_i operating \leq S_{i max. rate} \\ \log \left(\Psi_{L(OL)} * \left(\frac{S(MVA)_i operating}{S(MVA)_{i max. rate}} \right)^{2 * R} \right) & ,if S_i operating > S_{i max. rate} \end{cases}$$

$$V(BV) = \begin{cases} 0 & ,if 0.95 \leq V_j \leq 1.05 \\ \log \left(\Psi_{V(BV)} * abs \left(\frac{V_j nominal - V_j}{V_j} \right)^Q \right) & ,otherwise \end{cases}$$

In some simulations, the log relations can be replaced with linear relations, according to the penalty of overloading and voltage violations values.

5.2.3. UPFC Modeling for Power Flow

The equivalent circuit of UPFC will be attached to the power system equation, and programmed for output results, and is shown Figure (5.3). It consists of two synchronous voltage sources (SVS), which are simultaneously coordinated together to achieve the required performance mode.

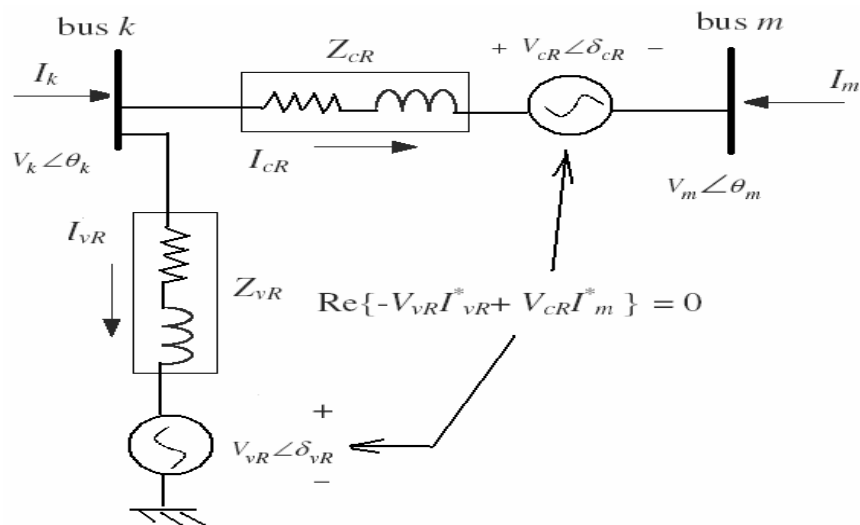


Fig. 5.3. Unified power flow controller equivalent circuit.

$$E_{vR} = V_{vR} * (\cos \delta_{vR} + j \sin \delta_{vR}) \quad (5.9)$$

$$E_{cR} = V_{cR} * (\cos \delta_{cR} + j \sin \delta_{cR}) \quad (5.10)$$

Where

V_{vR} represents the magnitude of the shunt SVS voltage.

δ_{vR} represents the value of the shunt SVS angle.

V_{cR} represents the magnitude of the series SVS voltage.

δ_{cR} represents the value of the series SVS angle.

Equations (5.4) and (5.5) will be adjusted to represent the active and reactive power equations for bus k and m , then combined with Equations (5.9) and (5.10) to get:

$$P_{cR} = V_{cR}^2 G_{mm} + V_{cR} V_k (G_{km} \cos(\delta_{cR} - \theta_k) + B_{km} \sin(\delta_{cR} - \theta_k)) \\ + V_{cR} V_m (G_{mm} \cos(\delta_{cR} - \theta_m) + B_{mm} \sin(\delta_{cR} - \theta_m)) \quad (5.11)$$

$$Q_{cR} = -V_{cR}^2 B_{mm} + V_{cR} V_k (G_{km} \sin(\delta_{cR} - \theta_k) - B_{km} \cos(\delta_{cR} - \theta_k)) \\ + V_{cR} V_m (G_{mm} \sin(\delta_{cR} - \theta_m) - B_{mm} \cos(\delta_{cR} - \theta_m)) \quad (5.12)$$

$$P_{vR} = -V_{vR}^2 G_{vR} + V_{vR} V_k (G_{vR} \cos(\delta_{vR} - \theta_k) + B_{vR} \sin(\delta_{vR} - \theta_k)) \quad (5.13)$$

$$Q_{vR} = V_{vR}^2 B_{vR} + V_{vR} V_k (G_{vR} \sin(\delta_{vR} - \theta_k) - B_{vR} \cos(\delta_{vR} - \theta_k)) \quad (5.14)$$

Where

V_k and V_m : the voltage magnitudes at bus k and bus m .

θ_k and θ_m : the voltage magnitudes at bus k and bus m .

P_{cR} and Q_{cR} : the series SVS active and reactive powers.

P_{vR} and Q_{vR} : the shunt SVS active and reactive powers.

G_{mm} , G_{kk} , G_{km} , G_{mk} : the conductance elements for bus k , m and for lines between buses.

B_{mm} , B_{kk} , B_{km} , B_{mk} : the susceptance elements for bus k , m and for lines between buses.

G_{vR} , B_{vR} , G_{cR} , B_{cR} : the susceptances and conductances for shunt and series SVS.

5.2.4. Problem Constraints:

⇒ Equality Constraints

The active and reactive power balance equations at each bus in the network, which are described as

$$\sum_{lines \Rightarrow bus_i} PowerLinesFlow = PowerGenerator_i - PowerDemand_i \\ P_{Gi} - P_{Di} - P_{Lines \Rightarrow bus_i}(V, \theta) = 0.0 \quad (5.15)$$

$$Q_{Gi} - Q_{Di} - Q_{Lines \Rightarrow bus_i}(V, \theta) = 0.0 \quad (5.16)$$

This is in addition to the active and reactive power flow equations for the series and shunt SVS for UPFC device, which is indicated from Equations (5.11) to (5.14).

⇒ **Inequality Constraints**

- Generation Power Limits:

$$P_{Gi}^{\min} \leq P_{Gi} \leq P_{Gi}^{\max}, i=1, 2, \dots, n_G \quad (5.17)$$

$$Q_{Gi}^{\min} \leq Q_{Gi} \leq Q_{Gi}^{\max}, i=1, 2, \dots, n_G \quad (5.18)$$

- Bus Voltage Limits:

$$V_i^{\min} \leq V_i \leq V_i^{\max}, i=1, 2, \dots, n_{bb} \quad (5.19)$$

- Phase Angles Limits:

$$\delta_i^{\min} \leq \delta_i \leq \delta_i^{\max}, i=1, 2, \dots, n_{bb} \quad (5.20)$$

- Parameters UPFC Constraints:

$$\begin{aligned} V_{vR}^{\min} &\leq V_{vR} \leq V_{vR}^{\max} \\ V_{cR}^{\min} &\leq V_{cR} \leq V_{cR}^{\max} \end{aligned} \quad (5.21)$$

- Power Lines Limits:

$$P_{ij} \leq P_{ij}^{\max}, i=1, 2, \dots, n_{tl} \quad (5.22)$$

5.3 Performance Ranking Index

For applying UPFC installation, the optimal locations and optimal parameters setting (V_{cR} , V_{vR}) will be adjusted by the designed Genetics Algorithm which will be shown later. As indicated before, the installation of UPFC with optimal locations and optimal parameters setting will eliminate or at least reduce the overloading of the transmission lines and the violations of the bus voltage.

The installations of UPFC will be performed on the system during the normal operations and also during contingency conditions. Ranking process is occurred on the network post the contingency study. There will be some single contingencies. We calculate the following performance indices at each single line outage:

- $\hat{K}_{(LOLN)}$: the index which indicates the Lines Over Loaded Number.
- $\Gamma_{(VBVN)}$: the index which indicates the Violation of Voltage Buses Number.

Then we rank the lines according to the severity of the contingency, in other words, according to:

- The Performance Index $\mathcal{J} = \hat{K}_{(LOLN)} + \Gamma_{(VBVN)}$

As will be shown later in simulations and results, Performance Index \mathcal{J} is zero for the remaining cases, which have no transmission line overloading nor buses voltage violation, as a short example for this process (as Numerical explanations):

Table 5.1 Ranking for the severity contingency cases

Ranking Case	Line Number	Connecting Bus		$\dot{K}_{(LOLN)}$	$\Gamma_{(VBVN)}$	\mathcal{J} $= \dot{K}_{(LOLN)} + \Gamma_{(VBVN)}$
		From	To			
1	11	9	2	3	2	5
2	15	8	5	2	1	3
3	1	6	12	2	0	2

5.4 The Proposed Genetics Algorithm

In the genetic algorithm, the individuals are coded to chromosomes that contain variables of the problem. The configuration of chromosomes to reach the optimal installation of the UPFC has two categories of parameters: location of UPFC and parameters setting V_{cR} , V_{vR} as decoupled model parameters of UPFC. In Figure 5.4, the chromosome for the proposed algorithm has been shown.

Objective Function	Location of UPFC	V_{cR}	V_{vR}
---------------------------	-------	-------------------------	----------	----------

Fig. 5.4 The Chromosome of Proposed GA.

- The first group of chromosomes inside the individual points to the positions locations of UPFCs hardware in the power system. This group defines in which transmission line the UPFCs should be structured.
- The second group (starting from the end of the first set) represents the value of V_{cR} for series SVS. The range for this set is randomly generated according to the working range [0.001, 0.3].
- At last, the third set (starting from the end of the second set) represents the value of V_{vR} for shunt SVS. The range for this set is randomly generated according to the range [0.8, 1.2].

A genetic algorithm is governed by three factors: mutation rate, crossover rate and population size. The GA is a search process, which can be applied to constrained problems; the constraints may be included into the fitness function. In this algorithm, issues for optimization that must be performed on the objective function and all equality and inequality constraints including the UPFC equations, these all explained in the previous sections. The structure of the GA execution can be separated into the following three constituent phases namely: initial population generation, fitness evaluation and genetic operations.

In the following steps, we describe the process of the implemented GA technique:

Phase 1: Definitions for the optimization controlling parameters such as the population size, crossover and mutation and their probabilities, maximum generation number, stopping criterion. In addition, the power flow data is defined.

Phase 2: Generation a primary population for individuals, this process performed for optimizing variables, which are the positions, and the parameters setting of UPFC. Three chromosomes for the individual show a meaningful point inside the optimization problem's region solution.

Phase 3: Using the objective function, we start to calculate the individual's fitness inside the population. The fitness is computed by considering the fitness function F_t . The population on-line performance $P(n)$ is defined as

$$P(n) = \frac{1}{P} \sum_{p=1}^N F_t^n(p) \quad n=0, 1, \dots, T-1 \quad (5.23)$$

Where

N = Total population size;

T = total generations;

$F_t^n(p)$ = the fitness function of the p th chromosome in the n th generation.

Phase 4: GA depends on genes rules and the Darwin principle of the survival of the fittest, so we eliminate the worse individuals, and continue with the most highly fit members to generate a new population, keeping information for the next generation. That process is preformed by comprising selection, crossover, and mutation.

To maintain diversity in the population, we consider d_{ij} the variable distance between two solutions $X^{(i)}$ and $X^{(j)}$

$$d_{ij} = \sqrt{\sum_{k=1}^S \left(\frac{X_k^{(i)} - X_k^{(j)}}{X_k^{\max} - X_k^{\min}} \right)^2} \quad (5.24)$$

Where

S : the no. of the variables included in the optimizes

X_k^{\max} and X_k^{\min} respectively the upper and the lower bounds of variables of X_k

Phase 5: Trying multiplies epochs with the selection, crossover, and mutation until achieving the desired individuals for the new generation. Then we use the fitness values, which are the best and which are the worst, to rank the individuals, and use the ranking process to define the selection probability. Considering the individual at rank i :

$$\text{Probability}_i = \frac{1}{\|P\|} \left(2 - \alpha + (2\alpha - 1) \frac{i - 1}{\|P\| - 1} \right) \quad (5.25)$$

Where α is the selection bias and its value between 1, 2; higher values for more directing the cursor on selecting only the well individuals. The best individual in the population is thus selected with the probability $\frac{\alpha}{\|P\|}$; the worst individual is selected with the probability

$\frac{2 - \alpha}{\|P\|}$. That procedure keeps the best individual in the new next generation.

Phase 6: Generation maximum number defines the stopping point of the system. Let z denote the bits number inside the chromosome and N population size as mentioned before, then the expected number of generations until convergence is,

$$E(N_G) = 1.4 N (0.5 \ln(z) + 1) \quad (5.26)$$

This is valid for random mating with recombination but without selection and mutation. This procedure causes small selection intensities to decrease the probability to find the optimum. Reaching to the maximum number and achieving both function and constraints with the final best individual lead to end the procedure and prints the final result.

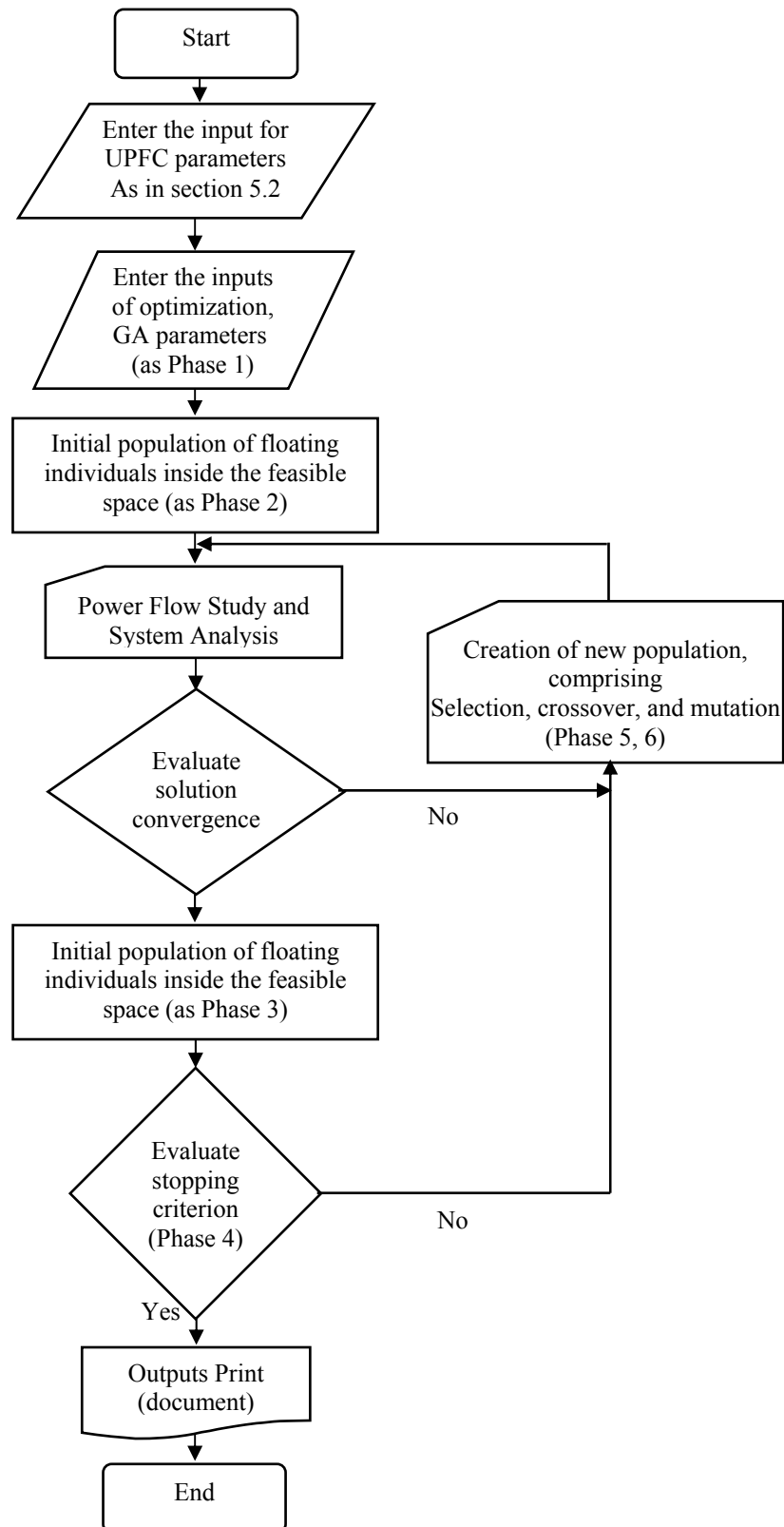


Fig. 5.5 Flowchart of optimization procedure for GA.

5.5 Scope on the Simulations Files (UPFC files , GA files)

Matlab Codes for GA (with the main GA file, the fitness function and the constraints) and a modified power flow algorithm to include UPFC are developed. Programmed M-files are incorporated to include the updates for adjust the algorithm according to the required indices and terms. In addition, the automatic contingency analysis with performance indices and ranking the severity cases were developed and incorporated together for the simulation purposes. During the following sections, we will be concerned with the steady state data of the UPFC. That data affects the steady state performance of the UPFC and the power network; where the dynamics date will be concerned after in a later stage.

- **UPFC Data:**

% NUPFC : Number of UPFC's
 % UPFCsend : Shunt converter's bus and series converter' sending bus
 % UPFCrec : Series converter' receiving bus
 %UPFCtln : UPFC Transmission Line Number (Insertion Location)
 % Xcr : Inductive reactance of Shunt impedance (p.u.)
 % Xvr : Inductive reactance of Series impedance (p.u.)
 % Flow : Power flow direction
 % Psp : Target active power flow (p.u.)
 % PSta : control status for active power : 1 is on; 0 is off
 % Qsp : Target reactive power flow (p.u.)
 % QSta : control status for reactive power : 1 is on; 0 is off
 % Vcr : Initial condition for the series source voltage magnitude (p.u.)
 % Tcr : Initial condition for the series source voltage angle (rad.)
 % VcrLo : Lower limit of series source voltage magnitude (p.u.)
 % VcrHi : Higher limit of series source voltage magnitude (p.u.)
 % Vvr : Initial condition to the shunt source voltage magnitude (p.u.)
 % Tvr : Initial condition to the shunt source voltage angle (rad.)
 % VvrLo : Lower limit of shunt source voltage magnitude (p.u.)
 % VvrHi : Higher limit of shunt source voltage magnitude (p.u.)
 % VvrTar : Target nodal voltage magnitude to be controlled by shunt branch (p.u.)
 % VvrSta : Control status for nodal voltage magnitude: 1 is on; 0 is off

• **Designed GA Program**

Table 5.2 the designed values for the GA parameters

GA Parameters	
Input Variables	x(1)= UPFCtl x(2)= Vcr(1) x(3)= Vvr(1)
Lower bound for Variables	LB = [1 1 0.001 0.8];
Upper bound for Variables	UB = [5 5 0.3 1.2];
Options. PopulationType	Double Vector
Options. PopulationSize	Adapted
Options. EliteCount	2
Options. CrossoverFraction	0.8
Options. MigrationDirection	Forward
Options. MigrationInterval	20
Options. MigrationFraction:	0.2
Options. Generations	200
Options. TimeLimit	Inf
Options. FitnessLimit	-Inf
Options. StallGenLimit	50
Options. StallTimeLimit	Inf
Options. TolFun	1e-6
Options. TolCon	1e-6
Options. InitialPenalty	10
Options. PenaltyFactor	100
Options. FitnessScalingFcn	'Rank'
Options. SelectionFcn	'Stochastic Uniform'
Options. CrossoverFcn	'Scattered'
Options. MutationFcn	@mutationadaptfeasible

5.6 Dynamics Studies on the system (Concept and Building)

The unified power flow controller was proposed for flexible AC transmission systems applications. UPFC has various tasks, one of them as power flow controller. The secondary functions of the UPFC can be voltage control, transient stability improvement, oscillation damping, and others. UPFC can be very effective to damp power system oscillations.

Because FACTS devices have very fast dynamics compared to generators, they can play important roles in enhancing the dynamics response. This is usually accomplished through controls associated with these devices.

Using a damping controller with the UPFC, it can enhance the electromechanical mode damping. That controller can be one of inherent UPFC PI damping controllers. UPFC main controllers can enhance system dynamics but first the dynamics parameters setting should be selected to damp and fine tuning the response. The damping controller for UPFC may affect the system response. The effect of different controllers as conventional and adaptive AI controllers can be compared to conclude the most effective controller.

The operating conditions can be changed according to the disturbance, which has an effect on the power system. In the steady state analysis section, we considered the increasing in loading conditions, which lead to a change from one certain operating condition to another operating point. In addition, we considered the contingency outage cases, which produce a loading increase in the power of all network elements.

For making stress on the correlation between the steady state and the dynamic analysis, we will consider the cases and the operating conditions from the steady state analysis. The steady state analysis leads to the importance of installing the UPFC in certain optimal locations with certain optimal settings. That may be considered as a comparison between installing and not installing the UPFC in the system. After we installed the UPFC at these optimal locations to achieve enhanced steady state performance, we should adapt the dynamic parameters to achieve also the optimal dynamic response, where UPFC at this location may not lead to perfect dynamics response. The mechanical modes of the generators in the system can be good indicator for the dynamic response; the speed deviation response ($\Delta\omega$) and the mechanical rotors angle dynamic response ($\Delta\delta$) can be shown.

The link between the steady state and the dynamic analysis can be achieved by considering the results from the steady state as a primary part to install the optimal UPFC in the system then we investigate the dynamics response analysis. Building and adapting the system configuration to be suitable for the dynamic response analysis will be achieved using the derivation and programming of dynamics equation in Chapter 4, Section 4.4 by m-file codes linked with simulink blocks models. Some scope on the dynamic model of UPFC and also dynamic model of multi-machine power system equipped with UPFC will appear in the Appendix section

5.6.1 Data for dynamics studying of UPFC installation

1- Synchronous Machine:

* Reactances d and q axis; steady state, transient and sub-transient

$$[X_d, X_d', X_d'', X_q, X_q', X_q''].$$

* d and q axis time constants: (Short-circuit , Open-circuit)

$$[T_d', T_d'', T_{qo}'', \dots].$$

- * Stator resistance (R_s).
- * Inertia coefficient, friction factor and pole pairs.
- * Initial conditions [$\Delta\omega$, $\delta(\text{deg})$, i_a , i_b , i_c , ϕ_a , ϕ_b , $\phi_c(\text{deg})$, V_{field}].
- * Rotor Type : Salient-pole or Round.

2- Hydraulic Turbine and Governor:

- * Servo-motor parameters [K_a , T_a].
- * Gate opening limits [g_{min} , g_{max} , $V_{g_{\text{min}}}$, $V_{g_{\text{max}}}$].
- * Permanent droop and regulator [R_p , K_p , K_i , K_d , T_d].
- * Hydraulic turbine settings [β , T_w].
- * Droop reference (0=power error, 1=gate opening).
- * Initial mechanical power.

3- Excitation System:

- * Low-pass filter time constant T_r .
- * Regulator gain and time constant [K_a , T_a]
- * Exciter parameters [K_e , T_e]
- * Transient gain reduction [T_b , T_c]
- * Damping filter gain and time constant [K_f , T_f]
- * Regulator output limits and gain [$E_{f_{\text{min}}}$, $E_{f_{\text{max}}}$, K_p]
- * Initial values of terminal voltage and field voltage [V_{t_0} , V_{f_0}]

4- Power System Stabilizer:

- * Sensor time constant
- * Wash-out time constant
- * Lead-lag time constant [T_{num} , T_{den}]
- * Output limits [$V_{s_{\text{min}}}$, $V_{s_{\text{max}}}$]

5- Transformer Data:

* Primary Winding parameters:

Voltage, Resistance, Reactance, Magnetizing Resistance, Magnetizing reactance

* Secondary Winding parameters:

Voltage, Resistance, Reactance, Magnetizing Resistance, Magnetizing reactance

5.7 Importance of Dynamics Tuning

To show the importance of tuning the dynamic parameters of the UPFC, we will focus on a case study from the cases discussed before in steady state performance enhancing. In the previous cases, this stage concerned with enhancing the performance of the network related to the overloading of transmission lines and violation of bus voltage profile. This performed on the normal configuration of the system with increasing the load pattern on the system until the year 2020. The results lead to optimal location and optimal settings of UPFC to be installed to achieve the required performance.

After installing the UPFC at these optimal locations with optimal settings, the dynamic parameters of the UPFC will have a significant effect on the dynamic response specially the mechanical variables response as the speed deviation response ($\Delta\omega$) and the mechanical rotor angle dynamic response ($\Delta\delta$) of the generating units. The dynamics parameters for the UPFC blocks should be well selected and be set to fine tune the response and damp the oscillation and enhance the settling time of the response.

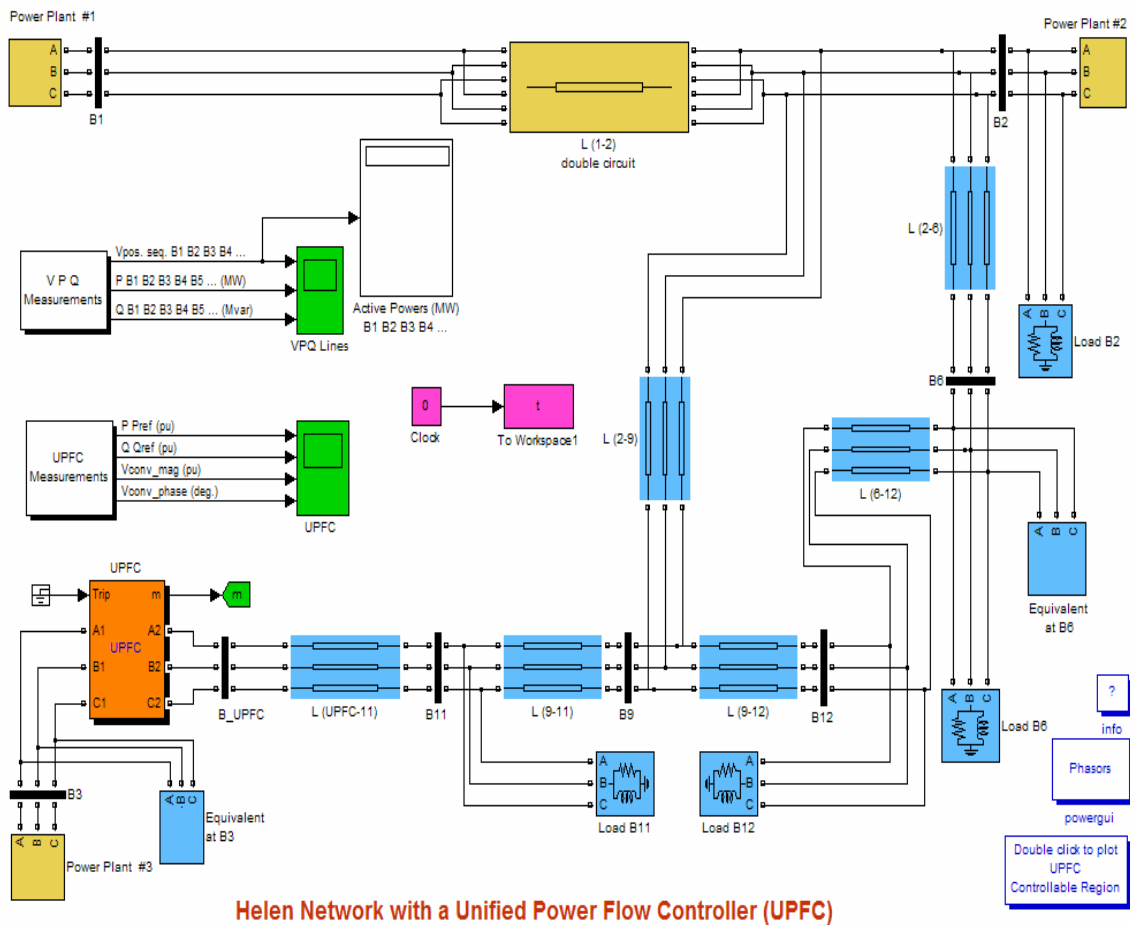


Fig. 5.6, Dynamic blocks for section of Helen (Helsinki Network).

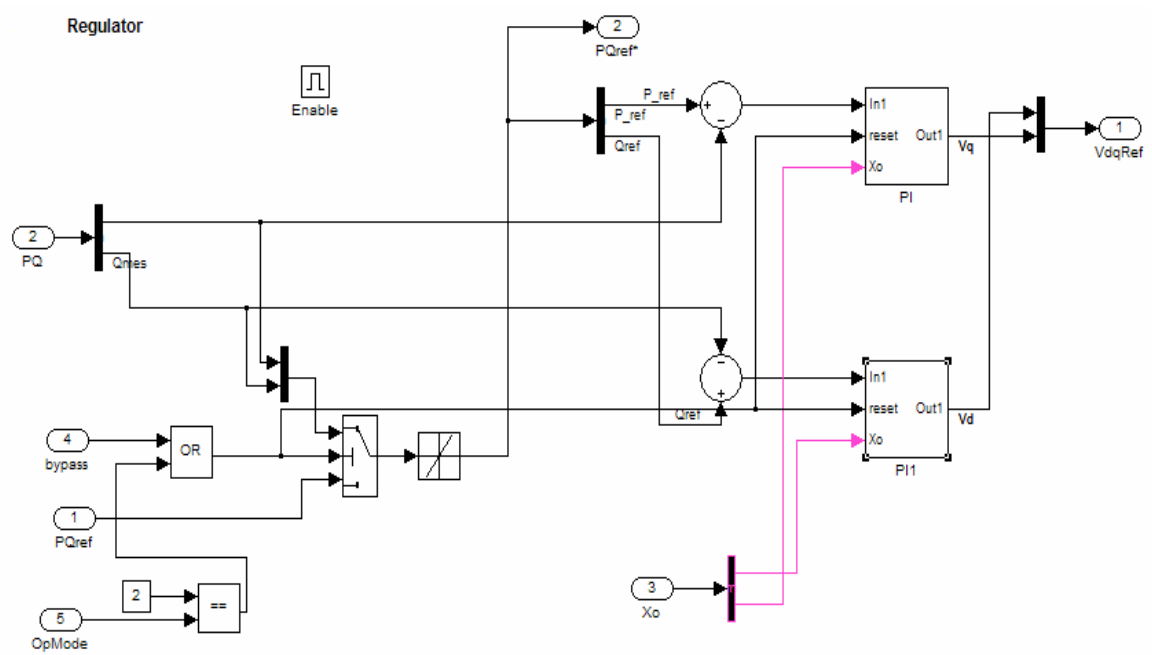


Fig. 5.7, General Structure for Dynamic Blocks for UPFC regulator (UPFC controller).

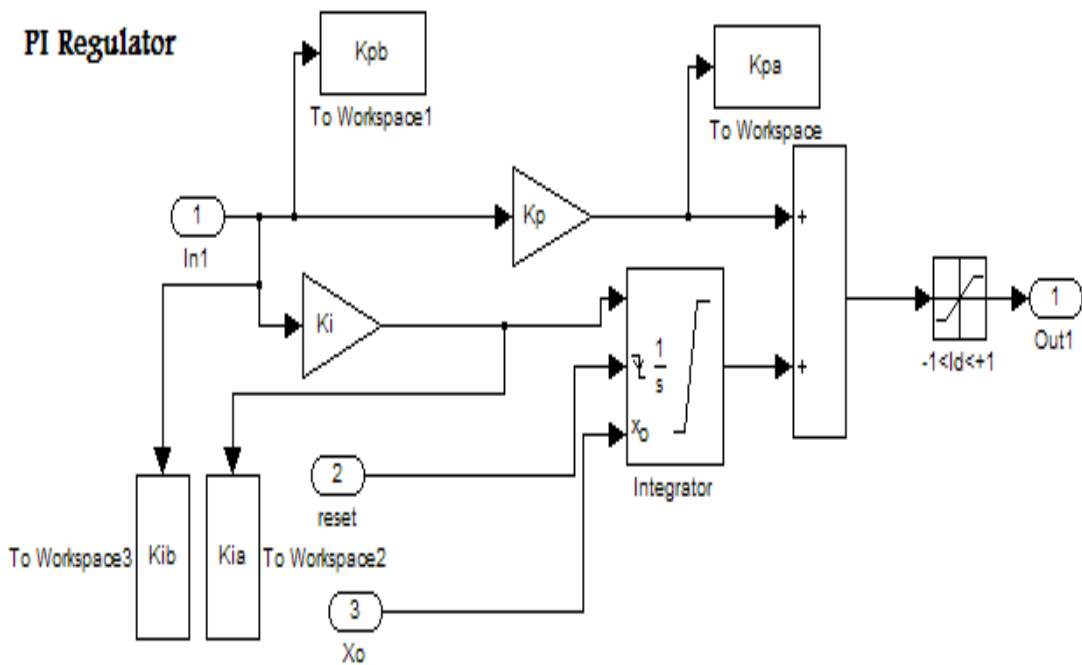


Fig. 5.8, Inherent Dynamic Blocks for UPFC regulator (UPFC controller).

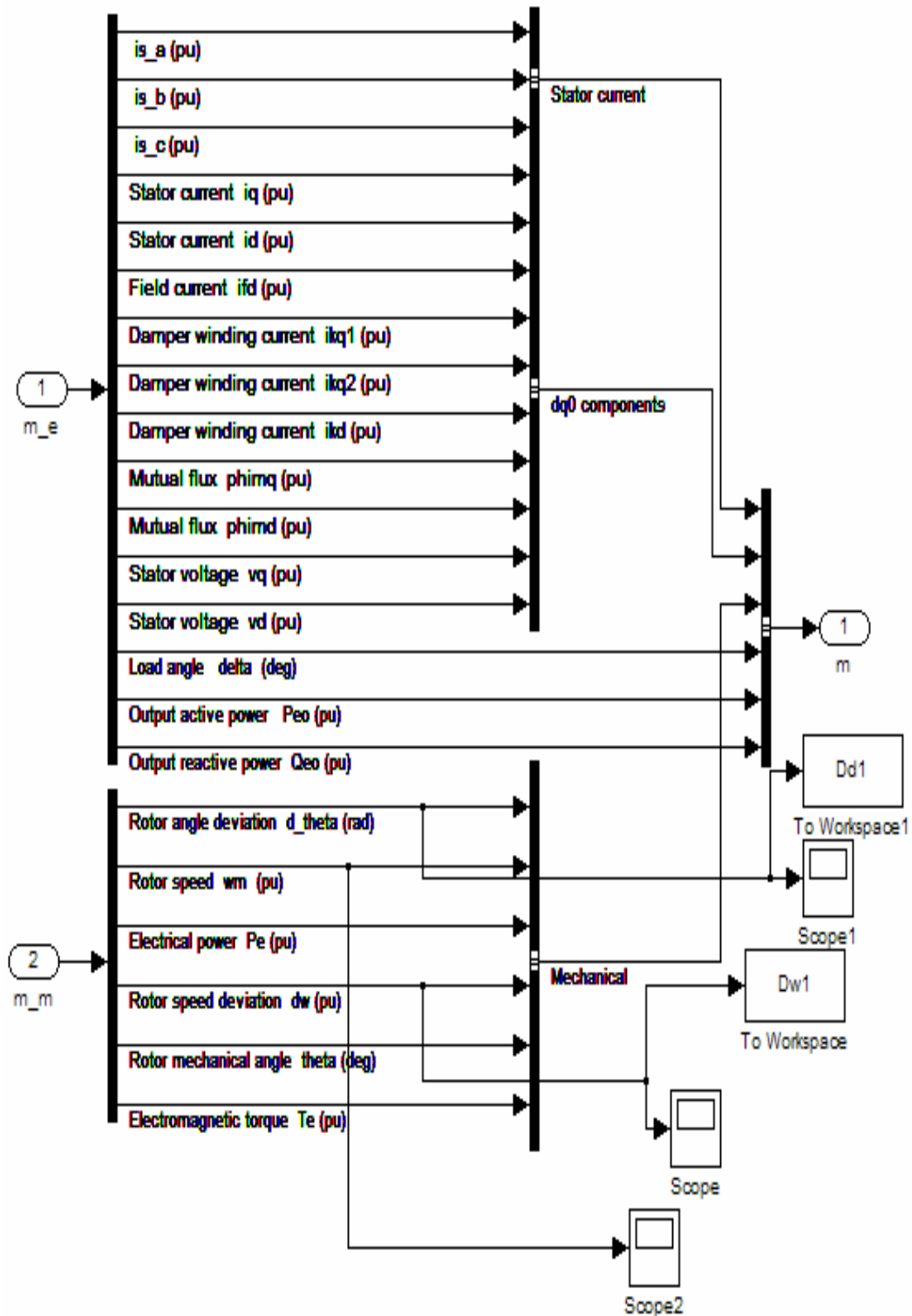


Fig. 5.9, Measurement variables prepared for Dynamic response.

The dynamic response of the mechanical variables as the speed deviation response ($\Delta\omega$) and the mechanical rotor angle ($\Delta\delta$) of the generating units will be varied according to the adjusting of the dynamic parameters of the UPFC.

Some examples of the dynamic response for various operating cases with related UPFC dynamic parameters will show the importance of getting the significant setting of that parameters to enhance the dynamic response.

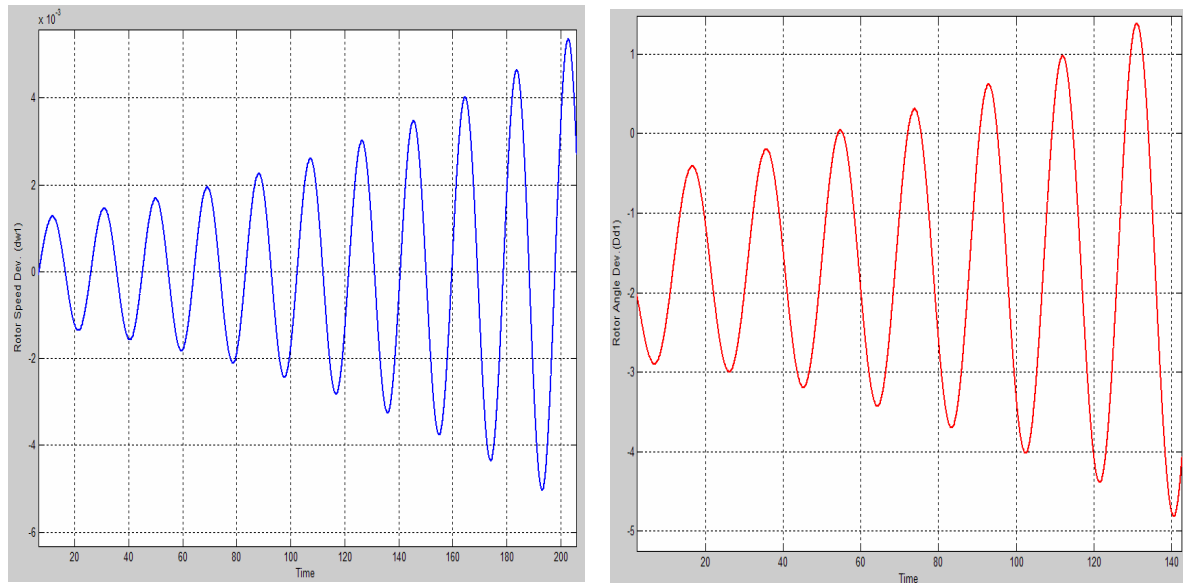


Fig. 5.10, Increased Instability Dynamic Response.

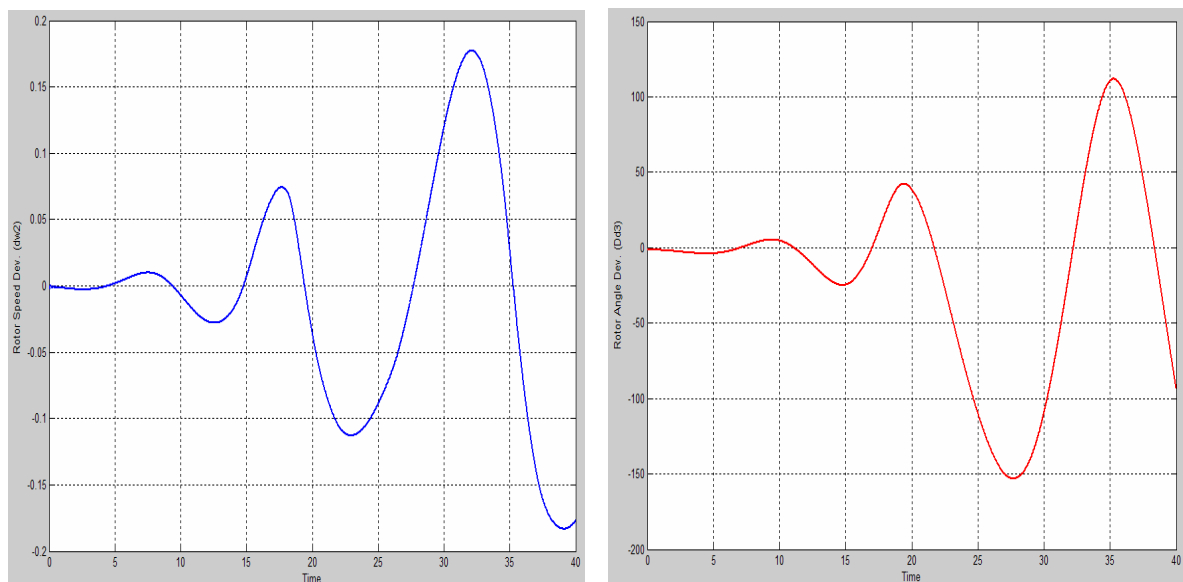


Fig. 5.11, Fast Instability Dynamic Response.

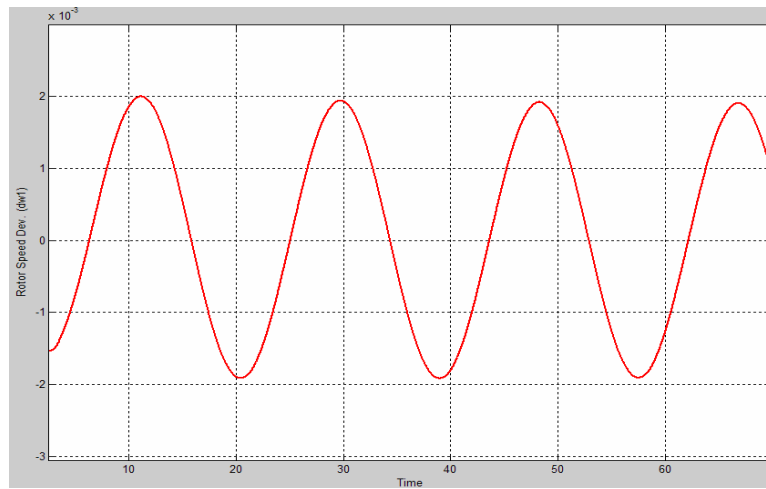


Fig. 5.12, Critical Stability (Naturally Damped) Dynamic Response.

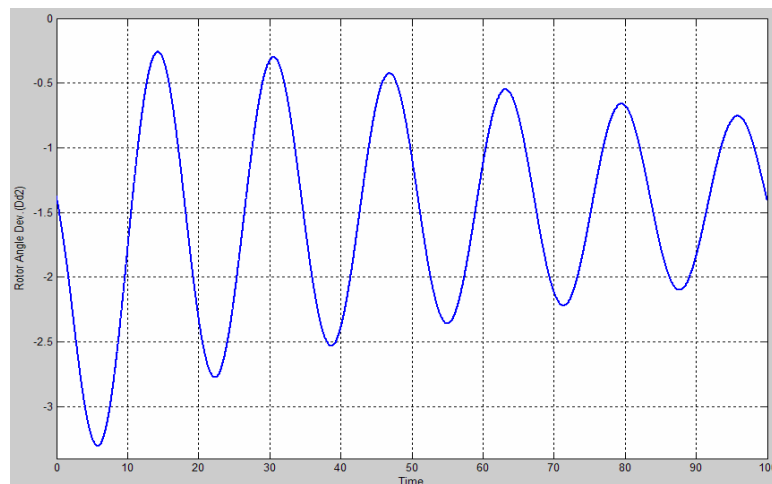


Fig. 5.13, High-Timed Damped Dynamic Response.

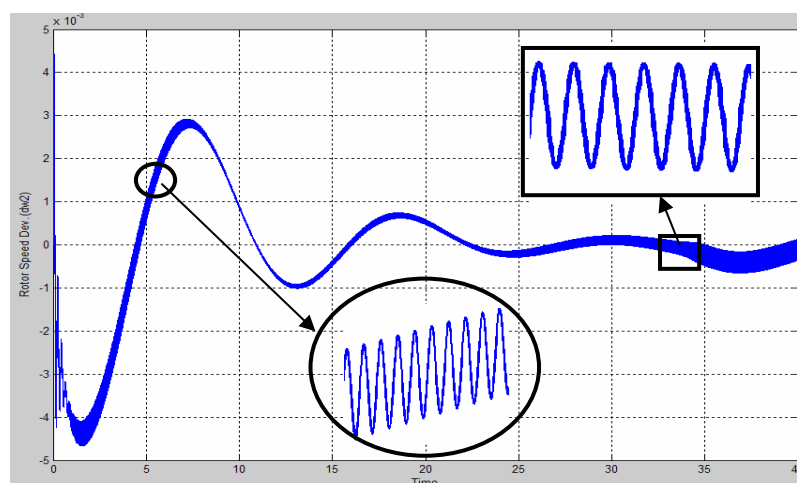


Fig. 5.14, High Oscillatory Dynamic Response.

5.8 Conventional PI Controller

The modelling of a PI controller can be considered mainly in software such as Simulink using Laplace operators:

$$C = \frac{G(1 + \tau s)}{\tau s}$$

Where

$G = K_p$ = proportional gain

$G / \tau s = K_i$ = integral gain

Setting a value for G is often tuned between decreasing overshoot and increasing settling time, also finding a proper value for τs is an iterative process. The problem with using a PI controller is careful design considerations with respect to the gain must be considered.

- Proportional term

In the case of high value for the proportional gain, the performance can act in unstable mode. In the opposite situation, a small gain causes a small output response to a large input error, and a less sensitive controller. If the proportional gain is too low, the control action may be too small during occurrence of system disturbances. Both tuning theory and industrial practice indicate that it is the proportional term that should contribute the bulk of the output change.

- Integral term

The task of the integral term is proportional to both the value of the error and the time of the error. The magnitude of the integral part to the resultant control action is calculated by the integral gain, K_i . The integral part increases the speed of the motion in the direction of the set-point and minimizes the steady-state error that occurs with a proportional only controller. However, since the integral term is responding to accumulated errors from the past, it can cause the present value to overshoot the set-point.

- Loop tuning

The selection process of the PI controller parameters, which are the proportional and integral gains, should be chosen in a proper way that makes the controlled process more stable. Tuning a control loop is the adaptation of its control parameters to the optimum values for the desired control response.

Mostly, stability of response is requested and the process must not oscillate under any circumstances. Increasing the value of the proportional gain, K_p , will make faster response, and more proportional term compensation. An increase in the proportional gain will direct to instable and oscillated behaviour. With respect to integral gain, K_i , larger values imply steady state errors are fast minimized. An integral control (K_i) will affect on eliminating the steady-state error, but it may worse the transient response.

There are many traditional manual techniques for tuning a PI loop. The most efficient techniques essentially have the investment of some phases of the process model, then select

P and I according to the dynamic model parameters. Manual tuning methods can be relatively inefficient.

The most effective tuning method has the effect of applying a step change in input to the system, evaluating the output as a function of time, and using this response to calculate the control parameters.

- Manual tuning

The procedure to keep the system online starts with selecting one tuning method to set K_i values to zero. Larger the K_p value until the output oscillates, then the K_p should be set to approximately half of that value for a quarter amplitude decay response. Then increase K_i until any offset is proper in sufficient time for the process. We should note that too much K_i will lead to instability.

The tuning of the PI settings is quite a subjective procedure, depending mainly on the skill and experience of the control engineer and operator. Although tuning guidelines are available, the process of controller tuning takes some time with the result that many plant control loops are improperly tuned and the complete effect of the control system does not occur.

Table 5.3 shows the effects of increasing a parameter independently on the system dynamics response.

Table 5.3 Effects of increasing a parameter independently

Parameter	Rise time	Overshoot	Settling time	Steady-state error	Stability
K_p	Decrease	Increase	Small change	Decrease	Degrade
K_i	Decrease	Increase	Increase	Decrease significantly	Degrade

Referring to the tables, these correlations may not be exactly accurate, because K_p and K_i are dependent on each other. In fact, altering one of them can change the effect of the another one. For this reason, the table should only be used as a reference when calculating the values for K_i and K_p .

- PI tuning software

Various modern industrial options no longer tune loops using the manual procedure shown above. Instead, PI tuning and loop optimization software is applied to achieve the desired results. These software packages will collect the information, develop process models, and suggest optimal tuning.

An impulse tuning is produced by a mathematical PI loop during the process, and then applies the controlled system's frequency response to design the PI loop values. The response times which take some minutes, mathematical loop tuning is better, due to trial and error can spend a long time just to get a stable group of loop values. Optimal values are more difficult to reach. Some digital loop controllers save self-tuning attributes in which very small set-point changes are activated in the process, leaving the controller itself to determine optimal tuning values. Other formulas are available to tune the loop according to different performance criteria.

5.9 UPFC Dynamic Controller

The shunt converter of UPFC operates as a STATCOM. The shunt converter governs the AC voltage at its terminals and the voltage of the DC bus. It applies a dual voltage regulation loop: an inner current control loop and an outer loop regulating AC and DC voltages. The control system includes:

- A phase-locked loop (PLL) which handles the positive-sequence item of the three-phase AC voltage. The output of the PLL is applied to calculate the d-axis and q-axis items of the AC three-phase voltage and currents.
- Measuring devices for the d-axis and q-axis parts of AC positive-sequence voltage and currents to be under control like the DC voltage V_{dc} .
- An external regulation loop has an AC voltage regulator and a DC voltage regulator.
- An internal current regulation loop has a current regulator.

That regulator controls the voltage supplied by the PWM converter. Control of the series branch inside a UPFC has two levels of functions where it is used to control the active power and the reactive power. A schematic diagram of the series converter is in Figure 5.15.

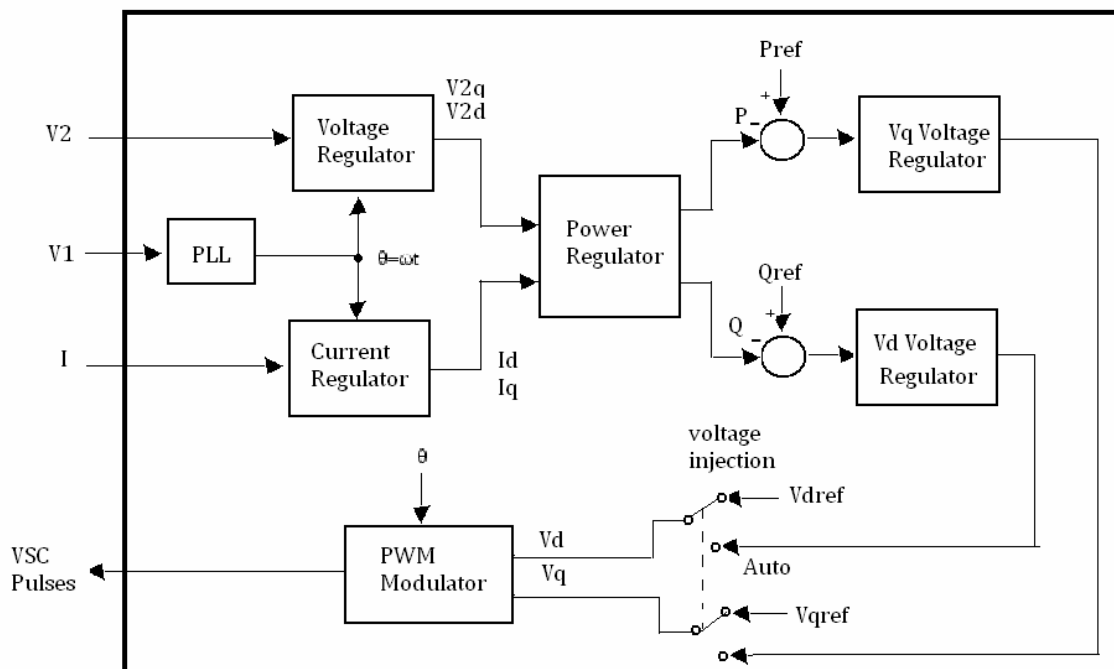


Fig. 5.15, Simplified Block Diagram of the Series Converter Control System.

The series converter can work controlling the power flow and also in voltage control mode. In power control mode, the real operating active power and reactive power are compared with reference values to develop P and Q errors. The P error and the Q error are applied by two PI regulators to calculate respectively the V_q and V_d components of voltage to be synthesized by the VSC.

The analysis of the Helen (Helsinki network) during all the previous power flow studies and the corresponding results showed that the network has an efficient topology which is well tied and interconnected that made it always has no effectively dangerous problems in its voltage profile. Under most operating conditions, the voltage of the majority of the system buses has high significant values near the required base values. So most of the problems which face the network are due to the power flow in the lines, not in the voltage profile of the buses. These options direct us to focus on examining the control elements, which mainly have a contribution and effect on the line power flow. According to the former statements, there are many control elements as Vac Regulator, Vdc Regulator and Power regulator and more. The most effective one on the power flow and its dynamics is the power flow regulator. So the main concerned control element will be inside the series SVS part to control the power flow which will be a power PI regulator containing Integral gain (K_i) and proportional gain (K_p).

We will try to adjust the values of the power PI regulator containing Integral gain (K_i) and proportional gain (K_p) to reach to optimum dynamic response. First we will use the conventional method described in the previous section to tune the parameters values of the PI controller. Then we will apply the Artificial Intelligence techniques to get the optimal tuning of the PI controller parameters values; this gives us all the options and benefits which are available in the AI concept and the controlling will gain process the required adaptivity, flexibility and intelligent characteristics.

5.10 Why AI?

In recent years, AI theory applications have received increasing attention in various areas of power systems such as operation, planning, and control.

AI techniques play a prominent role in power system management and control. The electric power industry is always looking for methods to enhance the performance efficiency. Although the basic technologies of power generation, transmission, and distribution change quite slowly, the power industry has been quick to explore new technologies that might assist its search to show benefits.

This general layout has an effect on the appearance of the various artificial intelligence technologies. General planners, expert systems, artificial neural networks, fuzzy logic algorithms, genetic algorithms have applied almost every form of AI tool in at least prototype form to one or more problem applications in the power systems, and new practical applications of AI appear with increasing frequency. In some cases, AI tools change existing techniques. In others, AI tools provide solutions to problems previously appeared only by natural intelligence, creating new applications for computers.

A number of research articles which have appeared recently indicate the applicability of AI systems to power systems for wider operating conditions under uncertainties. While most of these systems are still under investigation, however, there already exist several practical applications of AI systems.

Because of multiple AI systems, they can be applied as a general methodology to provide knowledge or theory into controllers and decision makers. There are analytical solution techniques for power system problems. However, the mathematical formulations of power systems problems are derived during specific restrictive assumptions and even with these assumptions, the solution of large-scale power system problems is not simple.

On the other hand, there are various uncertainties in power system problems, due to those power systems are large-scale, complex, wide spread in geographical places, and affected by unplanned conditions. These reasons lead to difficulty in handling many power systems problems through strict mathematical formulations alone.

Therefore, the AI approach has emerged in recent years as a complement tool to mathematical approaches for solving power system problems. Since expert knowledge, experience, and intuition are essential in power systems operations, AI can be effectively used in power system problems to represent uncertainties based on preferences and/or experience.

Artificial intelligence (AI) analysis depends on the past history data of a system, the designer should understand and appreciate this data than other theoretical and empirical methods. AI may be applied to provide innovative ways of solving design issues and will allow designers to get an almost instantaneous expert opinion on the effect of a proposed change in a design.

Figure 5.16 shows the percentages of some significant AI researches on applications to power systems.

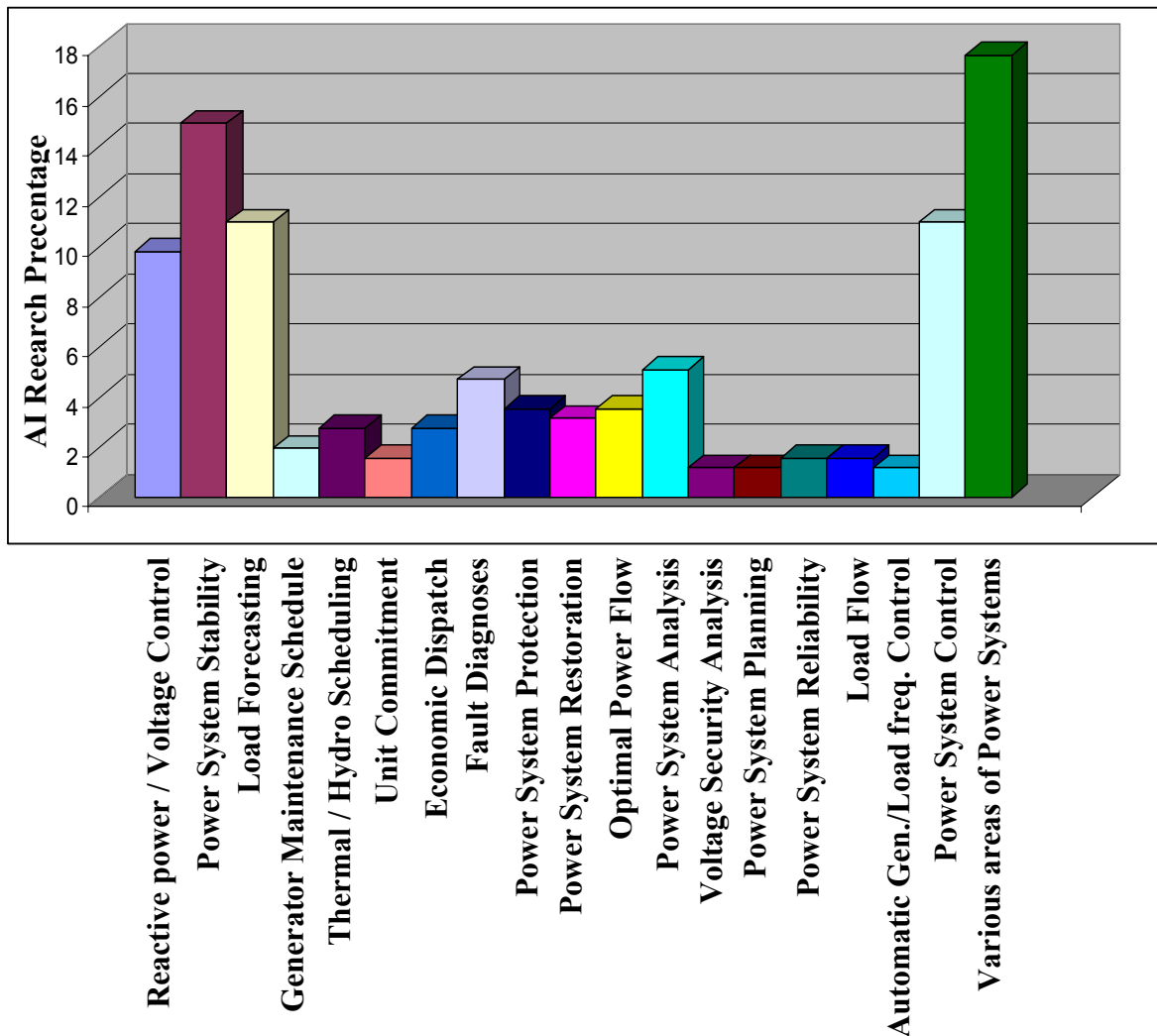


Fig. 5.16 Some Applications of AI in Power Systems [83].

5.10.1 Why GA with ANFIS?

Adaptive control is the updating of controller parameters online based on the changes in system operating conditions. Adaptive controllers based on analytical techniques can save wonderful response and enhance the dynamic performance of the plant by allowing the parameters of the controller to adapt the operating conditions change. Proper care is required to let them be robust, especially under large disturbances. Controller robustness can be enhanced by applying artificial intelligence (AI) techniques. It is available to achieve the entire algorithm using AI techniques or integrating analytical and AI techniques for executing some tasks using analytical approach and the rest using AI techniques.

The main benefit in using the genetics algorithm is the ability of GA to reach the optimal solution, which guarantee that if the GA is well self designed and trained that will lead to the most achieved level from the desired performance for the system under any problem space. About the Adaptive Neuro-Fuzzy Inference (ANFIS), we can first state that ANFIS is a merging system between the neural network system and fuzzy logic system. Therefore, it has the resultant benefits of both systems. The fuzzy system is a very efficient tool in the controlling actions and the neural networks (NN) are powerful in patterns classifications and patterns recognitions. The NN can be merged with the fuzzy system to adapt the parameters of the fuzzy systems to reach the best collection of fuzzy parameters leading to the required controlling procedure. Therefore, we get the positive options from each AI system and merge them to get the global benefits.

- **Why Use Fuzzy Logic?**

Here is a list of general characteristics about fuzzy logic:

- Fuzzy logic is basically easy to understand.

The theory behind fuzzy learning is very simple. Fuzzy logic is a more self-evident technique without complex principles.

- Fuzzy logic is flexible.

With any specific process, it is simple to apply on more flexibility without working from scratch.

- Fuzzy logic has more clearance to deal with imprecise data.

when we work closely enough, everything may be considered imprecise but more than that, most things are imprecise even on careful inspection.

- Fuzzy logic can deal with nonlinear complex functions.

We can design a fuzzy system to any set of input-output data. This process is applied particularly easy by adaptive techniques like (ANFIS) systems.

- Fuzzy logic can be integrated with traditional control techniques.

Fuzzy systems do not necessarily exchange traditional controllers. In most situations, fuzzy systems link with them and enhance their implementation.

- Fuzzy logic building depends on natural language.

The core of fuzzy logic is the core of for people communication. This concept explains many features about fuzzy logic. Because fuzzy logic is structured on the structures of normal language description used in our life, the fuzzy logic algorithm is easy to apply.

- **Why Use ANFIS?**

The fuzzy logic has processed only certain membership functions that were selected at the beginning of the design. The fuzzy system is used to only handling processes, those have rules are basically determined by the user's design of the features of the variables in the system.

During the fuzzy logic design, the shape of the membership functions is based on parameters, and altering these parameters alters the shape of the membership function. In some modeling cases, we can select the shapes of the membership functions simply from looking at data. Considering selecting the parameters with respect to a specific membership function arbitrarily, these parameters could be selected to tailor the membership functions to the input/output data in order to account for these types of variations in the data values. In such situations, we can apply the Neural networks; neuro-adaptive learning techniques (ANFIS) to provide a method for the fuzzy modeling procedure to learns information about a data set and to calculate the membership function parameters that best allow the associated fuzzy inference system to track the given input/output data.

The ANFIS establishes a fuzzy inference system (FIS), which has membership function parameters that are updated. This updating permits fuzzy systems to learn from the data they are modeling. The parameters of the membership functions change through the learning process. A gradient vector processes the updating of these parameters. This gradient vector saves a judge of the quality of the fuzzy inference system by handling the input/output data for a certain group of parameters. When the gradient vector occurs, various optimization actions can be used in order to update the parameters to minimize some error measure.

- **Why Use GA?**

The genetic algorithm is a technique for solving optimization problems that depend on natural selection, the procedure that simulates biological evolution. The genetic algorithm repeatedly adapts a population of individual solutions. In each phase, the genetic algorithm chooses individuals at random from the current population to become parents and applies them to develop the children for the next generation. Over successive generations, the population flows toward an optimal solution.

We can use the genetic algorithm to solve many optimization problems that are not solved by standard optimization algorithms, especially problems, have an extremely nonlinear objective function.

5.10.2 Construction of the adaptive intelligent Controller

ANFIS will be used in this work to adapt the dynamic controllers' gains of the UPFC controllers in real time. Before ANFIS can be used, it is necessary to determine a proper set of training patterns. Each training pattern comprises a set of input data and corresponding output data. For UPFC controller, an ANFIS will be designed to update its gains. The inputs for ANFIS will be the desired line active power and line reactive power, and also the operating line active power and line reactive power.

To obtain this data, the operating conditions of the power system is varied covering the situations of light loaded system (25 % of the normal loading) to 150 over loading. Also conditions such as different generation levels are included. The training data contains the training patterns obtained by GA for ANFIS. The GA feeds the ANFIS with the training patterns. The GA itself has been trained and designed well to guarantee the achieving and validation of the data. That procedure gives the controller high power characteristics; where it focuses on the optimal solutions using the inherent structure of the GA system. Another power characteristic of the proposed controller is that ANFIS has the option to cover very wide operating conditions and it continuously adapts itself where there some operation conditions that GA cannot reach, the ANFIS can reach in fast action. In addition, the connection between the GA and ANFIS achieves that each one of them corrects and helps the another one where each one can be considered as a checker tool for its neighbor system.

The structure of the adaptive controller can be presented in working layers. As the neural network layer can be considered as co-operative with the fuzzy logic layer to construct the ANFIS system. Where the genetics algorithm system is a co-operative layer for the totally ANFIS system as a pre-training tool, it provides the ANFIS with the training patterns. The above structure can be indicated in the following Figure 5.17, which gives more details about the connection and link between the adaptive controller sections.

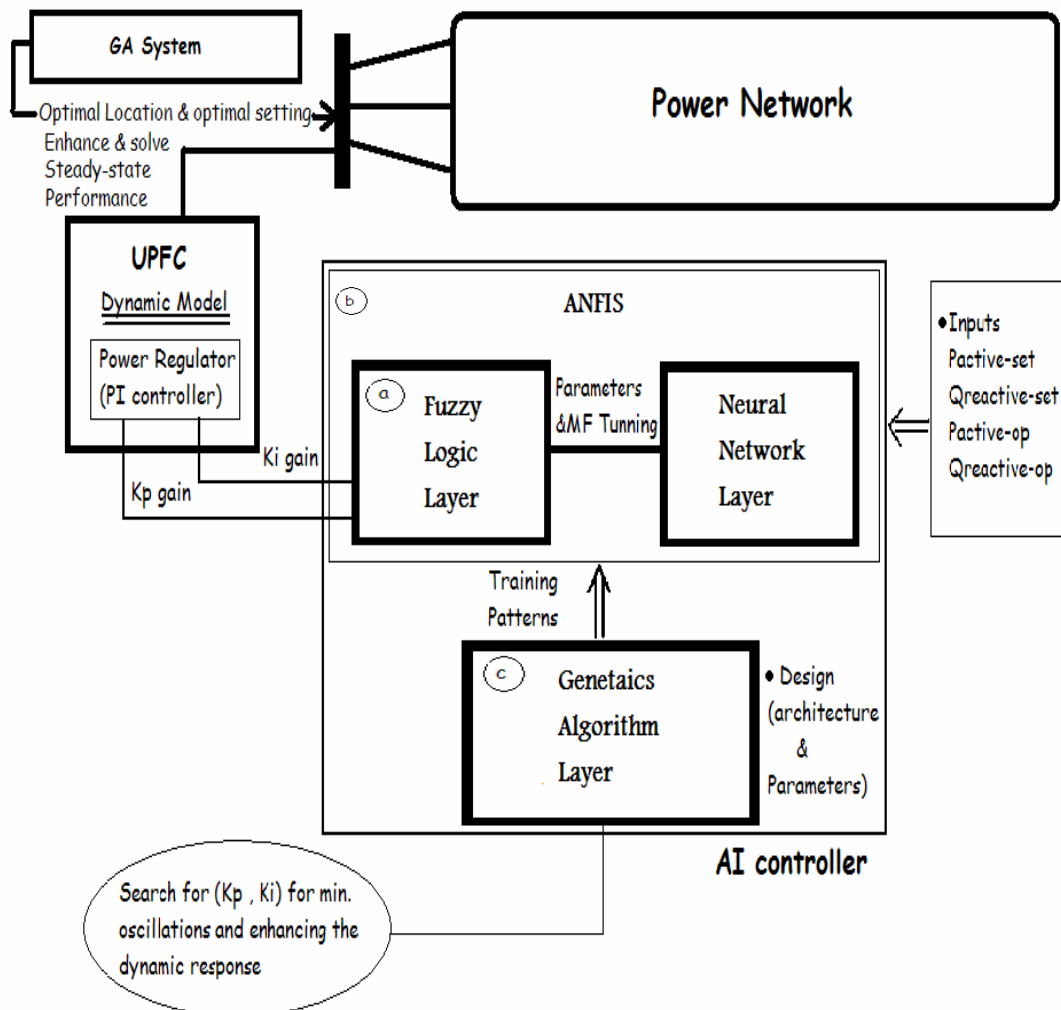


Fig. 5.17 Structure of UPFC adaptive controller.

More details of the inherent structure of the blocks and systems in the general structure of the adaptive controller can be indicated in the following figures.

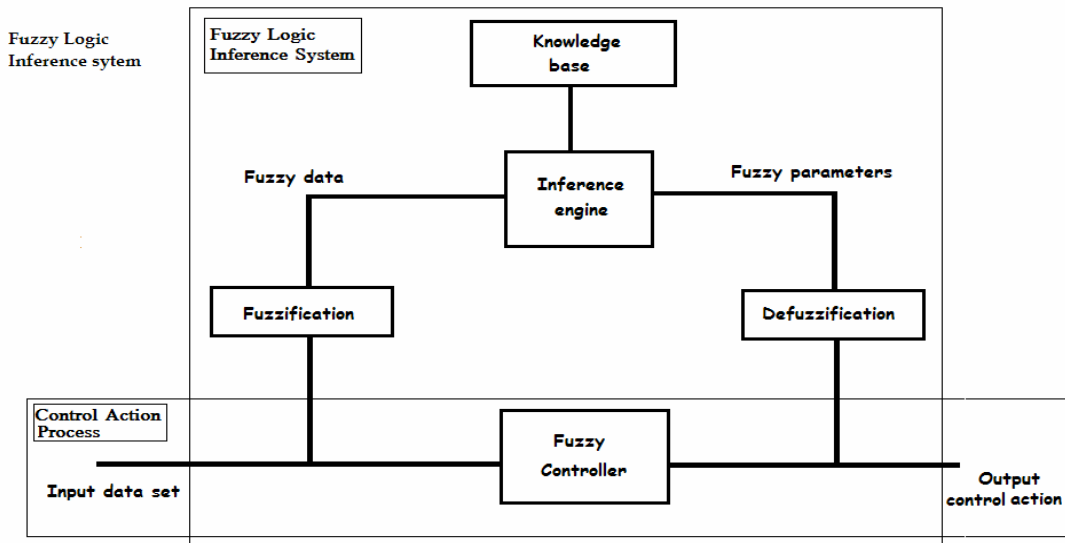


Fig. 5.18 Structure of Fuzzy logic control, section (a).

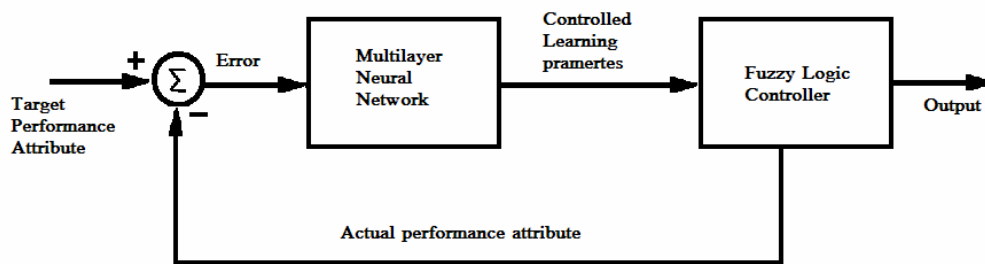


Fig. 5.19 Fuzzy Logic controlled multilayer neural network, section (b).

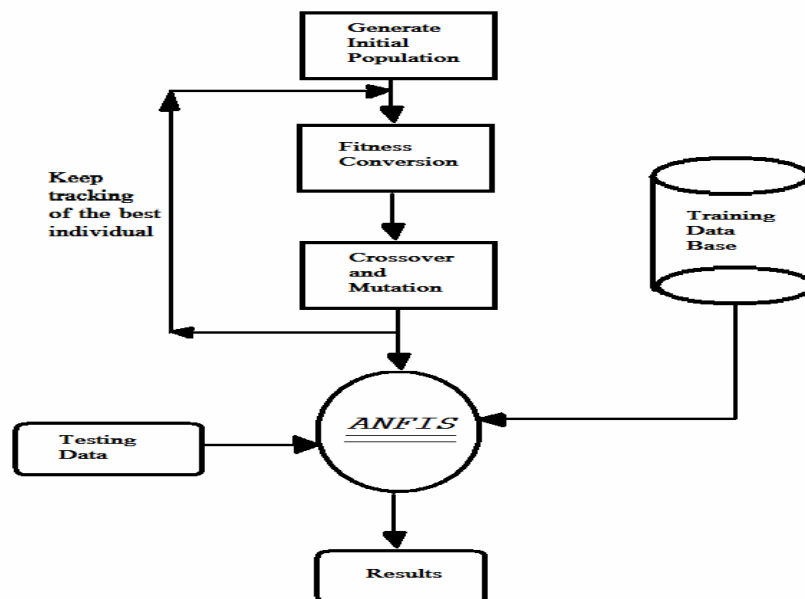
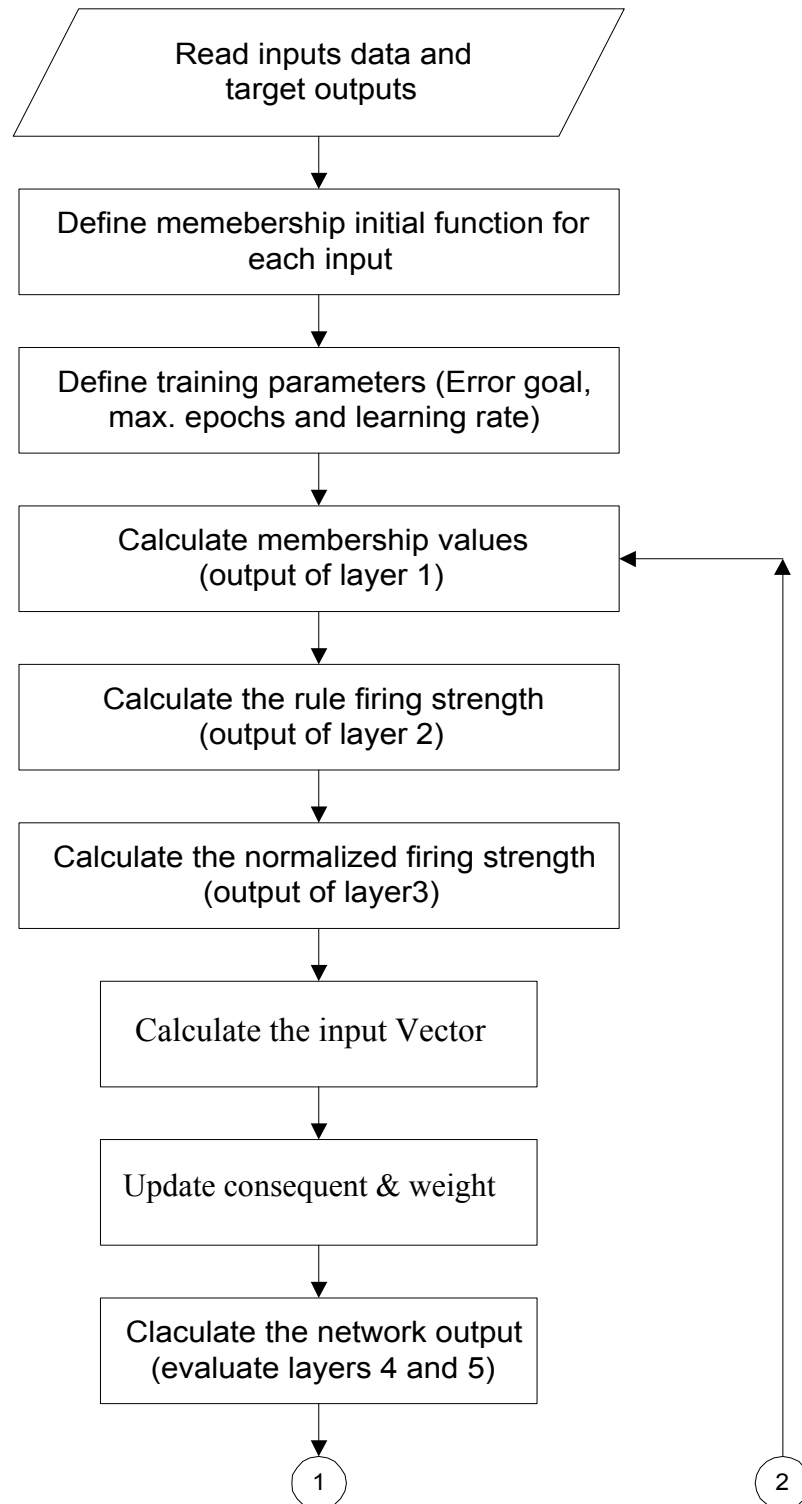


Fig. 5.20 Genetic algorithm linked ANFIS, section (c).

The following flow charts indicate the algorithms of the ANFIS procedure for designing, training and testing. In addition, it shows section of the genetic algorithm, which describes the fitness function.



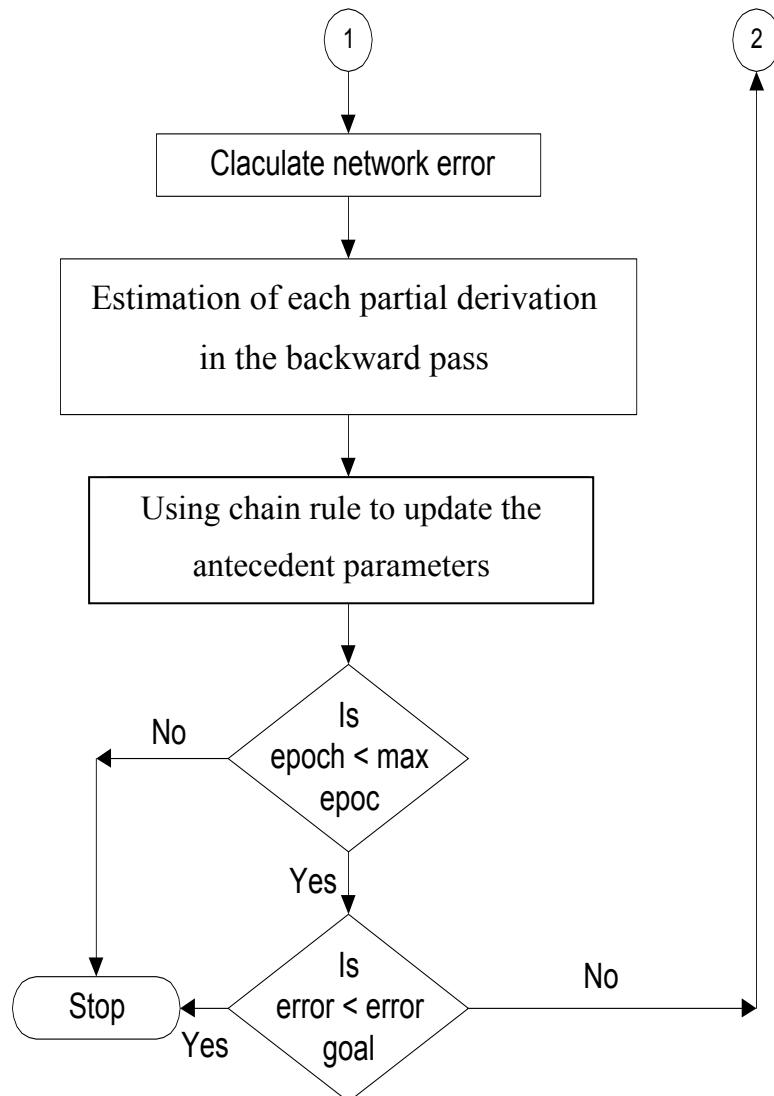


Fig. 5.21 ANFIS Flow chart structure.

Referring to Chapter 3, it describes all the details about ANFIS. Definitions, parameters, equations, relations and procedure sequence are indicated.

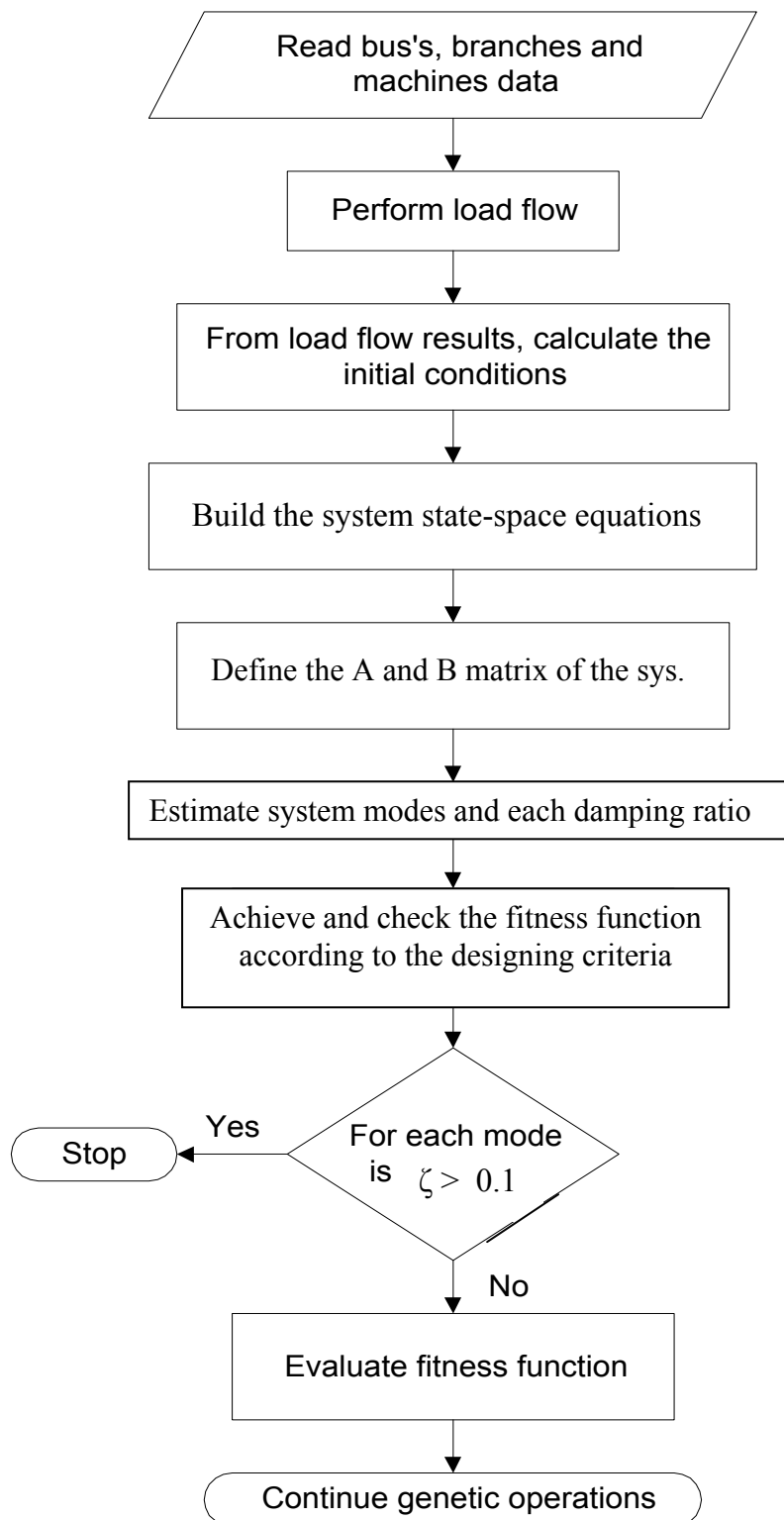


Fig. 5.22 Flow chart for genetic algorithm, describe the fitness function

- **GA System.**

The Genetic algorithm is used to tune the parameters of the P-I controller to obtain the optimal dynamic response for the system. The fitness function of the genetic controller is to minimize the difference between the required designed performance and the current actual performance

$$\text{Fitness function} = \text{Min} \left[\beta * e^{-\alpha * t} R_i(X, U) - R_i(X, U) \right]$$

Where

$R_i(X, U)$: The current actual performance of the dynamic variable i

$\beta * e^{-\alpha * t} R_i(X, U)$: The required designed performance; damped performance of the dynamic variable i . The dynamic variable are the variables as the speed deviation response ($\Delta\omega$) and the mechanical rotor angle ($\Delta\delta$) of the generating units and others, which will be varied according to the adjusting of the dynamic parameters of the UPFC.

U : The designed control variables, the parameters of UPFC controller.

β and α : parameters used for Tuning the controller issue.

According to the operating conditions, you can add some constraints:

- Damping ratio for all modes is not less than 0.1.
- The searching space of K_p and K_i is between ± 3 .

One of operating patterns, Floating point GA with a maximum generation number of 200, population size of 20 and a shape parameter $b = 3$ is used. The solution converged after 120 generations to $K_p = 0.02421$ and $K_i = 0.4514$. The fitness function versus the generation number is shown in Figure 5.23, Because GA minimizes the difference between the required designed performance and the current actual performance, system response with GA based damping controller is a superior based UPFC controller.

The results show the capability of the UPFC to enhance power system performance by controlling its power flow. The GA controller is added to give the UPFC more flexibility and to increase its capability to damp the power system oscillations; where the GA technique is used for tuning of UPFC.

GA will search the parameters space (K_p and K_i) to find the optimal values of the damping controller gains to achieve the fitness function. The floating point GA with maximum generation number of 200 is used. The solution converged after 120 generations to K_p and K_i , these parameters will applied to the system to realize the required dynamic performance.

Table 5.4. Designed values for the GA

GA Parameters	
Input Variables	$x(1) = K_P$ $x(2) = K_I$
Variables Lower bound	LB = [-3 -3];
Variables Upper bound	UB = [3 3];
Options. PopulationType	Double Vector
Options. PopulationSize	20
Options. EliteCount	Adapted (in the simulations)
Options. CrossoverFraction	Adapted (in the simulations)
Options. MigrationDirection	Forward
Options. MigrationInterval	20
Options. MigrationFraction:	0.2
Options. Generations	200

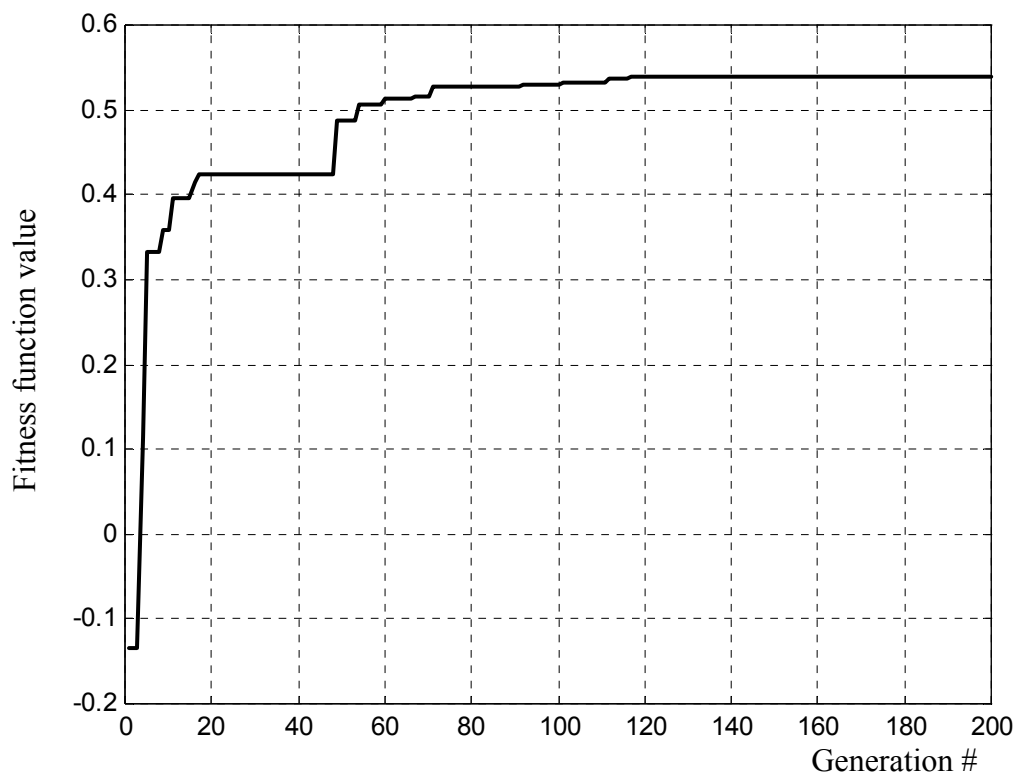


Fig. 5.23, Variation of the fitness function with the generations.

- **ANFIS System.**

In reality, the operating conditions change with time and, as a result, the dynamic performance of the system will change. Thus, to maintain good dynamic response under all possible operating conditions, the controllers' gains need to be adapted based on system operating conditions. ANFIS will be used in this work to adapt the controllers' gains of UPFC controllers in real time. Before ANFIS can be used, it is necessary to determine a proper set of training patterns. Each training pattern comprises a set of input data and corresponding output data. The inputs for ANFIS will be the line active and reactive power (current operating and settled).

For input patterns, we can proceed to determine a set of PI controllers' gains using GA, and the results are employed as the ANFIS outputs. To obtain this data, the operating conditions of the power system is varied covering the situations of light loaded system (25 % of the normal loading) to the highest loading of Year 2020. In addition, conditions such as different generation levels are included.

Trials should be done to choose a suitable number of membership functions to represent the inputs. A low number of membership functions leads to bad learned network, and high error in the network outputs, while a high number of membership functions leads to a complicated structure, to many parameters which have to be updated and a long training time. Input data is represented by a different number of membership functions and finally each input universe of discourse is represented by gaussian membership functions. The training algorithm is used with the following training parameters: learning rate (η) = 0.0001:0.0006, error goal of 0.05 and maximum epochs of 3000. There will be a noticeable change in the membership functions levels before and after training, the training process of adapting the shape and the number of membership functions during the training epochs.

The following figures will indicate the structure and the procedure of the ANFIS system.

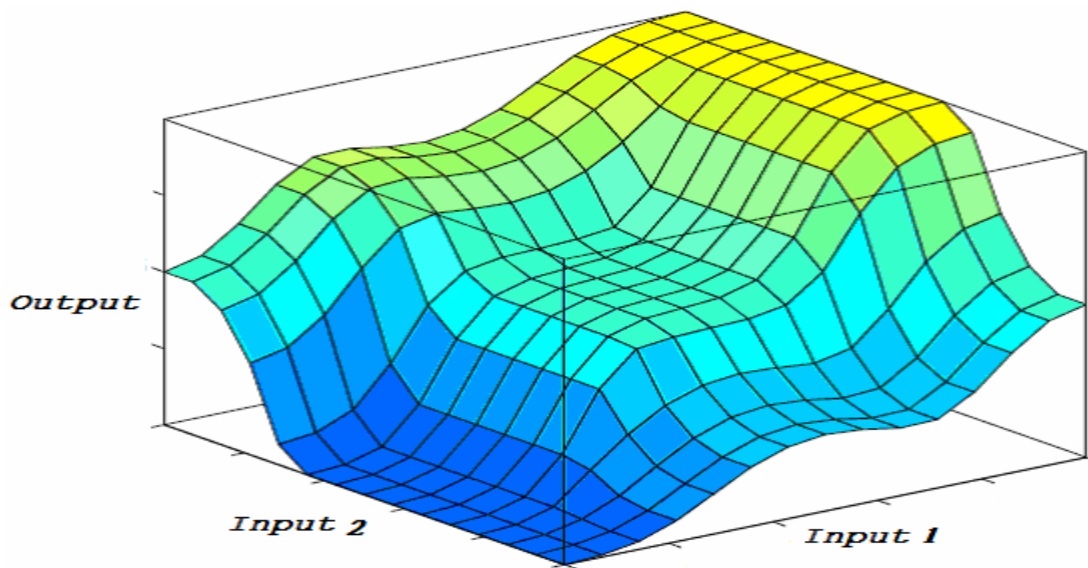


Fig. 5.24 Surface 3D for some input/output relations.

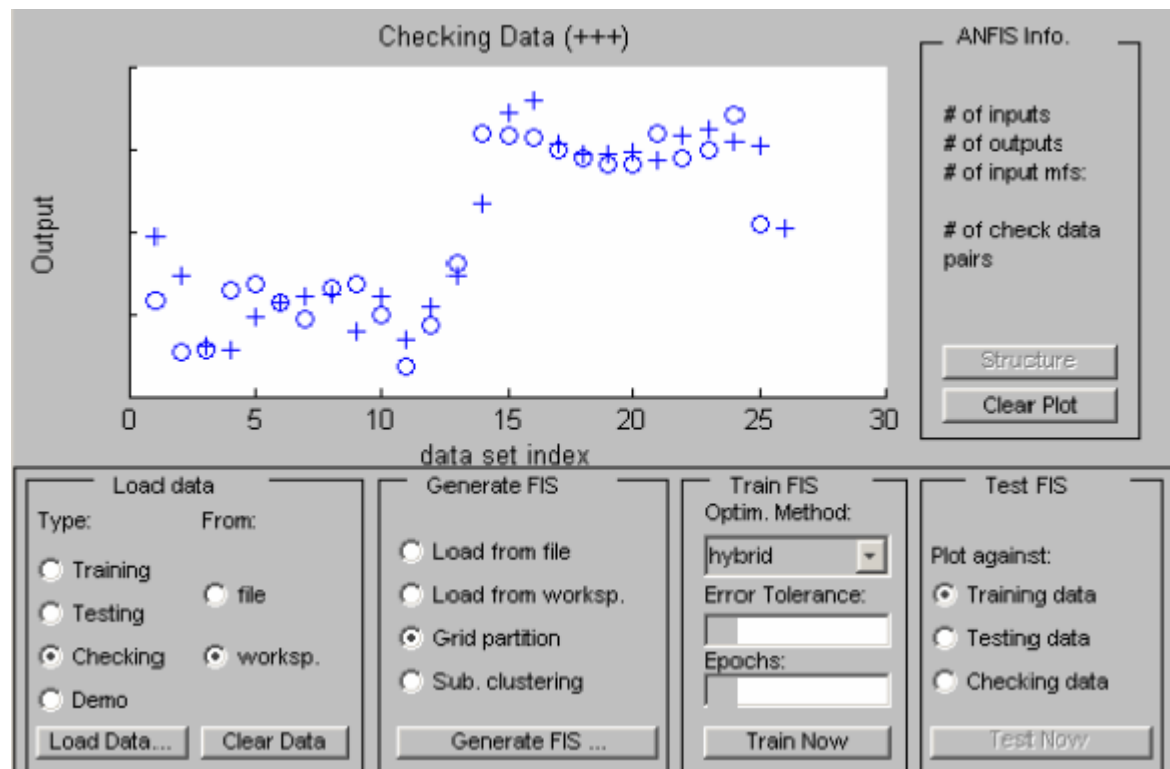


Fig. 5.25 Samples of the training Data, checked and training.

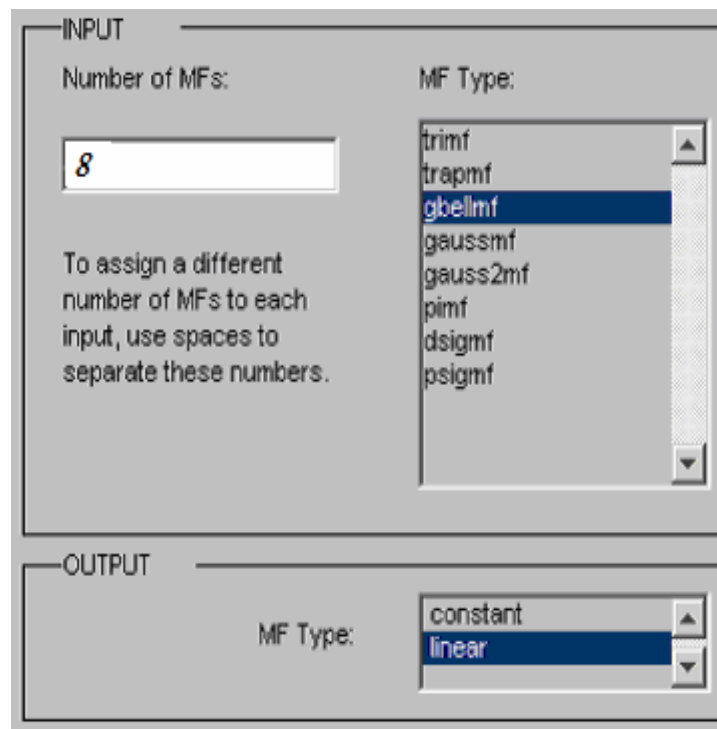


Fig. 5.26 Initial Membership number and shapes for one of inputs.

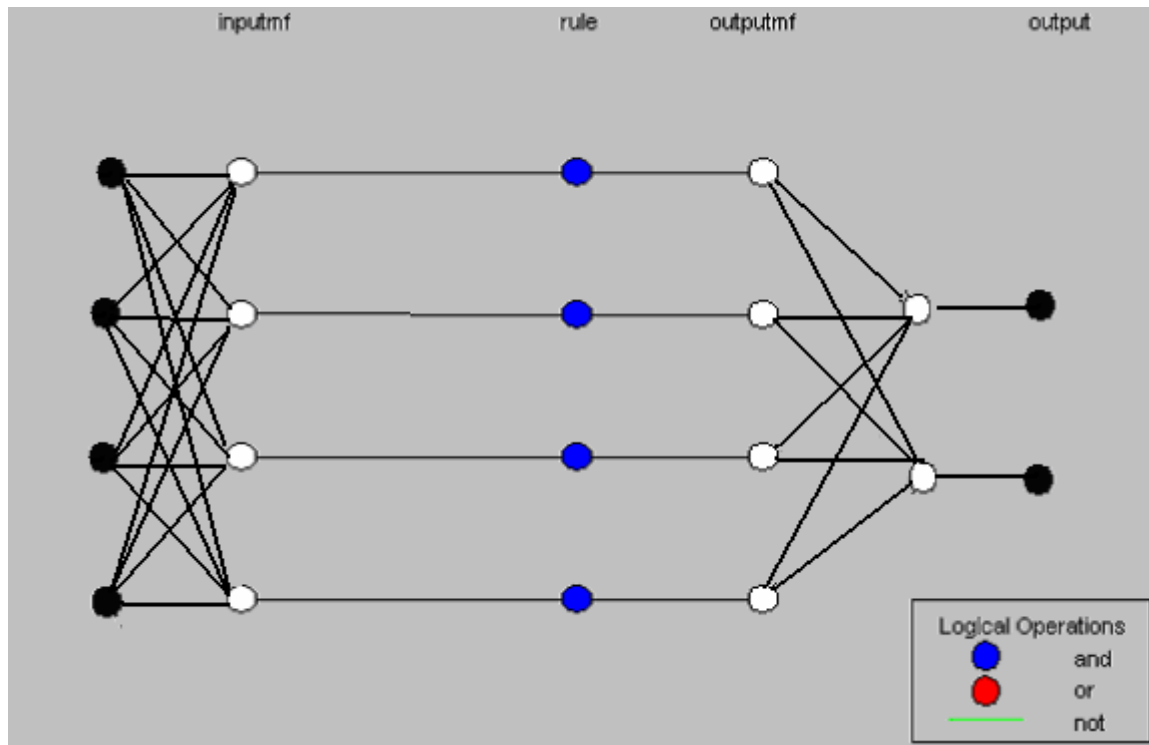


Fig. 5.27 Initial structure of the connected training neural network.

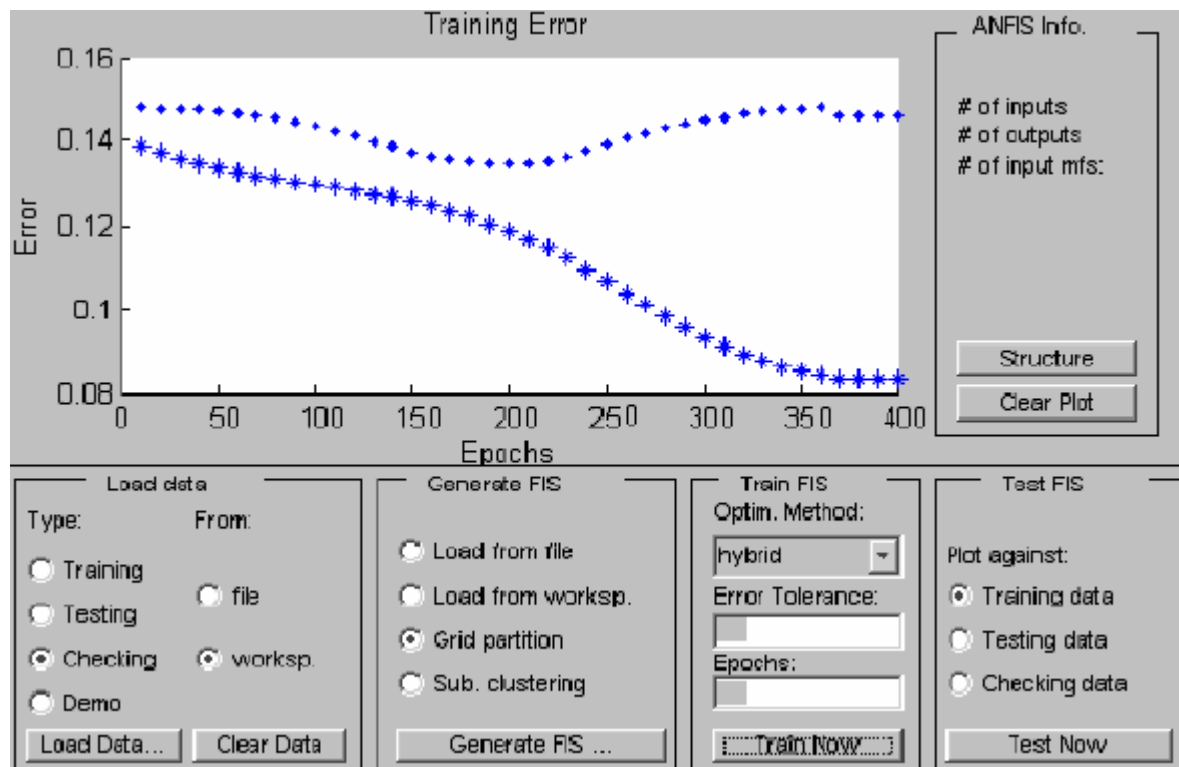


Fig. 5.28 Training and updating of the errors.

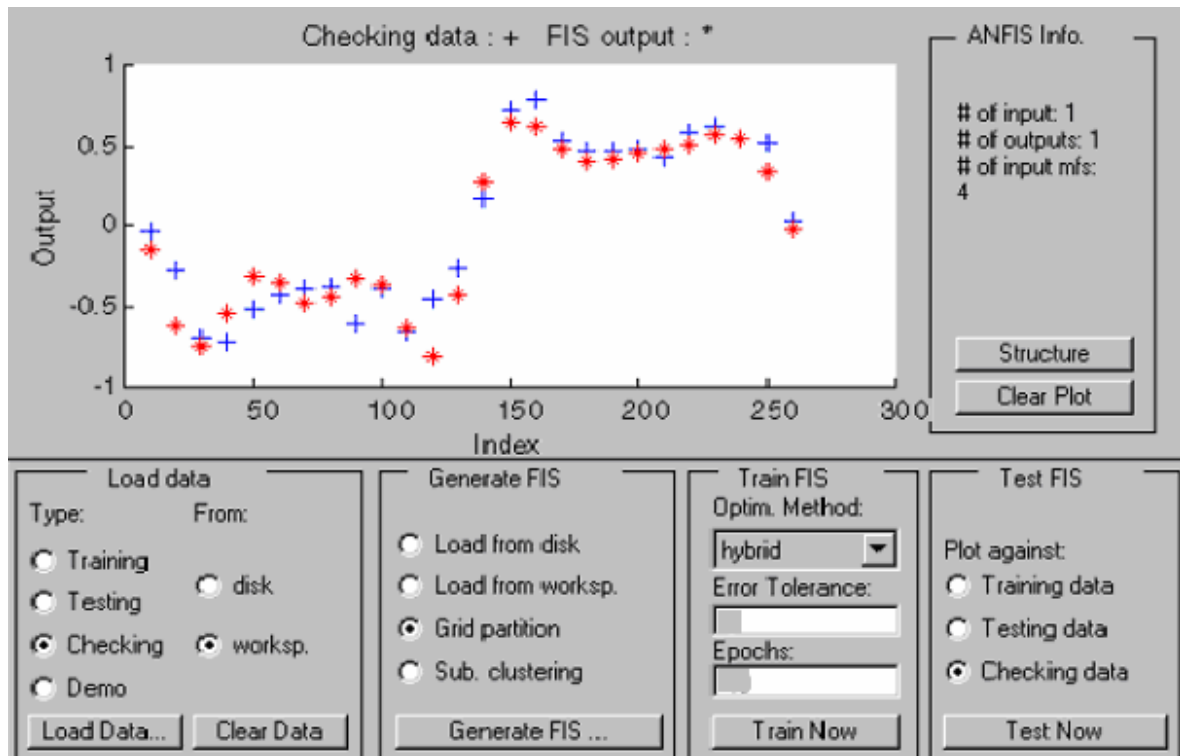


Fig. 5.29 Snapshot of training and updating of the output, checking patterns.

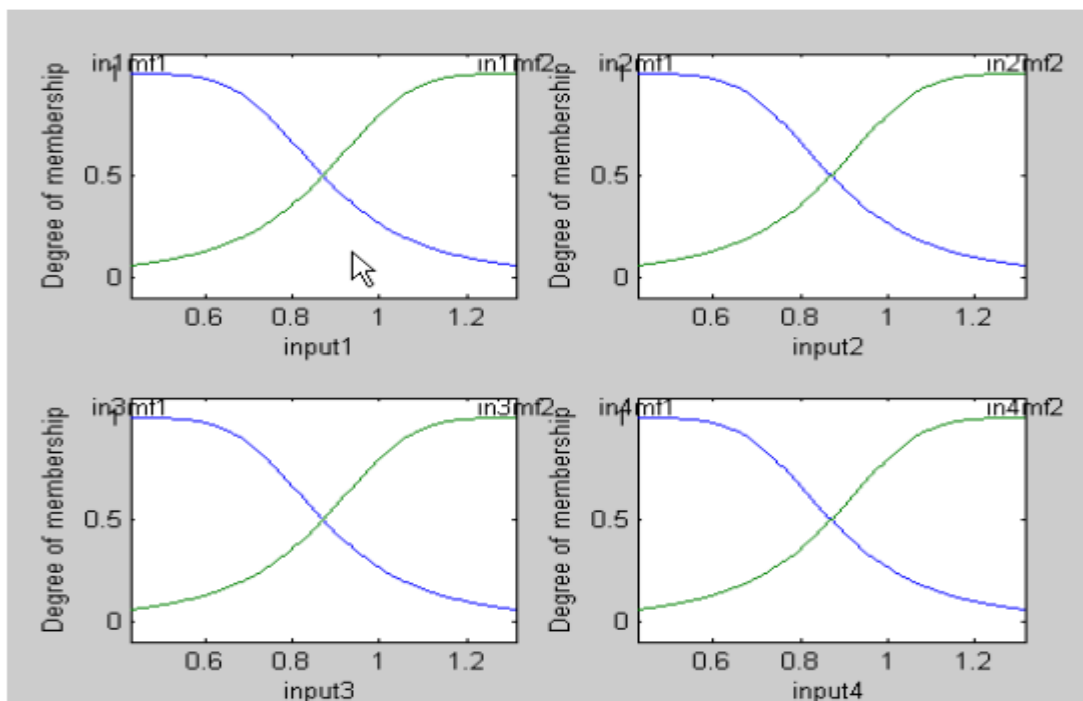


Fig. 5.30 Sample of inputs membership functions during training and updating.

Table 5.5 Snapshot of training of the ANFIS

ANFIS info:		
Number of nodes: 55		
Number of linear parameters: 80		
Number of nonlinear parameters: 24		
Total number of parameters: 104		
Number of training data pairs: 30		
Number of checking data pairs: 21		
Number of fuzzy rules: 16		
number of data is related to number of modifiable parameters		
Start training ANFIS ...		
1	1.41227e-005	1.38815e-005
2	1.34061e-005	1.31808e-005
3	1.27213e-005	1.25105e-005
4	1.2068e-005	1.18707e-005
5	1.14463e-005	1.12615e-005
::	::	::
Step size increases to 0.011000 after epoch 15.		
16	1.08566e-005	1.06836e-005
17	1.02456e-005	1.00849e-005
18	9.67494e-006	9.52589e-006
19	9.14526e-006	9.00735e-006
::	::	::
Step size increases to 0.012100 after epoch 22.		
23	8.65688e-006	8.52974e-006
::	::	::
Designated epoch number reached --> ANFIS training completed at epoch 400.		

Chapter 6

Case Studies

Case Studies

6.1 Introduction

The primary function of the UPFC devices is to control the load flow of the power system. An additional function of them is to add a damping torque component to enhance the dynamic stability of the system. In this chapter, UPFC devices will be generally applied to the power network and especially to real electric power, the Finnish network, HELENSÄHKÖVERKKO OY 110 KV NETWORK. The applied algorithm and technique will be used to solve real problems in this Finnish network.

The optimal locations and the optimal settings will be detected using the AI concepts to reach the best performance area during the normal operation of the network. In addition, the technique will merged with the contingency analysis to solve the overloading issues in the line outage cases and to enhance the network response by detecting the optimal positions and the settings for UPFC. The cases of the contingency study will be ranked with respect to the severity of the outage case, the ranking will be indicated by indices to show the bus voltage profile and the lines rating, the most sever cases will be handled by using the applied technique.

The criteria for the optimality will depend on some fitness functions, these fitness functions will involve the indices terms to include the network buses voltage profile and explain how to reduce the voltage violations of the network. In addition to, the network line loading and explain how to reduce the lines overloading related to the network lines rate. Some comparisons will be achieved in the UPFC settings and locations when we use the bus voltage index only and when we use the line-loading index only and at including both of them.

The mode of UPFC application can be adjusted according to the required characteristics where the UPFC can work as an SVC to improve the network voltage profile by controlling the shunt elements of the UPFC only. And also it can work as an SSSC to improve the network lines loading by controlling the series element of the UPFC only. UPFC has the ability to handle both of SVC and SSSC performance simultaneously, and all of theses UPFC modes will be applied and investigated. The multiple optimal operation issues will be achieved for the UPFC installing by multiple optimization to achieve the optimum technical aspects, and this procedure will be applied for both the normal operation of the network and the contingency operation of the network to keep the performance of the network in a stable range.

The effect of UPFC, in enhancing the dynamics of the system performance and in improving the oscillations damping of the system will be discussed. The dynamic controller will be based on modern control theory with a damping effect and will be designed to insure good damping under various operating conditions and disturbances.

Steady state and dynamic simulation results throughout the thesis are obtained by using the Matlab environment and its various toolboxes such as the Control System Toolbox, Genetic Algorithm and Direct Search and Simulink, and others tools; all the required codes for the simulations are programmed in m-files.

6.2 Helen Network Definition

The main task of the thesis is to solve real problems in a real Finnish network, so we will first present our main network that is our objective application. The Finnish network, HELENSÄHKÖVERKKO OY 110 KV NETWORK, has a total number of buses equal to

24, and the total number of the generators equal 5 generators. The network has in total 42 transmission lines.

The bus data, the load data and the generator data for the network are indicated in table 6.1; the data is in per units where the base value of the voltage 110 KV and the base value of the VA is 100 MVA.

Table 6.2 indicates the data for the network transmission lines, which the transmission line connecting buses, transmission line resistance, transmission line reactance, transmission line substance, and also it indicates MVA rates for the transmission lines. The configuration of the network is indicated in Figure 6.1, showing the type and the length for each line.

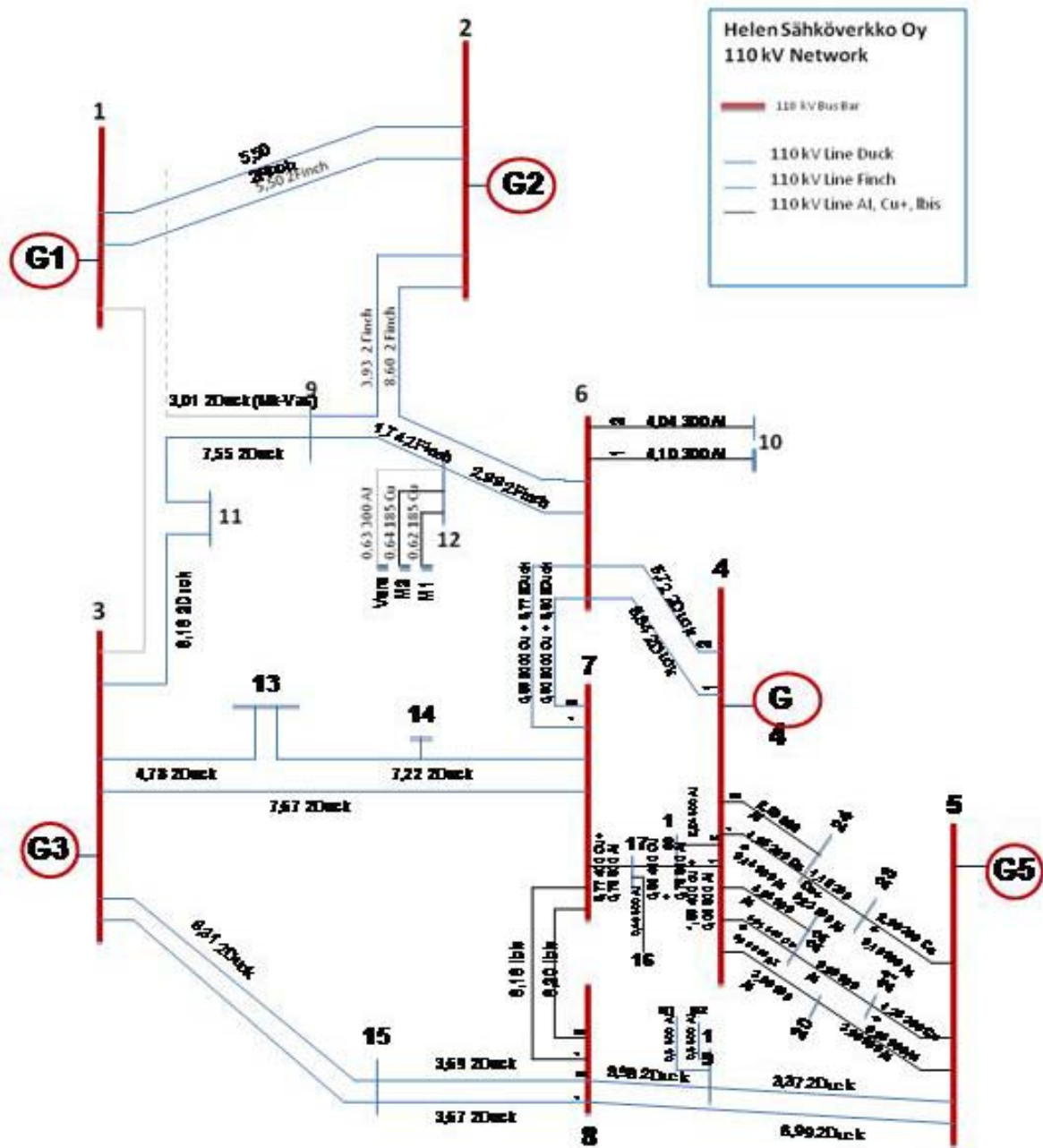


Fig. 6.1 the configuration of HELENSÄHKÖVERKKO OY
110 Kv network.

Table 6.1 Base Bus Data for the System

Bus Type	Bus Type	Vt (p.u.)	θ (degree)	P_g (p.u.)	P_l (p.u.)	Q_l (p.u.)
1	Slack	1.0	0.0	Slack	0	0
2	Gen.	1.0	0.0	5.5900	0.3800	0.0700
3	Gen.	1.0	0.0	1.2240	0	0
4	Gen.	1.0	0.0	0.8950	0.4500	0.1700
5	Gen.	1.0	0.0	1.4970	0.4000	0.1100
6	Load	1.0	0.0	-	0.4500	0.0800
7	Load	1.0	0.0	-	0.9000	0.1300
8	Load	1.0	0.0	-	0.7200	0.1700
9	Load	1.0	0.0	-	0	0
10	Load	1.0	0.0	-	0.2900	0.0230
11	Load	1.0	0.0	-	0.5100	0.0560
12	Load	1.0	0.0	-	0.5700	0.1100
13	Load	1.0	0.0	-	0.6400	0.1000
14	Load	1.0	0.0	-	0.1600	0.0560
15	Load	1.0	0.0	-	0.7400	0.1100
16	Load	1.0	0.0	-	0.1700	0.0630
17	Load	1.0	0.0	-	0.4600	0.0780
18	Load	1.0	0.0	-	0.3600	0.1700
19	Load	1.0	0.0	-	0.3700	0.1000
20	Load	1.0	0.0	-	0.3700	0.1100
21	Load	1.0	0.0	-	0.3100	0.0900
22	Load	1.0	0.0	-	0.4400	0.1000
23	Load	1.0	0.0	-	0.5600	0.1400
24	Load	1.0	0.0	-	0.5000	0.1200

Table 6.2 Base Transmissions Data for the System

T. L. No.	From Bus	To Bus	Impedance		Shunt Susceptance (μ S)	T. L. Rate (MVA)
			R Series Resistance (Ω)	X Series Reactance (Ω)		
1	6	12	0.0820	0.7800	6.5000	410
2	6	4	0.2880	1.6640	11.8000	281
3	6	4	0.2830	1.6390	11.6000	281
4	6	7	0.2710	1.1720	17.2600	225
5	6	7	0.2700	1.1770	17.4000	225
6	6	2	0.2330	2.2850	18.2000	410
7	15	8	0.1810	1.0400	7.5000	281
8	15	8	0.1810	1.0400	7.5000	281
9	15	3	0.4080	2.4400	16.1000	281
10	15	3	0.4080	2.4400	16.1000	281
11	9	2	0.1060	1.0280	8.4000	410
12	19	8	0.1760	1.0300	7.1000	281
13	19	5	0.1640	1.0000	6.4000	281
14	12	9	0.0480	0.4500	3.9000	410
15	8	5	0.3410	2.0700	13.3000	281
16	8	7	0.8760	2.4000	8.8000	110
17	8	7	0.8810	2.4200	8.9000	110
18	3	7	0.3760	2.2100	15.1000	281
19	13	14	0.1775	1.0400	14.3000	281
20	14	7	0.1775	1.0400	14.3000	281
21	3	13	0.2350	1.3700	9.5000	281
22	11	3	0.4040	2.6620	15.7000	281
23	9	11	0.3690	2.2170	14.7000	281
24	2	1	0.1480	1.4560	11.0000	410
25	2	1	0.1480	1.4560	11.0000	410
26	6	10	0.5130	0.5780	97.0000	82
27	6	10	0.5050	0.5700	95.0000	82

Continue Table 6.2 Base Transmissions Data for the System

Trans. Line No.	From Bus	To Bus	Impedance		Shunt Susceptance (μ S)	T. L. Rate (MVA)
			R Series Resistance (Ω)	X Series Reactance (Ω)		
28	21	22	0.0520	0.1140	32	134
29	22	4	0.2670	0.4630	191	104
30	22	4	0.2460	0.5820	143	134
31	23	24	0.1020	0.1960	65	104
32	24	4	0.1590	0.2770	102	104
33	24	4	0.1390	0.3260	81	134
34	23	5	0.2590	0.4070	155	104
35	17	18	0.0890	0.1960	76	120
36	17	7	0.2960	0.5110	243	120
37	17	16	0.0650	0.0880	11	134
38	21	5	0.1780	0.3060	98	104
39	5	20	0.1640	0.3590	102	134
40	4	20	0.1820	0.4430	119	134
41	18	4	0.1130	0.2310	112	134
42	18	4	0.1190	0.2870	70	120

6.3 Application Results on IEEE 6-Bus System

For the validation of the proposed techniques, the GA algorithms have been tested on the following test system, an IEEE-6 bus system (shown in Figure 6.2).

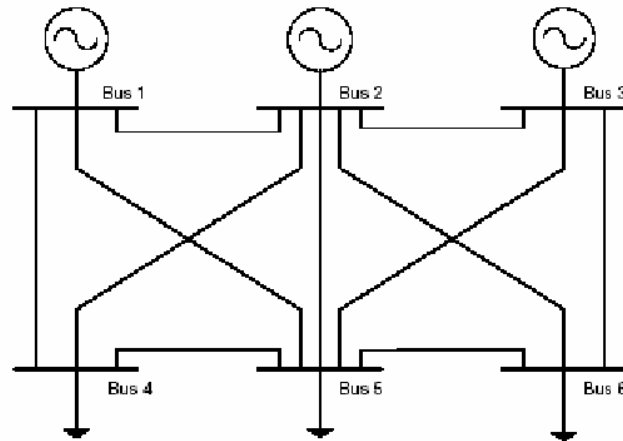


Fig. 6.2, The IEEE 6-Bus System.

This system consists of three generators, six buses, eleven transmission lines, and three loads; the data of the system is shown in Table 6.3

Table 6.3 the data of IEEE 6-Bus System

From Bus	To Bus	Resistance	Reactance	Susbtance	Line Rate(Mw)	Bus	VM
1	2	0.10	0.20	0.02	30		
1	4	0.05	0.20	0.02	50		
1	5	0.08	0.30	0.03	40	1	1.05
2	3	0.05	0.25	0.03	22	2	1.05
2	4	0.05	0.10	0.01	45	3	1.07
2	5	0.10	0.30	0.02	20	4	1.00
2	6	0.07	0.20	0.025	40	5	1.00
3	5	0.12	0.26	0.025	20	6	1.00
3	6	0.02	0.10	0.01	60		
4	5	0.20	0.40	0.04	20		
5	6	0.10	0.30	0.03	20		

Matlab Codes for the techniques were developed for simulation purposes. The following variables are considered as the optimization variables:

- a) The location of the UPFC in the power grid is the first variable in the GA process, and the position for this variable is a certain transmission line in the system where the UPFC should be located.
- b) The series voltage value of the UPFC is the second parameter in the optimization, and the operating range for this parameter is [0.001, 0.3]
- c) The shunt voltage value of the UPFC is considered as the third parameter to be optimized, and the operating range for this parameter is [0.8, 1.2].

6.3.1 Normal Operating with Heavy Loading Pattern

The increasing in the complexity of AC power networks requires a high-performance power flow control system in order to obtain the desired power flow and to enhance static and dynamic stability. One of the most efficient power electronics systems, to satisfy these requirements, is a UPFC (Unified Power Flow Controller) employing self-commutated converters. UPFCs are proven to be effective in power grids in well-developed countries (e.g. USA, Canada, Sweden). The economical viability of these controllers is justified through the long list of benefits that these controllers have, compared to the traditional controllers. UPFC technology can boost power transfer capability by increasing the flexibility of the systems. Power interchange with neighboring countries becomes easier and effective with these controllers.

UPFC can also increase the loadability and the distance to voltage collapse of a power system, so that additional loads can be added in the system without the addition of new transmission and generating facilities. Moreover, the current trend of the deregulated electricity market also favors UPFC in many ways. UPFC in the deregulated electricity market allow the system to be used in a way that is more flexible with increases in various stability margins.

This stage will concern the solving the problems of the network related to overloading of transmission lines and violation of bus voltage profile. This task will be performed on the normal configuration of the system with an increase in the load pattern on the system.

During the results, the index $\dot{K}_{(LOLN)}$ indicates the Lines Over Loaded Number and $\Gamma_{(VBVN)}$: the index which indicates the Violation of Voltage Buses Number. While Y1 will penalize the value of overall overloading for all lines of the system and Y2 will penalize the value of overall voltage violations for all buses of the system. The calculations for Y1 and Y2 will depend on Equations (5.4) and (5.6).

The loading pattern will be increased in uniform rate to create the overloading of the transmission lines, starting from one overloading for one transmission line and so on for multiple overloading in the system. The results will concern comparing the performance of the system before installing UPFC and after installing UPFC at optimal location with optimal settings to achieve the required performance criteria, enhancing the operating conditions of the power system.

Table 6.4 Case Study (1) of IEEE 6-Bus System

Case Study 1							
\Rightarrow Increasing Load Pattern at each bus with 140% (for all Load buses)							
\Rightarrow Before UPFC Installation							
$\dot{K}_{(LOLN)}$	$Y1$	Overloaded Line	Connecting Bus		Overloading %	$\mathcal{A} = \dot{K}_{(LOLN)} + \Gamma_{(VBVN)}$	$Y = Y1 + Y2$
			From	To			
1	0.144	1	1	2	109.56%	1	0.144
\Rightarrow After UPFC Installation							
\Rightarrow Optimal Location Line (10) \equiv Buses (4-5), Optimal Setting (0.0023 , 1.1057)							
$\dot{K}_{(LOLN)} = 0$	$Y1 = 0$	$\Gamma_{(VBVN)} = 0$	$Y2 = 0$	$\mathcal{A} = 0$	$Y = 0$		
\Rightarrow No Overloading , No Voltage Violation $0.95 \leq V_i \leq 1.05$							

Table 6.5 Case Study (2) of IEEE 6-Bus System

Case Study 2							
\Rightarrow Increasing Load Pattern at each bus with 143% (for all Load buses)							
\Rightarrow Before UPFC Installation							
$\dot{K}_{(LOLN)}$	$Y1$	Overloaded Line	Connecting Bus		Overloading %	$\mathcal{A} = \dot{K}_{(LOLN)} + \Gamma_{(VBVN)}$	$Y = Y1 + Y2$
			From	To			
1	0.1595	1	1	2	112.38%	1	0.1595
\Rightarrow After UPFC Installation							
\Rightarrow Optimal Location Line (1) \equiv Buses (1-2), Optimal Setting (0.0242 , 1.1911)							
$\dot{K}_{(LOLN)} = 0$	$Y1 = 0$	$\Gamma_{(VBVN)} = 0$	$Y2 = 0$	$\mathcal{A} = 0$	$Y = 0$		
\Rightarrow No Overloading , No Voltage Violation $0.95 \leq V_i \leq 1.05$							

Table 6.6 Case Study (3) of IEEE 6-Bus System

Case Study 3					
\Rightarrow Increasing Load Pattern at each bus with 145% (for all Load buses)					
\Rightarrow Before UPFC Installation					
$\dot{K}_{(LOLN)} = 2$	$Y1 = 0.2804$	$\mathcal{A} = \dot{K}_{(LOLN)} + \Gamma_{(VBVN)} = 2$		$Y = Y1 + Y2 = 0.2804$	
Overloaded Line	Connecting Bus		Overloading		
	From	To	%		
1	1	2	115.2%		
3	1	5	102%		
\Rightarrow After UPFC Installation					
\Rightarrow Optimal Location Line (1) \equiv Buses (1-2), Optimal Setting (0.008 , 1.1923)					
$\dot{K}_{(LOLN)} = 0$	$Y1 = 0$	$\Gamma_{(VBVN)} = 0$	$Y2 = 0$	$\mathcal{A} = 0$	$Y = 0$
\Rightarrow No Overloading , No Voltage Violation $0.95 \leq V_i \leq 1.05$					

Table 6.7 Case Study (4) of IEEE 6-Bus System

Case Study 4					
\Rightarrow Increasing Load Pattern at each bus with 146% (for all Load buses)					
\Rightarrow Before UPFC Installation					
$\dot{K}_{(LOLN)} = 3$	$Y1 = 0.4072$	$\mathcal{A} = \dot{K}_{(LOLN)} + \Gamma_{(VBVN)} = 3$		$Y = Y1 + Y2 = 0.4072$	
Overloaded Line	Connecting Bus		Overloading		
	From	To	%		
1	1	2	118.04%		
2	1	4	101%		
3	1	5	102.77%		
\Rightarrow After UPFC Installation					
\Rightarrow Optimal Location Line (2) \equiv Buses (1-4), Optimal Setting (0.0425 , 1.194)					
$\dot{K}_{(LOLN)} = 0$	$Y1 = 0$	$\Gamma_{(VBVN)} = 0$	$Y2 = 0$	$\mathcal{A} = 0$	$Y = 0$
\Rightarrow No Overloading , No Voltage Violation $0.95 \leq V_i \leq 1.05$					

Table 6.8 Case Study (5) of IEEE 6-Bus System

Case Study 5					
\Rightarrow Increasing Load Pattern at each bus with 150% (for all Load buses)					
\Rightarrow Before UPFC Installation					
$\dot{K}_{(LOLN)} = 3$	$Y1 = 0.4775$	$\mathcal{A} = \dot{K}_{(LOLN)} + \Gamma_{(VBVN)} = 3$		$Y = Y1 + Y2 = 0.4775$	
Overloaded Line	Connecting Bus		Overloading		
	From	To	%		
1	1	2	123.74%		
2	1	4	103.69%		
3	1	5	107.29%		
\Rightarrow After UPFC Installation					
\Rightarrow Optimal Location Line (1) \equiv Buses (1-2), Optimal Setting (0.0195, 1.1868)					
$\dot{K}_{(LOLN)} = 0$	$Y1 = 0$	$\Gamma_{(VBVN)} = 0$	$Y2 = 0$	$\mathcal{A} = 0$	$Y = 0$
\Rightarrow No Overloading, No Voltage Violation $0.95 \leq V_i \leq 1.05$					

Table 6.9 Case Study (6) of IEEE 6-Bus System

Case Study 6					
\Rightarrow Increasing Load Pattern at each bus with 182% (for all Load buses)					
\Rightarrow Before UPFC Installation					
$\dot{K}_{(LOLN)} = 4$	$Y1 = 2.6363$	$\mathcal{A} = \dot{K}_{(LOLN)} + \Gamma_{(VBVN)} = 4$		$Y = Y1 + Y2 = 2.6363$	
Overloaded Line	Connecting Bus		Overloading		
	From	To	%		
1	1	2	198.90%		
2	1	4	146%		
3	1	5	150.3%		
7	2	6	101%		
\Rightarrow After UPFC Installation					
\Rightarrow Optimal Location Line (1) \equiv Buses (1-2), Optimal Setting (0.001, 1.2)					
$\dot{K}_{(LOLN)} = 0$	$Y1 = 0$	$\Gamma_{(VBVN)} = 0$	$Y2 = 0$	$\mathcal{A} = 0$	$Y = 0$
\Rightarrow No Overloading, No Voltage Violation $0.95 \leq V_i \leq 1.05$					

From the previous results, we can note that all line overloading is cancelled by positioning UPFC in an optimal location with optimal parameters setting by GA. While for the bus voltage profile, the optimal location and settings resulted from the GA keep the voltage profile for all the buses in the system inside the required limit.

6.3.2 Contingency Operating with Outage Pattern

According to the change in network configuration caused by the outage, undesired high or low voltage conditions can appear and thermal limits may be exceeded. Low voltage following an outage may lead to transmission limitations. The maximum acceptable voltage drop sets most major transmission line loading levels and the minimum voltage at line loss would appear at other locations in the network, and may in neighboring systems. The voltage drop due to the loss of a major line can be accompanied by circuit overloads, at the same voltage or at lower voltage levels. The introduction of the FACTS devices extends the possibility that current through a line can be controlled at a reasonable cost enables the large potential of increasing the capacity of existing lines, and the use of one of the FACTS devices to enable corresponding power to flow through such lines under normal and contingency conditions.

This stage is concern with solving the problems of the network related to overloading of transmission lines and the violation of bus voltage profile during the contingency operating with an outage pattern.

A ranking process is performed on the network after the contingency analysis. There will be some single contingencies. For each single line outage, we find the following performance indices $\hat{K}_{(LOLN)}$ and $\Gamma_{(VBVN)}$, which are described in Chapter 5. Then we rank the lines according to the severity of the contingency, in other words, according to $\mathcal{Y} = \hat{K}_{(LOLN)} + \Gamma_{(VBVN)}$. The remaining cases will not be concerned where the total performance indices equal zero.

Table 6.10 Ranking for the severity contingency cases for IEEE 6-bus system

Ranking Case	Line Number	Connecting Bus		$\hat{K}_{(LOLN)}$	$\Gamma_{(VBVN)}$	\mathcal{Y} $= \hat{K}_{(LOLN)} + \Gamma_{(VBVN)}$
		From	To			
1	9	3	6	3	1	4
2	5	2	4	2	1	3
3	2	1	4	1	1	2
4	6	2	5	1	0	1
5	3	1	5	1	0	1
6	4	2	3	1	0	1
7	11	5	6	1	0	1

Table 6.11 Outage Case Study (1) of IEEE 6-Bus System

Outage Case Study 1					
\Rightarrow Outage of Line (9) \equiv (3-6), Severity Rank =1					
\Rightarrow Before UPFC Installation					
$\hat{K}_{(LOLN)} = 3$	$Y1 = 1.3040$	$\Gamma_{(VBVN)} = 1$	$Y2 = 0.0115$	$\mathcal{A} = 4$	$Y = 1.3155$
Overloaded Line	Connecting Bus		Overloading		
	<i>From</i>	<i>To</i>	%		
4	2	3	108.63%		
7	2	6	101%		
8	3	5	180.51%		
Bus Violation		Bus 6			
\Rightarrow After UPFC Installation					
\Rightarrow Optimal Location Line (4) \equiv (2-3), Optimal Setting (0.008, 0.9931)					
$\hat{K}_{(LOLN)} = 1$	One Overloading	Line (8)	Eliminate Overloading at line 4, 7		
$\Gamma_{(VBVN)} = 0$	No Voltage Violation		$0.95 \leq V_i \leq 1.05$		

Table 6.12 Outage Case Study (2) of IEEE 6-Bus System

Outage Case Study 2					
\Rightarrow Outage of Line (5) \equiv (2-4), Severity Rank =2					
\Rightarrow Before UPFC Installation					
$\hat{K}_{(LOLN)} = 2$	$Y1 = 0.3205$	$\Gamma_{(VBVN)} = 1$	$Y2 = 0.0103$	$\mathcal{A} = 3$	$Y = 0.3308$
Overloaded Line	Connecting Bus		Overloading		
	<i>From</i>	<i>To</i>	%		
6	2	5	101%		
8	3	5	121.53%		
Bus Violation		Bus 4			
\Rightarrow After UPFC Installation					
\Rightarrow Optimal Location Line (3) \equiv (1-5), Optimal Setting (0.1779, 0.977)					
$\hat{K}_{(LOLN)} = 0$	No Overloading	$\Gamma_{(VBVN)} = 0$	No Voltage Violation $0.95 \leq V_i \leq 1.05$		

Table 6.13 Outage Case Study (3) of IEEE 6-Bus System

Outage Case Study 3					
\Rightarrow Outage of Line (2) \equiv (1-4), Severity Rank =3					
\Rightarrow Before UPFC Installation					
$\hat{K}_{(LOLN)} = 1$	$Y1 = 0.1560$	$\Gamma_{(VBVN)} = 1$	$Y2 = 0.0068$	$\mathcal{A} = 2$	$Y = 0.1628$
Overloaded Line	Connecting Bus		Overloading %		
	<i>From</i>	<i>To</i>			
5	2	4	111.75%		
Bus Violation		Bus 4			
\Rightarrow After UPFC Installation					
\Rightarrow Optimal Location Line (1) \equiv (1-2), Optimal Setting (0.012, 1.1903)					
$\hat{K}_{(LOLN)} = 0$	No Overloading	$\Gamma_{(VBVN)} = 0$	No Voltage Violation $0.95 \leq V_i \leq 1.05$		

Table 6.14 Outage Case Study (4) of IEEE 6-Bus System

Outage Case Study 4					
\Rightarrow Outage of Line (6) \equiv (2-5), Severity Rank =4					
\Rightarrow Before UPFC Installation					
$\hat{K}_{(LOLN)} = 1$	$Y1 = 0.1716$	$\Gamma_{(VBVN)} = 0$	$Y2 = 0.0$	$\mathcal{A} = 1$	$Y = 0.1716$
Overloaded Line	Connecting Bus		Overloading %		
	<i>From</i>	<i>To</i>			
8	3	5	114.45%		
Bus Violation		---			
\Rightarrow After UPFC Installation					
\Rightarrow Optimal Location Line (3) \equiv (1-5), Optimal Setting (0.1297, 0.8758)					
$\hat{K}_{(LOLN)} = 0$	No Overloading	$\Gamma_{(VBVN)} = 0$	No Voltage Violation $0.95 \leq V_i \leq 1.05$		

Table 6.15 Outage Case Study (5) of IEEE 6-Bus System

Outage Case Study 5					
\Rightarrow Outage of Line (3) \equiv (1-5), Severity Rank =5					
\Rightarrow Before UPFC Installation					
$\dot{K}_{(LOLN)} = 1$	$Y1 = 0.1880$	$\Gamma_{(VBVN)} = 0$	$Y2 = 0.0$	$\mathcal{A} = 1$	$Y = 0.1880$
Overloaded Line	Connecting Bus		Overloading		
	<i>From</i>	<i>To</i>	%		
8	3	5	117.09%		
Bus Violation		---			
\Rightarrow After UPFC Installation					
\Rightarrow Optimal Location Line (9) \equiv (3-6), Optimal Setting (0.1349, 0.9185)					
$\dot{K}_{(LOLN)} = 0$	No Overloading	$\Gamma_{(VBVN)} = 0$	No Voltage Violation $0.95 \leq V_i \leq 1.05$		

Table 6.16 Outage Case Study (6) of IEEE 6-Bus System

Outage Case Study 6					
\Rightarrow Outage of Line (4) \equiv (2-3), Severity Rank =6					
\Rightarrow Before UPFC Installation					
$\dot{K}_{(LOLN)} = 1$	$Y1 = 0.1031$	$\Gamma_{(VBVN)} = 0$	$Y2 = 0.0$	$\mathcal{A} = 1$	$Y = 0.1031$
Overloaded Line	Connecting Bus		Overloading		
	<i>From</i>	<i>To</i>	%		
8	3	5	101%		
Bus Violation		---			
\Rightarrow After UPFC Installation					
\Rightarrow Optimal Location Line (1) \equiv (1-2), Optimal Setting (0.001, 0.8)					
$\dot{K}_{(LOLN)} = 0$	No Overloading	$\Gamma_{(VBVN)} = 0$	No Voltage Violation $0.95 \leq V_i \leq 1.05$		

Table 6.17 Outage Case Study (7) of IEEE 6-Bus System

Outage Case Study 7					
\Rightarrow Outage of Line (11) \equiv (5-6), Severity Rank =7					
\Rightarrow Before UPFC Installation					
$\dot{K}_{(LOLN)} = 1$	$Y1 = 0.1014$	$\Gamma_{(VBVN)} = 0$	$Y2 = 0.0$	$\mathcal{A} = 1$	$Y = 0.1014$
Overloaded Line	Connecting Bus			Overloading	
	<i>From</i>	<i>To</i>		%	
8	3	5		101%	
Bus Violation			---		
\Rightarrow After UPFC Installation					
\Rightarrow Optimal Location Line (2) \equiv (1-4), Optimal Setting (0.012 ,0.9015)					
$\dot{K}_{(LOLN)} = 0$	No Overloading	$\Gamma_{(VBVN)} = 0$	No Voltage Violation $0.95 \leq V_i \leq 1.05$		

From the previous tables, we can find that all bus voltage violations are eliminated by placing UPFC in an optimal location with optimal parameter settings by GA. While for overloaded lines, despite that, placing UPFC in the system did not result in eliminating all of them, but most of overloaded lines are eliminated and the power flow distribution in the rest-overloaded lines is significantly reduced.

The optimal installation of FACTS devices plays a key role in achieving the proper functionality of these devices. The tables, we have simulated, show that the application can efficiently get the proper settings and locations of UPFC. Optimal UPFC in these locations can enhance the performance of a power system by preventing the overloading in lines and the bus voltage violations.

6.3.3 Genetic Algorithms Versus another advanced optimization tool (PSO)

Particle Swarm Optimization (PSO) is a technique based on a stochastic optimization process developed by Dr. Eberhart and Dr. Kennedy in 1995 without explicit knowledge of the gradient of the problem to be optimized. PSO is originally attributed first to be requested for simulating social behavior. The algorithm was simplified and it was observed to be performing optimization.

PSO applies optimization by keeping a population of proposed solutions called particles and moving these particles around in the search-space with respect to simple formulae. The motions of the particles are directed by the best positions in the search-space, which are continually updated as better positions are found by the particles.

Concept of Particle Swarm Optimization (PSO)

PSO participate various identical feature with evolutionary computation methods like Genetic Algorithms (GA). The system is started with a population of stochastic solutions and looks for optimality by updating generations. However, PSO doesnot have evolution process like crossover and mutation. In PSO, the potential solutions are the particles, which move in the problem space by succeeding the current optimum particles.

Each particle maintains track of its coordinates in the space-solution that is accompanied with the best record it has occurred. The fitness is also memorized. This value is called P_{best} . The second best value that is followed by the particle swarm optimizer is the best value, obtained by any particle in the neighbors of the particle. This position is referred as L_{best} . When a particle takes all the population as its topological neighbors, the best value is a global best and is called g_{best} .

The particle swarm optimization idea depends on changing the speed of accelerating of each particle directed to its P_{best} and L_{best} positions. Acceleration is controlled by a random parameter, with separate random values being determined for acceleration directed to P_{best} and L_{best} locations.

Many publications are concerned with choosing well PSO parameters. The method for tuning PSO parameters is called meta-optimization because another optimization method is used in an overlapping way to tune the PSO parameters. The best performing PSO parameters were found to be contrary to the guidelines in the literature and often yielded satisfactory optimization performance for simple PSO variants.

PSO Technique

There is a randomized velocity corresponding to a potential solution, called a particle, and harmonized with individuals. Each particle in PSO moves in the D-dimensional problem space with a speed dynamically adapted with respect to the flying experiences of particles.

The position of the i th particle is described as $X_i = [x_{i1}, x_{i2}, \dots, x_{iD}]$, where, $x_{id} \in [l_d, u_d]$, $d \in [1, D]$. l_d and u_d , are the lower and upper bounds for d th dimension, respectively. The best previous position, which calculates the best fitness value of the i th particle is saved and represented as $P_i = [P_{i1}, P_{i2}, \dots, P_{iD}]$, which is also called P_{best} .

The index of the best particle between all particles in the population is described by the symbol g . The location P_g is also called as g_{best} . The speed of the i th particle is described as $V_i = [v_{i1}, v_{i2}, \dots, v_{iD}]$ and is clamped to a maximum speed $V_{max} = [v_{max1}, v_{max2}, \dots, v_{maxD}]$ which is defined by the designer. At each time step, the particle swarm optimization concept regulates the velocity and location of each particle toward its P_{best} and g_{best} locations according to the following equations

$$v_{id}^{n+1} = wv_{id}^n + c_1r_1^n (P_{id}^n - x_{id}^n) + c_2r_2^n (P_{gd}^n - x_{id}^n)$$

$$x_{id}^{n+1} = x_{id}^n + v_{id}^{n+1}$$

$$i = 1, 2, \dots, m, \quad d = 1, 2, \dots, D$$

Where:

c_1 and c_2 are two positive constants, called cognitive and social parameters respectively, m is the size of the swarm,
 D is the number of members in a particle,
 r_1 and r_2 , are random numbers, uniformly distributed in $[0,1]$,
 n is the pointer of iterations (generations), and
 w is the inertia weight, which achieve a balance between global and local investigation and thus leading to lower iteration to calculate a appropriate optimal solution.

It is specified by the following equation:

$$w = w_{\max} - \frac{w_{\max} - w_{\min}}{iter_{\max}} \times iter$$

Where:

w_{\max} is the initial weight,

w_{\min} is the final weight,

$iter$ is the current iteration number, and

$iter_{\max}$ is the maximum iteration number (generations).

We can summery particle swarm optimization algorithm in steps:

1. Initialise particles in the search space at random.
2. Assign random initial velocities for each particle.
3. Evaluate the fitness of each particle according a user defined objective function.
4. Calculate the new velocities for each particle.
5. Move the particles.
6. Repeat steps 3 to 5 until a predefined stopping criterion is satisfied.

Particle Swarm: Controlling Velocities

- During PSO, it is available for increasing the magnitude of the speed.
- Performance can be improper if V_{\max} is set in the wrong way.
- Several techniques were proposed for controlling the growth of velocities:
 - A effectively updated inertia weight factor,
 - A effectively updated acceleration coefficients
 - Re-initialization of stagnated particles and swarm size.
 - Robust Settings for (c_1 and c_2).

Outline of the Basic Genetic Algorithm

The concept of Genetic algorithms is simulated to Darwin's theory of evolution. GAs were appeared and promoted by John Holland with his research group.

The outline of the GA technique is:

1. Produce stochastic population of n chromosomes (proper solutions for the problem).
2. Calculate the fitness of each chromosome x in the population.
3. Produce a new population by sequencing following actions for ending the new population process.
 - a. Refer to two parent chromosomes from a population with respect to their fitness (the more well fitness, the higher chance to be chosen).
 - b. With a crossover probability cross over the parents to generate new offspring (new children). If no crossover was occurred, children are the exact copies of parents.

- c. With a mutation probability mutate new offspring at each location in chromosome.
4. Locate new offspring in the new population.
5. Apply new generated population for a further run of the algorithm.
6. If the end condition is satisfied, stop, and return the best solution in current population.
7. Go to step 2.

Case Study: IEEE 6-bus System

This system consists of three generators, six buses, eleven transmission lines, and three loads; the data of the system is shown in Table 6.3. Eleven possible single outage contingencies are included. Ranking process is performed on the network after the contingency analysis. The applied GA and PSO algorithms were implemented to find the optimal values of UPFC variables.

The GA parameters and PSO parameters are:

GA parameters	
Parameter	Value
Variables Numbers	3
Population Size	40
Generations Number	100
Crossover Probability	0.85
Mutation Probability	0.1

PSO parameters	
Parameter	Value
Variables Numbers	3
Max. weight	0.8
Min. weight	0.1
Max. iteration	100
c1 , c2	0.5
r1 , r2	[0, 1]
Swarm beings Number	25

Table 6.18: Overloaded lines and bus voltage violations before and after Placing UPFC for IEEE 6-bus system with optimal location and optimal parameters setting of UPFC by GA

Severity	Outaged Line	Without UPFC			UPFC Optimal Location Line No.	UPFC Optimal Settings		With Optimal UPFC		
	Line No. ≡ (From – To) Buses	Voltage Violation Buses	Overloaded Lines	Overloading %		V_{CR}	V_{VR}	Voltage Violation Buses	Overloaded Lines	Overloading %
1	2 ≡ (1 – 4)	Bus 4	1-5 1-2 2-4	106.64 123.53 117.95	10 ≡ (4–5)	0.0517	1.098	-	- - 2-4	- - 111.1
2	3 ≡ (1 – 5)	-	1-4 1-2 3-5	116.24 109.14 104.85	11 ≡ (5–6)	0.1142	1.089	-	1-4 - -	109.1 - -
3	5 ≡ (2 – 4)	Bus 4	1-4 3-5	159.95 105.85	10 ≡ (4–5)	0.0769	1.059	-	1-4 -	112.8 -
4	9 ≡ (3 – 6)	Bus 6	2-6 3-5	128.97 145.39	11 ≡ (5–6)	0.2169	1.090	-	- -	- -
5	7 ≡ (2 – 6)	-	2-3 3-6	137.25 115.35	11 ≡ (5–6)	0.0534	1.099	-	- -	- -
6	6 ≡ (2 – 5)	-	3-5	103.54	2 ≡ (1–4)	0.2010	1.088	-	-	-

Table 6.19: Overloaded lines and bus voltage violations before and after placing UPFC for IEEE 6-bus system with optimal location and optimal parameters setting of UPFC by PSO

Severity	Outaged Line	Without UPFC			UPFC Optimal Location Line No.	UPFC Optimal Settings		With Optimal UPFC		
	Line No. ≡ (From - To) Buses	Voltage Violation Buses	Overloaded Lines	Overloading %		V_{CR}	V_{VR}	Voltage Violation Buses	Overloaded Lines	Overloading %
1	2 ≡ (1 - 4)	Bus 4	1-5 1-2 2-4	106.64 123.53 117.95	6 ≡ (2-5)	0.2081	1.041	-	- - 2-4	- - 116.2
2	3 ≡ (1 - 5)	-	1-4 1-2 3-5	116.24 109.14 104.85	10 ≡ (4-5)	0.2035	1.1	-	1-4 - -	114.7 - -
3	5 ≡ (2 - 4)	Bus 4	1-4 3-5	159.95 105.85	10 ≡ (4-5)	0.1424	1.0291	-	1-4 -	124.1 -
4	9 ≡ (3 - 6)	Bus 6	2-6 3-5	128.97 145.39	11 ≡ (5-6)	0.1173	1.0564	-	- -	- -
5	7 ≡ (2 - 6)	-	2-3 3-6	137.25 115.35	11 ≡ (5-6)	0.0946	1.0361	-	- -	- -
6	6 ≡ (2 - 5)	-	3-5	103.54	10 ≡ (4-5)	0.0776	1.0913	-	-	-

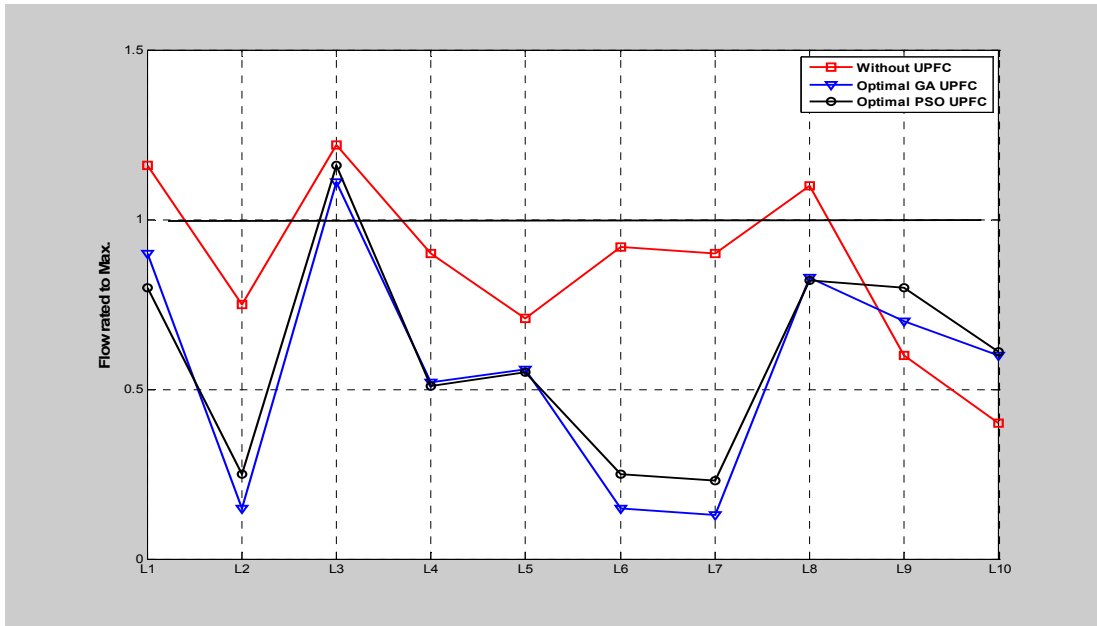


Fig. 6.3: Power flow distribution for IEEE 6-bus system when line 2 is outage by GA and PSO.

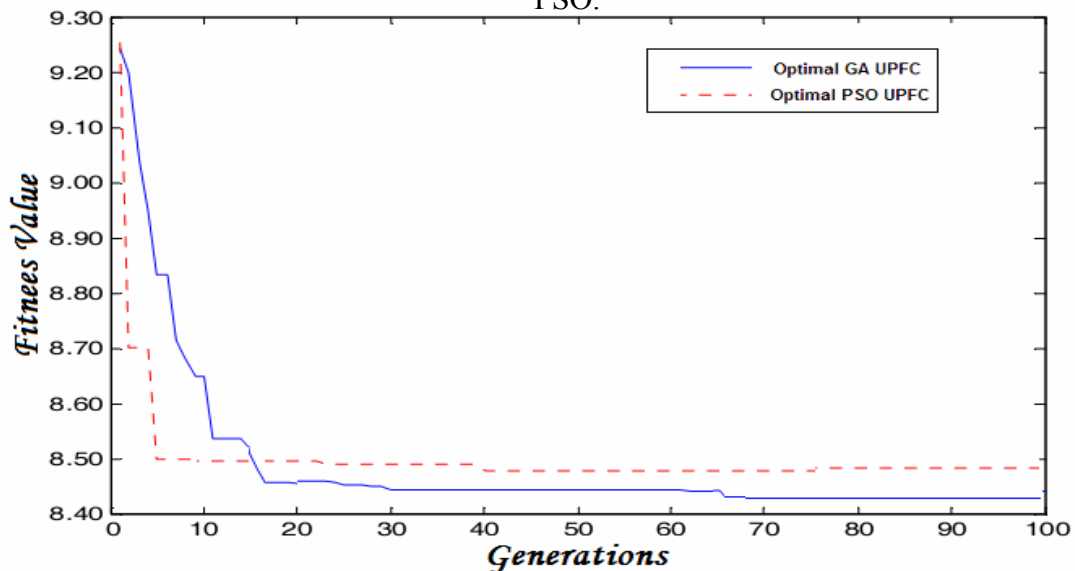


Fig. 6.4: Minimization of the objective function by both GA and PSO techniques for IEEE 6-bus system when line 2 is outage.

Analyzing the simulation results, from the convergence point of view, it is clear that with the increase of generation, it can be noted that the performance of GA is better than the performance of PSO as indicated. This is because the GA technique has selection, crossover, and mutation actions, while PSO doesnot have such actions; the GA more efficient and effective to achieve the optimal solution. The solutions, which we got from the GA, minimize the overloading better than the ones through PSO. The most advantageous part in GA that we apply the rules of evolution to the individuals. GA finds the individuals with the best suggestions to the problem and then combine these individuals into new individuals. Using this method repeatedly, the population will evolve good solutions. Specifically, the elements of a GA are: selection, cross-over, and mutation. As we can see, Darwin's principles have been a major inspiration to GAs.

A GA owns many advantages. It can quickly scan a vast solution group. Unwell solutions do not affect the final results negatively as they are simply disappearing.

6.4 Application Results on IEEE Large Scale 57-Bus System

For the validation of the proposed technique on a large-scale power system, it has been tested on the following test system, an IEEE-57 bus system. This system consists of seven generators, fifty-seven buses, and eighty transmission lines.

6.4.1 Normal Operating with Heavy Loading Pattern

This stage concerns solving a network problem related to the overloading of transmission lines. This will be performed on the normal configuration of the system with increasing the load pattern on the system.

Table 6.20 Case Study (1) of IEEE 57-Bus System

⇒ Increasing Load Pattern at each bus with 120% (for all Load buses)					
⇒ Before UPFC Installation					
$\dot{K}_{(LOLN)}$	YI	Overloaded Line	From Bus	To Bus	Overloading %
1	0.1573	8	8	9	112%
⇒ After UPFC Installation					
⇒ Optimal Location Line (18) ≡ (3-15), Optimal Setting (0.2997, 1.1995)					
$\dot{K}_{(LOLN)} = 0$		$YI = 0$	- No Overloading		

Table 6.21 Case Study (2) of IEEE 57-Bus System

⇒ Increasing Load Pattern at each bus with 150% (for all Load buses)					
⇒ Before UPFC Installation					
$\dot{K}_{(LOLN)}$	YI	Overloaded Line	From Bus	To Bus	Overloading %
1	0.236	8	8	9	103.77 %
		15	1	15	104.82 %
⇒ After UPFC Installation					
⇒ Optimal Location Line (18) ≡ (3-15), Optimal Setting (0.13241, 1.2)					
$\dot{K}_{(LOLN)} = 0$		$YI = 0$	- No Overloading		

From the previous simulations, we can note that all line overloading is prevented by applying an optimal installation of UPFC using GA. That means the applied technique is successful in achieving the desired performance.

6.4.2 Contingency Operating with Outage Pattern

This stage is to do with solving the problems of the network related to overloading of transmission lines during the contingency operating with a single outage pattern.

Table 6.22 Outage Case Study (1) of IEEE 57-Bus System

Outage Case Study 1			
\Rightarrow Outage of Line (8) \equiv (8-9)			
\Rightarrow Before UPFC Installation			
$\dot{K}_{(LOLN)} = 1$	$YI = 0.1558$		- One overloading
Overloaded Line	Connecting Bus		Overloading %
	From	To	
21	7	8	111.73 %
\Rightarrow After UPFC Installation			
\Rightarrow Optimal Location Line (6) \equiv (6-7), Optimal Setting (0.02387, 0.8002)			
$\dot{K}_{(LOLN)} = 0$	$YI = 0.0$		- No Overloading

Table 6.23 Outage Case Study (2) of IEEE 57-Bus System

Outage Case Study 2			
\Rightarrow Outage of Line (15) \equiv (1-15)			
\Rightarrow Before UPFC Installation			
$\dot{K}_{(LOLN)} = 2$	$YI = 0.2452$		- Two overloading
Overloaded Line	Connecting Bus		Overloading %
	From	To	
1	1	2	102 %
8	8	9	108.37 %
\Rightarrow After UPFC Installation			
\Rightarrow Optimal Location Line (8) \equiv (8-9), Optimal Setting (0.10438, 0.8)			
$\dot{K}_{(LOLN)} = 0$	$YI = 0.0$		- No Overloading

6.5 Application Results on HELENSÄHKÖVERKKO OY 110 KV NETWORK

The data of HELENSÄHKÖVERKKO OY 110 KV NETWORK was introduced in Table 6.1 and Table 6.2. In addition, the configuration of the network was indicated in Figure 6.1. The load and generation data are valid through Aalto (TKK) University. The data is taken for 24 hours each day monthly for twelve months. The applications of UPFC for this network will be studied until the year 2020 using the load forecasting coefficient which will be available until the year 2020. To show the effectiveness of the UPFC installation, the design of the UPFC will be applied for the worst cases, which are the highest loading conditions, of each loading value at each bus at the same time. This procedure will be applied for current loading pattern and also for the worst cases of the year 2020. Increasing load patterns will be performed with two procedures, the first one is multiplying all the entire loads in the system by increasing the percentage factor. The second one is multiplying all the entire loads in the system by their individual forecasted load coefficient for the future year. The contingency analysis with outage cases will be enhanced through the UPFC installation. This analysis will also be studied through the worst case scenario with the maximum load value at each bus at the same time in the current loading pattern until the year 2020 conditions. Estimating loadability of a generation and transmission system is practically important in power system operations and planning. Increasing the loadability of the system will be indicated during the analysis to measure the utilization of the network after the UPFC installation. The loadability of the transmission grid will be calculated according to the transmission lines flow related to the transmission lines maximum capacity, for all the transmission lines, considering the number of the lines to get the total average loadability. The enhancement in the loadability is achieved in some cases as additional benefits besides the main objective of minimizing overloading and voltage violations. Simulations show that UPFC can be used to enhance loadability in the power system even with solving one, two or more in overloading boundaries. UPFC is a powerful control device that can efficiently control powerful, both transmitted real and reactive flows power as well as bus independently voltages.

6.5.1 Normal Operating with Heavy Loading Pattern until 2020

This stage deals with enhancing the performance of the network related to the overloading of the transmission lines and violation of the bus voltage profile. This task will be performed on the normal configuration of the system with an increasing load pattern on the system until the year 2020.

Table 6.24 Case Study (1) of HELEN Network

Case Study 1					
- Normal Loading (Base Case) Max. Load for each load bus at the same time - Before UPFC Installation					
$\dot{K}_{(LOLN)} = 0$	$Y1 = 0$		$\mathcal{A} = \dot{K}_{(LOLN)} + \Gamma_{(VBVN)} = 0$		$Y = Y1 + Y2 = 0$
Loadability			24.04 %		
\Rightarrow After Optimal UPFC Installation: Location (4 \equiv 6-7), Setting (0.1219 , 0.996)					
$\dot{K}_{(LOLN)} = 0$	$Y1 = 0$	$\Gamma_{(VBVN)} = 0$	$Y2 = 0$	$\mathcal{A} = 0$	$Y = 0$
Loadability			24.1512%		
- No Overloading , No Voltage Violation				$0.98 \leq V_i \leq 1.02$	

Table 6.25 Case Study (2) of HELEN Network

Case Study 2					
\Rightarrow Max. Load for each load bus at the same time with 110% increase for all.					
\Rightarrow Before UPFC Installation					
$\dot{K}_{(LOLN)} = 0$	$Y1 = 0$	$\mathcal{A} = \dot{K}_{(LOLN)} + \Gamma_{(VBVN)} = 0$		$Y = Y1 + Y2 = 0$	
Loadability			28.17%		
\Rightarrow After UPFC Installation					
\Rightarrow Optimal Location Line (2) \equiv (6-4), Optimal Setting (0.0573 , 0.8286)					
$\dot{K}_{(LOLN)} = 0$	$Y1 = 0$	$\Gamma_{(VBVN)} = 0$	$Y2 = 0$	$\mathcal{A} = 0$	$Y = 0$
Loadability			30.5788%		
\Rightarrow No Overloading , No Voltage Violation $0.98 \leq V_i \leq 1.02$					

Table 6.26 Case Study (3) of HELEN Network

Case Study 3					
\Rightarrow Max. Load for each load bus at the same time with 115% increase for all.					
\Rightarrow Before UPFC Installation					
$\dot{K}_{(LOLN)} = 0$	$Y1 = 0$	$\mathcal{A} = \dot{K}_{(LOLN)} + \Gamma_{(VBVN)} = 0$		$Y = Y1 + Y2 = 0$	
Loadability			30.26%		
\Rightarrow After UPFC Installation					
\Rightarrow Optimal Location Line (2) \equiv (6-4), Optimal Setting (0.0036 , 0.934)					
$\dot{K}_{(LOLN)} = 0$	$Y1 = 0$	$\Gamma_{(VBVN)} = 0$	$Y2 = 0$	$\mathcal{A} = 0$	$Y = 0$
Loadability			31.454%		
\Rightarrow No Overloading , No Voltage Violation $0.98 \leq V_i \leq 1.02$					

Table 6.27 Case Study (4) of HELEN Network

Case Study 4					
\Rightarrow Max. Load for each load bus at the same time with 118% increase for all.					
\Rightarrow Before UPFC Installation					
$\dot{K}_{(LOLN)} = 1$	$Y1 = 0.1124$	$\mathcal{A} = \dot{K}_{(LOLN)} + \Gamma_{(VBVN)} = 1$		$Y = Y1 + Y2 = 0.1124$	
Loadability			31.52%		
Overloaded Line (11) \equiv (9-2)			102.96%		
\Rightarrow After UPFC Installation					
\Rightarrow Optimal Location Line (22) \equiv (11-3), Optimal Setting (0.1366 , 1.1958)					
$\dot{K}_{(LOLN)} = 0$	$Y1 = 0$	$\Gamma_{(VBVN)} = 0$	$Y2 = 0$	$\mathcal{A} = 0$	$Y = 0$
Loadability			34.8819%		
\Rightarrow No Overloading , No Voltage Violation $0.98 \leq V_i \leq 1.02$					

Table 6.28 Case Study (5) of HELE Network

Case Study 5					
\Rightarrow Max. Load for each load bus at the same time with 120% increase for all.					
\Rightarrow Before UPFC Installation					
$\dot{K}_{(LOLN)} = 1$	$Y1 = 0.1242$	$\mathcal{A} = \dot{K}_{(LOLN)} + \Gamma_{(VBVN)} = 1$		$Y = Y1 + Y2 = 0.1242$	
Loadability			32.37%		
Overloaded Line (11) \equiv (9-2)			105.56%		
\Rightarrow After UPFC Installation					
\Rightarrow Optimal Location Line (22) \equiv (11-3), Optimal Setting (0.1508 , 0.9716)					
$\dot{K}_{(LOLN)} = 0$	$Y1 = 0$	$\Gamma_{(VBVN)} = 0$	$Y2 = 0$	$\mathcal{A} = 0$	$Y = 0$
Loadability			37.1451%		
\Rightarrow No Overloading , No Voltage Violation $0.98 \leq V_i \leq 1.02$					

Table 6.29 Case Study (6) of HELEN Network

Case Study 6					
\Rightarrow Max. Load for each load bus at the same time multiplied by 96% of 2020 coefficient.					
\Rightarrow Before Optimal UPFC (UPFC at line 13, for case 90% of 2020 coefficient)					
$\dot{K}_{(LOLN)} = 2$	$Y1 = 0.2328$	$\mathcal{A} = \dot{K}_{(LOLN)} + \Gamma_{(VBVN)} = 2$	$Y = Y1 + Y2 = 0.2328$		
Loadability			35.42%		
Overloaded Line (11) \equiv (9-2)			107%		
Overloaded Line (36) \equiv (7-17)			101%		
\Rightarrow After UPFC Installation					
\Rightarrow Optimal Location Line (22) \equiv (11-3), Optimal Setting (0.1812, 0.9356)					
$\dot{K}_{(LOLN)} = 0$	$Y1 = 0$	$\Gamma_{(VBVN)} = 0$	$Y2 = 0$	$\mathcal{A} = 0$	$Y = 0$
Loadability			37.23%		
\Rightarrow No Overloading, No Voltage Violation $0.98 \leq V_i \leq 1.02$					

Table 6.30 Case Study (7) of HELEN Network

Case Study 7					
\Rightarrow Max. Load for each load bus at the same time multiplied by 98% of 2020 coeff.					
\Rightarrow Before Optimal UPFC (UPFC at line 22, for case 96% of 2020 coefficient)					
$\dot{K}_{(LOLN)} = 2$	$Y1 = 0.2068$	$\mathcal{A} = \dot{K}_{(LOLN)} + \Gamma_{(VBVN)} = 2$	$Y = Y1 + Y2 = 0.2068$		
Overloaded Line (11) \equiv (9-2)			102.07%		
Overloaded Line (36) \equiv (7-17)			101%		
\Rightarrow After UPFC Installation					
\Rightarrow Optimal Location Line (14) \equiv (12-9), Optimal Setting (0.196, 1.0928)					
$\dot{K}_{(LOLN)} = 0$	$Y1 = 0$	$\Gamma_{(VBVN)} = 0$	$Y2 = 0$	$\mathcal{A} = 0$	$Y = 0$
\Rightarrow No Overloading, No Voltage Violation $0.98 \leq V_i \leq 1.02$					

Table 6.31 Case Study (8) of HELEN Network

Case Study 8					
\Rightarrow Max. Load for each load bus at the same time multiplied by 98% of 2020 coefficient.					
\Rightarrow Before UPFC installation.					
$\dot{K}_{(LOLN)} = 1$	$Y1 = 0.1487$	$\mathcal{A} = \dot{K}_{(LOLN)} + \Gamma_{(VBVN)} = 1$	$Y = Y1 + Y2 = 0.1487$		
Overloaded Line (11) \equiv (9-2)		110.42%			
\Rightarrow After UPFC Installation					
\Rightarrow Optimal Location Line (14) \equiv (12-9), Optimal Setting (0.2032, 0.8447)					
$\dot{K}_{(LOLN)} = 0$	$Y1 = 0$	$\Gamma_{(VBVN)} = 0$	$Y2 = 0$	$\mathcal{A} = 0$	$Y = 0$
\Rightarrow No Overloading, No Voltage Violation $0.98 \leq V_i \leq 1.02$					

Table 6.32 Case Study (9) of HELEN Network

Case Study 9					
\Rightarrow Max. Load for each load bus at the same time multiplied by 100% 2020 coeff.					
\Rightarrow Before Optimal UPFC (UPFC at line 14, for case 98% of 2020 coefficient)					
$\dot{K}_{(LOLN)} = 2$	$Y1 = 0.2091$	$\mathcal{A} = \dot{K}_{(LOLN)} + \Gamma_{(VBVN)} = 2$	$Y = Y1 + Y2 = 0.2091$		
Overloaded Line (6) \equiv (6-2)		103%			
Overloaded Line (11) \equiv (9-2)		101%			
\Rightarrow After UPFC Installation					
\Rightarrow Optimal Location Line (14) \equiv (12-9), Optimal Setting (0.215, 0.9883)					
$\dot{K}_{(LOLN)} = 0$	$Y1 = 0$	$\Gamma_{(VBVN)} = 0$	$Y2 = 0$	$\mathcal{A} = 0$	$Y = 0$
\Rightarrow No Overloading, No Voltage Violation $0.98 \leq V_i \leq 1.02$					

Table 6.33 Case Study (10) of HELEN Network

Case Study 10					
\Rightarrow Max. Load for each load bus at the same time multiplied by 100% 2020 coeff.					
\Rightarrow Before UPFC installation.					
$\dot{K}_{(LOLN)} = 1$	$Y1 = 0.1577$	$\mathcal{A} = \dot{K}_{(LOLN)} + \Gamma_{(VBVN)} = 1$	$Y = Y1 + Y2 = 0.1577$		
Overloaded Line (11) \equiv (9-2)			112.07%		
\Rightarrow After UPFC Installation					
\Rightarrow Optimal Location Line (14) \equiv (12-9), Optimal Setting (0.215, 0.9629)					
$\dot{K}_{(LOLN)} = 0$	$Y1 = 0$	$\Gamma_{(VBVN)} = 0$	$Y2 = 0$	$\mathcal{A} = 0$	$Y = 0$
\Rightarrow No Overloading, No Voltage Violation			$0.98 \leq V_i \leq 1.02$		

The tables show that the UPFC can enhance the performance of power systems with optimal location and optimal settings. Locating UPFC in the network prevents all of the overloading in the lines. However, all of the bus voltage violations are eliminated, or the technique can achieve the solution region to eliminate the overloaded lines and at the same moment keeping the voltage profile. Increasing the system loadability of a power system as an index to evaluate the impact of UPFC in power system is achieved with respect to the line thermal limits and the bus voltage magnitude limits. Loading increase studies on the system can be applied at different cases and aspects. UPFC in optimal placement can restore the system operating condition to the steady state point.

Figure 6.5 shows the effect of the UPFC at an optimal location with optimal settings on the transmission line flow at the maximum loading pattern of the year 2020.

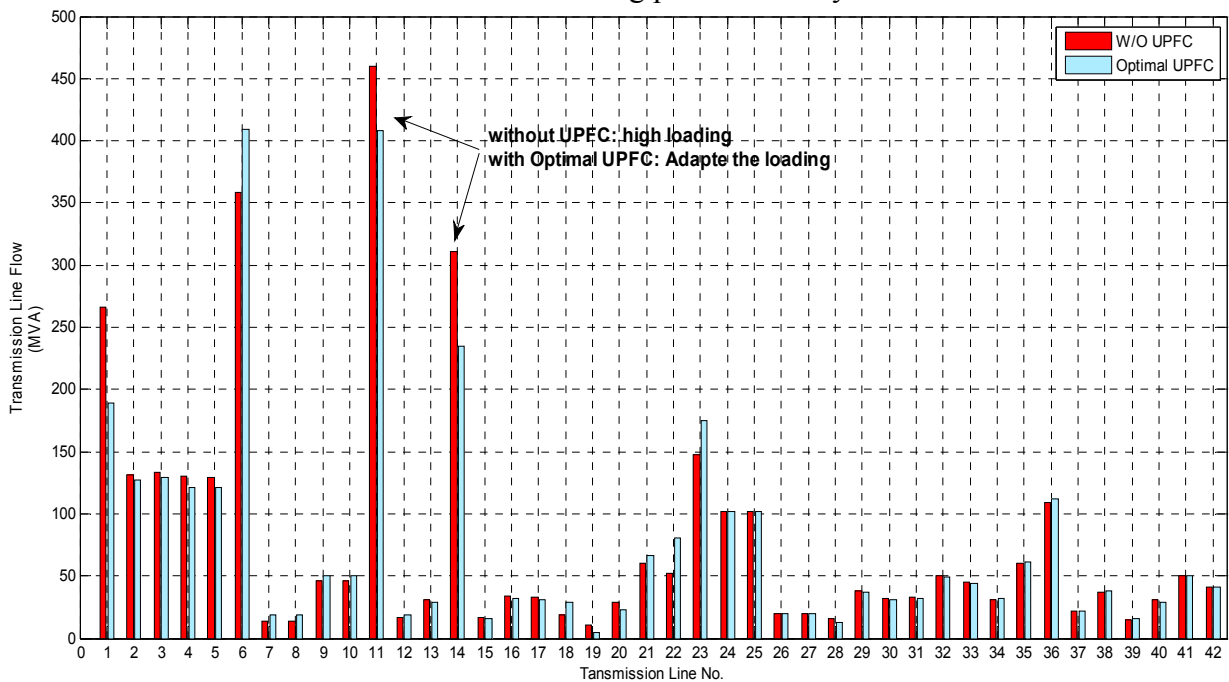


Fig. 6.5 the effect of the UPFC at the maximum loading pattern of the year 2020.

6.5.2 Contingency Operating with Outage Pattern

Most electric power grids are widely interconnected, and are extend to inter-utility interconnections and then to inter-regional and internal connections. That is because of economic issues, to minimize the cost of electricity, and to enhance the reliability of the power supply. However, as power transfer grows, the power system becomes increasable more complex to operate and the system can become less secure for riding through the major outages. It may cause a large power flow with inadequate control, excessive reactive power in various portions of the system, large dynamic swings between different parts of the system and bottlenecks. Thus the full potential of transmission interconnections cannot be utilized. Power system stability and thermal constraints restrict the transmission capacity. To meet the increasing load demand and satisfy the stability and reliability criteria, both existing transmission and generation facilities must be utilized more efficiently, or new facilities should be added to the systems. Given the constraints, such as lack of investment and difficulties in getting new transmission line right-of ways, the later is often difficult. The former can be achieved by using UPFC as seen in well-developed power systems throughout the world.

This stage is related to enhancing the performance of the HELENSÄHKÖVERKKO network with regard to the overloading of transmission lines and violation of bus voltage profile during the contingency operating with an outage pattern.

A ranking process is performed on the network after the contingency analysis. There will be some single contingencies. For each single line outage, we will find the following performance indices $\dot{K}_{(LOLN)}$ and $\Gamma_{(VBVN)}$.

Then we rank the lines according to the severity of the contingency, in other words, according to $\mathcal{Y} = \dot{K}_{(LOLN)} + \Gamma_{(VBVN)}$. The remaining cases will not be of concern where the totally performance indices equal zero.

The results will be performed on the HELENSÄHKÖVERKKO network with the maximum loading value for each bus individual at the same time to achieve the worst loading pattern of the system. Also using these conditions, the simulation and the analysis will be verified on the maximum loading pattern of the year 2020 to improve the performance and solve the related problems in the network.

Table 6.34 Ranking for the severity contingency cases for the HELENSÄHKÖVERKKO Network

(Max. Load for each load bus at the same time multiplied by Year 2020 coefficient)

Ranking Case	Line Number	Connecting Bus		$\dot{K}_{(LOLN)}$	$\Gamma_{(VBVN)}$	$\mathcal{Y} = \dot{K}_{(LOLN)} + \Gamma_{(VBVN)}$
		From	To			
1	6	2	6	3	0	3
2	11	9	2	1	0	1
3	14	12	9	1	0	1
4	3	6	4	1	0	1
5	2	6	4	1	0	1
6	1	12	6	1	0	1

Table 6.35 Outage Case Study (1) of HELEN Network

Outage Case Study 1					
\Rightarrow Outage of Line (6) \equiv (2-6), Severity Rank =1					
\Rightarrow Before UPFC Installation					
$\dot{K}_{(LOLN)} = 3$	$Y1 = 1.2227$	$\mathcal{A} = \dot{K}_{(LOLN)} + \Gamma_{(VBVN)} = 3$		$Y = Y1 + Y2 = 1.2227$	
Loadability			32.74%		
Overloaded Line (1) \equiv (6-12)			115.72%		
Overloaded Line (11) \equiv (9-2)			168.2%		
Overloaded Line (14) \equiv (12-9)			125.3%		
\Rightarrow After UPFC Installation					
\Rightarrow Optimal Location Line (22) \equiv (11-3), Optimal Setting (0.2546, 0.98)					
$\dot{K}_{(LOLN)} = 1$	$Y1 = 0.8$	$\Gamma_{(VBVN)} = 0$	$Y2 = 0$	$\mathcal{A} = 1$	$Y = 0.8$
Loadability			33.85%		
\Rightarrow One Overloading		Line (11)	Eliminate Overloading at line 1, 14		
\Rightarrow No Voltage Violation		$0.98 \leq V_i \leq 1.02$			

Table 6.36 Outage Case Study (2) of HELEN Network

Outage Case Study 2					
\Rightarrow Outage of Line (11) \equiv (9-2), Severity Rank =2					
\Rightarrow Before UPFC Installation					
$\dot{K}_{(LOLN)} = 1$	$Y1 = 0.8053$	$\mathcal{A} = \dot{K}_{(LOLN)} + \Gamma_{(VBVN)} = 1$		$Y = Y1 + Y2 = 0.8053$	
Overloaded Line (6) \equiv (6-2)			168.46 %		
\Rightarrow After UPFC Installation					
\Rightarrow Optimal Location Line (6) \equiv (6-2), Optimal Setting (0.20, 0.80)					
$\dot{K}_{(LOLN)} = 1$	$Y1 = 0.15$	$\Gamma_{(VBVN)} = 0$	$Y2 = 0$	$\mathcal{A} = 1$	$Y = 0.15$
- One Overloading		Line (6)	Reduced Overloading (168.46% to 110%)		
\Rightarrow No Voltage Violation		$0.98 \leq V_i \leq 1.02$			

Table 6.37 Outage Case Study (3) of HELEN Network

Outage Case Study 3					
\Rightarrow Outage of Line (14) \equiv (12-9), Severity Rank =3					
\Rightarrow Before UPFC Installation					
$\dot{K}_{(LOLN)} = 1$	$Y1 = 0.1762$	$\mathcal{A} = \dot{K}_{(LOLN)} + \Gamma_{(VBVN)} = 1$		$Y = Y1 + Y2 = 0.1762$	
Loadability			27.88%		
Overloaded Line (6) \equiv (6-2)			115.21%		
\Rightarrow After UPFC Installation					
\Rightarrow Optimal Location Line (22) \equiv (11-3), Optimal Setting (0.239, 0.9525)					
$\dot{K}_{(LOLN)} = 0$	$Y1 = 0$	$\Gamma_{(VBVN)} = 0$	$Y2 = 0$	$\mathcal{A} = 0$	$Y = 0$
Loadability			29.4468%		
\Rightarrow No Overloading , No Voltage Violation				$0.98 \leq V_i \leq 1.02$	

Table 6.38 Outage Case Study (4) of HELEN Network

Outage Case Study 4					
\Rightarrow Outage of Line (3) \equiv (6-4), Severity Rank =4					
\Rightarrow Before UPFC Installation					
$\dot{K}_{(LOLN)} = 1$	$Y1 = 0.1624$	$\mathcal{A} = \dot{K}_{(LOLN)} + \Gamma_{(VBVN)} = 1$		$Y = Y1 + Y2 = 0.1624$	
Loadability			30.9%		
Overloaded Line (36) \equiv (7-17)			112.89 %		
\Rightarrow After UPFC Installation					
\Rightarrow Optimal Location Line (15) \equiv (8-5), Optimal Setting (0.0872, 0.9260)					
$\dot{K}_{(LOLN)} = 0$	$Y1 = 0$	$\Gamma_{(VBVN)} = 0$	$Y2 = 0$	$\mathcal{A} = 0$	$Y = 0$
Loadability			32.4554%		
\Rightarrow No Overloading , No Voltage Violation				$0.98 \leq V_i \leq 1.02$	

Table 6.39 Outage Case Study (5) of HELEN Network

Outage Case Study 5					
\Rightarrow Outage of Line (2) \equiv (6-4), Severity Rank =5					
\Rightarrow Before UPFC Installation					
$\dot{K}_{(LOLN)} = 1$	$Y1 = 0.1578$	$\mathcal{A} = \dot{K}_{(LOLN)} + \Gamma_{(VBVN)} = 1$		$Y = Y1 + Y2 = 0.1578$	
Loadability			30.85%		
Overloaded Line (36) \equiv (7-17)			112.07%		
\Rightarrow After UPFC Installation					
\Rightarrow Optimal Location Line (15) \equiv (8-5), Optimal Setting (0.1104 , 0.8402)					
$\dot{K}_{(LOLN)} = 0$	$Y1 = 0$	$\Gamma_{(VBVN)} = 0$	$Y2 = 0$	$\mathcal{A} = 0$	$Y = 0$
Loadability			34.100%		
\Rightarrow No Overloading , No Voltage Violation				$0.98 \leq V_i \leq 1.02$	

Table 6.40 Outage Case Study (6) of HELEN Network

Outage Case Study 6					
\Rightarrow Outage of Line (1) \equiv (6-12), Severity Rank =6					
\Rightarrow Before UPFC Installation					
$\dot{K}_{(LOLN)} = 1$	$Y1 = 0.1386$	$\mathcal{A} = \dot{K}_{(LOLN)} + \Gamma_{(VBVN)} = 1$		$Y = Y1 + Y2 = 0.1386$	
Loadability			27.57%		
Overloaded Line (6) \equiv (6-2)			108.5%		
\Rightarrow After UPFC Installation					
\Rightarrow Optimal Location Line (23) \equiv (9-11), Optimal Setting (0.2912 , 0.8249)					
$\dot{K}_{(LOLN)} = 0$	$Y1 = 0$	$\Gamma_{(VBVN)} = 0$	$Y2 = 0$	$\mathcal{A} = 0$	$Y = 0$
Loadability			28.9328%		
\Rightarrow No Overloading , No Voltage Violation				$0.98 \leq V_i \leq 1.02$	

The results indicate that the UPFC can efficiently enhance the characteristics of power systems with optimal position and optimal parameter settings. Positioning UPFC in the network cancels the overloading in the lines in most of the conditions. In other cases, most of the overloaded lines are cancelled and the power flow in the rest-overloaded lines is efficiently decreased.

Increasing of the system loadability of a power system as an index to evaluate the impact of UPFC in power system is achieved with respect to the line thermal limits and the bus voltage magnitude limits. Load increasing studies on the system can be applied at different cases and aspects. Figure 6.6 shows the effect of the Optimal UPFC on the transmission line flow at the year 2020 during the Outage of Line (14).

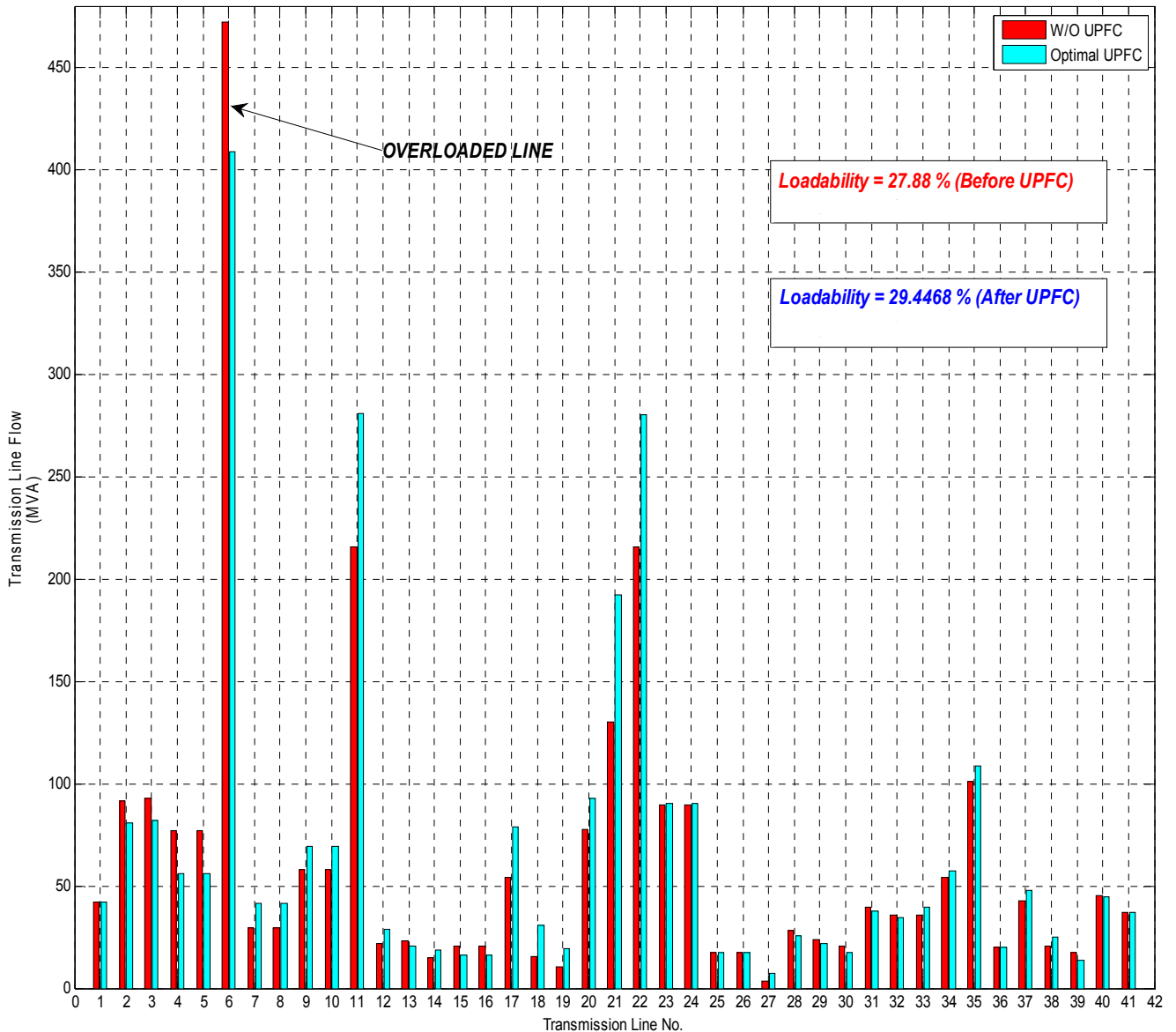


Fig. 6.6 the effect of the Optimal UPFC on the transmission line flow at Year 2020 during the Outage of Line (14).

6.6 Cases Study: Optimal Installation for Load Profile Period

6.6.1 Normal Configuration with high loading

We will start by selecting one of the highly loading conditions for the Helen Network in the year 2020, using the hourly loading profile and forecasting the coefficient for the year 2020. Then, to generate the load profile period for that highly loaded condition, we will focus on the week that contains that highly case.

Table 6.41, Case (1) Normal Configuration

$K_{(LOLN)}=2$	$Y1=2.7$	$\Gamma_{(VBVN)}=0$	$Y2=0$	$\mathcal{A}=2$	$Y=Y1$
Overloaded Line 17-18			121.67 %		
Overloaded Line 17-7			224.58 %		

→ **Without UPFC** :

- For a given loading scenario in 2020, one loading pattern on the week that contains highly loading conditions.
(Considering 168 loading cases with one-hour load steps for the 42 lines of Helen Network)
- Total number of overloads
(out of a possible number of 168 loading cases x 42 lines) = 179
- Number of overloads in current concerned scenario = 2.

$K_{(LOLN)}=0$	$Y1=0$	$\Gamma_{(VBVN)}=0$	$Y2=0$	$\mathcal{A}=0$	$Y=0$
→ No overloading, no voltage violation $0.95 \leq V_i \leq 1.05$					

→ **With UPFC** :

- For the same load scenario
- The optimal location is on line (36) and the optimal setting is:
[0.097257 , 0.93716]
- Total number of overloads
(out of a possible number of 168 loading cases x 42 lines) with UPFC = 2
- Number of overloads in current concerned scenario = 0

Naturally, the study forms required part for planning the upgrading of a sub-transmission network that will cope with future load and contingency requirements in the most effective manner. We will simply state that the line is secure for the future load scenario. Optimal location and the optimal parameter settings of the UPFC in the power network eliminate or minimize the overloaded lines and the bus voltage violations. These results prove to be successful in solving the steady-state problems and in enhancing performance in the majority of the cases.

Table 6.42, Case (2) Normal Configuration

→ **Without UPFC** :

- For another given loading scenario in 2020, which is the maximum loading

Pattern.

(Considering 168 loading cases with one-hour load steps for the 42 lines of Helen Network)

- Total number of overloads

(out of a possible number of 168 x 42) with UPFC = 179

- Number of overloads in current concerned scenario = 2

$\dot{K}_{(LOLN)}=2$	Y1=1.76	$\Gamma_{(VBVN)}=0$	Y2=0	$\mathcal{A}=2$	Y=Y1
Overloaded Line 17-18			105.73 %		
Overloaded Line 17-7			201.18 %		

* Without UPFC line 17-7 exceeds the thermal limit given by a transient thermal analysis, i.e., the overload percentage of 201% exceeds the cyclic rating factor of approximately 155%.

→ **With UPFC** :

- For the same load scenario

- Optimal location at line (36) with optimal setting: [0.097257, 0.93716]

- Total no. of overloads (out of 168 x 42) with UPFC = 2

- Number of overloads in current concerned scenario = 1

Overloaded Line 21-5			104.22 %		
$\dot{K}_{(LOLN)}=1$	Y1=0.12	$\Gamma_{(VBVN)}=0$	Y2=0	$\mathcal{A}=1$	Y=Y1

→ No voltage violation $0.95 \leq V_i \leq 1.05$

The thermal overload, which occurs on 38, is only slight. This line is split between an old oil cable, which will most likely have been upgraded by the time this simulation is valid for, and a 3 x AHXLMK 800 installation, which are more modern XLPE cables with 800 mm² stranded aluminum conductors. If the entire overloaded line section has been upgraded by 2020, then the projected overload will not be an overload at all, even in steady-state terms, but if the old oil cables still remain in use, a transient rating shows that they are, at least thermally, in no danger. The cyclic loading factor for these cables is approximately 155%, which is much greater than the projected overload based on a steady-state rating of 104.22%. Thus, we can safely say, for this case the projected thermal overload is not a thermal overload when a full transient analysis is performed.

6.6.2 The contingency Study

During the same load profile for the highly loaded conditions, The total number of overload cases for each of 42 single contingency outage cases. Each contingency case has 168 loading patterns ⇒ 3677 cases. The most severe case is the outage of line 24, which gives

rise to the highest number of overloaded lines – 140 overloaded cases from the 168 loading cases.

The second most severe case is the outage of line 2, which has the second highest number of overloaded lines – 106 overload cases from the 168 loading cases.

Table 6.43, Contingency Case (1)

$\dot{K}_{(LOLN)}=2$	Y1=0.56	$\Gamma_{(VBVN)}=0$	Y2=0	$\mathcal{R}=2$	Y=Y1
Overloaded Line 1-2			102.18 %		
Overloaded Line 23-5			127.65 %		
Overloaded Line 17-18			115.29 %		

→ **Without UPFC** :

- Severity case Rank 1 = outage of line 24, For a given loading scenario in 2020, one loading pattern on the week that contains highly loading conditions.
- Total number of overloads (out of 168 x 41) without UPFC = 140
- Number of overloads in current concerned scenario = 3

→ **With UPFC** :

- For the same loading scenario; with outage of line 24.
- Optimal location at line (4) with optimal setting: [0.24324 , 0.98349]
- Total number of overloaded lines (out of 168 x 41) when there is an outage of line 24 with UPFC = 13
- Number of overloads in current concerned scenario = 0

$\dot{K}_{(LOLN)}=0$	Y1=0	$\Gamma_{(VBVN)}=0$	Y2=0	$\mathcal{R}=0$	Y=Y1
→ No overloading, no voltage violation $0.95 \leq V_i \leq 1.05$					

Table 6.44, Contingency Case (2)

One of the (13) cases with overloads after UPFC Optimal placement

→ **Without UPFC** :

- Severity case Rank 1 = outage of line 24, for the given loading scenario, which the maximum loading pattern.
- Total number of overloads (out of 168 x 41) without UPFC = 140

→ **With UPFC** :

- For an outage of line 24
- Optimal location at line (4) with optimal setting: [0.24324 , 0.98349]
- Total number of overloads (out of 168 x 41) with UPFC = 13
- One of the (13) cases, after UPFC Optimal placement

Overloaded Line 17-18			106.23%		
$\dot{K}_{(LOLN)}=0$	Y1=0.13	$\Gamma_{(VBVN)}=0$	Y2=0	$\mathcal{R}=1$	Y=Y1
→ No voltage violation $0.95 \leq V_i \leq 1.05$					

In this case, the cyclic rating factor is only 107.5 % and so the full thermal response is shown in Fig. 6.7.

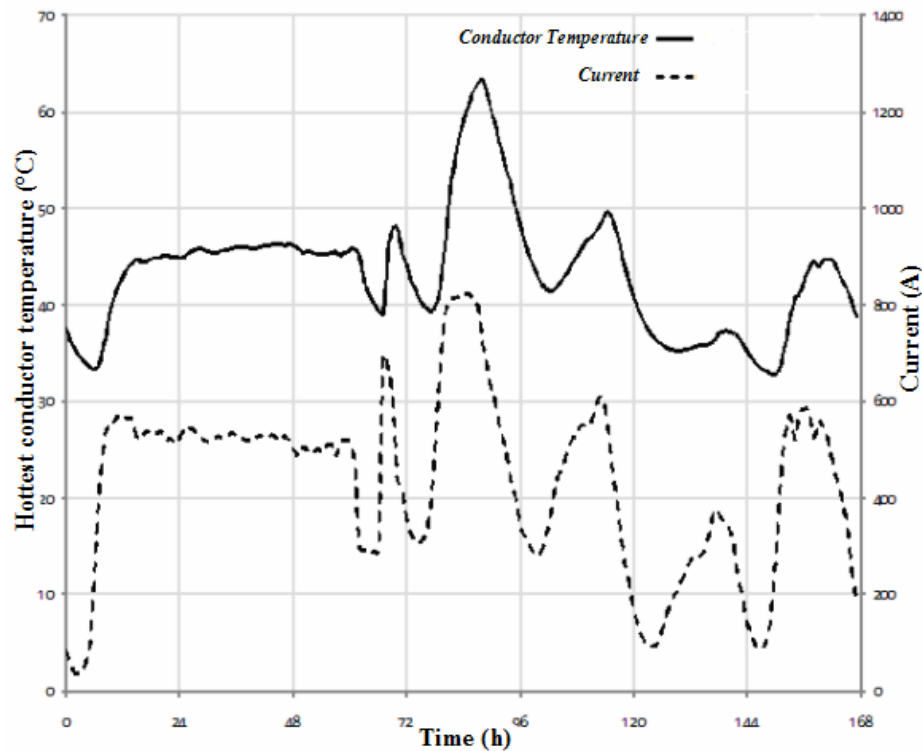


Fig. 6.7. Temperature response of cable for the 1st severity case (Contingency Case (2)).

As can be seen in Fig. 6.7, the temperature does not rise above 65 °C in the hottest conductor, so we can conclude that even with conservative thermal modeling, the cables will not overheat in the projected future loading scenario due to this contingency. The second severity case is the outage of line 2; it has the second highest number of overloaded lines, 106 out of a possible 168 loading cases.

Table 6.45, Contingency Case (3)

→ **Without UPFC** :

- Severity case Rank 2 = outage of line 2
- Total number of overloaded lines (out of 168 x 41) without UPFC = 106

→ **With UPFC** :

- at outage of line 2
- Optimal location at line (4) with optimal setting: [0.24324 , 0.98349]
- Total number of overloaded lines (out of 168 x 41) at outage of line 2 with UPFC = 38
- One of these cases, after UPFC Optimal placement

Overloaded Line 17-18			117.65 %		
$\dot{K}_{(LOLN)}=0$	Y1=0.36	$\Gamma_{(VBVN)}=0$	Y2=0	Я=1	Y=Y1

→ No voltage violation $0.95 \leq V_i \leq 1.05$

This thermal overload is the most severe out of the cases considered and its thermal response is given below in Fig. 6.8.

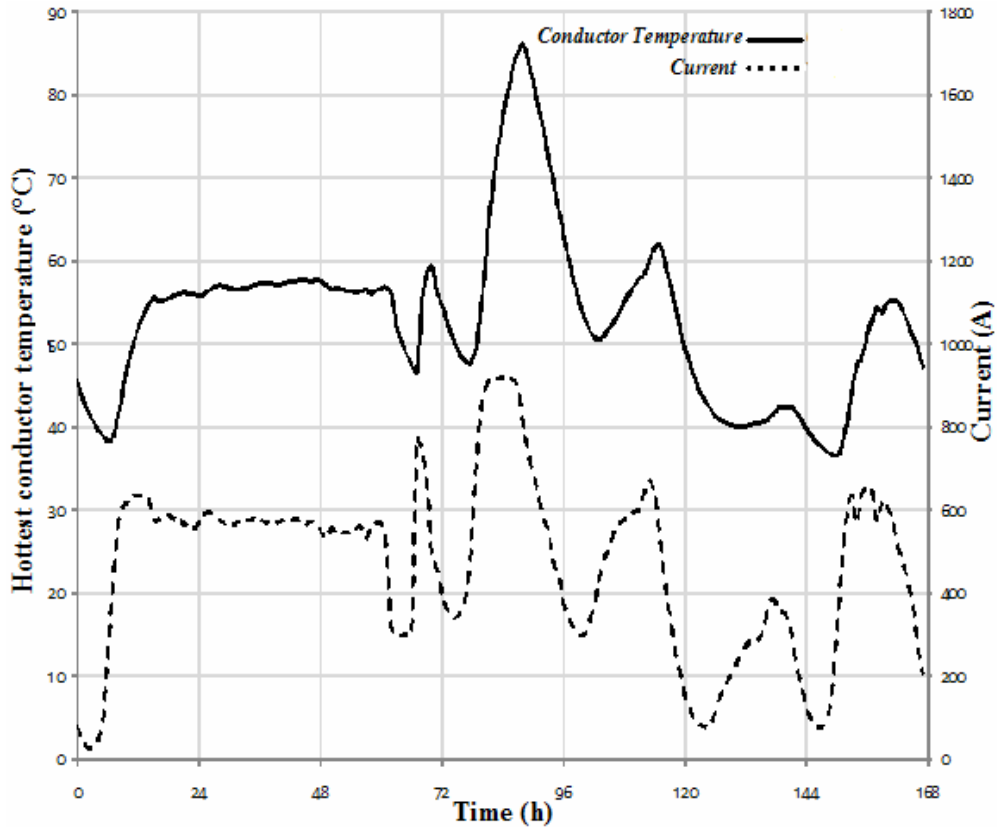


Fig. 6.8. Temperature response of cable for the 2nd severity case (Contingency Case (3)).

It can be seen that the temperature exceeds 65 °C in contingency 2. 65 °C has normally been used as the maximum allowable conductor temperature in underground cables in order to avoid moisture migration problems. Now, however, we have conservatively modeled moisture migration in the transient analysis, which means that the catalogue maximum temperature for continuous operation of 90 °C can be considered – and, as Fig. 6.8 shows, the temperature stays below 90 °C. If moisture migration occurs at lower temperatures, however, 90 °C will be exceeded.

6.7 Case Study: Fixed Location with Optimal Setting

The following case study involves studying the effect of searching for only the optimal settings at fixed locations of UPFC. To achieve a link between the results, we will use the results of Section 6.5.1; Table 6.29 indicates that using proposed GA the optimal UPFC is in location of line 13, for case 90 % of operating conditions of the year 2020. However, for the loading pattern of 96 % of operating conditions of the year 2020, this location should be modified using the proposed GA to location of line 22 with optimal settings of (0.1812 , 0.9356) to solve the problem of overloading of line 11 and line 36 and also to enhance the loadability. The analysis now will study fixing the location of UPFC at line 13 for the two cases 90 % and 96 % of operating conditions of the year 2020, and search for the optimal settings only.

Table 6.46 Case Study (1) for optimal settings of UPFC only.

Case Study					
\Rightarrow Max. Load for each load bus at the same time multiplied by 96% of 2020 coeff.					
\Rightarrow Before Optimal Process , UPFC at Line (13) , Setting (0.001 , 0.800)					
(UPFC at Optimal Location and settings of previous pattern 90 % of year 2020)					
$\dot{K}_{(LOLN)} = 2$	$YI = 0.2328$	$\mathcal{A} = \dot{K}_{(LOLN)} + \Gamma_{(VBVN)} = 2$	$Y = 0.2328$		
Loadability			35.42%		
Overloaded Line (11) \equiv (9-2)			107%		
Overloaded Line (36) \equiv (7-17)			101%		
\Rightarrow Performing Optimal Process for UPFC settings with fixed Location					
\Rightarrow UPFC at Location Line (13) , Optimal Setting (0.0750 , 0.8000)					
$\dot{K}_{(LOLN)} = 1$	$YI = 0.1310$	$\mathcal{A} = \dot{K}_{(LOLN)} + \Gamma_{(VBVN)} = 1$	$Y = 0.1310$		
Loadability			35.48%		
Overloaded Line (11) \equiv (9-2)			106%		
\Rightarrow With UPFC for Optimal Location Line (22), Optimal Setting (0.1812 , 0.9356)					
$\dot{K}_{(LOLN)} = 0$	$YI = 0$	$\Gamma_{(VBVN)} = 0$	$Y2 = 0$	$\mathcal{A} = 0$	$Y = 0$
Loadability			37.23%		
\Rightarrow No Overloading , No Voltage Violation $0.98 \leq V_i \leq 1.02$					

Also, Table 6.30 indicates the optimal location and settings for 98% of operating conditions of the year 2020; this loading pattern will be used again but with fixing the location of UPFC and uses the optimal process for the optimal settings only.

Table 6.47 Case Study (2) for optimal settings of UPFC only.

Case Study					
\Rightarrow Max. Load for each load bus at the same time multiplied by 98% of 2020 coefficient.					
\Rightarrow Before Optimal Process , UPFC at Line (22) , Setting (0.1812 , 0.9356)					
(UPFC at Optimal Location and settings of previous pattern 96 % of year 2020)					
$\dot{K}_{(LOLN)} = 2$	$YI = 0.2068$	$\mathcal{A} = \dot{K}_{(LOLN)} + \Gamma_{(VBVN)} = 2$		$Y = 0.2068$	
Overloaded Line (11) \equiv (9-2)		101.07%			
Overloaded Line (36) \equiv (7-17)		101%			
\Rightarrow Performing Optimal Process for UPFC settings with fixed Location					
\Rightarrow UPFC at Location Line (22) , Optimal Setting (0.1784 , 1.1980)					
$\dot{K}_{(LOLN)} = 1$	$YI = 0.1048$	$\mathcal{A} = \dot{K}_{(LOLN)} + \Gamma_{(VBVN)} = 1$		$Y = 0.1048$	
Overloaded Line (11) \equiv (9-2)		101.119%			
\Rightarrow Performing Optimal Process, for Optimal Location and Optimal Setting					
\Rightarrow With UPFC for Optimal Location Line (14), Optimal Setting (0.1960 , 1.0928)					
$\dot{K}_{(LOLN)} = 0$	$YI = 0$	$\Gamma_{(VBVN)} = 0$	$Y2 = 0$	$\mathcal{A} = 0$	$Y = 0$
\Rightarrow No Overloading , No Voltage Violation				$0.98 \leq V_i \leq 1.02$	

The previous results show that the effective actions of UPFC are achieved when performing the optimal process for the optimal location and the optimal settings together. Table 6.46 indicates that the optimal process for the optimal setting with fixed location from the previous loading pattern does not achieve the maximum benefits where the network will still have overloaded lines. In addition, the enhancing in the loadability is significantly slight low with searching for the optimal settings only, where with optimal location and optimal settings together the enhancing in the loadability is clearer. In addition, Table 6.47 shows that the optimal process for the optimal setting with fixed location from the previous loading pattern does not get the desired performance for totally no overloading.

6.8 Case Study: Multiple Optimal UPFC Installation

The following case study is concerned with modifying the proposed GA to install multiple UPFCs according to optimal locations and optimal settings for each UPFC in order to enhance the network performance. To achieve a link between the results, we will use the results of Section 6.5.1. Table 6.30 indicates that used proposed GA, the optimal UPFC is in the location of line 14 for case of 98 % of operating conditions for the year 2020, with optimal settings of (0.1960 , 1.0928) to solve the problem of the overloading of line 11 and line 36 with one optimal UPFC. The analysis now will study installing multiple UPFCs instead of only of only a single UPFC.

Table 6.48 Case Study (1) for Multiple Optimal UPFC Installation

<i>Case Study</i>					
\Rightarrow <i>Max. Load for each load bus at the same time multiplied by 98% of 2020 coeff.</i>					
\Rightarrow <i>Before Optimal Process for Multiple UPFC.</i>					
\Rightarrow <i>UPFC at Line (22) , Setting (0.1812 , 0.9356)</i>					
<i>(UPFC at Optimal Location and settings of previous pattern 96 % of year 2020)</i>					
$\dot{K}_{(LOLN)} = 2$	$YI = 0.2068$	$\mathcal{A} = \dot{K}_{(LOLN)} + \Gamma_{(VBVN)} = 2$		$Y = 0.2068$	
Overloaded Line (11) \equiv (9-2)		101.07%			
Overloaded Line (36) \equiv (7-17)		101%			
- Performing Optimal Process for Multiple UPFC (optimal locations & settings)					
\Rightarrow <i>UPFC(1) at Location Line (39) , Optimal Setting (0.0138 , 0.8975)</i>					
\Rightarrow <i>UPFC(2) at Location Line (14) , Optimal Setting (0.2228 , 0.9238)</i>					
$\dot{K}_{(LOLN)} = 0$	$YI = 0$	$\Gamma_{(VBVN)} = 0$	$Y2 = 0$	$\mathcal{A} = 0$	$Y = 0$
\Rightarrow <i>No Overloading , No Voltage Violation</i>				$0.98 \leq V_i \leq 1.02$	

In addition, Table 6.33 indicates the optimal location and settings for 100% of operating conditions of the year 2020, this loading pattern will be used again but with installing multiple UPFCs with optimal locations and setting for each UPFC.

Table 6.49 Case Study (2) for Multiple Optimal UPFC Installation.

Case Study					
⇒ Max. Load for each load bus at the same time multiplied by 100% of 2020 coefficient.					
⇒ Before Optimal Process for Multiple UPFC.					
⇒ Without UPFC Installation					
$\dot{K}_{(LOLN)} = 1$	$Y1 = 0.1577$	$\mathcal{A} = \dot{K}_{(LOLN)} + \Gamma_{(VBVN)} = 1$		$Y = Y1 + Y2 = 0.1577$	
Overloaded Line (11) \equiv (9-2)			112.07%		
- Performing Optimal Process for Multiple UPFC (optimal locations & settings)					
⇒ UPFC(1) at Location Line (14), Optimal Setting (0.2186, 0.9657)					
⇒ UPFC(2) at Location Line (10), Optimal Setting (0.0282, 0.8620)					
$\dot{K}_{(LOLN)} = 0$	$Y1 = 0$	$\Gamma_{(VBVN)} = 0$	$Y2 = 0$	$\mathcal{A} = 0$	$Y = 0$
⇒ No Overloading, No Voltage Violation				$0.98 \leq V_i \leq 1.02$	

The previous tables state that multiple optimal UPFC can fulfill the required performance and enhance the features of the grid. However, by comparing Table 6.30 with 6.48 and Table 6.33 with 6.49, we can note that one optimal UPFC will achieve the same outputs of multiple optimal UPFCs. In addition, the tables show that the process of one optimal UPFC reaches the same optimal location that multiple optimal UPFC reach. However, with tuning the optimal settings of one optimal UPFC, it achieves the objective function without installing more UPFCs. From an economical point of view, when one optimal UPFC can fulfill the required performance, so there is no need for multiple optimal UPFC, due to the high cost of installing more UPFC devices. Also, from a technical perspective, more UPFC installation may cause itself to overloading.

6.9 Optimal Power Flow Case

The FACTS technology is a solution for the transmission level in the power system. Due to the power market and Deregulated power system concepts, which are now applicable in most of real power networks, we should obtain many solution related to each power system level and section. The power market concept divides the power system operation into many levels and sections. Each level is controlled by a certain authority or company. There are many principles, which consider that the ultimate open supplier is the Transmission System Operator (TSO). The optimal power flow sometimes is unable to solve the technical problems of the power network; also in some cases it strikes or hits the bounds of the system variables. Some variables needs to lambda multiplier to just be kept

at the limits. The main issue is that the optimal power flow requires actions from the generation, transmission and distribution levels.

Table 6.50 IEEE 30-Bus Case Study OPF and Optimal UPFC

System Summary							
Buses No.	30	Generators No.	6	Lines No.	41		
Loads No.	20	Shunts No.	2				
I. OPF Simulation							
Objective Function Value = 576.89 \$/hr							
Lambda P	(min) 3.66 \$/MWh @ bus 1			(max) 5.38 \$/MWh@bus 8			
Lambda Q	(min) -0.06 \$/MWh @ bus 29			(max) 1.40 \$/MWh@bus 8			
Voltage Constraints							
Bus #	Vmin mu	Vmin	V	Vmax	Vmax mu		
29	-	0.950	1.050	1.050	29.810		
Line Flow Constraints							
Line #	From Bus	"From" End Sf mu Sf		Limit Smax	"To" End St St mu		To Bus
10	6	2.387	32.00	32.00	31.63	-	8
35	25	-	15.62	16.00	16.00	0.024	27
II. Optimal UPFC Placement							
- After UPFC Installation							
- Optimal Location Line (10) \equiv (6-8), Optimal Setting (0.0023794 , 0.99983)							
$\dot{K}_{(LOLN)} = 0$	$Y1 = 0$	$\Gamma_{(VBVN)} = 0$	$Y2 = 0$	$\mathcal{A} = 0$	$Y = 0$		
- No Overloading , No Voltage Violation $0.95 \leq V_i \leq 1.05$							

6.10 Dynamics of the system (Concept and Building)

The unified power flow controller was proposed as a device of flexible AC transmission systems. This is a multiple functional FACTS controller with the main task to control the power flow. The additional jobs of UPFC are to provide voltage control, transient stability enhancement, oscillation damping. UPFC can be very effective to damp power system oscillations.

Because FACTS devices have very fast dynamics compared to generators, they can play important roles to enhance the dynamics response. This is usually accomplished through controls associated with these devices. Using a damping controller with the UPFC can enhance the electromechanical mode damping. That controller can be one of inherent UPFC PI damping controller. UPFC main controllers can enhance system dynamics but the dynamics parameters setting should first be selected to damp and fine tuning the response. Damping controller for UPFC may affect the system response.

The effect of different controllers as conventional and adaptive AI controllers can be compared to conclude the most effective controller.

The operating conditions can be changed according to the disturbance, which affect the power system response. In the steady state analysis section, we considered the increasing in loading conditions, which lead to a change from one certain operating condition to another operating point. In addition, we considered the contingency outage cases, which produce an increase in the loading of all network elements.

For making stress on the correlation between the steady state and the dynamic analysis, we will consider the cases and the operating conditions from the steady state analysis. The steady state analysis leads to the importance of installing the UPFC in certain optimal locations with certain optimal settings. That may be considered as a comparison between installing and not installing the UPFC in the system. After we installed the UPFC at these optimal locations to achieve enhanced steady state performance, we should adapt the dynamic parameters to achieve also the optimal dynamic response.

The mechanical modes of the generators in the system can be good indicators for the dynamic response; the speed deviation response ($\Delta\omega$) and the mechanical rotor angle dynamic response ($\Delta\delta$) can be shown.

The link between the steady state and the dynamic analysis can be achieved by considering the results from the steady state as a part for the dynamic response analysis. So the same operating conditions will be assumed, we will select some different cases and patterns from the previous analysis in Sections 6.5.1 and 6.5.2 to complete the analysis with the dynamic response analysis. Building and adapting the system configuration to be suitable for the dynamic response analysis will be achieved using the derivation and programming of dynamics equation in Chapter 4, Section 4.4 by m-file codes linked with Simulink blocks models. Some scope on the dynamic model of UPFC and the dynamic model of a multi-machine power system equipped with UPFC will appear in the Appendix section.

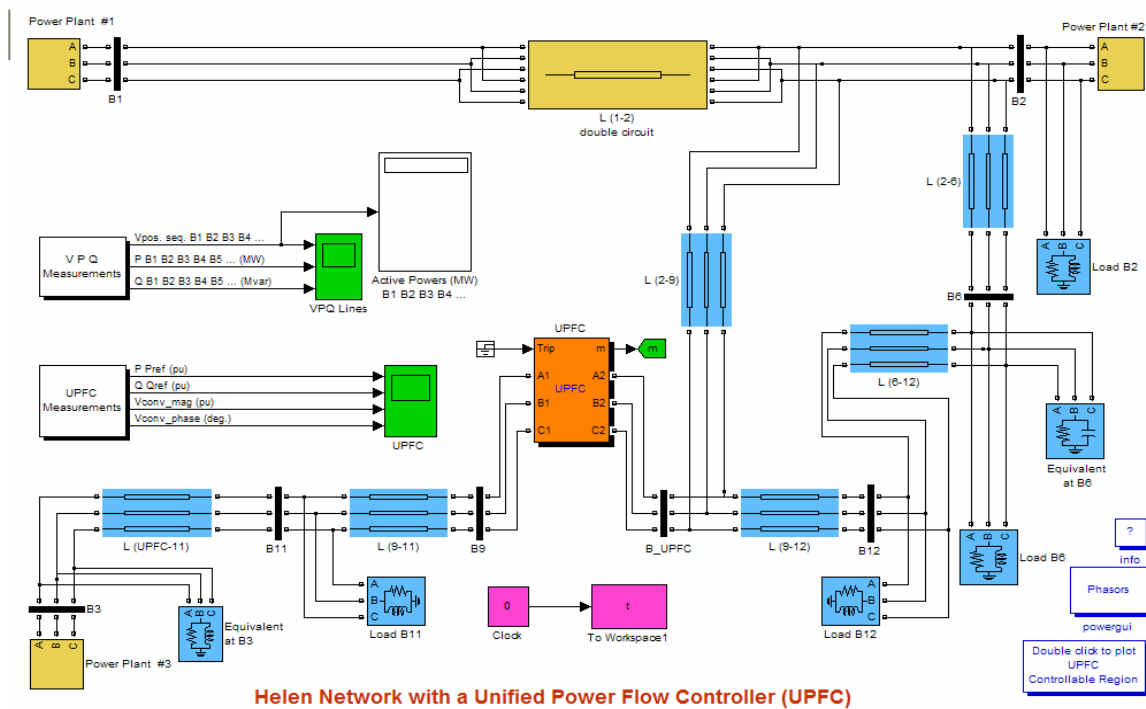


Fig. 6.9, a zone scope of dynamic blocks for Helen Network at certain case study from steady state analysis.

6.11 Dynamics Data of the System

The data for getting the optimal locations and optimal settings for installation of UPFC in the Helen network for enhancing the steady state performance was introduced in Section 6.2. This data has the total number of buses, the total number of the generators and the total number of transmission lines. The bus data, the load data and the generator data for the network were indicated in Table 6.1.

Table 6.2 indicated the data for the network transmission lines, which included the transmission line connecting buses, transmission line resistance, transmission line reactance, transmission line substance, and also, it indicated MVA rates for the transmission lines. The following section concerns the required data for studying dynamics of the UPFC installation in the HELEN network.

6.11.1 Scope on some dynamics data values of the HELEN network

A sample of the dynamic parameters values, which are used, will be indicated. The transformers data and the generators data is shown. Table 6.51 indicates the scope of the dynamic details data for the network and especially for the synchronous generators.

Table 6.51 Sample of some network generators dynamic data.

Generator	G1	G2	G3	G4	G5	G6	G1	G2	G1	G2	G3
Sn (MVA)	70	70	50	190	190	200	137.5	137.5	188	64	64
Un (kV)	10.5	10.5	10.5	10.5	10.5	13	10.5	10.5	15	10.5	10.5
Xd''	17.10%	17.10%	19%	24.40%	24.40%	17.70%	23.70%	23.70%	16.10%	15.40%	15.40%
Xd'	20.50%	20.50%	23%	33.30%	33.30%	23.20%	29.80%	29.80%	22.10%	21.30%	21.30%
Xd	190%	190%	206%	248.40%	248.40%	175%	239%	239%	211%	185%	185%
Xq''	18.80%	18.80%	19%	26.80%	26.80%	21%	23.70%	23.70%	20.80%	15.40%	15.40%
Xq'	39.20%	39.20%	42%	61.70%	61.70%	28%	24.70%	24.70%	45%	34.10%	34.10%
Xq	180%	180%	184%	235.90%	235.90%	159%	203%	203%	195%	157%	157%
Ra (ohm)	0.00127	0.00127	0.00187	0.000562	0.000562	0.000470	0.00206	0.00206	0.000850	0.001500	0.001500
Tdo'' (s)	0.04	0.04	0.04	0.043	0.043	0.142	0.0566	0.068	0.052	0.040	0.040
Tdo' (s)	7.6	7.6	6.1	9.590	9.590	7.800	3.8300	6.120	8.170	16.300	16.300
Tqo'' (s)	0.150	0.150	0.045	0.150	0.150	0.045	0.150	0.150	0.045	0.150	0.150
Tqo' (s)	2.500	2.500	0.730	2.500	2.500	0.730	2.500	2.500	0.730	2.500	2.500
Td'' (s)	0.03	0.03	0.03	0.030	0.030	0.107	0.0453	0.054	0.040	0.030	0.030
Td' (s)	0.75	0.75	0.64	1.203	1.203	1.100	0.7630	0.760	0.930	1.500	1.500
Tq'' (s)	0.071	0.071	0.030	0.071	0.071	0.030	0.071	0.071	0.030	0.071	0.071
Tq' (s)	0.539	0.539	0.180	0.539	0.539	0.180	0.539	0.539	0.180	0.539	0.539
Pole pairs	1	1	1	1	1	1	1	1	1	1	1
Generator transformer											
Sn (MVA)	63	63	50	180	180	210	140	140	188	75	75
Un1 (kV)	10.5	10.5	10.5	10.5	10.5	13	10.5	10.5	15	10.5	10.5
Un2 (kV)	118	118	118	118	118	118	118	118	118	118	118
ux	10%	10%	10%	12.5 %	12.5 %	12.5 %	9.90%	9.90%	12.50%	10%	10%
ur	0.30%	0.30%	0.30%	0.30%	0.30%	0.30%	0.28%	0.28%	0.25%	0.30%	0.30%

6.12 Importance of Dynamics Tuning

To show the importance of tuning the dynamic parameters of the UPFC, we will introduce a case study from the cases indicated before in steady state performance enhancing. In the previous cases, this stage was concerned with enhancing the performance of the network related to overloading of the transmission lines and violation of the bus voltage profile. This task performed on the normal configuration of the system with an increasing the loading pattern until the year 2020. The results lead to optimal location and optimal settings of UPFC to be installed to achieve the required performance.

After installing the UPFC at these optimal locations with optimal settings, the dynamic parameters of the UPFC will have a significant effect on the dynamic response especially the mechanical variables response as the speed deviation response ($\Delta\omega$) and the mechanical rotor angle dynamic response ($\Delta\delta$) of the generating units. The dynamic blocks of the UPFC are indicated in Chapter 4, Section 4.5. The dynamics parameters for the UPFC blocks should be well selected and be set to fine tune the response and damp the oscillation and enhance the settling time of the response. More focus on the UPFC parameters, and the ones which should be adapted, will be shown in the following sections.

Table 6.52 indicates the case study, which will be the start to show the importance of adapting the dynamic parameters of the UPFC after its installation in the optimal location with the optimal settings.

Table 6.52 Case Study for the optimal location and setting of UPFC on Helen network (Start Point).

Case Study					
- Max. Load for each load bus at the same time multiplied by 97% of 2020 coeff.					
⇒ Before Optimal UPFC.					
$\dot{K}_{(LOLN)} = 2$	$Y1 = 0.24$	$\mathcal{A} = \dot{K}_{(LOLN)} + \Gamma_{(VBVN)} = 2$		$Y = Y1 + Y2 = 0.24$	
Loadability			33%		
Overloaded Line (11) \equiv (9-2)			108%		
⇒ After UPFC Installation					
- Optimal Location Line (22) \equiv (3-11), Optimal Setting (0.1812 , 0.9356)					
$\dot{K}_{(LOLN)} = 0$	$Y1 = 0$	$\Gamma_{(VBVN)} = 0$	$Y2 = 0$	$\mathcal{A} = 0$	$Y = 0$
Loadability			37.63%		
⇒ No Overloading , No Voltage Violation				$0.98 \leq V_i \leq 1.02$	

After installing the UPFC at the optimal location line (22) \equiv (3-11), with optimal setting ($V_{VR} = 0.1812$, $V_{CR} = 0.9356$), we should build up the dynamic model of the Helen network including UPFC at the optimal location. That building will use the dynamic equations of UPFC from Equations (4.5) to (4.21) incorporated with the block models for the Helen network elements and UPFC blocks; the Appendix section will present a part of equations and programming codes for constructing the model.

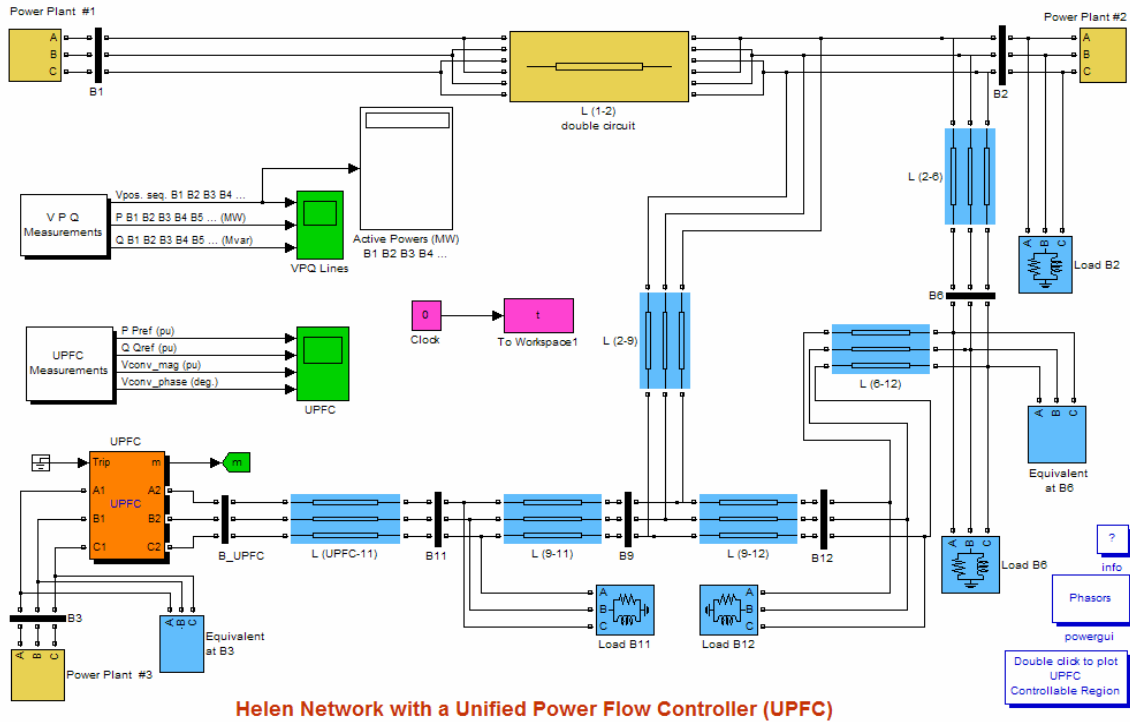


Fig. 6.10 Dynamic blocks zone for Helen Network for above mentioned case.

The dynamic response of the mechanical variables as the speed deviation response ($\Delta\omega$) and the mechanical rotor angle ($\Delta\delta$) of the generating units will be varied according to the adjusting of the dynamic parameters of the UPFC.

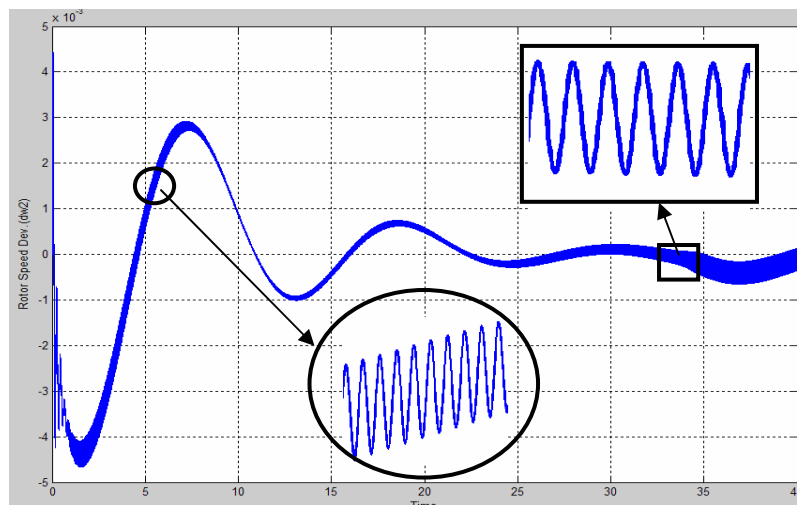


Fig. 6.11, Highly Oscillatory Dynamic Response

6.13 Effect of Adjusting PI Controller on Dynamics

To show the effect of tuning the dynamic parameters of the UPFC, we examine the case study from the cases indicated before in the steady state performance enhancing. The simulations calculate the optimal location and optimal settings of the UPFC to be installed to achieve the required performance.

The dynamic buildings of the network and the UPFC are constructed. The dynamics parameters for the UPFC blocks will be adapted according to the conventional manual tuning method described in Section 5.8. As in Section 5.9, the main concerned control element will be inside the series SVS part to control the power flow, which will be power PI regulator containing Integral gain (K_i) and propotional gain (K_p). That will be the controlling element, which will be adapted to enhance the dynamic response for the system. According to Table 6.52 that shows the case study, which will be the used to demonstrate the effect of adapting the dynamic parameters of the UPFC after its installation in the optimal location with the optimal settings.

The simulation of the case study indicated that the operating loading conditions are considered as follows: the loading of each load bus is the maximum loading values at all of them then multiplying that loading pattern in the load forecasting coefficients of the year 2020 to achieve most loading constraints. That operating conditions leads to some overloading cases. After applying the GA technique to reach the optimal location and settings which are optimal location line (22) \equiv (3-11), optimal settings (0.1812 , 0.9356), there will be no overloading in the network with keeping the voltage profile of the network in the required limits.

The dynamic response for that operating case with related UPFC dynamic parameters will show the effect to get the significant setting of that parameters to enhance the dynamic response. Without adapting the UPFC paramerters, we may lose the benefits that we got from installing the UPFC in the optimal location, where may lead to instability or osclliations in the dynamic response which means that we enhanced certain performance and impaired another one.

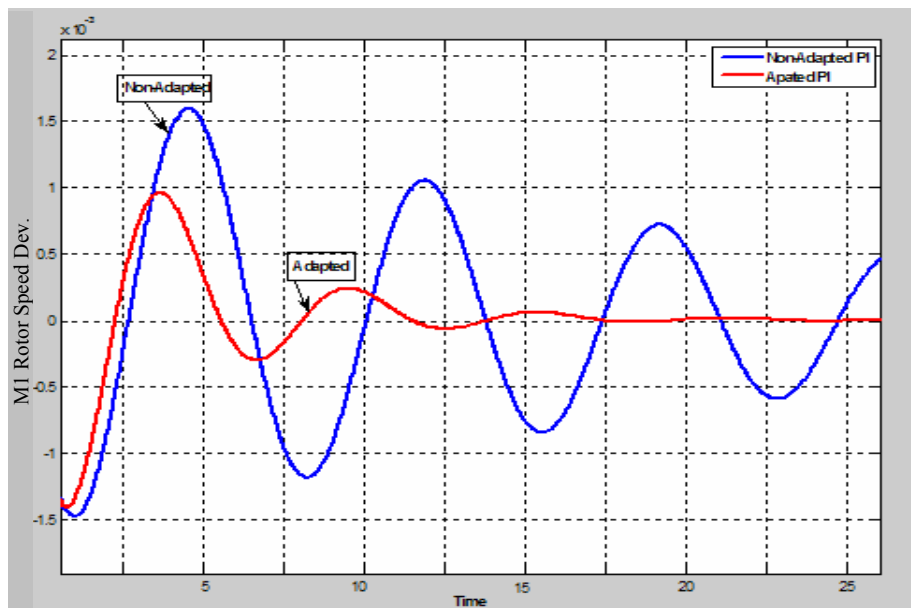


Fig. 6.12, Rotor Speed Deviation of Machine #1.

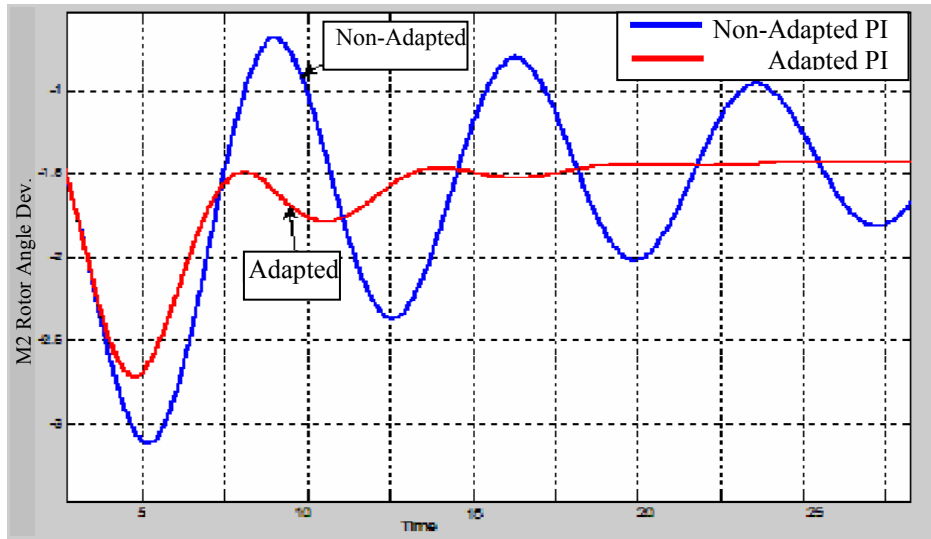


Fig. 6.13, Rotor Angle Deviation of Machine #2.

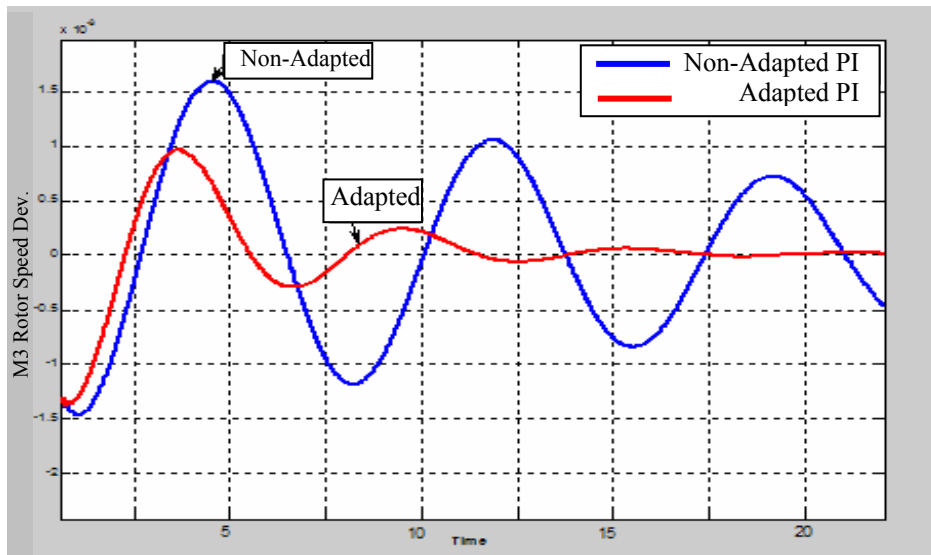


Fig. 6.14, Rotor Speed Deviation of Machine #3.

6.15 Effect of AI Controller Installation on the System

We select a case study from the cases indicated before in steady state performance enhancing, to study the effect of adaptive controller installation to adapt the dynamic parameters of the UPFC. In that case, we will enhance the performance of the network related to the overloading of transmission lines and violation of the bus voltage profile, during the normal configuration of the system with an increasing load pattern on the system until the year 2020. The results lead to optimal location and optimal settings of UPFC to be installed to achieve the required performance.

After installing the UPFC at these optimal locations with optimal settings, the dynamic parameters of the UPFC will have a significant effect on the dynamic response specially the mechanical variables response as the speed deviation response ($\Delta\omega$) and the mechanical rotor angle dynamic response ($\Delta\delta$) of the generating units. The dynamics

parameters for the UPFC blocks should be well-selected and set to fine tune the response and damp the oscillation and enhance the settling time of the response. Table 6.53 indicates the case study, which will be concerned to show the effect of adapting the dynamic parameters of the UPFC after its installation in the optimal location with the optimal settings.

Table 6.53 Case Study of HELEN Network for optimal UPFC.

Case Study					
- Max. Load at all load bus at the same time multiplied by 98% of 2020 coeff.					
⇒ Before Optimal UPFC (UPFC at line 22, for case 96% of 2020 coefficient)					
$\dot{K}_{(LOLN)} = 2$	$Y1 = 0.2068$	$\mathcal{A} = \dot{K}_{(LOLN)} + \Gamma_{(VBVN)} = 2$	$Y = Y1 + Y2 = 0.2068$		
Overloaded Line (11) \equiv (9-2)		101.07%			
Overloaded Line (36) \equiv (7-17)		101%			
⇒ After UPFC Installation					
- Optimal Location Line (14) \equiv (12-9), Optimal Setting (0.196 , 1.0928)					
$\dot{K}_{(LOLN)} = 0$	$Y1 = 0$	$\Gamma_{(VBVN)} = 0$	$Y2 = 0$	$\mathcal{A} = 0$	$Y = 0$
⇒ No Overloading , No Voltage Violation				$0.98 \leq V_i \leq 1.02$	

After installing the UPFC at the optimal location line (14) \equiv (9-12), with optimal setting ($V_{VR} = 0.196$, $V_{CR} = 1.0928$), we will build up the dynamic model of the Helen network including UPFC at the optimal location.

The dynamic behavior aspects of the systems that can be improved with the use of UPFC controllers include transient stability and dynamic stability for damping oscillations. Dynamic instability is characterized by sustained or growing power oscillations between generators or groups of generators. Application of UPFC to enhance the stability of the power system is an important issue. The problems faced in planning and operation are where to place, what size is the appropriate size for these controllers, and what appropriate control input signal should be used to improve dynamic performance.

Figures 6.15, 6.16 and 6.17 show the variation of the change in the generator speed deviation and generator angle deviation and in the generator speed respectively. In the dynamic system responses $\Delta\delta$, $\Delta\omega$ and ω , which will be shown in the following figures, the mechanical oscillations in addition to the system settling down times are noticed. To ensure the robustness of the proposed controller, the design process takes into account a wide range of operating conditions and system configurations.

While the major advantage of UPFC controllers is flexible power scheduling under various operating conditions, the fast controllability also ensures improvement of the dynamic of power systems where system stability is threatened. We take up the problem of oscillations and their damping by appropriate controllers. The UPFC controller damps out

the oscillation effectively, which means that the presence of UPFC damping controller enhances system dynamics. Demonstrating the effectiveness of the UPFC controller, the settling time of the system enhanced with the UPFC controller.

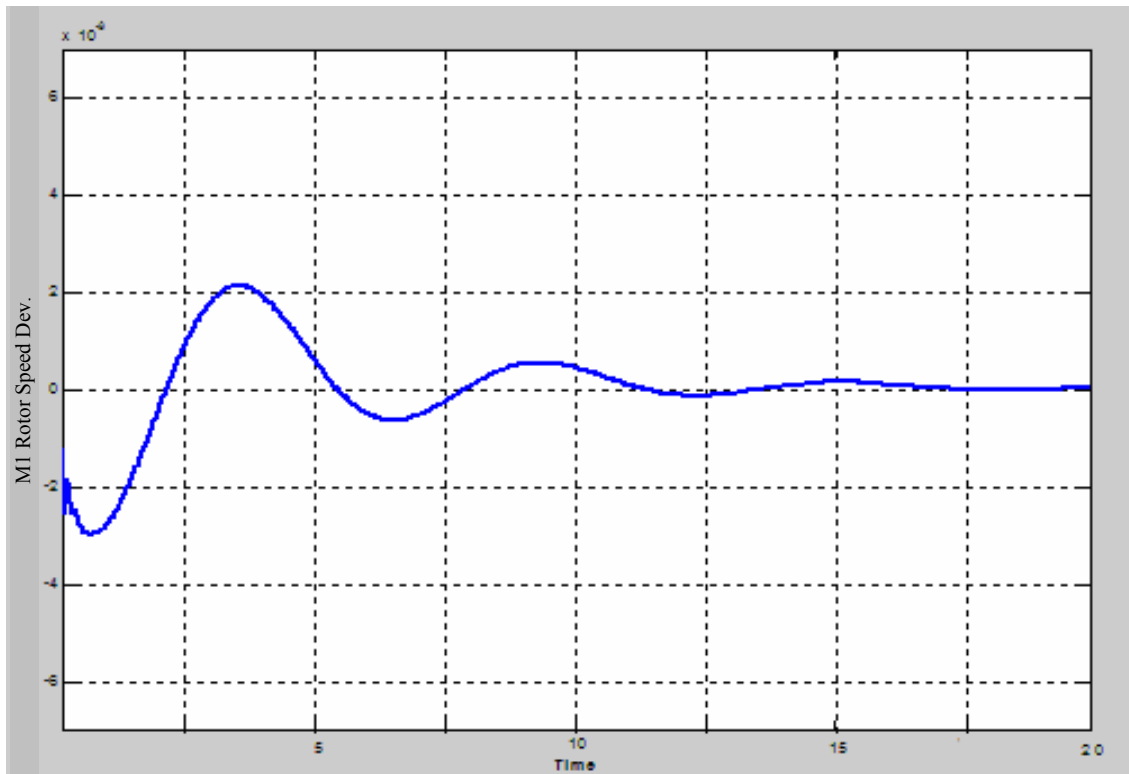


Fig. 6.15 Rotor Speed Deviation Response with AI-adapted optimal UPFC.

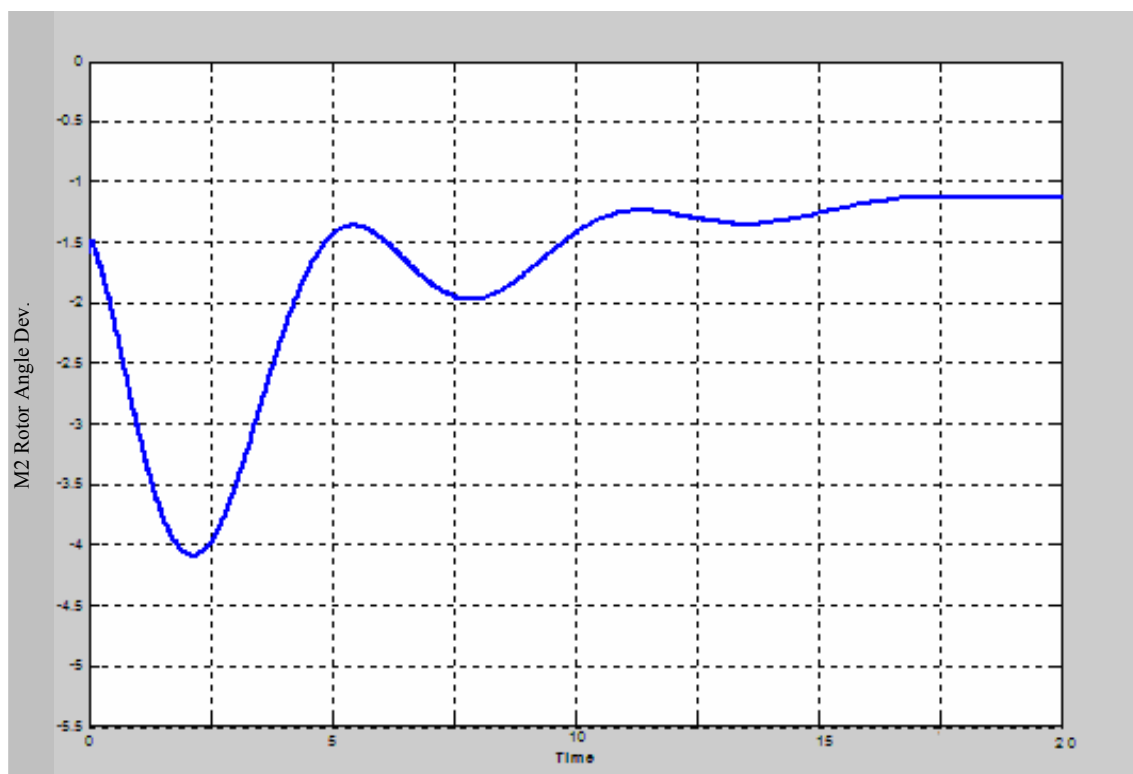


Fig. 6.16 Rotor Angle Deviation Response with AI-adapted optimal UPFC.

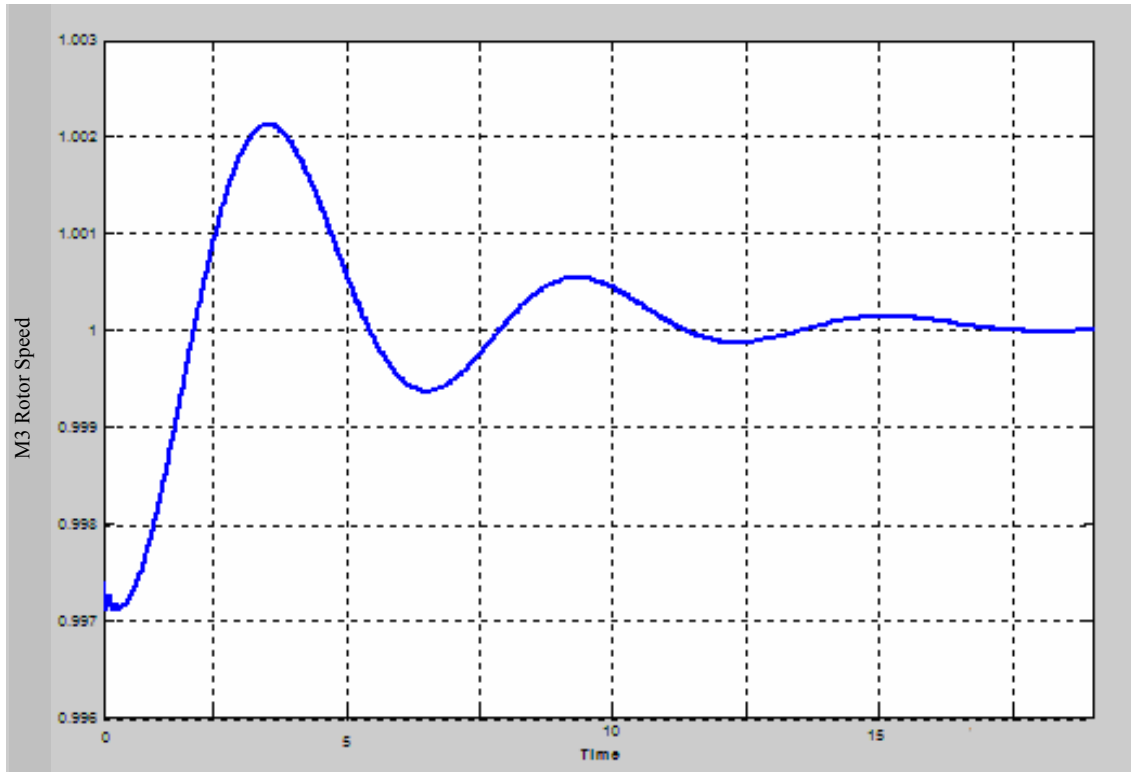


Fig. 6.17 Rotor Speed Response with AI-adapted optimal UPFC.

6.15 Comparing Conventional Fixed PI with Adaptive AI Controller

The performance of the proposed ANFIS controllers has been investigated. The response of the system with fixed-gain controllers designed by GA under normal operating conditions and with the adaptive ANFIS controllers is compared.

The controllers' gains as calculated by GA under normal operating conditions and are held constant and the system loading is increased by 30 %. System responses for this condition with fixed gains damping controllers and with ANFIS are shown in Figures from 6.18 to 6.20. System performance is greatly enhanced by the tuning action of ANFIS.

The figures will show the dynamic response of the system without and with installing an AI-adapted UPFC controller. The AI-adapted UPFC controller makes the system settle down in less cycles and less overshoot, which means the presence of the UPFC controller enhances the system dynamics. We considered the application of UPFC controllers for damping power oscillations in the system. The objective is to improve the stability of power systems that implies the ability of the power systems to maintain synchronism under disturbances that are always present. We are concerned with the improvement of the dynamic response of power systems by suitable control of UPFC controllers. To show the comparison effect of adaptive controller installation to adapt the dynamic parameters of the UPFC, we will now turn to another case study from the cases indicated before in steady state performance enhancing. After installing the UPFC in these optimal locations with optimal settings, the dynamic parameters of the UPFC will have a noticeable effect on the dynamic response. Transient stability is concerned with the stability of power systems when subjected to a severe or large disturbance such as a high increase in loading

conditions. Transient stability depends on the location and nature of the disturbance in addition to the initial operating point.

Table 6.54 Outage Case Study HELEN Network

Outage Case Study					
\Rightarrow Outage of Line (1) \equiv (6-12), Severity Rank =6					
\Rightarrow Before UPFC Installation					
$\dot{K}_{(LOLN)} = 1$	$Y1 = 0.1386$		$\mathcal{A} = \dot{K}_{(LOLN)} + \Gamma_{(VBVN)} = 1$		$Y = Y1 + Y2 = 0.1386$
Loadability			27.57%		
Overloaded Line (6) \equiv (6-2)			108.5%		
\Rightarrow After UPFC Installation					
\Rightarrow Optimal Location Line (23) \equiv (9-11), Optimal Setting (0.2912 , 0.8249)					
$\dot{K}_{(LOLN)} = 0$	$Y1 = 0$	$\Gamma_{(VBVN)} = 0$	$Y2 = 0$	$\mathcal{A} = 0$	$Y = 0$
Loadability			28.9328%		
\Rightarrow No Overloading , No Voltage Violation				$0.98 \leq V_i \leq 1.02$	

After installing the UPFC at the optimal location line (23) \equiv (9-11), with an optimal setting ($V_{VR} = 0.2912$, $V_{CR} = 0.8249$), we will build up the dynamic model of the Helen network including UPFC at an optimal location.

Figures 6.18, 6.19, 6.20 and 6.21 show the variation of the change in the generator speed deviation and generator angle deviation and in the generator speed respectively. In the dynamic system responses $\Delta\delta$, $\Delta\omega$ and ω , which will be shown in the following figures, the mechanical oscillations in addition to the system settling down times are noticed. The figures will show the dynamic response of the system with a fixed controller (without the AI-adapted UPFC controller) and with an installed AI-adapted UPFC controller. The AI-adapted UPFC controller makes the system settle down in less cycles and less overshoot, which means the presence of UPFC controller enhances system dynamics. System performance is greatly enhanced by the tuning action of ANFIS.

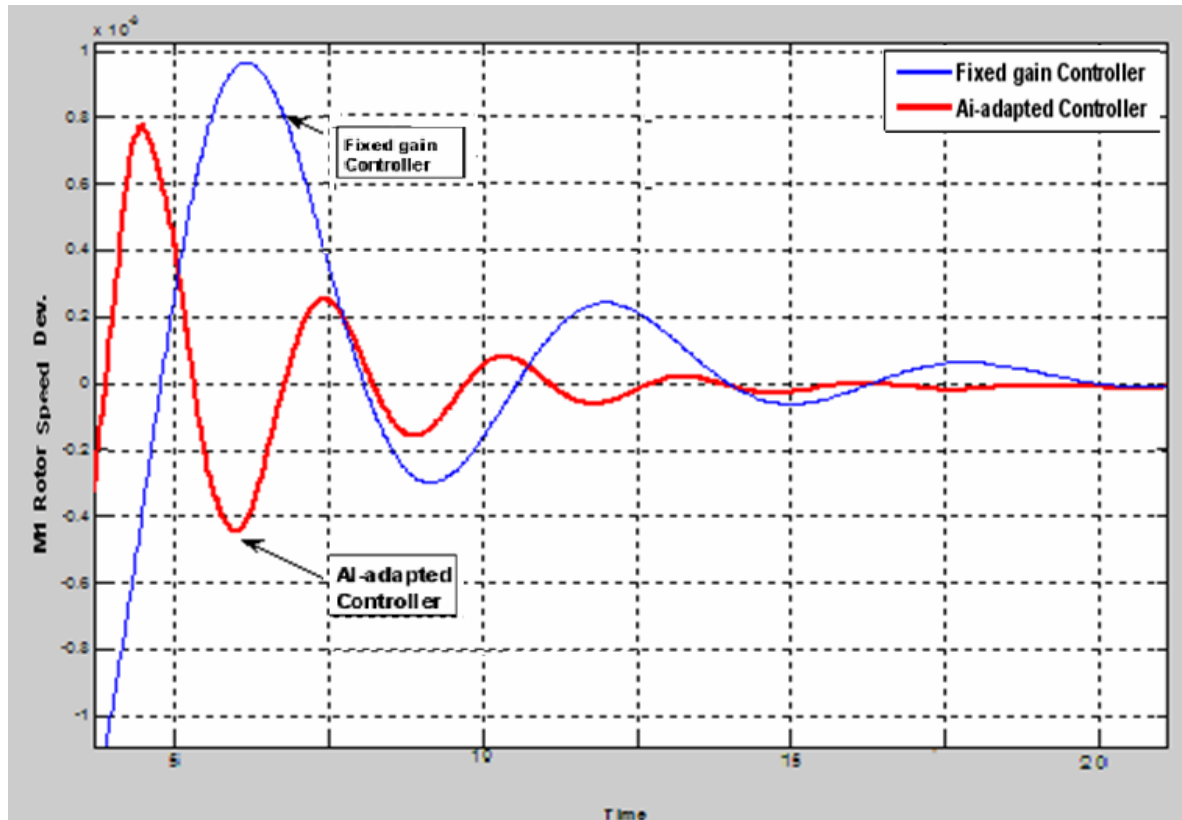


Fig. 6.18 Comparison of Rotor Speed Deviation Response.

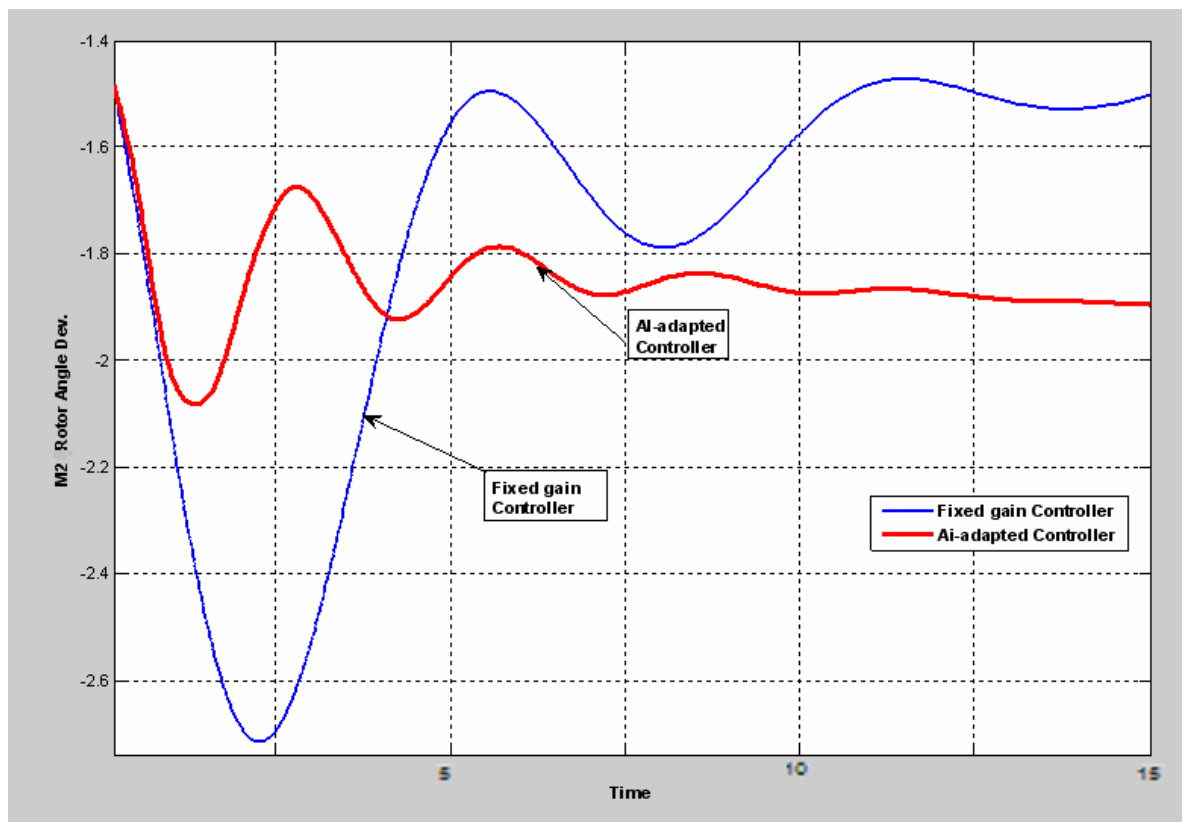


Fig. 6.19 Comparison of Rotor Angle Deviation Response.

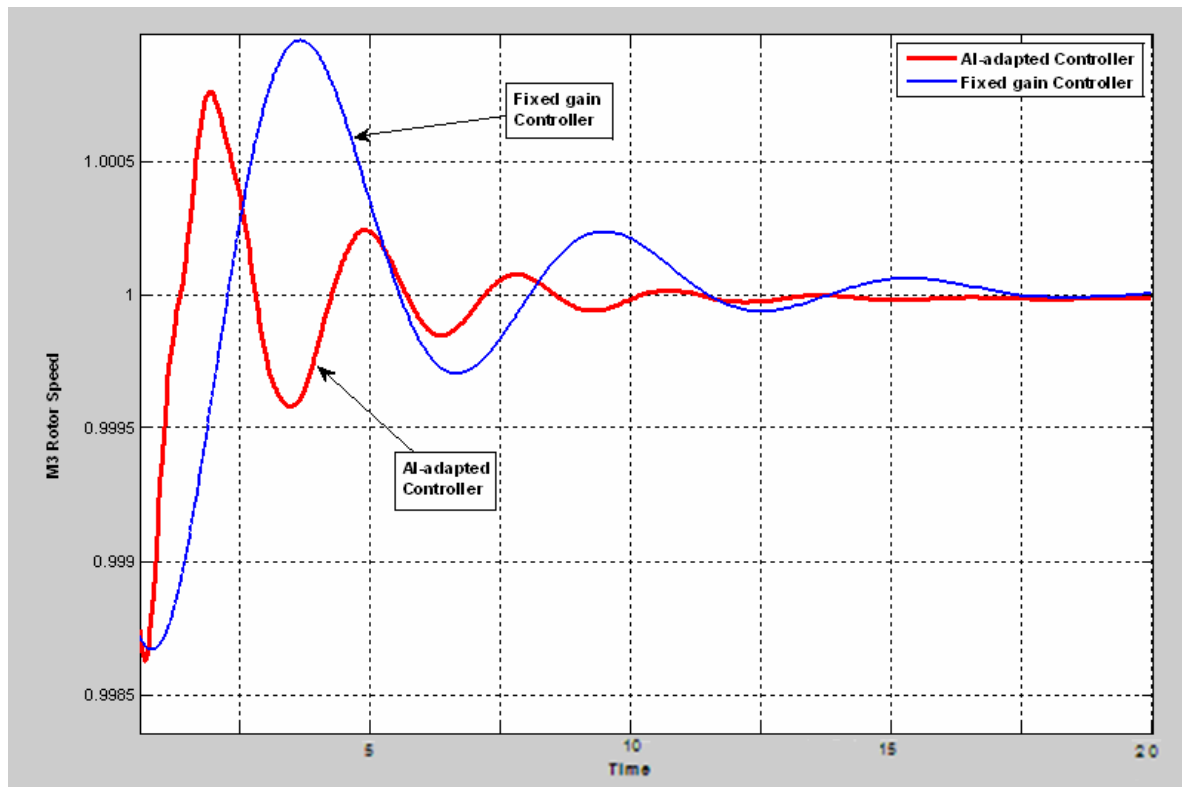


Fig. 6.20 Comparison of Rotor Speed Response.

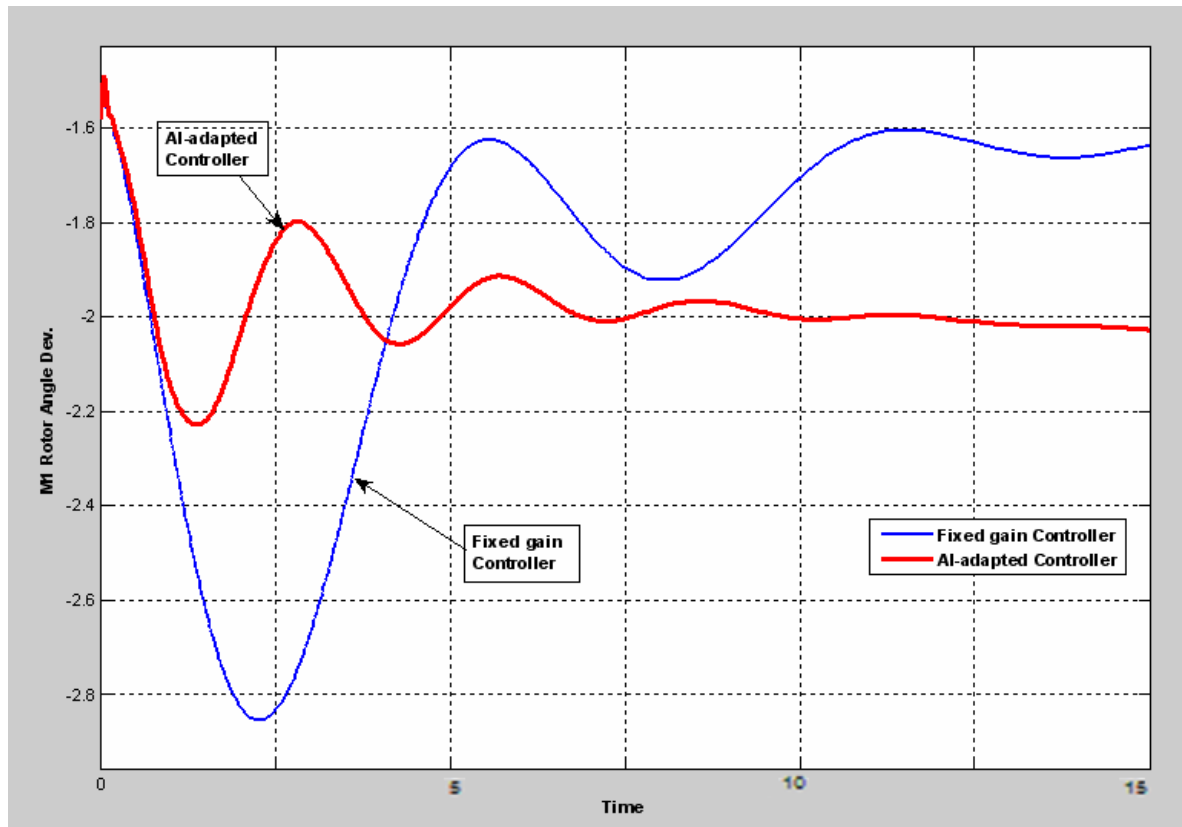


Fig. 6.21 Comparison of Rotor Angle Dev. Response.

Chapter 7

Conclusions

Conclusions

- Flexible Alternating Current Transmission System (FACTS) devices represent very efficient tools for controlling the operations and enhancing the performances of the electrical power network.
- A Unified Power Flow Controller (UPFC) is considered as a powerful member of the Flexible Alternating Current Transmission System (FACTS) family, where it has both the shunt and series controller inside its frame.
- We can use the Genetic Algorithm (GA) to find the optimal location and the optimal settings of the UPFC to improve the performance of the power system specially solving the transmission lines overloading and buses voltage violations during normal operation at increasing loading condition and during the contingency outage cases. When the transmission lines are overloaded and the buses are subjected to voltage violations, the Genetic Algorithm (GA) is also applied to find the optimal location and the optimal settings of the UPFC to improve the performance of the power system at the contingency of the transmission lines outage.
- In this thesis, the optimal UPFC is used to maximize the loadability of the transmission grid. Loadability is an index of the utilization of the transmissions lines and the capability of the power transfer.
- This procedure is proposed to be applied on a Finnish 110 kV NETWORK in Helsinki, until the operating conditions of the year 2020. To show the validity of the technique, it was tested on the IEEE 6-bus, IEEE 30-bus and IEEE 57-bus system.
- Indices have been proposed to evaluate the performance and are used to determine the suitable location and parameter settings of the UPFC in the network.
- These optimal UPFCs enhance the steady-state performance of the network; but the dynamic performance needs another adaptive stage to improve it.

- The performance of the system depends on the model parameters and loading conditions, which varied according to operating point of the network. Therefore, the system performance is studied to get analysis before the control stage under different loading conditions on different system models parameters.
- A novel hybrid technique based on ANFIS, ANFIS merged with a GA system, is used to tune the dynamic parameters of the optimal UPFC to achieve the optimal characteristics; steady-state and dynamic.
- The adaptive controller is better than the fixed parameters controller in how it adapts the control action according to the system performance and can be applied over a wide range of operating conditions.
- Simulation results show that the proposed genetic based ANFISs controller is a very effective means for improving the dynamic performance of the power system compared to fixed-gains controllers.

Contributions of the Thesis

The contributions of the thesis start with formatting, deriving, coding and programming the network equations required to link UPFC steady-state and dynamic models to the power systems. One of the other contributions of the thesis is deriving GA applications on the UPFC to achieve real criteria on a real world sub-transmission network.

An enhanced GA technique is proposed by enhancing and updating the working phases of the GA; the simulations and results show the advantages of using the proposed technique. Integrating the results by linking the case studies of the steady-state and the dynamic analysis is achieved. In the dynamic analysis section, a new idea for integrating the GA with ANFIS to be applied on the control action procedure is presented.

In addition to, packages of Software for genetic algorithm and adaptive neuro-fuzzy system were developed. In other related works, GA only was used to enhance the system dynamic performance considering the whole working

range of the power system at a time that made it difficult and unable in some cases to reach the solution criteria. In this thesis, for every operating point GA is used to search for the controllers' parameters, parameters found at a certain operating point are different from those found at other points. ANFISs are required in this case to recognize the appropriate parameters for each operating point.

FUTURE WORK

- More focusing on the economical issues should be applied to investigate the benefits of UPFC devices versus other options such as network reinforcement.
- The study can be extended to examine the relation and the effect of UPFC devices with magnetic energy storage elements.
- More reliability analysis of the UPFC considering the outage cost analysis and Demand Not Supplied (DNS), Energy Not Supplied (ENS) indices.

References

- [1] T. J. Miller, “Reactive power Control in Electric Systems”, John Willey & Sons, 1982.
- [2] E. Wanner, R. Mathys, M. Hausler, “Compensation Systems for Industry,” *Brown Boveri Review*, vol. 70, pp.330-340, Sept./Oct. 1983.
- [3] P. Kundur, “Power System Stability and Control”, McGraw-Hill, 1994.
- [4] A. Hammad, B. Roesle, “New Roles for Static VAR Compensators in Transmission Systems,” *Brown Boveri Review*, vol. 73, pp. 314-320, June 1986.
- [5] Enrique Acha, C. R. Fuerte, Hugo A. Pe´rez, C. A. Camacho, “FACTS Modelling and Simulation in Power Networks”, John Wiley & Sons Ltd, West Sussex PO19 8SQ, England, ISBN 0-470-85271-2, Copyright © 2004
- [6] N. G. Hingorani, L. Gyugyi, “Understanding FACTS: Concepts and Technology of Flexible AC Transmission Systems”, Institute of Electrical and Electronic Engineers, New York, 2000.
- [7] C.R. Fuerte-Esquivel, “Steady State Modelling and Analysis of Flexible ac Transmission Systems”, Department of Electronics and Electrical Engineering, University of Glasgow, Glasgow, 1997.
- [8] H. Ambriz-Perez, 1998, “Flexible AC Transmission Systems Modelling in Optimal Power Flows Using Newton's Method”, Department of Electronics and Electrical Engineering, University of Glasgow, Glasgow, 1998.
- [9] C. H. Liang, C. Y. Chung, , K. P. Wong, and X. Z. Duan, “Parallel Optimal Reactive Power Flow Based on Cooperative Co-Evolutionary Differential Evolution and Power System Decomposition”, *IEEE Transactions On Power Systems*, Vol. 22, No. 1, February 2007.
- [10] Wei Yan, Fang Liu, C. Y. Chung, and K. P. Wong, “A Hybrid Genetic Algorithm–Interior Point Method for Optimal Reactive Power Flow”, *IEEE Transactions On Power Systems*, Vol. 21, No. 3, August 2006.
- [11] Wei Yan, Juan Yu, David C. Yu, and Kalu Bhattarai, “A New Optimal Reactive Power Flow Model in Rectangular Form and its Solution by Predictor Corrector Primal Dual Interior Point Method”, *IEEE transactions on power systems*, Vol. 21, No. 1, February 2006.
- [12] Luis A. Ll. Zarate, Carlos A. Castro, Jose Luis Martinez Ramos, and Esther Romero Ramos, “Fast Computation of Voltage Stability Security Margins Using Nonlinear Programming Techniques”, *IEEE Transactions On Power Systems*, Vol. 21, No. 1, February 2006.

- [13] Arthit Sode-Yome, Nadarajah Mithulananthan, and Kwang Y. Lee, "A Maximum Loading Margin Method for Static Voltage Stability in Power Systems", *IEEE Transactions On Power Systems*, Vol. 21, No. 2, May 2006.
- [14] Ivan Smon, Gregor Verbič, and Ferdinand Gubina, "Local Voltage-Stability Index Using Tellegen's Theorem", *IEEE Transactions On Power Systems*, Vol. 21, No. 3, August 2006.
- [15] Joong-Rin Shin, Byung-Seop Kim, Jong-Bae Park, and Kwang Y. Lee, "A New Optimal Routing Algorithm for Loss Minimization and Voltage Stability Improvement in Radial Power Systems", *IEEE Transactions On Power Systems*, Vol. 22, No. 2, May 2007.
- [16] Andrzej Wiszniewski, "New Criteria of Voltage Stability Margin for the Purpose of Load Shedding", *IEEE Transactions on Power Delivery*, Vol. 22, No. 3, July 2007.
- [17] Jing Zhang, J. Y. Wen, S. J. Cheng, and Jia Ma, "A Novel SVC Allocation Method for Power System Voltage Stability Enhancement by Normal Forms of Diffeomorphism", *IEEE Transactions On Power Systems*, Vol. 22, No. 4, November 2007.
- [18] Carson W. Taylor, "Improving Grid Behavior", *IEEE Spectrum*, Vol. 36, No. 6, pp. 40-45, June 1999.
- [19] Canadian Electrical Association, "Static Compensators for Reactive Power Control," Context Publications, 1984.
- [20] Laszlo Gyugyi, "Solid-State Synchronous Voltage Sources for Dynamic Compensation and Real-Time Control of AC Transmission Lines", *Emerging Practices in Technology*, IEEE standards Press, 1993.
- [21] G. Bonnard, "The Problems Posed by Electrical Power Supply to Industrial Installations," in *Proc. of IEE Part B*, vol. 132, pp. 335-340, Nov. 1985.
- [22] Nadarajah Mithulananthan, "Hopf Bifurcation Control and Indices for Power System with Interacting Generator and FACTS Controllers", Ph.D. Thesis, University of Waterloo, Ontario, Canada, 2002.
- [23] "FACTS Technology for Open Access", CIGRE Report, August 2000.
- [24] Naihu Li, Yan Xu, and Heng Chen, "FACTS-Based Power Flow Control in Interconnected Power Systems", *IEEE Transaction on Power System*, Vol. 15, No. 1, pp. 257-262, Feb. 2000.
- [25] R. Mihalic, "Power Flow Control with Controllable reactive series elements", *IEE Proceeding., Generation, Transmission and. Distribution*, Vol. 145, No. 5, pp. 493-498, Sept. 1998.

- [26] S. Y. Ge and T S Chung, “Optimal power flow incorporating Power Flow Control Needs in Flexible AC Transmission Systems”, *IEEE Transaction on Power System*, Vol. 14, No. 2, pp. 738-744, May 1999.
- [27] C.R. Fuerte-Esquivel, E. Acha and H. Amprez-Pêrez, “A Thyristor Controlled Series Compensation Model for the Power Flow Solution of Practical Power Networks”, *IEEE Transaction on Power System*, Vol. 15, No. 1, pp. 58-64, Feb. 2000.
- [28] C.R. Fuerte-Esquivel, E. Acha and H. Amprez-Pêrez, “A Comprehensive Newton-Raphson UPFC Model for the Quadratic Power Flow Solution of Practical Power Networks”, *IEEE Transaction on Power System*, Vol. 15, No. 1, pp. 102-109, Feb. 2000.
- [29] F. P. De Mello and T. F. Laskowski, “Concepts of Power System Dynamic Stability,” *IEEE Trans. PAS*, Vol. 94, pp. 827-833, 1979.
- [30] G. N. Taranto, D. M. Falcao, “Robust Decentralized Control Design Using Genetic Algorithm in power System Damping Control”, *IEE Proc., Generation, Transmission, Distribution*, Vol. 145, No. 1, pp. 1-6, Jan. 1998.
- [31] Tain-Syyh Luor, Yuan-Yih Hsu, Tzong-Yih Guo, Jiann-Tyng Lin, and Chiung-Yi Huang, “Application of Thyristor-Controlled Series Compensators to Enhance Oscillatory Stability and Transmission Capability of Longitudinal Power System”, *IEEE Transaction on Power System*, Vol. 14, No. 1, pp. 179-185, Feb. 1999.
- [32] L.L. Li, and J.T. Ma, “Power Flow Control with UPFC Using Genetic Algorithms”, *International Conference on Intelligent Systems Applications to Power Systems*, Orlando, FL, Feb 1996.
- [33] H.C. Leung, and T. S. Chung, “Optimal Power Flow with a Versatile FACTS controller by Genetic Algorithm Approach”, *Power Engineering Society IEEE Winter Meeting*, Vol. 4, pp. 2806 – 2811, 2000.
- [34] T. K. Mok, Yixin Ni and F. F. Wu, “Design of Fuzzy Damping Controller of UPFC through Genetic Algorithm”, *Power Engineering Society IEEE Winter Meeting*, Vol. 3, pp. 1889 - 1894, 2000.
- [35] S. Gerbex, R. Cherkaoui, and A. J. Germond, “Optimal Location of FACTS Devices to Enhance Power System Security”, *PowerTech IEEE Conference*, Bologna, 23-26 June 2003.
- [36] A. Parizad, A. Khazali, and M. Kalntar, “Application of HAS and GA in Optimal Placement of FACTS devices considering Voltage Stability and Losses”, *Conference on Electric Power & Energy Conversion Systems, EPECS '09*, pp. 1 - 7, Nov. 2009.
- [37] S. O. Faried and A. A. Eldamaty, “Damping Power System Oscillations Using A Genetic Algorithm Based Unified Power Flow Controller”,

- Conference on Electrical & Computer Engineering, Vol. 1, pp. 65 - 68, May 2004.
- [38] L. Khan, K. L. Lo, and N. Ahmed, "Micro-GA based Fuzzy Logic Controllers for Coordinated FACTS Control", 7th International Conference on Multi Topic INMIC 2003. , pp. 269 - 275, Dec. 2003.
- [39] L. Khan, N. Ahmed, and C. Lozano "GA Neuro-Fuzzy Damping Control System for UPFC to Enhance Power System Transient Stability", 7th International Conference on Multi Topic INMIC 2003. , pp. 276 - 282 , Dec. 2003.
- [40] H. R. Baghaee, M. Jannati, and B. Vahidi, "Improvement of Voltage Stability and Reduce Power System Losses by Optimal GA-based Allocation of Multi-type FACTS Devices", 11th International Conference on Optimization of Electrical and Electronic Equipment, OPTIM 2008, pp. 209 – 214, May 2008.
- [41] K. R. Saidi, N. P. Padhy, and R. N. Patel, "Congestion Management in Deregulated Power System using FACTS Devices", International IEEE Power India Conference, June 2006.
- [42] A. Kazemi, D. Arabkhabori, M. Yari, and J. Aghaei, "Optimal Location of UPFC In Power Systems for Increasing Loadability By Genetic Algorithm", Universities Power Engineering Conference, UPEC '06, Vol. 2, pp. 774 – 779, Sept. 2006.
- [43] D. Arabkhabori, A. Kazemi, M. Yari, and J. Aghaei, "Optimal Placement of UPFC In Power Systems using Genetic Algorithm", Industrial Technology ICIT IEEE International Conference, pp. 1694 - 1699, Dec. 2006.
- [44] H. C. Leung, and T. S. Chung, "A Hybrid GA Approach for Optimal Control Setting Determination of UPFC", Power Engineering Review, IEEE , Vol. 21, pp. 62 - 65, Dec. 2001.
- [45] K. Vijayakumar, R. P. Kumudinidevi, and D. Suchithra, "A Hybrid Genetic Algorithm for Optimal Power Flow Incorporating FACTS Devices", Conference on Computational Intelligence and Multimedia Applications, Vol. 1, pp. 463 - 467, Dec. 2007.
- [46] B. Mahdad, T. Bouktir, and K. Srairi, "Dynamic Methodology for Control of Multiplie-UPFC to Relieve Overloads and Voltage Violations", 2007. The International Conference on (Computer as a Tool) EUROCON; pp. 1579 - 1585, Vol. 1, pp. 463 - 467, Sept. 2007.
- [47] F. Taki, S. Abazari, and G. R. Markadeh, "Transient Stability Improvement using ANFIS Controlled UPFC based on Energy Function", 18th Iranian Conference Electrical Engineering (ICEE), pp. 994 – 948, May 2010.

- [48] G. Li, T. T. Lie, G. B. Shrestha, and K. L. Lo, “Design and application of coordinated Multiple FACTS Controllers”, IEE Proceeding., Generation, Transmission and. Distribution, Vol. 147, No. 2, pp. 112-120, , March 2000.
- [49] Laszlo Gyugyi, “Power Electronics in Electric Utilities: Static Var Compensator”, Proc. of the IEEE, Vol. 76, No. 4, pp. 483-494, , April 1988.
- [50] Zeno T. Faur, “Effects of FACTS Devices on Static Voltage Collapse”, Master Thesis, University of Waterloo, Ontario, Canada, 1996.
- [51] T. J. E. Miller, “Reactive Power Control in Electric Systems”, John Wiley & Sons, 1982.
- [52] X. Zhou and J. Liang, “Overview of Control Methods for TCSC in Enhance the Stability of Power Systems”, IEE Proceeding., Generation, Transmission and. Distribution, Vol. 146, No. 2, pp. 125-130, March 1999.
- [53] Claudio A. Canizares, “Power Flow and Transient Stability Models of FACTS Controllers for Voltage and Angle Stability Studies”, IEEE/PES Panel on Modeling, Simulation and Application of FACTS Controller in Angle and Voltage Stability Studies, Singapore, pp. 1-8, Jan. 2000.
- [54] Edward Y. Y Ho and Paresh C. Sen, “Effect of Gate-Drive Circuits on GTO Thyristor Characteristics”, IEEE Transaction on Industrial Electronics, Vol. IE-33, No. 3, pp. 325-331, August 1986.
- [55] Laszlo Gyugyi, “Solid-State Synchronous Voltage Sources for Dynamic Compensation and Real-Time Control of AC Transmission Lines”, Emerging Practices In Technology, IEEE standards Press, 1993.
- [56] Handbook of Measuring System Design, edited by Peter H. Sydenham and Richard Thorn. 2005 John Wiley & Sons, Ltd. ISBN: 0-470-02143-8.
- [57] A. Abraham, “Neuro-Fuzzy Systems: State-of-the-art Modeling Techniques, Connectionist Models of Neurons, Learning Processes, and Artificial Intelligence”, Lecture Notes in Computer Science, Vol. 2084, Springer Verlag, Germany, pp. 269–276, 2001
- [58] A. Abraham, “Intelligent Systems: Architectures and Perspectives, Recent Advances in Intelligent Paradigms and Applications, in Studies in Fuzziness and Soft Computing”, Springer Verlag Germany, pp. 1–35, 2002.
- [59] C.M. Bishop, “Neural Networks for Pattern Recognition”, Oxford University Press, UK, 1995.
- [60] T. K. Mok, Yixin Ni and Flex F. Wu, “Design of Fuzzy Damping Controller of UPFC through Genetic Algorithm”, IEEE Transaction on Power Systems, Vol. 1, No. 2, pp. 1889-1894, Nov. 2000.

- [61] D.B. Fogel, “Evolutionary Computation: Toward a New Philosophy of Machine Intelligence”, 2nd edn, IEEE Press, Piscataway, NJ, 1999.
- [62] L.J. Fogel, A.J. Owens, and M.J. Walsh, “Artificial Intelligence through Simulated Evolution”, John Wiley & Sons, New York, 1967.
- [63] D.E. Goldberg, “Genetic Algorithms in Search, Optimization, and Machine Learning”, Addison-Wesley Publishing Corporation, Inc, Reading, MA, 1989.
- [64] J. Holland, “Adaptation in Natural and Artificial Systems”, University of Michigan Press, Ann Harbor, MI, 1975.
- [65] T. Kohonen, “Self-organization and Associative Memory”, Springer-Verlag, New York, 1988.
- [66] J.R. Koza, “Genetic Programming”, MIT Press, Cambridge, MA, 1992.
- [67] H. T. Nguyen, and E. A. Walker, “A First Course in Fuzzy Logic”, CRC Press, USA, 1999.
- [68] J. Pearl, “Probabilistic Reasoning in Intelligent Systems: Networks of Plausible Inference”, Morgan Kaufmann Publishers, San Francisco, CA, 1997.
- [69] A. M. Turing, “Computing Machinery and Intelligence”, <http://abelard.org/turpap/turpap.htm>, VOL. LIX. No.236, October 1950.
- [70] Turing Machine, <http://www.turing.org.uk/turing/>, 2004
- [71] L. A. Zadeh, “Fuzzy Sets”, *Journal of Information and Control*, 8, 338–353, 1965.
- [72] Randy L. Haupt and Sue Ellen Haupt, “Practical Genetic Algorithms”, John Wiley & Sons, 1998.
- [73] Sushmita Mitra and Yoichi Hayashi, “Neuro-Fuzzy Rule Generation: Survey in Soft Computing Framework”, *IEEE Transaction on Neural Networks*, Vol. 11, No. 3, pp. 748-768, May 2000.
- [74] Hong-Chan Chang and Mang-Hui Wang, “Neural Network-Base Self-Organizing Fuzzy Controller for Transient Stability of Multi-machine Power Systems”, *IEEE Transaction on Energy Conversion*, Vol. 10, No. 2, June 1995, pp. 339-346.
- [75] J. Wesley Hines, “MATLAB Supplement to Fuzzy and Neural Approaches in Engineering”, John Wiley & Sons, 1997.

- [76] M. Reformat, E. Kuffel, D. Woodford and W. Pedrycz, “Application of Genetic Algorithm for Control Design in Power systems”, IEE Proc., Generation, Transmission and Distribution., Vol. 145, No. 4, pp. 345-354, July 1998.
- [77] Jyh-Shing R. Jang, Chuen-Tsai Sun, Eiji Mizutani, “Neuro-Fuzzy and Soft Computing”, Prentice-Hall, 1997.
- [78] P. M. Anderson and A. A. Fouad, “Power System Control and Stability”, Iowa State University Press, Iowa, 1977.
- [79] A. Nabavi Niaki and M. R. Iravani, “Steady-State and Dynamic Models of Unified Power Flow Controller (UPFC) for Power System Studies”, IEEE Transaction on Power Systems, Vol. 11, No. 4, pp. 1937-1943, Nov. 1996.
- [80] Haifeng Wang, “A Unified Model for the Analysis of FACTS Devices in Damping Power System Oscillations Part III: Unified power Flow Controller”, IEEE Transaction on Power Delivery, Vol. 15, No. 3, pp. 978-983, July 2000.
- [81] K. R. Padiyar, “FACTs Controllers in Power Transmission and Distribution”, ISBN (13): 978-81-224-2541-3, New Age International (P) Limited, Publishers, New Delhi, 2007.
- [82] K. Schoder, A. Hasanovic, and A. Feliachi , “Load-Flow and Dynamic Model of the Unified Power Flow Controller (UPFC) within the Power System Toolbox (PST) ”, Circuits and Systems Proceedings of the 43rd IEEE Midwest Symposium, Vol. 2, pp. 634 – 637, 2000.
- [83] I. Dahhaghchi, R.D. Christie, G:W: Rosenwald, and Chen-Ching Liu, “AI application areas in power systems”, IEEE Expert Magazine, Volume: 12 pp. 58 – 66, Jan/Feb 1997.
- [84] D. Radu, Y.Besanger, “Blackout prevention by optimal insertion of FACTS devices in power systems”, Future Power Systems, 2005 International Conference on Volume 6, Issue 18, pp. 9-18, Nov. 2005.

Appendix

[I] Genetics Algorithm Programming

```

%Main GA core program
%PowerFlowsData; %Function to read network data
%UPFCdata; %Function to read the UPFC data

ObjectiveFunction = @UPFCobjective;
nvars = 3; % Number of variables
LB = [1 0.001 0.8]; % Lower bound
UB = [42 0.3 1.2]; % Upper bound
ConstraintFunction = @UPFCconstraint;

options = gaoptimset('MutationFcn',@mutationadaptfeasible,
'PopulationSize',500,'Generations',30);
options =
gaoptimset(options,'PlotFcns',{@gaplotbestf,@gaplotmaxconstr},'Display',
'iter');

[X,FVAL,EXITFLAG,OUTPUT,POPULATION,SCORES] =
ga(ObjectiveFunction,nvars,[],[],[],[],LB,UB,[],options)
%[X,FVAL,EXITFLAG,OUTPUT,POPULATION,SCORES] =
GA(FITNESSFCN,NVARS,A,b,Aeq,beq,lb,ub,NONLCON,options)

% Objective function programming
function y = UPFCobjective(x)

UPFCtln(1)=x(1);
Vcr(1)=x(2);
Vvr(1)=x(3);

NetworkData; %Function to read network data

NUPFC=1;
UPFCrec(1)=25;

nbb=25;
bustype(25) = 3 ; VM(25) = 1 ; VA(25) =0 ;

Xcr(1)=0.1; Xvr(1)=0.1;
Psp(1)= -4.49 ; Qsp(1)=0.099;
Flow(1)=-1; PSta(1)=0; QSta(1)=0;
%Vcr(1)= 0.21855 ;
Tcr(1)=-87.13/57.3; VcrLo(1)=0.001; VcrHi(1)=0.3;
%Vvr(1)= 1.0155 ;
Tvr(1)=0.0; VvrLo(1)=0.8; VvrHi(1)=1.2;
VvrTar(1)=1.0; VvrSta(1)=0;

UPFCtln(1)=fix(UPFCtln(1));
UPFCsend(1)=tlsend(UPFCtln(1));
tlsend(UPFCtln(1))=25;

[YR,YI] = YBus(tlsend,tlrec,tlresis,tlreac,tl suscep,tlcond,shbus,...
shresis,shreac,ntl,nbb,nsh);

```

```

[VM,VA,it,Vcr,Tcr,Vvr,Tvr,DPQ] =
UPFCNewtonRaphson(nmax,tol,itmax,ngn,nld,...
nbb,bustype,genbus,loadbus,PGEN,QGEN,QMAX,QMIN,PLOAD,QLOAD,YR,YI,...
VM,VA,NUPFC,UPFCsend,UPFCrec,Xcr,Xvr,Flow,Psp,PSta,Qsp,QSta,Vcr,...
Tcr,VcrLo,VcrHi,Vvr, Tvr,VvrLo,VvrHi,VvrTar,VvrSta);
[PQsend,PQrec,PQloss,PQbus] = PQflows(nbb,ngn,ntl,nld,genbus,...
loadbus,tlsend,tlrec,tlresis,tlreac,tlcond,tlsuscep,PLOAD,QLOAD,...
VM,VA);
tlflow=zeros(1,ntl);
for n=1:ntl
    if abs(PQsend(1,n)) > abs(PQrec(1,n))
        tlflow(1,n)=abs(PQsend(1,n));
    else
        tlflow(1,n)=abs(PQrec(1,n));
    end
end
Vmref=ones(1,nbb);
q=2; r=2;
Q=2*q; R=2*r; wm=1 ; wl=0.1 ; y1=0; y2=0;
for i=1:nbb
    if VM(1,i) > 1.05 || VM(1,i) < 0.95
        y1=y1+(wm*((Vmref(1,i)-VM(1,i))./Vmref(1,i)).^R);
    else
        y1=y1+0;
    end
end
for i=1:ntl
    if tlflow(1,i)*100 <= tlrates(1,i)
        y2=y2+0;
    else
        y2=y2+(wl*(tlflow(1,i)*100./tlrates(1,i)).^Q);
    end
end
y = y1+y2;
%y(1)=abs(imag(sum(PQloss))); y(2)=real(sum(PQloss));
%End Main Program
function [x,fval,exitFlag,output,population,scores] =
ga(fun,nvars,Aineq,bineq,Aeq,beq,lb,ub,nonlcon,options)
%GA Constrained optimization using genetic algorithm.
defaultopt = struct('PopulationType','doubleVector',...
'PopInitRange',[0;1],...
'PopulationSize',20,...
'EliteCount',2,...
'CrossoverFraction',0.8,...
'MigrationDirection','forward',...
'MigrationInterval',20,...
'MigrationFraction',0.2,...
'Generations',100,...
'TimeLimit',inf,...
'FitnessLimit',-inf,...
'StallGenLimit',50,...
'StallTimeLimit',inf,...
'TolFun',1e-6,...
'TolCon',1e-6,...
'InitialPopulation',[],...
'InitialScores',[],...
'InitialPenalty',10,...
'PenaltyFactor',100,...
'PlotInterval',1,...

```

```

    'CreationFcn',@gacreationuniform, ...
    'FitnessScalingFcn', @fitscalingrank, ...
    'SelectionFcn', @selectionstochunif, ...
    'CrossoverFcn',@crossoversscattered, ...
    'MutationFcn',{@mutationgaussian 1 1}}, ...
    'HybridFcn',[], ...
    'Display', 'final', ...
    'PlotFcns', [], ...
    'OutputFcns', [], ...
    'Vectorized','off', ...
    'UseParallel', 'never');
% Check number of input arguments
errmsg = nargchk(1,10,nargin);
if ~isempty(errmsg)
    error('gads:ga:numberOfInputs',[errmsg, ' GA requires at least 1
input argument.']);
end
% If just 'defaults' passed in, return the default options in X
if nargin == 1 && nargout <= 1 && isequal(fun,'defaults')
    x = defaultopt;
    return
end
if nargin < 10, options = [];
    if nargin < 9, nonlcon = [];
        if nargin < 8, ub = [];
            if nargin < 7, lb = [];
                if nargin < 6, beq = [];
                    if nargin < 5, Aeq = [];
                        if nargin < 4, bineq = [];
                            if nargin < 3, Aineq = [];
                                end
                            end
                        end
                    end
                end
            end
        end
    end
end
end
end
end
end
end
end
end
end
% Is third argument a structure
if nargin == 3 && isstruct(Aineq) % Old syntax
    options = Aineq; Aineq = []; end
% One input argument is for problem structure
if nargin == 1
    if isa(fun,'struct')
        [fun,nvars,Aineq,bineq,Aeq,beq,lb,ub,nonlcon,rngstate,options]
= separateOptimStruct(fun);
        % Reset the random number generators
        resetDfltRng(rngstate);
    else % Single input and non-structure.
        error('gads:ga:invalidStructInput','The input should be a
structure with valid fields or provide at least two arguments to GA.'
);    end
end
% If fun is a cell array with additional arguments get the function
handle
if iscell(fun)
    FitnessFcn = fun{1};
else
    FitnessFcn = fun;
end

```

```

end
% Only function handles or inlines are allowed for FitnessFcn
if isempty(FitnessFcn) || ~(isa(FitnessFcn, 'inline') ||
isa(FitnessFcn, 'function_handle'))
    error('gads:ga:needFunctionHandle', 'Fitness function must be a
function handle.');
```

```

end
% We need to check the nvars here before we call any solver
valid = isnumeric(nvars) && isscalar(nvars) && (nvars > 0) ...
    && (nvars == floor(nvars));
if ~valid
    error('gads:ga:notValidNvars', 'Number of variables (NVARs) must be
a positive integer.');
```

```

end
user_options = options;
% Use default options if empty
if ~isempty(options) && ~isa(options, 'struct')
    error('gads:ga:optionsNotAstruct', 'Tenth input argument must
be a valid structure created with GAOPTIMSET.');
```

```

elseif isempty(options)
    options = defaultopt;
end
% Take defaults for parameters that are not in options structure
options = gaoptimset(defaultopt, options);
% All inputs should be double
try
    dataType = superiorfloat(nvars, Aineq, bineq, Aeq, beq, lb, ub);
    if ~isequal('double', dataType)
        error('gads:ga:dataType', ...
            'GA only accepts inputs of data type double.')
```

```

    end
catch
    error('gads:ga:dataType', ...
        'GA only accepts inputs of data type double.')
```

```

end
[x, fval, exitFlag, output, population, scores, FitnessFcn, nvars, Aineq, bineq
, Aeq, beq, lb, ub, ...
    NonconFcn, options, Iterate, type] =
gacommon(nvars, fun, Aineq, bineq, Aeq, beq, lb, ub, nonlcon, options, user_opti
ons);
if exitFlag < 0
    return;
end
% Call appropriate single objective optimization solver
switch (output.problemtype)
    case 'unconstrained'
        [x, fval, exitFlag, output, population, scores] =
gaunc(FitnessFcn, nvars, ...
        options, output, Iterate);
    case {'boundconstraints', 'linearconstraints'}
        [x, fval, exitFlag, output, population, scores] =
galincon(FitnessFcn, nvars, ...
        Aineq, bineq, Aeq, beq, lb, ub, options, output, Iterate);
    case 'nonlinearconstr'
        [x, fval, exitFlag, output, population, scores] =
gacon(FitnessFcn, nvars, ...
```

```

        Aineq, bineq, Aeq, beq, lb, ub, NonconFcn, options, output, Iterate, type);
end
```

III Network, UPFC Model Programming

```

SavedCharacterEncoding "US-ASCII"
SaveDefaultBlockParams on
ScopeRefreshTime 0.035000
OverrideScopeRefreshTime on
DisableAllScopes off
DataTypeOverride "UseLocalSettings"
MinMaxOverflowLogging "UseLocalSettings"
MinMaxOverflowArchiveMode "Overwrite"
Creator "hyp01"
UpdateHistory "UpdateHistoryNever"
ModifiedByFormat "%<Auto>"
LastModifiedBy "Amo"
ModifiedDateFormat "%<Auto>"
RTWModifiedTimeStamp 0
ModelVersionFormat "1.%<AutoIncrement:1027>"
ConfigurationManager "None"
SampleTimeColors off
SampleTimeAnnotations off
LibraryLinkDisplay "none"
WideLines off
ShowLineDimensions off
ShowPortDataTypes off
ShowLoopsOnError on
IgnoreBidirectionalLines off
ShowStorageClass off
ShowTestPointIcons on
ShowSignalResolutionIcons on
ShowViewerIcons on
SortedOrder off
ExecutionContextIcon off
ShowLinearizationAnnotations on
BlockNameDataTip off
BlockParametersDataTip off
Array {
  Type "Handle"
  Dimension 1
  Simulink.ConfigSet {
    $ObjectID 1
  }
}
Array {
  Type "Handle"
  Dimension 8
  Simulink.SolverCC {
    $ObjectID 2
    Version "1.6.0"
    StartTime "0"
    StopTime "40"
    AbsTol "1e-3"
    FixedStep "auto"
    InitialStep "auto"
    MaxNumMinSteps "-1"
    MaxOrder 5
    ZcThreshold "auto"
    ConsecutiveZCsStepRelTol "10*128*eps"
    MaxConsecutiveZCs "1000"
    ExtrapolationOrder 4
    NumberNewtonIterations 1
    MaxStep "1/60"
  }
}

```

```

    MinStep          "auto"
    MaxConsecutiveMinStep "1"
    RelTol           "1e-4"
    SolverMode       "SingleTasking"
    Solver           "ode23tb"
    SolverName       "ode23tb"
    ShapePreserveControl "DisableAll"
    ZeroCrossControl "UseLocalSettings"
    ZeroCrossAlgorithm "Nonadaptive"
    AlgebraicLoopSolver "TrustRegion"
    SolverResetMethod "Fast"
    PositivePriorityOrder off
    AutoInsertRateTranBlk off
    SampleTimeConstraint "Unconstrained"
    InsertRTBMode       "Whenever possible"
    SignalSizeVariationType "Allow only fixed size"
  }
  PropName          "Components"
  }
  Name              "Configuration"
  CurrentDlgPage    "Real-Time Workshop/Interface"
  ConfigPrmDlgPosition " [ -2, 26, 927, 740 ] "
  }
  PropName          "ConfigurationSets"
  }
  Simulink.ConfigSet {
    $PropName        "ActiveConfigurationSet"
    $ObjectID        1
  }
  BlockDefaults {
    ForegroundColor  "black"
    BackgroundColor  "white"
    DropShadow       off
    NamePlacement    "normal"
    FontName         "Helvetica"
    FontSize         10
    FontWeight       "normal"
    FontAngle        "normal"
    ShowName         on
    BlockRotation    0
    BlockMirror      off
  }
  AnnotationDefaults {
    HorizontalAlignment "center"
    VerticalAlignment  "middle"
    ForegroundColor    "black"
    BackgroundColor    "white"
    DropShadow         off
    FontName           "Helvetica"
    FontSize           10
    FontWeight         "normal"
    FontAngle          "normal"
    UseDisplayTextAsClickCallback off
  }
  LineDefaults {
    FontName          "Helvetica"
    FontSize          9
    FontWeight        "normal"
    FontAngle         "normal"
  }

```

```

}
BlockParameterDefaults {
  Block {
    BlockType      BusCreator
    Inputs          "4"
    DisplayOption  "none"
    UseBusObject    off
    BusObject       "BusObject"
    NonVirtualBus   off
  }
  Block {
    BlockType      Outport
    Port           "1"
    UseBusObject    off
    BusObject       "BusObject"
    BusOutputAsStruct off
    PortDimensions "-1"
    SampleTime      "-1"
    OutMin           "[]"
    OutMax           "[]"
    DataType        "auto"
    OutDataType     "fixdt(1,16,0)"
    OutScaling      "[]"
    OutDataTypeStr  "Inherit: auto"
    LockScale       off
    SignalType      "auto"
    SamplingMode    "auto"
    SourceOfInitialOutputValue "Dialog"
    OutputWhenDisabled "held"
    InitialOutput   "[]"
    DimensionsMode  "auto"  }
  Block {
    BlockType      PMComponent
    SubClassName    "unknown"  }
  Block {
    BlockType      PMIOPort
  }
  Block {
    BlockType      Product
    Inputs          "2"
    Multiplication  "Element-wise(.*)"
    CollapseMode    "All dimensions"
    CollapseDim     "1"
    InputSameDT     on
    OutMin           "[]"
    OutMax           "[]"
    OutDataTypeMode "Same as first input"
    OutDataType     "fixdt(1,16,0)"
    OutScaling      "[]"
    OutDataTypeStr  "Inherit: Same as first input"
    LockScale       off
    RndMeth         "Zero"
    SaturateOnIntegerOverflow on
    SampleTime      "-1"  }
  Block {
    BlockType      RateLimiter
    RisingSlewLimit "1"
    FallingSlewLimit "-1"
    SampleTimeMode "continuous"

```

```

        InitialCondition      "0"
        LinearizeAsGain      on
    }
    Block {
        BlockType              RealImagToComplex
        Input                  "Real and imag"
        ConstantPart          "0"
        SampleTime            "-1"
    }
    Block {
        BlockType              RelationalOperator
        Operator               ">="
        InputSameDT           on
        LogicOutDataTypeMode  "Logical (see Configuration Parameters:
Optimization)"
        LogicDataType         "uint(8)"
        OutDataTypeStr        "Inherit: Logical (see Configuration
Parameters: Optimization)"
        ZeroCross             on
        SampleTime            "-1"
    }
    Block {
        BlockType              Saturate
        UpperLimit            "0.5"
        LowerLimit            "-0.5"
        LinearizeAsGain      on
        ZeroCross             on
        SampleTime            "-1"
        OutMin                "[]"
        OutMax                "[]"
        OutDataTypeMode       "Same as input"
        OutDataType           "fixdt(1,16,0)"
        OutScaling            "[]"
        OutDataTypeStr        "Inherit: Same as input"
        LockScale             off
        RndMeth               "Floor"    }
    Block {
        BlockType              Scope
        ModelBased            off
        TickLabels            "OneTimeTick"
        ZoomMode              "on"
        Grid                  "on"
        TimeRange             "auto"
        YMin                  "-5"
        YMax                  "5"
        SaveToWorkspace       off
        SaveName              "ScopeData"
        LimitDataPoints       on
        MaxDataPoints         "5000"
        Decimation            "1"
        SampleInput           off
        SampleTime            "-1"    }
    Block {
        BlockType              Selector
        NumberOfDimensions    "1"
        IndexMode             "One-based"
        InputPortWidth        "-1"
        SampleTime            "-1"
    }
}

```

[III] Dissertation's Publications and Author's Contribution

- Paper " Real World Optimal UPFC Placement and its Impact on Reliability ", **Ahmed M. Othman**, Alexander Gaun, Matti Lehtonen, Mahdi M. Alarini, For The 5th IASME / WSEAS International Conference on (EE'10), Cambridge University, UK, February 23-25, 2010, accepted for publishing in The World Scientific and Engineering Academy and Society Journal Transaction.
- Paper "Enhancing the Contingency Performance of HELENSÄHKÖVERKKO OY 110 KV NETWORK by Optimal Installation of UPFC based on Genetics Algorithm", **Ahmed M. Othman**, Matti Lehtonen, Mahdi M. Alarini, IEEE Power & Energy Society 2010 GM July 25-29, 2010 , Minneapolis, Minnesota, USA.
- Paper "Optimal UPFC based on Genetics Algorithm to Improve the Steady-State Performance of HELEN SÄHKÖVERKKO 110 KV NETWORK at Increasing the Loading Pattern", **Ahmed M. Othman**, Matti Lehtonen, Mahdi M. Alarini, For Ninth International Conference On Electrical Eng., 9th IEEEIC, co-sponsored by IEEE, 2010, Prague.
- Paper "Optimal UPFC Installation based on GA in a Real Finnish Sub-transmission Network considering Performance Measures and Reliability", **Ahmed M. Othman**, Alexander Gaun, Matti Lehtonen, Mahdi M. Alarini, For WSEAS Journal Transactions on Power Systems, ISSN: 1790-5060 .
- Paper " Heavy Loading Conditions Studies by Optimal UPFC on a Real Finnish 110 KV Network to Solve Technical Problems of 2020", **Ahmed M. Othman**, Matti Lehtonen, Mahdi M. Alarini, Electrical Review Journal Transaction ISSN 0033-2097, R. 86 NR 11a/2010, Volume December 2010, p.p 23-27
- Paper "Integrated GA with ANFIS as UPFC Controller for Dynamics Response Fine-Tuning applied on a Real Finnish 110 KV Network until Year 2020", Ahmed M. Othman, Matti Lehtonen, Mahdi M. Alarini, IEEE Transactions on Smart Grid, under reviewing.

This work has been carried out under joint supervision between Zagazig University, Egypt and Aalto University School of Science and Technology, Finland. Professor Mahdi El-Arini participated from Zagazig University and Professor Matti Lehtonen participated from Aalto University. The author of this dissertation has had the main responsibility of all research work and publications.

